THE UNIVERSITY OF HULL

Unknown Input Observer Approaches to Robust Fault Diagnosis

Being a Thesis submitted for the Degree of Doctor of Philosophy

in the University of Hull

by

Xiaoyu Sun

MSc Electronics Shenyang (China)
BSc Automation Shenyang (China)

July, 2013

Acknowledgements

I would like to express my appreciation to my supervisor, Professor Ron.J.Patton for his unbounded encouragement, guidance, support and help during my PhD studies. It has no doubt that it is his solicitude and professional experience inspiring me to go to the end of my PhD with confidence.

I also would like to give my thanks to my colleagues Fengming Shi, Dr Lejun Chen and Dr. Chenglei Nie, Dr. Zheng Huang, Yimeng Tang, Dr. Shaodong Ma, Dr. Montadher Sami Shaker and Dr. Eshag Yousef Larbah, for their help and discussion on the subject of Fault detection and diagnosis and their best friendship.

I would like to acknowledge financial support from ADDSAFE Project. ADDSAFE was an FP7 project funded by the European Union and coordinated by Dr Andres Marcos of Deimos Aerospace of Madrid. A PhD scholarship form the Department of Engineering, University of Hull is also acknowledged.

Also, I would like to acknowledge the financial support from a HEFCE HEIF5 research infrastructure funding award (2012-2013) through the Centre for Adaptive Systems and Sustainability (CASS), University of Hull.

Finally, I would like to give special acknowledgment to my parents and my fiancé for their support, encouragement, and understanding and love as always.

Abstract

This thesis focuses on the development of the model-based fault detection and isolation /fault detection and diagnosis (FDI/FDD) techniques using the unknown input observer (UIO) methodology. Using the UI de-coupling philosophy to tackle the robustness issue, a set of novel fault estimation (FE)-oriented UIO approaches are developed based on the classical residual generation-oriented UIO approach considering the time derivative characteristics of various faults. The main developments proposed are:

- Implement the residual-based UIO design on a high fidelity commercial aircraft benchmark model to detect and isolate the elevator sensor runaway fault. The FDI design performance is validated using a functional engineering simulation (FES) system environment provided through the activity of an EU FP7 project Advanced Fault Diagnosis for Safer Flight Guidance and Control (ADDSAFE).
- Propose a linear time-invariant (LTI) model-based robust fast adaptive fault estimator (RFAFE) with UI de-coupling to estimate the aircraft elevator oscillatory faults considered as actuator faults.
- Propose a UI-proportional integral observer (UI-PIO) to estimate actuator multiplicative faults based on an LTI model with UI de-coupling and with added H_∞ optimisation to reduce the effects of the sensor noise. This is applied to an example on a hydraulic leakage fault (multiplicative fault) in a wind turbine pitch actuator system, assuming that the first derivative of the fault is zero.
- Develop an UI–proportional multiple integral observer (UI-PMIO) to estimate the system states and faults simultaneously with the UI acting on the system states. The UI-PMIO leads to a relaxed condition of requiring that the first time derivative of the fault is zero instead of requiring that the finite time fault derivative is zero or bounded.
- Propose a novel actuator fault and state estimation methodology, the UI–proportional multiple integral and derivative observer (UI-PMIDO), inspired by both of the RFAFE and UI-PMIO designs. This leads to an observer with the comprehensive feature of estimating faults with bounded finite time derivatives and ensuring fast FE tracking response.
- Extend the UI-PMIDO theory based on LTI modelling to a linear parameter varying (LPV) model approach for FE design. A nonlinear two-link manipulator example is used to illustrate the power of this method.

Table of Contents

List of Figures

List of Tables

List of Symbols and Abbreviations

Symbols

$\Re$	The set of real numbers
$\Re^n$	The set of real-valued *n*-dimensional vectors
$\Re^{n\times m}$	The set of real-valued n by m matrices
I_n	The *n* by *n* identity matrix
$\|\cdot\|$	Euclidean norm (vectors) or induced spectral norm (matrices)
A^T	The transpose of the matrix A
A^{-1}	The inverse of the matrix A

Abbreviations

ADDSAFE	Advanced Fault Diagnosis for Sustainable Flight Guidance and Control
AFTC	Active fault tolerant control
CFIT	Controlled flight into terrain
FAFE	Fast adaptive fault estimation
FA	False alarm
FAR	False alarm rate
FCC	Flight control computer
FD	Fault detection
FDD	Fault detection and diagnosis
FDI	Fault detection and isolation
FDR	Fault detection rate
FDT	Fault detection time
FE	Fault estimation
FES	Functional engineering system
FIR	Fault isolation rate
FTC	Fault tolerant control
GARTEUR	Group for Aeronautical Research and Technology in Europe
G&C	Guidance and control

IFAC	International Federation Automatic Control
IFD	Instrument fault detection
LMI	Linear matrix inequality
LMIs	Linear matrix inequalities
LPV	Linear parameter varying
LTI	Linear time invariant
LTV	Linear time varying
LoC	Loss-of-Control
LoC-I	Loss of Control In-flight
MDT	Mean detection time
MAR	Missed alarm rate
OFC	Oscillatory fault case
PIO	Proportional integral observer
RFAFE	Robust fast adaptive fault estimator
SISO	Single input single output
S.P.D	Symmetric positive definite
SVD	Singular value decomposition
UI	Unknown input
UIO	Unknown input observer
UIOs	Unknown input observers
UI-PIO	Unknown input-proportional integral observer
UI-PMIDO	Unknown input–proportional multiple integral and derivative observer
UI-PMIO	Unknown input–proportional multiple integral observer

List of Publications

Within the period of this research the following works were published:

Sun, X., Patton, R. J., Robust actuator multiplicative fault estimation with unknown input decoupling for a wind turbine system. IEEE Conference on Control and Fault-Tolerant Systems SysTol'13, October 9-11, 2013, Nice, France (accepted)

Sun, X. Y., Patton, R. J. and Goupil, P. (2012). Robust adaptive fault estimation for a commercial aircraft oscillatory fault scenario. *Proc. of the 2012 UKACC International Conference on Control*, Cardiff, 595-600, 3-5 Sept.

Chapter 1
Introduction

1.1 Introduction

It has become inevitable that human daily activities have been technologically assisted by increasing advanced computer-based automation. The services provided by automatic, mechatronic systems fundamentally aim at ensuring safety and improving life quality and enhance availability. Computer-assisted living can, however, be easily threatened without enough time to generate a warning if the computer-controlled systems provide unintended services, especially in safety-critical scenarios such as transportation (Wikipedia, 1992), chemical and nuclear power plants (Rogovin, 1979; Patton, Frank and Clark, 1989).

Considering the following two examples of fatal accidents in transportations: *El Al Flight 1862* on October the 4th 1992, involved a Boeing 747 cargo plane that crashed into a residential apartment in Bijlmermeer near southeast Amsterdam, causing 47 dead and many more injured on the ground (Wikipedia, 1992). Figure 1-1 shows the aircraft that crashed and the buildings that were destroyed.

Figure 1-1 Boeing 747–200 of El Al Flight 1862 and the Bijlmermeer apartment building (Wikipedia, 1992)

The accident investigation results unveiled that one engine broke away from the starboard wing shortly after take-off, causing structural damage. This was followed by the break-away of the second engine on the same wing. The pilots had to circle around

Amsterdam (about 80kms) to try to come back to Schipol airport. Unfortunately, on line up with the instrument landing system the aircraft rolled excessively became uncontrollable and crashed.

In Wenzhou province, China, two high-speed trains collided on a viaduct in the suburbs (Wikipedia, 2011) among which 40 people were killed and the 192 were injured. An official accident investigation report released that one of the causes was that the trains failed to correctly respond to equipment malfunction attributed to lightning. The elevated impact on human life in both of these incidents is a sign of the lack of hazard prevention in these systems compared with the huge amount of technical development. The underlying reason causing the above catastrophes is that electronic and computer-based systems are assumed to deliver the expected capacity correctly, whilst lacking systematic procedures for identifying the causes of system malfunctions in real-time.

With the early days of the development of automatic supervisory control, very significant attention to these safety and security issues were paid by academic researchers (Clark, Fosth and Walton, 1975; Patton, Frank and Clark, 1989). This is especially the case in aeronautics and astronautics which have stringent requirements on stability, performance and reliability. Heavy demands can be placed on an automatic system to help to avoid repetition of tragedies and devastating economic loss. In the context of research on fault diagnosis the term *system* usually refers to an operational plant or process in conjunction with basic feedback control elements such as the actuator sensors. The causes leading to unintended system executions or unusual sensing are called *faults*, which are conceptually defined as *unpermitted deviations of at least one characteristic property or parameter of the system from the acceptable/usual/standard operating conditions* according to (Isermann and Ballé, 1997). As a consequence of each fault occurring during operations, *failure* is understood as *the complete breakdown of a system component or function*. *It describes the situation that the system no longer performs the required function* (Isermann and Ballé, 1997). Faults occurring in actuators, sensors or other system components may lead to unsatisfactory performance or even worse instability. The monitoring system takes the responsibility of detecting and diagnosing the unanticipated functions. The supervisory system is the so-called fault detection isolation/diagnosis (FDI/FDD) system. FDI/FDD

systems should not only provide alarms when the supervised plant suffers a malfunction, but should also classify and identify the erroneous behaviour occurring during the entire plant operation. The FDI/FDD systems should also provide information and reports to prevent further loss of system function. The operators should be informed of the fault situations and of important actions to be taken to avoid total system breakdown and catastrophe (Patton, Frank and Clark, 1989). Hence, a reliable and affordable fault diagnosis system is very critical from safety and sustainability perspective and plays a significantly important role in technical processes of the industry sectors (Chen and Patton, 1999).

The traditional fault diagnosis approach localises the faults by making use of *hardware redundancy* (replicates all system components including actuators, sensors, computers to measure and/or control a particular variable). The location of a fault can be inferred using a majority voting scheme, three or more redundant lanes of system hardware are used to provide the same function. However, the complexity and system volume of modern industrial appliances render the hardware redundancy approach much less applicable in terms of maintenance and operational costs, even in terms of weight restriction and strictly regulated ecological requirements.

An alternative to the use of redundant hardware is to develop systems that have analytical redundancy or functional redundancy based on the use of model-based information. Analytical redundancy effectively transforms the hardware redundancy into realisable software estimation problems. Redundant or additional/repeated estimates of the measured signals are used to derive estimates of other variables of the system without the use of additional measurement sensors (Chen and Patton, 1999). The only required information for the model-based FDI/FDD approach is the use of a valid system model and the measured inputs and outputs of the system being monitored. However, to achieve reliability and robustness special methods must be used to ensure that the estimated variables are faithful replicas of the measured quantities. The expected outcomes from the model-based FDI/FDD approach are multiple symptoms (residuals or FE signals) indicating the differences between nominal and faulty system status in a timely manner. Figure 1-2 shows a concise, open-loop FDI/FDD structure using analytical redundancy compared to the conventional FDI/FDD hardware redundancy method.

The growing demands on safety, reliability, maintainability and survivability in industrial processes motive and accelerate the development of many model-based fault diagnosis strategies (Chen and Patton, 1999; Blanke, Kinnaert, Lunze and Staroswiecki, 2003; Simani, Fantuzzi and Patton, 2003; Ding, 2008; Edwards, Lombaerts and Smaili, 2010; Isermann, 2011).

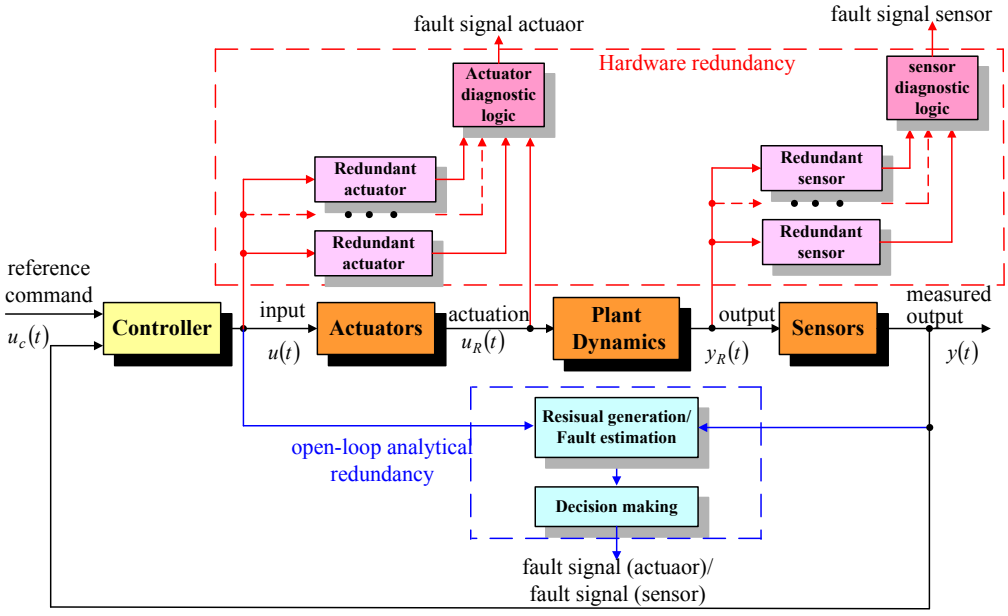

Figure 1-2 FDI/FDD hardware redundancy *vs* open-loop analytical redundancy

1.2 The need for FDI/FDD in Fault tolerant control (FTC)

Increasing demands from the supervised plant for safety, reliability, availability, maintainability, survivability and sustainability also motives to develop FTC designs with the capability of tolerating system malfunctions preventing loss of life, mitigating against hazards, and avoiding economic loss, etc. FTC is also expected to maintain desirable and robust performance and stability properties in the case of malfunctions in actuators, sensors or other system components (Patton, 1997a; Blanke, Kinnaert, Lunze and Staroswiecki, 2003).

FTC schemes have been widely investigated for potential applications. As an example, the Group for Aeronautical Research and Technology in Europe (GARTEUR) Flight Mechanics Action Group 16 (FM-AG (16)) project "Fault tolerant Flight Control" based on the 'Bijlmermeer disaster' (outlined in Section 1.1) case is introduced briefly here to demonstrate how fault diagnosis together with FTC can assist in accident prevention.

The main task of the FM-AG (16) project is to explore the FTC approach to recovery of flight following in flight failure. The FM-AG (16) project was initiated to investigate the use of FTC in attempting to sustain the flight of the damaged El Al Flight 1862 Boeing 747 aircraft of the 'Bijlmermeer disaster', to enable the aircraft to land successfully after the structural failure. Different fault monitoring systems (*fault diagnosis systems)* and fault-tolerant control (FTC) strategies were applied on the 'GARTEUR RECOVER benchmark'(GARTEUR, 2004) model which includes the fault scenarios of the El Al Flight 1862 flight and is validated with accident flight data. The FTC strategies were continuously experimented according to the reconstructed fault signals supplied from various kinds of fault diagnosis systems to restore stability and manoeuvrability of the aircraft for continuous and safe operation and provide survivable recovery to improve the resilience and safety of the aircraft. The simulated results demonstrated that the Bijlmermeer crash could have been avoided using appropriate fault diagnosis-assisted FTC action (Smaili and Mulder, 2000; Maciejowski and Jones, 2003; Smaili, Breeman, Lombaerts and Stroosma, 2008; Alwi and Edwards, 2010; Edwards, Lombaerts and Smaili, 2010).

FDD information can certainly be important in FTC, for example the control system can be reconfigured subsequent to detect that a fault has occurred. If the location, fault onset time and severity of the fault are determined either from an FDI residual signal or using estimates of a fault, then appropriate action can be taken to switch or reconfigure the control system either using on-line or off-line computed control laws corresponding to various potential fault scenarios. When the FTC system makes use of fault information for reconfiguration this is known as *active* FTC (AFTC), whilst the alternative *passive* FTC methods do not require fault diagnosis information and are thus based mainly on robust control ideas (Patton, 1997a). The book by (Blanke, Kinnaert, Lunze and Staroswiecki, 2003) provides an in-depth analysis of the subject of FTC.

AFTC schemes are used to trigger specific control actions in real-time (based on fault information) to prevent plant damage as a consequence of malfunctions and ensure system availability and sustainability based on the use of redundancy (in either analytical or hardware forms). AFTC can also be used to ensure that the control system performance is not degraded when there is a loss of efficiency in closed-loop system components, i.e. corresponding to minor or incipient fault conditions (Patton, 1997a).

Figure 1-3 gives the general relationship among FDI/FDD, robust control as well as AFTC.

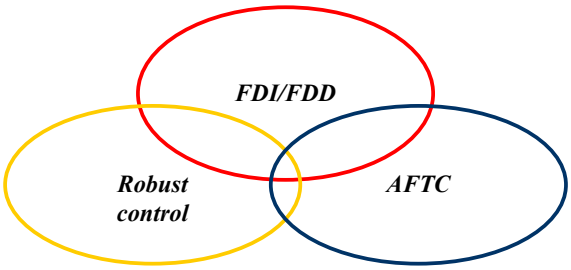

Figure 1-3 The three disciplines of FTC (adapted from: Patton, 1997a)

In an AFTC mechanism, sufficient real-time fault information is required to accommodate to the effects of faults by a reconfiguration mechanism. The AFTC performance is strongly affected by the degree to which accurate fault information is available. Whilst residual-based FDI methods can provide a high degree of fault information accuracy a preferable approach is to use on-line fault estimation (FE) signals that are designed to robustly reconstruct the time-variation of each fault. The reconfiguration in this case may use the FE signal to compensate for the fault in the closed-loop system. The more precisely the fault estimated information provides by on-line FE, the more favourably the AFTC scheme designs. (Patton, 1997a; Zhang and Jiang, 2008).

Of course many AFTC research studies assume that the fault information is richly and precisely known. However, although appropriately rich and accurate fault information is not easy to determine there are now several very powerful methods available for robust FE, subject to expected bounds in terms of the fault level or finite time derivatives (Koenig, 2005; Gao and Ding, 2007). Although this thesis is not about AFTC, in the light of the availability of these methods the work is very much concerned with developments of the FE approach (for FDD) that can be very effectively applied to AFTC. Figure 1-4 gives an overview of the structure of AFTC, showing the role of FDD (that also includes FDI).

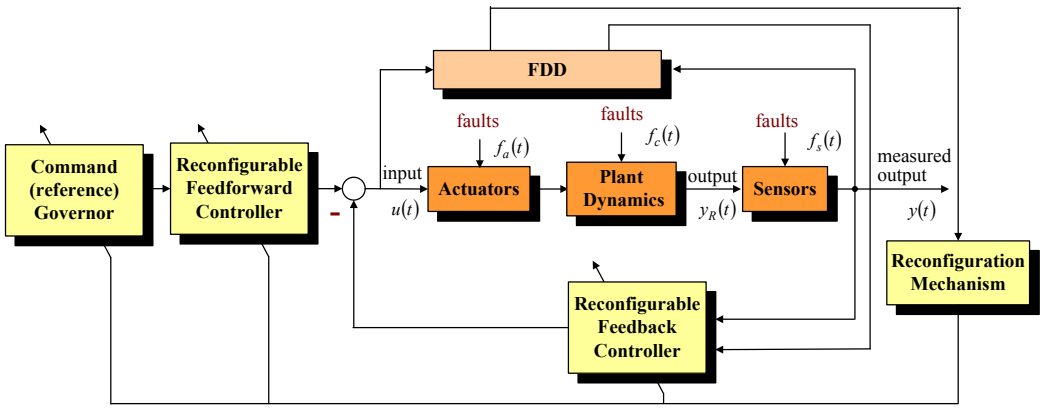

Figure 1-4 An overview structure of AFTC (Zhang and Jiang, 2008)

Detailed AFTC research concepts are described (Patton, 1997b; Blanke, Staroswiecki and Wu, 2001; Blanke, Kinnaert, Lunze and Staroswiecki, 2003; Blanke, Kinnaert, Lunze and Staroswiecki, 2006 ; Zhang and Jiang, 2008).

1.3 Fundamentals of FDI/FDD

This sub-section revisits and clarifies briefly some preliminary concepts and terminologies in fault diagnosis research field. All the terminologies defined in this thesis are based on information from the International Federation Automatic Control (IFAC) SAFEPROCESS Technical Committee and associate the updated literatures listed herein (Isermann and Ballé, 1997; Chen and Patton, 1999; Isermann, 2006), for example.

Fault: An unpermitted deviation of at least one characteristic property or parameter of the system from the acceptable/usual/standard condition.

Failure: A permanent interruption of a system's ability to perform a required function under specified operating conditions.

***Malfunction*:** An intermittent irregularity in the fulfilment of a system's desired function.

Error: A deviation between a measured or computed value of an output variable and its true or theoretically correct one.

***Modelling uncertainty*:** The overall system cannot be precisely described by a linear mathematical model. Uncertainties come from incomplete identification of the system and some unknown disturbances/control signals. Moreover, model aggregation or

simplification which is deliberately designed to make the system manageable may also lead to uncertainties.

***Disturbance*:** An unknown and uncontrolled input acting on a system.

Residual: A fault indicator, based on a deviation between measurements and model-equation based computations. Residuals should remain small as long as there is no fault, and become sufficiently large to be noticeable whenever faults occur.

It is very important to note that the terminology 'failure' denotes that a subsystem or an entire system loses its functionality completely. However, the word 'fault' has a wide definition which refers to any unwanted malfunctions of the system. For example, pump wear for which it turns out that the parameter variations can also be considered as fault (Blanke, Staroswiecki and Wu, 2001).

A fault diagnosis system is usually built to perform one or more functionalities as shown in Figure 1-5:

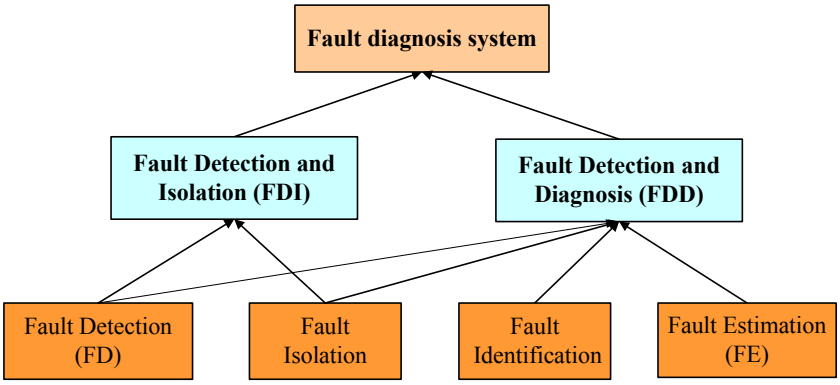

Figure 1-5 Topological illustration of fault diagnosis functional relationships

The difference between the roles of FDI and the FDD are clarified here to avoid the confusion since the terms '*isolation*' and '*identification*' share the same initials but correspond to different functional cases. FDI aims to locate and isolate the faulty components in the system. FDD, however, is intended to know the detailed attributes of detected faults e.g. faults severity and the *fault identification* is required in FDD. FE is the abbreviation of *fault estimation* which is functionally similar as *fault identification* but focuses on reconstruction of the fault signal using estimation-based methods (Ding, 2008).

A common purpose of the FDI/FDD functions is to serve either individually or in combination with others for the actuation of a particular fault accommodation scheme, to detect, isolate and estimate faults so that this information can be used in a fault accommodation scheme (AFTC) (Zhang and Jiang, 2008). The FDD system provides descriptive information to reconstruct a fault in the form of a signal and notify the AFTC which accommodates the faults by adaptively controlling system dynamics or reconfiguring system structure. A real-time FE function is nowadays regarded as a must-have feature as AFTC schemes require accurate fault information. The term FDD tends to be used totally in the aerospace flight control community, whereas the wider control-based fault diagnosis community tend to use the term 'FDI'. However, one should be clear that the most applicable term should be used. For example, FDI does not include fault reconstruction/estimation/identification and this should be reserved for the topic of FDD.

1.4 Fault classification

The faults are categorised according to different characteristics. As defined in Section 1.1, a fault is an unpermitted deviation of at least one characteristic property or parameter of the system from the acceptable/usual/standard condition. Three different classifications are defined in terms of the fault types, faults location and time dependency, respectively. They are described as following.

- **Fault types**

Two usually seen interactions, defined as *additive* or *multiplicative* faults, are modelled and structured in conjunction with system as shown in Figure 1-6.

***Additive fault*:** This behaves as an additional signal acting on the plant, for instant, unexpected exogenous motion on an actuator.

***Multiplicative fault**:* This is represented by the product of a system variable with the fault itself. They can appear as parametric deviation within a process, i.e. it may cause changes in the system dynamics.

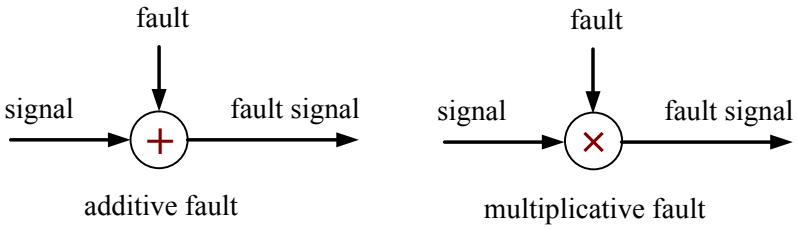

Figure 1-6 Additive fault and multiplicative fault

•**Fault location** (see Figure 1-7)

***Actuator fault*:** A fault occurring in the electro-mechanic drive subsystem such as electrical motors, pneumatic actuators, and hydraulic pistons. An actuator fault normally suggests partial or total loss of the actuator's control action effectiveness. Possible reason to cause actuator faults are jamming or oscillation, the sticking of mechanical dampers or levers or damage in the drive system e.g. due to bearings, gear wear or friction, caused by changes from the design characteristics or complete failure.

***Sensors fault*:** With reference to feedback control systems, a fault in a sensor in the feedback path can mislead the controller to drive the plants improperly and thereby lose performance. Likely reasons for *sensor faults* are inaccurate calibration, value bias, scaling errors, dynamical changes (disturbance) in sensors and physical breakdown in a control loop.

***Components fault*:** Dynamical, parametric variations in the system rendering the dynamics invalid. These plant variations in the plants are common phenomena since most realistic processes are time-varying and nonlinear and normally referred to as multiplicative faults. For instance, abnormal variations in the damping ratio or natural frequency of a mechanical or mechatronic system can be considered as *component fault.*

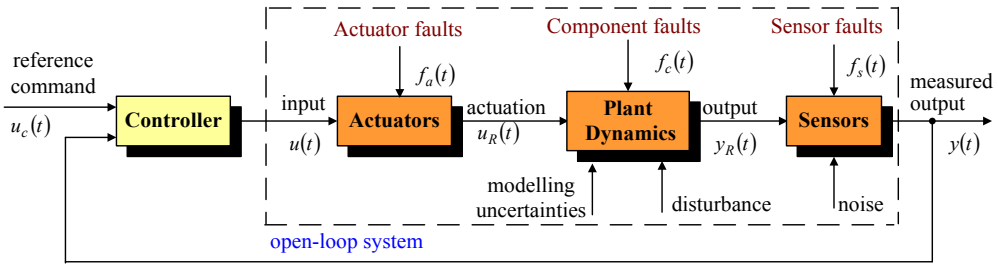

Figure 1-7 Actuator fault, sensor fault and component fault

•**Time dependency of faults**

Some typical fault signal types and their time dependency can be characterized as shown in Figure 1-8.

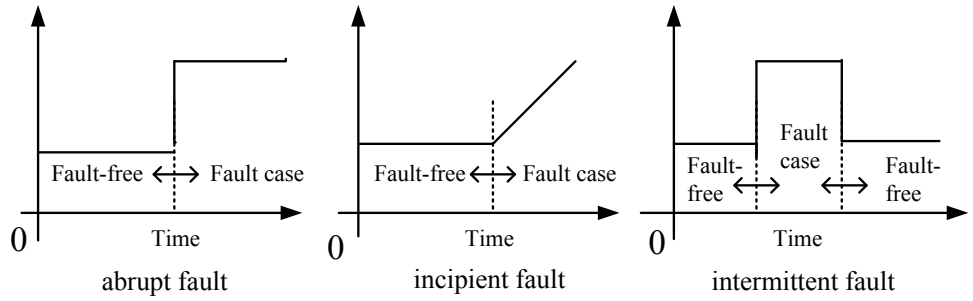

Figure 1-8 Abrupt fault, incipient fault and intermittent fault (Isermann and Ballé, 1997)

Abrupt fault: This fault typically can be modelled as stepwise signals and can be represented by a sudden change in some actuator or sensor characteristic.

***Incipient fault*:** A fault that can be modelled by using ramp signals typically and represents an unexpected drift of the monitored signal.

***Intermittent fault*:** The fault is not permanent, sometimes it is present and other instants the fault is absent, e.g. corresponding to a loose connection in an electronic system.

Considering, each of these in turn. Abrupt faults behave as variations that are faster than the nominal system dynamics, having a significant impact on the controlled system performance and stability. The effects of abrupt faults can be severe and hence the faults need to be detected and isolated quickly before they have an effect on system function and stability.

In contrast to an abrupt fault, an incipient fault (also known as a soft fault) has a very small but possibly developing effect on the system and is very hard to detect and hence also to isolate. The incipient fault may not lead rapidly to serious consequence, but may develop further into a more significant fault situation and hence must be detected and isolated (even identified) as quickly as possible to avoid system break-down or catastrophe. Finally, intermittent faults are faults that appear and disappear repeatedly.

Besides the aforementioned faults, there is another type of fault which is represented by

a sinusoidal signal, known as an oscillatory fault. It can be considered as a type of incipient fault in terms of its time characteristics which behaves smoothly, not abruptly.

1.5 Typical performance indices for FDI/FDD performance evaluation

It is very important to set a series of indices to evaluate the performance of an FDI/FDD method to determine if it is well suited for practical applications. A good FDI/FDD performance should detect and isolate faults as early as possible. Meanwhile, considering the further FTC action, FE design, in some cases should provide accurate fault information for the reconfiguration mechanism. A set of performance indices that can be used for an effective model-based FDI/FDD are listed in Table 1-1 (Baca, 1993; Lieber, Nemirovskii and Rubinstein, 1999; Hokayem and Abdallah, 2003; Bartys, Patton, Syfert, De las Heras and Quevedo, 2006; Patton, Uppal, Simani and Polle, 2010):

Table 1-1 FDI/FDD Performance Indices

Fault detection time (FDT)	t_{fd}	The time interval between the time instance at which a fault occurs and time instance at which a fault is declared as detected.
Fault isolation time (FIT)	t_{fi}	The time interval between the time instance at which a fault occurs and time instance at which a fault is declared as isolated.
False alarm rate (FAR)	r_{fa}	The number of wrongly detected faults divided by the total fault scenarios.
Missed alarm rate (MAR)	r_{mf}	For each fault, the total number of undetected faults divided by the total number of times that the fault occurs.
Fault detection rate (FDR)	r_{td}	For a particular fault, the number of times that it is correctly detected is divided by the total number of times that the fault occurs.
Fault isolation rate (FIR)	r_{ti}	For a particular fault, the number of times that it is correctly isolated is divided by the total number of times that the fault occurs.
Mean detection time (MDT)	t_{md}	For each fault, this is an average of the detection times, i.e. sum of FDT divided by the total number of times that fault occurs
Maximum detection time	t_{max_d}	Maximum fault detection time amongst total number of fault occurs.
Minimum detection time	t_{min_d}	Minimum FDT amongst total number of fault occurs.

In accordance with Table 1-1, the desirable FDI/FDD performances expected are rapid FDT, high FDR, low FAR & MAR, high accuracy of FE signal and accurate FE information (location, type, shape). The achievable performance is considered to be acceptable as long as it satisfies a relaxed requirement in Table 1-1, even though the system monitored system is affected by various forms of uncertainty in practice. It is quite challengeable and launches difficulties in model-based FDI/FDD methods.

1.6 Robustness issue in model-based FDI/FDD methods

To meet the indices listed in Section 1.5, one of the biggest challenges in FDI/FDD design is the robustness issue caused by unexpected signals, uncertainty and modelling errors as well as faults acting in the control system that all contribute to a deterioration of required system performance. The robustness issue can be raised in different ways (Patton, Frank and Clark, 1989; Chen and Patton, 1999).

On one aspect, the overall system cannot be precisely described by the mathematical model. Particularly, the parameters in the system may change with time, unexpected exogenous disturbance and noise. Therefore, unexpected discrepancies can be defined as a form of 'modelling uncertainty' between the actual system and its mathematical model description. Modelling uncertainties can also be caused by discrepancies between the model and the actual system that are generated as a consequence of the use of linear models for representing dynamic behaviour. The real system may have strongly nonlinear system dynamics so that linear modelling is limited only to small variations around operating points, causing modelling uncertainty as the systems moves away from these points. Moreover, model aggregation or simplification for managing the system to be designable may also lead to uncertainties. All of these uncertainties can be thought of as having a combined effect on the system acting through the so-called unknown input (UI) signals considered to act at the system inputs. Since the UI signals affect the system modelling, they also have an impact on the residuals/FE signals so that the FDI/FDD performance is degraded. In terms of performance indices in Section 1.5, the existence of the UI may extend the FDT, generate false alarm (FA) or lead to a higher MAR.

These uncertainty issues lead to the main challenge of FDI/FDD that is that the residuals/FE must all be robust against these uncertainties, i.e. they should be designed

to compensate for the effects of the UI to an appropriate degree of robustness to achieve satisfactory FDI/FDD performance.

Following this, for residual generation-based FDI design the robustness problem is defined as the minimised sensitivity of the effect of the UI to residual signals and the maximised sensitivity of the detectability and isolability to faults. For FE-based FDD design, the robustness problem is regulated as the minimised sensitivity of the effect of UI to the FE signals, yielding the most accurate FE signals (Chen and Patton, 1999; Ding, 2008; Zhang and Jiang, 2008). The performance indices given in Section 1.5 are hence very important for evaluating the robust performance of individual FDI/FDD designs.

In the last three decades, robustness issue has become a very significant research subject to guarantee an acceptable fault diagnosis system performance. Fruitful studies can be found in the excellent works (Chen and Patton, 1999; Patton, Frank and Clark, 2000; Shafai, Pi and Nork, 2002; Gao and Ding, 2005; Henry and Zolghadri, 2005; Ding, 2008; Alwi, Edwards and Tan, 2009; Falcoz, Henry and Zolghadri, 2010; Patton, Uppal, Simani and Polle, 2010; Chen, Patton and Klinkhieo, 2010).

1.7 The structure of the thesis

This thesis mainly focuses on the development of model-based FDI/FDD approaches using the UI de-coupling principle that are implemented in different examples according to the suitability of related UI de-coupling based FE theory. Various methods have properties which make them more or less suitable for particular FDI/FDD problems, according to fault types, degrees of robustness, applicability to nonlinear systems, accuracy of fault reconstruction, practical implementability, and so on. The thesis is outlined as follows:

In Chapter 2, a historical development of model-based FDI/FDD is reviewed. The role of model-based FDI/FDD within the framework of FTC is also discussed. The Chapter commences by outlining the core idea of model-based approaches to FDI/FDD based on a review of three most dominant methods. Then, two different techniques in terms of the functions of FDI or FDD, namely residual generation-based and FE-based techniques are described respectively. The central issues to be addressed in the thesis are concerned with the development of model-based FDI/FDD methods and algorithms

that take into account systems with uncertainties and exogenous disturbance considered acting in a UI format.

Throughout the thesis FDI/FDD designs are considered to be implemented using observer-based methods and hence the research focuses on both review and new developments of robust unknown input observer (UIO) methods involving either UI estimation/de-coupling or robust fault estimation, or both.

The state space structure of the UI-corrupted linear time invariant (LTI) models that are used for FDI/FDD designs are described. Then, according to this formulation, the detectability and isolability (two key conditions for FDI/FDD design) in terms of both additive and multiplicative faults are given, respectively.

The fundamental UIO theory is introduced according to the formulation of (Chen, Patton and Zhang, 1996) and (Chen and Patton, 1999) as a foundation for the following Chapters. The idea of de-coupling the structured UI for the purpose of overcoming the robustness issue in the FDI/FDD design is explained explicitly and an entire residual generation-based UIO design procedure together with the distribution matrix of UI estimation is described with reference to a simple nonlinear tutorial system example. This foundation is necessary at this stage since all the developed theory in the thesis focusses on the re-development of the UIO formulation into an FE-based approach, i.e. moving away from a residual-based strategy.

In Chapter 3, studies on aircraft FDI/FDD design and the residual-generated UIO application on the aircraft are reviewed briefly. A high fidelity commercial aircraft benchmark model provided by the FP7 "*ADDSAFE* (Advanced Fault Diagnosis for Safer Flight Guidance and Control)" project is used to test the UIO-based FDI strategy. The FDI performance validation and verification procedures are carried out in a functional engineering system (FES) environment to evaluate the proposed FDI design.

In Chapter 4, the studies move towards the UIO-based FE design, from the conventional UIO FDI design (residual generation-based FDI) introduced in Chapter 3.

An LTI model-based robust fast adaptive fault estimator (RFAFE) with UI de-coupling is proposed to estimate the aircraft elevator fault scenario in terms of oscillatory fault cases (OFC) in an elevator actuator. Since the proposed FE is a function of system

output errors, it is necessary to design the fault estimator with the capability of rejecting the influence of the UI acting on the system states. Hence, in Chapter 4, the FE signal generated by the RFAFE is de-coupled from the UI (modelling uncertainties herein) using the principle outlined in Chapter 2. In order to enhance the FE performance, an adaptive fault estimator is constructed by involving additional proportional action besides conventional integral action in the FE signal to enhance the fault estimation tracking performance. A Lyapunov stability analysis of the proposed fault estimator is given and the fault estimator dynamic response is achieved by pole assignment in sub-regions formed by Linear Matrix Inequality (LMI).

Finally, the proposed RFAFE is implemented on a high-fidelity nonlinear generic Airbus aircraft model (as described in Chapter 3) to estimate the elevator actuator oscillatory faults.

In Chapter 5, a robust FE design approach for detecting multiplicative faults acting is described by combining the UI de-coupling principle and H_∞ optimisation. The fault is constructed as an augmented system state and estimated by the augmented fault estimator which is a proportional integral observer (PIO). The UI de-coupling principle is chosen to improve the robustness of the FE signals against the UI, i.e. the UI de-coupling principle is used to de-couple the UI effect from the FE signal. The UIO gains are chosen (a) to achieve the de-coupling and (b) to satisfy FE performance requirements. In a novel step combined with UI de-coupling principle, the H_∞ optimisation is used to minimise the effect of exogenous disturbance in the fault estimation as a specific stage of the robust FE-oriented UIO design.

This new design approach is applied to a tutorial example comprising multiplicative (parametric) faults acting within one of the pitch actuation systems of an offshore wind turbine, based on a nonlinear benchmark system. Whilst the benchmark system is itself nonlinear, due to aerodynamic nonlinear dependence on wind speed. The design makes use of an LTI wind turbine model (derived from the benchmark system at a particular wind speed). During the linearisation, both the linearisation error and exogenous disturbance (the wind force) are combined together into an UI which is then de-coupled via the UI de-coupling principle. From a practical point of view, the actuator measurement sensors are considered corrupted by sensor measurement noise signals which are considered as exogenous (hence unknown) disturbances. As these noise

signals contaminate the FE performance, they are attenuated in the observer estimation error using H_∞ minimisation.

A hydraulic leakage fault occurring in a wind turbine pitch actuator is considered as a multiplicative fault that relates to the damping and natural frequency parameters of the actuator. A fault model modification is used to reformulate the multiplicative fault into an additive fault representation by which the fault can be estimated via the proposed observer-based FE scheme. Once the additive fault is reconstructed, a wind turbine operation look-up table is then used to determine the individual fault parameters.

In Chapter 6, the goal is to develop the FE method, called UI–proportional multiple integral observer (UI-PMIO) which is capable of estimating the system state and the faults simultaneously regardless of the existence of the UI influencing the system states. The UI-PMIO widens the practical application field of the UI-proportional integral observer (UI-PIO) described in Chapter 5 by removing the constraint that the FE signal has zero-valued first derivative (as in the UI-PIO case). The use of the multiple integrals in the FE structure facilitates a relaxation of the constraint applied to the FE signal so that the finite fault derivatives should only be bounded or have zero values.

In this UI-PMIO structure, the UI de-coupling strategy (as described in Section 2.3) is kept for handling the UI influence on the state estimation error. Besides, the H_∞ theory is investigated to guarantee the convergence condition of the augmented state estimation error dynamics in the case of the bounded finite time fault derivatives. This leads to accurate and robust fault and system state estimation. Noticeably, the UI-PMIO provides an enhancement to the UI-PIO observer in Chapter 5, from the perspective of FE type.

At the end of Chapter 6 a numerical tutorial example comprising an actuator fault is used to demonstrate the effectiveness of the proposed UI-PMIO approach.

In Chapter 7, a novel actuator fault and state estimation approach the UI–proportional multiple integral and derivative observer (UI-PMIDO) is proposed to enhance the FE performance which is inspired by both the RFAFE and UI-PMIO methods in Chapters 4 & 6, respectively. In the abbreviation of the 'UI-PMIDO' term, the 'D' represents the 'derivative' action in the observer structure which is inspired by the RFAFE method in Chapter 4. The UI-PMIDO proposed in this Chapter possesses comprehensive features of

both fast FE and multiple integral actions. Under this FE strategy, the FE signal involves the derivative action as well as multiple integral actions. Finally, a numerical example of a system with exogenous disturbance is used to demonstrate the effectiveness and efficiency of the novel FE methodology 'UI-PMIDO'. Comparisons between the UI-PMIO in Chapter 6 and UI-PMIDO in Chapter 7 are made using this tutorial by means of simulation results.

In Chapter 8, the main contribution is to extend the UI-PMIDO theory based on the LTI model developed in Chapter 7 to a polytopic linear parameter varying (LPV) system structure for the FE design. The LPV approach can be used to take into account an approximation to the nonlinear system via time-varying affine parameter dependence. At first, the fundamental theory of the model is introduced. Then, a polytopic robust UI-PMIDO FE method using an LPV modelling strategy is proposed for the purpose of estimating the bounded finite fault derivatives of the actuator faults as well as the states of a nonlinear system with the presence of the UI. The UI are considered here as exogenous disturbances. The polytopic UI-PMIDO stability conditions are formulated and solved via a set of linear matrix inequalities (LMIs). A tutorial example of a nonlinear two-link manipulator is used to illustrate the effectiveness of the proposed approach.

As stated above, a graphical description of the developed Chapters 3-8 is given as Figure. 1-9.

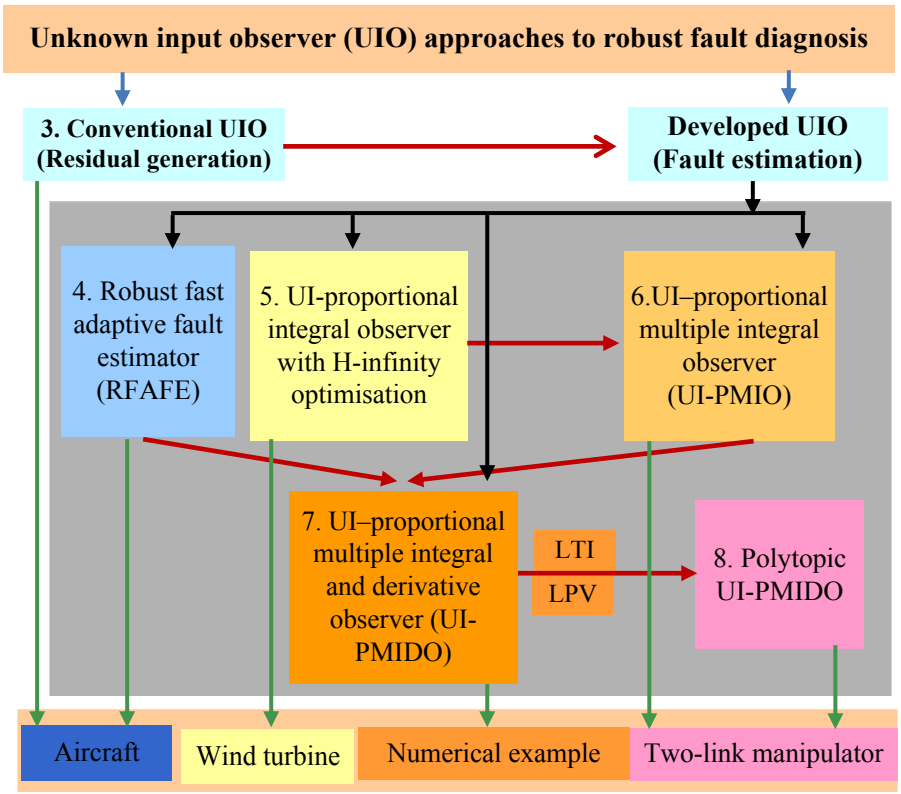

Figure 1-9 Graphical description of the developed Chapters 3-8

Note: The blue arrows point to the application Chapter 3 and the developed Chapters 4-8 based on residual-generation UIO design. The blacks and greens arrows point to the developed Chapters 4-8 and its corresponding applications, respectively. The red arrows represent the relationship between the Chapters, namely, the arrow directs to a further developed Chapter based on the arrow starting Chapter.

In Chapter 9, the original contributions from this research work are summarised and the context of the research of this thesis is outlined. Meanwhile, suggestions and recommendations for potential new work based on this thesis are discussed.

Chapter 2
Review of Model-based FDI/FDD

2.1 Introduction

This Chapter provides an overview of the development of model-based FDI/FDD, with a focus on observer-based approaches. The basic concepts, contexts and major issues that are associated with this subject are addressed in detail.

2.2 Model-based fault diagnosis methods

The model-based fault diagnosis techniques used in control can be traced back to the early 70's. Since then, the techniques have been developed with remarkable expansion and implemented in many industrial applications, thanks to the efficiency and good performance of many FDI/FDD designs. Successful applications can be seen in industrial sectors, for instance, space system (Patton, Uppal, Simani and Polle, 2010), automotive systems (Yacine, Ichalal, Oufroukh, Mammar and Djennoune, 2012), power systems (Ma and Jiang, 2011), process control systems (Venkatasubramanian, Rengaswamy, Yin and Kavuri, 2003), and so on. Some classical research outcomes have been assembled and published as textbooks such as: (Patton, Frank and Clark, 1989; Gertler, 1998; Mangoubi, 1998; Chen and Patton, 1999; Patton, Frank and Clark, 2000; Blanke, Kinnaert, Lunze and Staroswiecki, 2003; Venkatasubramanian, Rengaswamy, Yin and Kavuri, 2003; Blanke, Kinnaert, Lunze and Staroswiecki, 2006; Isermann, 2006; Ding, 2008; Isermann, 2011). Recent surveys on FDI/FDD are: (Frank, Ding and Köppen-Seliger, 2000; Simani, Fantuzzi and Patton, 2003; Venkatasubramanian, Rengaswamy, Yin and Kavuri, 2003; Isermann, 2005; Hwang, Kim, Kim and Seah, 2010; Ding, Zhang, Jeinsch, Ding, Engel and Gui, 2011; Marzat, Piet-Lahanier, Damongeot and Walter, 2012) and other references given throught the thesis.

The core idea of the model-based FDI/FDD approaches is to generate the fault indicator signals (residuals) or reconstruct fault signals on-line using FDI/FDD algorithms. To achieve on-line FDI/FDD, it is necessary to process the system input and output signals,

using mathematical models of the monitored system. Normally, a successful on-line implementation of the FDI/FDD algorithms requires powerful computer systems.

However, rapid development in computer technology have made the requirement is very achievable. The conventional way to achieve FD/FDI is to make use of residual signals based on models of the system being monitored. With the increasing demand from the developed AFTC described in Section 2.2.2, the fault diagnosis has been moving to the FDD subject which motivates the research on FE-based FDD to be more applicable and popular compared with residual generation-based FDI, especially in this decade. In the following Sections, both the residual generation-based FDI and the FE-based FDD are introduced, respectively.

2.2.1 Residual generation-based FDI design

Considerable research studies on model-based FDI have been developed in both academic studies and industrial applications during the last three decades. As outlined in Section 1.1 all these approaches are based on the principle of analytical redundancy in which the selected plant model operates in parallel with the real plant and is driven by the same inputs and outputs as the real plant. The discrepancies between the sensor measurements and the analytically computed values of the system variables are defined as residual signals (see Section 2.2.7 for details). As a result of generated residual, the faults can be detected and therefore isolated. Traditionally, the residual generation-based approaches have played the dominant role in FDI. Residual-based methods have the purpose of detecting faults promptly (with low FDT), with low FAR (see Section 1.5 for definitions), and with good potential for isolation of individual faults.

Many theoretical studies of FDI have been described in the academic literature (Patton, Frank and Clark, 1989; Gertler, 1998; Chen and Patton, 1999; Patton, Frank and Clark, 2000; Simani, Fantuzzi and Patton, 2003; Ding, 2008; Isermann, 2011). Several books describe interesting application studies (Patton, Frank and Clark, 1989; Simani, Fantuzzi and Patton, 2003; Isermann, 2011). Generally, residual generation-based FDI comprises two main stages ‘Residual Generation’ and ‘Decision making’, as illustrated in Figure 2-1.

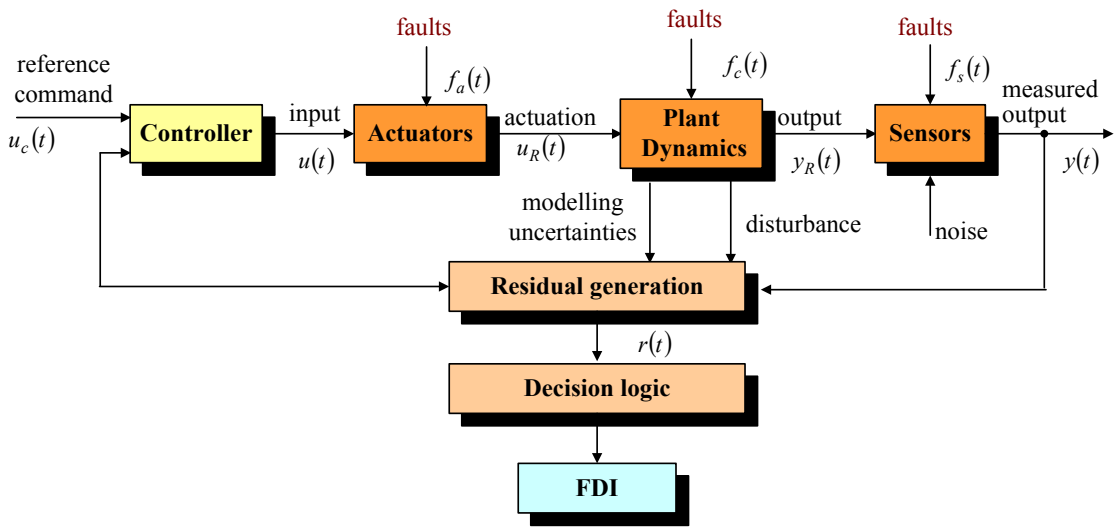

Figure 2-1 Model-based approaches to FDI method

Residual generation: This stage is used to generate a fault indicating signal via available input and output information from the monitored system (Chen and Patton, 1999). The required fault information is generated to decide promptly, reliably and robustly whether or not a fault has occurred and where it has occurred. In most robust FDI approaches, the residual signals are designed to be sensitive to specific fault (faults) whilst being insensitive to UI, i.e. the residuals are expected to be close to zero in fault-free conditions and deviate from zero after a fault has occurred but not deviate from zero when there is a modelling uncertainty or exogenous disturbance, represented by a UI.

Decision making: Using the generated residual, a decision is made to decide whether or not a fault has occurred through the use of a threshold function whose value can be fixed or variable. In this step, the choice of threshold is usually based on a hypothesis test to determine the statistical likelihood that a fault has occurred, whilst minimising the FAR and MAR rates. Using the threshold functions decisions are made as to the time of onset of a fault and it's likely time characteristic. The process of detecting the fault is referred to as FD, however once the fault is detected a suitable form of isolation logic based on analytical redundancy can be used to uniquely determine its location in the system.

2.2.2 FE-based FDD design

Most model-based FDI techniques have been developed mainly as fault monitoring systems to indicate the system working condition, as introduced in Section 2.2.1, with properties that depend on the method of generating the residuals.

In the literature, it is appreciated that FDI with fault occurrence and location information cannot satisfy the industrial requirements in terms of higher levels of safety, reliability and sustainability (Patton, 1997a). The more strict safety criteria require that suitable prompt action be taken when a monitored closed-loop system operates under abnormal conditions. In this context FTC and specifically AFTC is becoming demand-driven and aims to control the faulty systems to avoid failures and catastrophes. The need for FDI/FDD in FTC has been reviewed in Section 1.3.

Figure 2-2 illustrates the structure of FE-based FDD design, in which the FDD function often makes use of FE-based FDD design rather than residual-based FDI design.

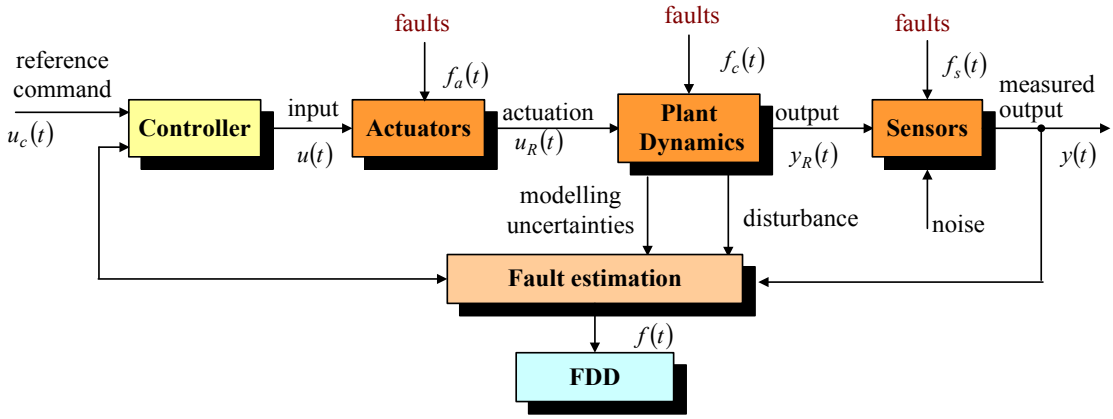

Figure 2-2 Model-based FDD method

2.2.3 Typical methodologies of model-based FDI/FDD design

Many fruitful research studies have been devoted to the subject of FDI/FDD in which a mathematical model is used to realise the FDI/FDD function in real-time. Of significance four model-based FDI/FDD design methodologies have been studied substantially based on (1) observer based methods; (2) parameter estimation; (3) parity space, introduced as follows:

- *Observer based FDI/FDD:* This technique has been developed under the framework of the well-studied advanced control theory. This is regarded as an effective method

for designing observers using efficient and reliable algorithms for data processing to reconstruct system variables. In this approach, the observer is used to estimate the actual system outputs. The residuals/FE signals are then constructed via suitable functions of the output estimation error between the measured and estimated outputs (Chen and Patton, 1999).

- *Parity equation based FDI:* A straightforward model-based method of FDI is to use an input-output model with fixed structure and run it in parallel with the process, thereby forming an output error. In this approach, the residual signals are generated based upon consistency checking (or parity checking) on system input and output data over a given time window. Actually, once the design objectives are determined, the parity equation and observer based designs have some correspondence or equivalence under certain conditions, as residual generation methods (Gertler, 1991; Patton and Chen, 1991).

- *Parameter estimation based FDI/FDD:* This approach is investigated in terms of system identification techniques. The faults are reflected in the physical system parameters and then the idea of the fault detection is based on the comparison between online estimation of system parameters and the parameters of the fault-free reference model. In most practical cases, the process parameters are only partially known or are not known at all. If the basic model structure of the process is known, the process parameters can be determined with parameter estimation methods by measuring input and output signals. Parameters can be identified by non-recursive or recursive methods or numerical optimisation methods. (Isermann, 1993).

2.2.4 Central issues in model-based FDI/FDD design

Three FDI/FDD model-based approaches have been introduced in Section 2.2.3 and the central issue of 'robustness issue' of FDI/FDD is introduced in Section 1.6. Some additional central issues in model-based FDI/FDD design are described in the literature for the purpose of assessing the developed approaches (Chen and Patton, 1999; Ding, 2008; Zhang and Jiang, 2008; Marzat, Piet-Lahanier, Damongeot and Walter, 2012):

- Ability to detect or estimate different types of faults (actuator, sensor, and component faults), i.e. ability of handling multiple faults.

- For ease of design tuning, normally require the least number of tuning parameters and with less complex tuning procedures. This is important for real application problems.

- Satisfaction of fault evaluation indices listed in Section 1.5. The indices should be different in terms of the requirements of the different monitored systems.

2.2.5 Mathematical description of model-based system

This Section outlines the basic LTI state space mathematical description of the monitored system used in FDI/FDD, followed by a brief description of most of the main issues to be solved (Chen and Patton, 1999).

- *Nominal LTI systems:*

A nominal LTI mathematical model of the monitored system is described by a state space model as:

$$\left.\begin{aligned}\dot{x}(t) &= Ax(t) + Bu(t)\\ y(t) &= Cx(t) + Du(t)\end{aligned}\right\} \tag{2-1}$$

where, $x \in \Re^n$ denotes the system state vector, $u \in \Re^r$ and $y \in \Re^m$ denote the input and measurement vectors, respectively. A, B, C, D are known system matrices with appropriate dimensions.

- *LTI systems with actuator faults*:

An LTI mathematical model of the monitored system with additive actuator faults is described by state space model as:

$$\left.\begin{aligned}\dot{x}(t) &= Ax(t) + Bu(t)+F_a f_a(t)\\ y(t) &= Cx(t) + Du(t)\end{aligned}\right\} \tag{2-2}$$

where, $x \in \Re^n$, $u \in \Re^r$ and $y \in \Re^m$ as well as A, B, C, D are defined as same as in (2-1). $f_a \in \Re^l$ represents a vector of time-varying actuator faults. The columns of the matrix $F_a \in \Re^{n\times l}$ denote the independent actuator fault distribution.

- *Systems with sensor faults*:

An LTI mathematical model of the monitored system with additive sensor faults is described by state space model as:

$$\left.\begin{aligned}\dot{x}(t) &= Ax(t) + Bu(t)\\ y(t) &= Cx(t)+Du(t) + F_s f_s(t)\end{aligned}\right\} \tag{2-3}$$

where, $x \in \Re^n$, $u \in \Re^r$ and $y \in \Re^m$ as well as A, B, C, D are defined as same as in (2-1). $f_s \in \Re^s$ represents a vector of time-varying sensor faults. The rows of the matrix $F_s \in \Re^{n\times s}$ denote the independent sensor fault distribution.

The faulty system (2-2) and (2-3) can be integrated into one expression for a system with both additive actuator and sensor faults. However, this does not mean that the actuator and sensor faults occur simultaneously. The integrated expression is given as:

$$\left.\begin{aligned}\dot{x}(t) &= Ax(t) + Bu(t)+F_a f(t)\\ y(t) &= Cx(t) + Du(t)+F_s f(t)\end{aligned}\right\} \tag{2-4}$$

An input–output transfer matrix representation for system (2-4) is described as:

$$y(s) = G_u(s)u(s) + G_f(s)f(s) \tag{2-5}$$

where,

$$\left.\begin{aligned}G_u(s) &= C(sI - A)^{-1}B + D\\ G_s(s) &= C(sI - A)^{-1}F_a + F_s\end{aligned}\right\} \tag{2-6}$$

- *LTI systems with multiplicative faults*:

As introduced in Chapter 1, the multiplicative fault (component faults) can be used to represent a parameter change. In this case, an LTI mathematical model of the monitored system with multiplicative faults is described by state space model as:

$$\left.\begin{aligned}\dot{x}(t) &= \left(A + \Delta A_f\right)x(t) + \left(B + \Delta B_f\right)u(t)\\ y(t) &= \left(C + \Delta C_f\right)x(t) + \left(D + \Delta D_f\right)u(t)\end{aligned}\right\} \tag{2-7}$$

where, $x \in \Re^n$, $u \in \Re^r$ and $y \in \Re^m$ as well as as A, B, C, D are defined as same as in (2-1), $\left(A + \Delta A_f\right)$, $\left(B + \Delta B_f\right)$, $\left(C + \Delta C_f\right)$, $\left(D + \Delta D_f\right)$ are the multiplicative faults repressed as:

$\Delta A_f = \sum_{i=1}^{N} A_i \alpha_{Ai}$, $\Delta B_f = \sum_{i=1}^{N} B_i \alpha_{Bi}$, $\Delta C_f = \sum_{i=1}^{N} C_i \alpha_{Ci}$, $\Delta D_f = \sum_{i=1}^{N} D_i \alpha_{Di}$.

A_i, B_i, C_i, D_i are known matrices with the same dimensions as A, B, C, D, respectively. α_{Ai}, α_{Bi}, α_{Ci}, α_{Di} are scalar factors. The fault is defined as a scalar

variable, either $\alpha_i \in \{\alpha_{Ai},\ \alpha_{Bi},\ \alpha_{Ci},\ \alpha_{Di}\}$

2.2.6 Fault detectability and isolability

This Section provides the necessary and sufficient conditions for the detectability and isolability of faults for cases of additive and multiplicative fault respectively, making use of the input-output transfer matrix representation for the system. The proofs of the following Theorems are omitted as these are provided in the references (Chen and Patton, 1999) and (Ding, 2008).

- Fault detectability condition

Theorem 2.1 Given system (2-4), then

- Additive fault f_i is detectable if and only if

$$G_{fi}(s) = C(sI - A)^{-1}F_{ai} + F_{si} \neq 0 \tag{2-8}$$

where, $F_{ai},\ F_{si}$ denotes the i_{th} column of matrix $F_a,\ F_s$, respectively.

- A multiplicative fault α_{Ai} is detectable if and only if:

$$G_{\alpha_{Ai}}(s) = C(sI - A)^{-1}A_i(sI - A)^{-1}B \neq 0 \tag{2-9}$$

- A multiplicative fault α_{Bi} defined in (2-7) is detectable if and only if:

$$G_{\alpha_{Bi}}(s) = C(sI - A)^{-1}B_i \neq 0 \tag{2-10}$$

- A multiplicative fault α_{Ci} defined in (2-7) is detectable if and only if:

$$G_{\alpha_{Ci}}(s) = C_i(sI - A)^{-1}B \neq 0 \tag{2-11}$$

- A multiplicative fault α_{Di} defined in (2-7) is detectable if and only if:

$$G_{\alpha_{Di}}(s) = D_i \neq 0 \tag{2-12}$$

Remark 2.1: (2-8) shows that an additive fault is detectable, if and only if the transfer function from the additive fault to the system outputs is not zero.

Remark 2.2: (2-9) shows that the multiplicative fault α_{Ai} can lead to a change in the system structure.

Remark 2.3: (2-10) & (2-11) shows that the detectability of the multiplicative faults α_{Bi} and α_{Ci} can be considered by equivalent input observability and output controllability problems, respectively in terms of the individual faults.

Remark 2.4: (2-9) shows that the multiplicative fault α_{Di} is always detectable.

Remark 2.5: The individual fault transfer matrices (2-8) to (2-12) can generally be expressed by $G_{F_i}(s)$, for which the fault vector is $F = [f_1 \quad f_2 \quad \cdots \quad f_i]^T$ $(i = 1, \cdots n_f)$ and the transfer between individual faults and selected residuals are considered individually (leading to a fault isolability property).

- Fault isolability condition

In Chapter 1, fault isolation is defined as 'to determine the location of the fault, e.g. sensor or actuator has become faulty' which lead to the fault isolability defined as 'whether the different faults occurring in a system can be distinguished in terms of their influences on the system. Theorem 2.2 is given as a test for fault isolability.

Theorem 2.2 Given system (2-4), with *remark 2.5*. Then any faults with fault transfer matrices $G_{F_1}(s), G_{F_2}(s), \cdots, G_{F_i}(s)$ are structurally isolable if and only if:

$$\begin{aligned} rank\big(G_F(s)\big) &= rank\,[G_{F_1}(s) \quad G_{F_2}(s) \quad \cdots \quad G_{F_i}(s)] \\ &= rank\left(G_{F_1}(s)\right) + rank\left(G_{F_2}(s)\right) + \cdots + G_{F_i}(s) \\ &= \sum_1^{n_f} rank\left(G_{F_i}(s)\right) \end{aligned} \tag{2-13}$$

As the thesis focusses mainly on additive faults, Corollary 2.1 corresponding to the isolability of additive faults is given here as a special case.

Corollary 2.1 Given system (2-4) and *Remark 2.5*. Let $F = [f_1 \quad f_2 \quad \cdots \quad f_i]^T$ $(i = 1, \cdots n_f)$. Then, these n_f faults are isolable if only if:

$$rank\big(G_F(s)\big) = n_f \tag{2-14}$$

where, $n_f \leq m$. m is defined in (2-1) as the number of the system outputs.

Remark 2.6: Corollary means that the isolability index number of the additive faults is not larger than the number of system outputs, so that (2-14) can be further interpreted as:

$$rank\big(G_F(s)\big) \leq \min\{m, n_f\} \tag{2-15}$$

A minimal state space realisation of $G_F(s)$ can be expressed as:

$$G_F(s) = C(sI - A)^{-1}F_a + F_s \tag{2-16}$$

In terms of (2-14) to (2-16), the state space description of (2-4) is given as Corollary 2.2.

Corollary 2.2 Given system (2-4) and *Remark 2.5*. Let $F = [f_1 \quad f_2 \quad \cdots \quad f_i]^T$ $(i = 1, \cdots n_f)$. Then, the n_f faults are isolable if and only if:

$$rank\begin{bmatrix} sI - A & F_a \\ C & F_s \end{bmatrix} = n + n_f \tag{2-17}$$

2.2.7 Representation of the FDI/FDD robustness issue

The importance of the robustness issue has been addressed in Section 1.6. In this Section, the specific mathematical representation of the robust issue is given, based on the LTI system described in Section 2.2.5. Hence, a simple representation of a fault-free state space system model of the monitored system with exogenous disturbance model parameter perturbations (corresponding to model uncertainty) can be described as:

$$\left.\begin{aligned} \dot{x}(t) &= (A + \Delta A)x(t) + (B + \Delta B)u(t) + E_1 d_e(t) \\ y(t) &= (C + \Delta C)x(t) + (D + \Delta D)u(t) + E_2 d_e(t) \end{aligned}\right\} \tag{2-18}$$

where, $x \in \Re^n$, $u \in \Re^r$ and $y \in \Re^m$ as well as A, B, C, D are defined as same as in (2-1). ΔA, ΔB, ΔC, ΔD are the parameter errors or variations which represent the modelling uncertainties, $d_e \in \Re^p$ is the exogenous disturbance. E_1 and E_2 are the distribution matrix of exogenous disturbance.

Remark 2.7: UI in (2-18) can refer to the modelling uncertainties, exogenous disturbance or the combination of modelling uncertainties and the exogenous disturbance. Particularly, in some FDI/FDD designs, the reformulation or the transformation should be taken to reconstruct the UI into two components: a UI distribution matrix and a UI

vector. Then, the effect of each UI should be de-coupled or minimised to satisfy a robustness requirement. The useful reformulation or transformation is provided in (Chen and Patton, 1999) and (Ding, 2008) to approximate the modelling uncertainties to construct the appropriate distribution matrix.

With accordance of (2-18), (2-19) is derived:

$$\Delta A \approx \sum_{i=1}^{N} a_i A_i,\ \Delta B \approx \sum_{i=1}^{N} b_i B_i,\ \Delta C \approx \sum_{i=1}^{N} c_i C_i,\ \Delta D \approx \sum_{i=1}^{N} d_i D_i \quad (2\text{-}19)$$

where, A_i, B_i, C_i, D_i have the same dimensions as known matrices A, B, C, D. a_i, b_i, c_i, d_i are scalar factors. Then, for the general case the modelling uncertainties can be reformulated in terms of two UI distribution matrices E_{u1} and E_{u2} as:

$$E_{u1}d_{u1}(t) = \Delta Ax(t) + \Delta Bu(t) = [A_1 \quad \cdots \quad A_N \quad B_1 \quad \cdots \quad B_N\ ] \begin{bmatrix} a_1x(t) \\ \cdots \\ a_Nx(t) \\ b_1x(t) \\ \cdots \\ b_Nx(t) \end{bmatrix} \quad (2\text{-}20)$$

$$E_{u2}d_{u2}(t) = \Delta Cx(t) + \Delta Du(t) = [C_1 \quad \cdots \quad C_N \quad D_1 \quad \cdots \quad D_N\ ] \begin{bmatrix} c_1x(t) \\ \cdots \\ c_Nx(t) \\ d_1x(t) \\ \cdots \\ d_Nx(t) \end{bmatrix} \quad (2\text{-}21)$$

Then further to (Chen and Patton, 1999), let $d_u(t) = [d_{u1}(t) \quad d_{u2}(t)]^T$, $E_{u1}^* = [\,E_{u1} \quad 0]$, $E_{u2}^* = [\,0 \quad E_{u2}]$. Then, (2-18) can be reformulated as:

$$\left.\begin{aligned} \dot{x}(t) &= Ax(t) + Bu(t) + E_{u1}^* d_u(t) + E_1 d_e(t) \\ y(t) &= Cx(t) + Du(t) + E_{u2}^* d_u(t) + E_2 d_e(t) \end{aligned}\right\} \quad (2\text{-}22)$$

Let UI represents the combination of the modelling uncertainties $d_u(t)$ and the exogenous disturbance $d_e(t)$ into the vector $d(t) = [d_u(t) \quad d_e(t)]^T$, with corresponding distribution matrix organised as $E_1^* = [\,E_{u1}^* \quad E_1]$ and $E_2^* = [\,E_{u2}^* \quad E_2]$. Then, (2-22) can be reformed as:

$$\left.\begin{aligned} \dot{x}(t) &= Ax(t) + Bu(t) + E_1^* d(t) \\ y(t) &= Cx(t) + Du(t) + E_2^* d(t) \end{aligned}\right\} \quad (2\text{-}23)$$

Assume that the additive faults occur in the system (2-23). Then, (2-23) can be

re-written in terms of (2-4) as:

$$\left.\begin{aligned}\dot{x}(t) &= Ax(t) + Bu(t) + E_1^* d(t) + F_a f(t)\\ y(t) &= Cx(t) + Du(t) + E_2^* d(t) + F_s f(t)\end{aligned}\right\} \tag{2-24}$$

The transfer matrix representation for the system (2-24) is given as:

$$G(s) = G_{yu}(s) + G_{yd}(s) + G_{yf}(s) \tag{2-25}$$

where,

$$G_{yu}(s) = C(sI - A)^{-1}B + D \tag{2-26}$$

$$G_{yd}(s) = E_2^* + C(sI - A)^{-1}E_1^* \tag{2-27}$$

$$G_{yf}(s) = F_s + C(sI - A)^{-1}F_a \tag{2-28}$$

As stated by (Chen and Patton, 1999), the FDI/FDD task is to design a filter $Q_r(s)$ such that the residual r, in terms of the system of (2-24) & (2-25), is defined by:

$$r(s) = Q_r(s)G_{yf}(s)f(s) + Q_r(s)G_{yu}(s)u(s) + Q_r(s)G_{yd}(s)d(s) \tag{2-29}$$

Then further to (Chen and Patton, 1999), alternatively, a filter $Q_f(s)$ can be designed in terms of a FE signal $\tilde{f}$, with the system of (2-24) & (2-25) defined by:

$$\tilde{f}(s) = Q_f(s)G_{yf}(s)f(s) + Q_f(s)G_{yu}(s)u(s) + Q_f(s)G_{yd}(s)d(s) \tag{2-30}$$

(2-29) & (2-30) indicate that robustness issue arises from the presence of the terms $Q_r(s)G_{yd}(s)d(s)$ and $Q_f(s)G_{yd}(s)d(s)$, respectively which can contaminate the performances of r or $\tilde{f}$ generating FA conditions in the residual case (2-29) and inaccurate estimates in the FE case (2-30). From this, it can be stated that robust FDI/FDD designs should satisfy either:

$$Q_r(s)G_{yd}(s)d(s) = 0 \tag{2-31}$$

or

$$Q_f(s)G_{yd}(s)d(s) = 0 \tag{2-32}$$

respectively.

In summary this Section provides a mathematical expression of the 'the robustness issue' in the context of the realisation of UI in FDI/FDD design. Following this an approach to perfectly de-couple or at least attenuate the UI effects from residual/FE signals is outlined as a critical problem or challenge in model-based FDI/FDD designs (Chen and Patton, 1999; Ding, 2008).

Note: For simplicity, the time subscript (t) is omitted in the remainder of the thesis.

2.2.8 Review of observer-based FDI/FDD design

The theoretical foundation of the UI de-coupling principle in this thesis comes from the UIO FDI scheme which is one kind of well-known observer-based FDI/FDD design. Hence, the aim of this Section is to review the classical observer-based approach to FDI/FDD. Its corresponding mathematical representation in the fault-free and fault cases as well as for the case of the system disturbed by UI are described respectively in the following.

Observer designs introduced in Section 2.2.3 have received increasing attention in the literature due to the availability of powerful control theory tools. The principle underling observer design is used to estimates of the actual system output (Frank, 1987). The output estimation error is obtained by comparing the estimated system outputs and their measured or expected values. Consequently, the residuals or FE signals are designed as a function of the output estimation error.

As a historical milestone in observer-based FDI/FDD, the first observer-based approach applied to the FDI problem (Clark, Fosth and Walton, 1975). Actually these authors refer to the "instrument fault detection (IFD) problem" as a special case of a sensor fault FDI problem. In their design Luenberger observer was constructed for FD since the Luenberger observers proposed by (Luenberger, 1966) allow the reconstruction of the state variables under deterministic hypotheses. Following this, (Frank, 1987) established a strong foundation for observer-based FDI. Since then, the observer approaches-based FDI/FDD are classical and have developed into a wide spread approach to the FDI/FDD design methodology.

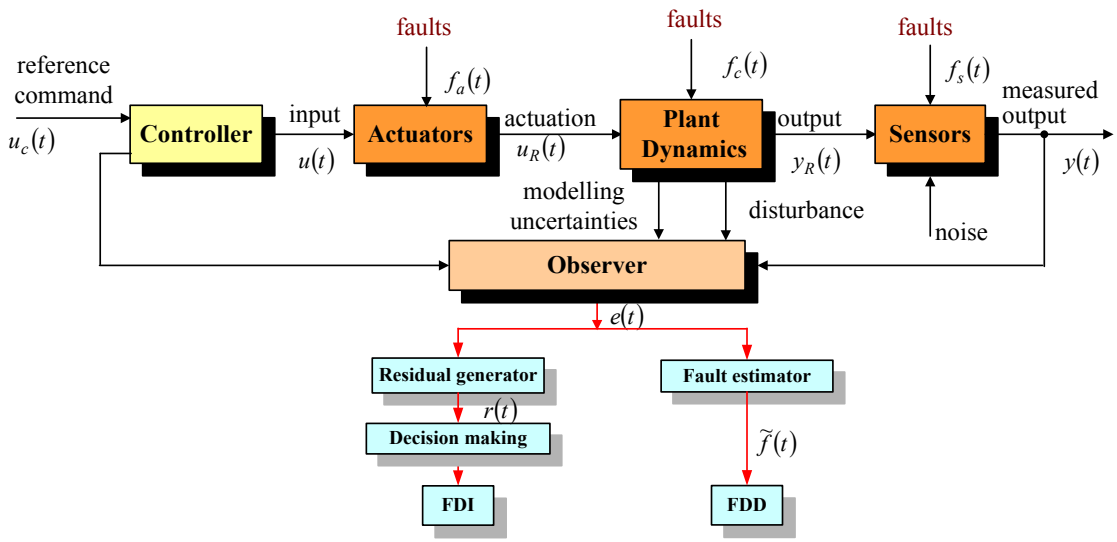

Figure 2-3 Observer-based FDD scheme

Particularly, at early stages in the development of the FDI field, some approaches in the literature are used to generate residuals that handle the central 'robustness problem' outlined in Section 2.2.7. One approach makes use of the UIO for de-coupling the UI from the residuals (Chen, Patton and Zhang, 1996; Xiong and Saif, 1998). The sliding mode observer (SMO) is inspired by the sliding model control theory due to the duality to generate residuals that are insensitive to the matched UI (Sreedhar, Fernandez and Masada, 1993; Yang and Saif, 1995). The H_-/H_∞ approach of (Hou and Patton, 1996) which was further developed by (Ding, Jeinsch, Frank and Ding, 2000), was introduced not only for deriving robust residuals following appropriate H_∞ minimisation of their UI influence but also possessing the capability of increasing the sensitivity of a fault to the residual using the H_- index. Noticeably, all these observer-based FDI methods endeavour to remove or attenuate the UI effect from the residuals in order to guarantee a satisfactory FDI performance.

Following that, substantial observer-based FE approaches were published with increasing demands from investigators working on AFTC methods. Accordingly, all the residual-based methods have been re-developed for the purpose of robust FE. The corresponding literature can be found in (Koenig and Mammar, 2001; Theilliol, Noura and Ponsart, 2002) for UIO, for SMO (Tan and Edwards, 2002; Alwi, Edwards and Tan, 2009), and considering norm-based approaches (Stoustrup and Niemann, 2002; Chen, Patton and Goupil, 2012).

Besides these, many other approaches for FE are reported using different observer-based frameworks. For example, (Shafai, Pi and Nork, 2002) used a PIO to estimate each fault by regulating the fault as an augmented state. (Jiang, Wang and Song, 2000), (Gao and Ho, 2004) and (Koenig, 2005) improved the PIO to a proportional multiple integral observer (PMIO) which augmented the multiple integrators into an observer structure as additional states for accounting for the finite time fault derivatives. The PMIO structure enables the observer to estimate more complex time-varying fault signals and is therefore not limited to constant or slow-time varying faults as in the PIO case. Adaptive observers were also used for FE in which the observer dynamics are updated by the fault information (Wang and Daley, 1996; Wang and Lum, 2007; Zhang, Jiang and Cocquempot, 2008; Zhao, Xie, Hong and Zhang, 2011).

As for the residual generation-based FDI, 'robustness' issues are also a challenging aspect in the FE design problems. The availability of accurate or robust FE signals are important both for FDD and also as an import function for modular AFTC design, e.g. using a two-step design approach involving (a) robust FE design and (b) AFTC design. As pointed out in Section 2.2.5, FE performance is easily corrupted by the presence of UI. To seek to overcome this problem, (Tan and Edwards, 2002) consider uncertainty dynamics. (Gao and Ho, 2004) also consider the robustness problem of FE by including sensor noise. However, many papers on FE hardly touch the FE robustness issue in 2.2.7, for instance in (Zhang, Jiang and Cocquempot, 2008) and (Zhang, Jiang and Shi, 2009).

As introduced in Chapter 1, the fault signal is a function of the error between the measured and estimated outputs and corrupted by existing measurement noise cannot be avoided. Some literature studies show that the FE signals require information about the derivatives of the measurements (Shafai, Pi and Nork, 2002). These derivatives can amplify the noise influence on the FE signal. It is, therefore, preferable that the robust FE designs should consider sensor noise related issues seriously.

This Section provides a fundamental review of observer-based FDI/FDD schemes focussed on robustness issues for both residual-based and FE-based methods. In Section 2.3, the UIO based FDI/FDD will be reviewed in detail since the study of the thesis is established using an UIO approach.

2.3 UIO for FDI/FDD design

In this sub-section, a brief review and outline of the preliminaries of the UIO theory is given to establish the core idea in the thesis by means of the UI de-coupling principle for solving the robustness issue in FDI/FDD design. This thesis is based on the principle of the UIO design approach described in (Chen, Patton and Zhang, 1996; Chen and Patton, 1999).

2.3.1 Overview of UIO approaches

As mentioned in Section 1.6, robust residual generation is the most important task in model-based FDI. Modelling uncertainties/exogenous disturbance acting on the dynamical system as UIO considered as extra input signals which can degrade the FDI/FDD performance. An approach to achieve the appropriate insensitivity to UI is to attempt to structure the UI and subsequently de-couple the structured UI using algebraic or geometric methods. The state estimation problem of de-coupling the UI is referred to as the UIO which was introduced by (Kudva, Viswanadham and Ramakrishna, 1980). Apparently, the objective of UIO-based FDI/FDD is to develop a robust FDI/FDD which is insensitive to modelling uncertainties without the use of a very accurate model, whilst sensitive to faults which implies that the UI signals must be de-coupled (Chen, Patton and Zhang, 1996). In the original form the UIO based FDD formulation is that the system output is compared with the output of an observer designed from a model of the monitored system and the error is applied to construct a residual or a set of residuals. This classical UIO structure does not make use of system state variable reconstruction. An linear transformation is normally applied to build new state variables by which the derived residuals are independent of the UI and of the state variables by a special selection of the design matrices. In this way, in the ideal case, the residuals only depend on the fault information (apart from the effect of initial conditions on the state estimation error).

Many types of full order and reduced order UIO designs are now available. Full order observers have been designed in (Yang and Wilde, 1988) and (Darouach, Zasadzinski and Xu, 1994). Reduced order UIO designs can be found in (Kudva, Viswanadham and Ramakrishna, 1980; Guan and Saif, 1991; Hou and Müller, 1992; Duan and Patton, 2001), to name only a few. Necessary and sufficient conditions for the existence of a UIO have been established in (Kudva, Viswanadham and Ramakrishna, 1980; Guan and

Saif, 1991; Hou and Müller, 1992; Darouach, Zasadzinski and Xu, 1994; Chen, Patton and Zhang, 1996; Chen and Patton, 1999; Koenig and Mammar, 2001).

Several systematic procedures for designing reduced-order UIO were proposed by partitioning the state vector into two parts through an linear transformation. One part is directly driven by the UI and has to be measured completely, and the other part is estimated by the reduced-order UIO, which is de-coupled from the input (Corless and Tu, 1998). It is noticed that conditions of the UI de-coupling for a full-order UIO are not very different from those of the reduced counterpart (Chen and Patton, 1999). The reduced-order observer may suffer a bad convergence rate which can degrade the FDI/FDD performance. The reduced-order UIO sacrifices some design freedom and may have decreased computational complexity but weakens the performance of the UIO dynamic response (Yang and Wilde, 1988; Chen and Patton, 1999). For the full-order UIO, it is interesting to see that it may provide extra freedom to generate a directional residual for the purpose of fault isolation (Chen, Patton and Zhang, 1995). On the other hand, for the purpose of only FDI/FDD, the reduced-order observer may be sufficient for providing the output estimation error. However, if the purpose is to apply the UIO problem to an AFTC scheme, the full-order observer is required to estimate the system states. In summary, whether or not a full or reduced order observer is selected depends on the purpose of the FDI/FDD problem to be solved.

The extension work based on the classical UIO methods (full order or reduced order cases) can be found in many literature. One interesting approach is to extend the system to a descriptor system form such as studied in (Pasand and Taghirad, 2010) and (Ting, Chang and Chen, 2011). The other extension of UIO design is the nonlinear UIO formulation. Nonlinear dynamic system behaviours governed by complex physical laws that are becoming more complex with the development of modern physical systems. In this context, single linear system models cannot be easily used for modelling the dynamic behaviour of such systems since the linear model is only valid within a neighbourhood of the operating point. However, the nonlinear system can be expressed as an Lipschitz system model, or a T-S fuzzy model or alternatively in LPV model format. Some of the studies are given as follows: for Lipschitz system model-based UIO: (Rajamani and Ganguli, 2004; Chen and Saif, 2006a; Chen and Saif, 2006b; Xian, Chun, Yu and Na, 2011); for fuzzy model based UIO: (Orjuela, Marx, Ragot and Maquin,

2009; Chen and Saif, 2010; Chadli and Karimi, 2012; Yacine, Ichalal, Oufroukh, Mammar and Djennoune, 2012); for LPV model-based UIO: (Bara, Daafouz, Kratz and Ragot, 2001; Rodrigues, Theilliol and Sauter, 2005a; Hamdi, Rodrigues, Mechmeche, Theilliol and BenHadjBraiek, 2009; Hamdi, Rodrigues, Mechmeche and BenHadjBraiek, 2012).

As discussed in Chapter 2, the original UIO design in FDI is the residual generation approach with the purpose of FD or FDI, not the FDD. Therefore, most of the aforementioned UIO designs for FD aim to play the role as fault indicator in the monitoring system via generating the residual to set the fault alarm. However, the residual cannot provide enough fault information for the demands from the state of art FDD/AFTC technology which is capable of tolerating potential faults in the monitored system in order to improve the reliability and availability while providing a desirable performance. In this context, many works has been published focusing on FDD (Marx, Koenig and Georges, 2003; Marx, Koenig and Ragot, 2007; Zhu and Cen, 2010, Xian, Chun, Yu and Na, 2011). Only a few papers are cited here, some further literature is included in Chapter 4, 5, 6, 7 & 8 in which the FE methods are developed based on the linear or nonlinear UIO design, aiming to deliver accurate and robust fault information.

The UIO development is reviewed in this Section to offer the motivation and vision of using the UI de-coupling principle. In the following Sections, the preliminaries of LTI-UIO theory are introduced. For simplicity and to demonstrate the core UI de-coupling principle for FD, an LTI design with only UI influence is considered first.

2.3.2 Preliminaries of UIO theory in fault-free case

An LTI system considering the UI (all actuators and sensors are assumed to be fault-free), represented by the term $E_u d_u$ is described as:

$$\left.\begin{aligned} \dot{x} &= Ax + Bu + E_u d_u \\ y &= Cx \end{aligned}\right\} \tag{2-33}$$

where, $x \in \Re^n$ denotes the system state vector, $u \in \Re^r$ and $y \in \Re^m$ denote the input and measurement vectors, respectively and $d_u \in \Re^p$ is a vector of UI. A, B, C are known system matrices with appropriate dimensions. The matrix $E_u \in \Re^{n\times p}$ is the UI distribution matrix.

Following (Chen and Patton, 1999), a functional observer is constructed as:

$$\left.\begin{aligned}\dot{z} &= Nz + TBu + Ky \\ \hat{x} &= z + Hy\end{aligned}\right\} \tag{2-34}$$

where, $\hat{x} \in \Re^n$ is the estimated state vector and $z \in \Re^n$ is the observer state vector. N, T, K and H are design matrices.

Definition 2.1: Observer (2-34) is defined as a robust UIO for the system (2-33), if its state and FE errors $e_x = x - \hat{x}$ approach zero asymptotically, in the presence of the system UI.

Assuming that E_u is known, the estimation error dynamics are governed by:

$$\begin{aligned}\dot{e}_x = {} & (A - HCA - K_1C)e_x \\ & + [N - (A - HCA - K_1C)]z \\ & + [K_2 - (A - HCA - K_1C)H]y \\ & + [T - (I - HC)]Bu \\ & + (HC - I)E_u d_u\end{aligned} \tag{2-35}$$

where,

$$K = K_1 + K_2 \tag{2-36}$$

If the following relations are satisfied:

$$(HC - I)E_u = 0 \tag{2-37}$$

$$T = I - HC \tag{2-38}$$

$$N = A - HCA - K_1C = A_1 - K_1C \tag{2-39}$$

$$K_2 = NH \tag{2-40}$$

The state estimation error is then refined as:

$$\dot{e}_x = Ne_x \tag{2-41}$$

$$e_y = Ce_x \tag{2-42}$$

$$r = y - C\hat{x} = Ce_x = e_y \tag{2-43}$$

Furthermore, if all eigenvalues of N are stable, r will approach zero asymptotically, i.e. $\hat{x} \to x$. The observer (2-34) is an UIO for the system (2-33) when conditions (2-36) to (2-40) are satisfied. Therefore, this UIO design involves the solution of (2-36) to (2-40) whilst placing all the eigenvalues of the system matrix N to be stable. Meanwhile, N, T, K and H are designed to achieve the required state estimation performance.

A particular solution to (2-37) can be calculated as follows:

$$H = E_u(CE_u)^+ \tag{2-44}$$

where, $(CE_u)^+ = [(CE_u)^T(CE_u)]^{-1}(CE_u)^T$ denotes the Moore-Penrose pseudo-inverse.

Theorem 2.3. The necessary and sufficient conditions for the existence of UIO (2-34) of system (2-33) are (Chen and Patton, 1999):

(1) $rank(CE_u) = rank(E_u)$

(2) $rank(C, A_1)$ is a detectable pair

Remark 2.8: with full measurement ($C = I$), Condition (1) in Theorem 2.3 is clearly satisfied. Condition (1) denotes that the maximum number of independent UI cannot be larger than the maximum number of independent measurements, i.e. the necessary condition for UI de-coupling in the state estimation error dynamics is $rank(E_u) \leq m$. If this condition is not satisfied, a rank approximation via a matrix E_u^* can be derived using Singular Value Decomposition (SVD) (Golub and Van Loan, 1996). The details in (Chen and Patton, 1999) are addressed in Section 2.3.5.

Remark 2.9: Condition (2) is equivalent to constrain the invariant zeros of the system described by (A_1, E_u, C) to be on the open left hand complex plane, i.e. $rank\begin{bmatrix} sI_n - A_1 & E_u \\ C & 0 \end{bmatrix} = n + p$. The proof is omitted in this study. (Chen and Patton, 1999) states the Condition (2).

Remark 2.10: Theorem 2.3 gives the necessary and sufficient conditions of UIO design. As introduced in Chapter 1, the incentive of the studies in this thesis is to investigate the FE-based FDD via improving the conventional residual generation-based UIO FDI

method. Under the circumstances, the proposed FE methods fully take advantage of the UIO design, namely, equipped with the robustness against the UI. Therefore, in the following Chapters, the conditions in Theorem 2.3 of the UI de-coupling principle will be restated within the context of FE design.

2.3.3 UIO-based robust FD scheme

Rewriting the system (2-33) by considering actuator faults and sensors as well as UI, then (2-45) is obtained as:

$$\left.\begin{aligned} \dot{x} &= Ax + Bu + E_u d_u + F_a f_a \\ y &= Cx + F_s f_s \end{aligned}\right\} \tag{2-45}$$

where, $x \in \Re^n$ denotes the system state vector, $u \in \Re^r$ and $y \in \Re^m$ denote the input and measurement vectors, respectively and $d_u \in \Re^p$ is a vector of UI. $f_a \in \Re^l$ represents a vector of time-varying actuator faults, $f_s \in \Re^s$ represents a vector of time-varying sensor faults. A, B, C are known system matrices with appropriate dimensions. The matrix $E_u \in \Re^{n\times p}$ represents the UI distribution matrix. The columns of the matrix $F_a \in \Re^{n\times l}$ denote the independent actuator fault directions. The rows of the matrix $F_s \in \Re^{n\times s}$ denote the independent sensor fault directions.

If the given LTI system (2-45) satisfies Theorem 2.3, construct the UIO using the functional observer structure as (2-34). Then, the state estimation error dynamics and the residual of system (2-45) are obtained as (2-46) and (2-47) respectively via solving (2-36) to (2-40).

$$\dot{e}_x = Ne_x + TF_a f_a - K_1 F_s f_s - HF_s \dot{f}_s \tag{2-46}$$

$$r = y - C\hat{x} = Ce_x + F_s f_s \tag{2-47}$$

(2-46) and (2-47) contribute the integrated formulation for both actuator and sensor faults. The separated estimation error and residual systems are given as follows:

- *Only actuator faults (sensor fault-free):*

$$\dot{e}_x = Ne_x + TF_a f_a \tag{2-48}$$

$$r = y - C\hat{x} = Ce_x \tag{2-49}$$

Remark 2.11: Condition (2) in Theorem 2.3, discussed in *Remark 2.9*, should be refined

as that invariant zeros of the system described by (A_1, M_1, C) are on the open left hand complex plane, i.e. $rank\begin{bmatrix} sI_n - A_1 & M_1 \\ C & 0 \end{bmatrix} = n + p + l$, where, $M_1 = [E_u \quad F_a]$ (Saif and Guan, 1993; Edwards, 2004).

- *Only sensor faults (actuator fault-free):*

$$\dot{e}_x = Ne_x - K_1F_sf_s - HF_s\dot{f}_s \tag{2-50}$$

$$r = y - C\hat{x} = Ce_x + F_sf_s \tag{2-51}$$

Remark 2.12: The same perspective is given as in *remark 2.11*. Condition (2) in Theorem 2.3 discussed in *Remark 2.9* should be refined as requiring that invariant zeros of the system described by (A_1, M_2, C) are on the open left hand complex plane, i.e. $rank\begin{bmatrix} sI_n - A_1 & M_2 \\ C & 0 \end{bmatrix} = n + p + s$, where, $M_2 = [E_u \quad F_s]$ (Saif and Guan, 1993; Edwards, 2004).

2.3.4 Residual evaluation based on UIO

In the light of the residual generation, fault alarm is reported by testing the residuals r by the residual evaluation step named as residual evaluation. The residual evaluation scheme that automatically interprets the time-behaviour of a residual into a Boolean decision function, indicates whether each signal is to be considered as small or not. Generally, this decision logic procedure involves the selection of threshold(s). Then, residual evaluation is necessary to transform the collection of decision-making functions into the actual FDI scheme that is used.

A residual evaluator is constructed by a fixed/variable threshold function as additional information, and then the fault is detected (decision-making step) by a logic depending on the threshold. In this Section, the norm-based statistical thresholds are built as follows:

$$\|r\| < Threshold \qquad \text{fault-free case} \tag{2-52}$$

$$\|r\| \geq Threshold \qquad \text{fault case} \tag{2-53}$$

where, $Threshold$ is a statistical detection threshold which is used to service for the decision making logic so that raise an alarm when fault occurred. The threshold can also

be considered as a tuning parameter in the UIO FDI design to achieve desired FDI performance criteria introduced in Section 1.5, for instance, FDT, FDR, MAR. Normally, an adequate tuning procedure should result in a satisfactory compromise amongst the contradictory objectives of minimising the FDT, and MAR. Therefore, the ease and computational load of the tuning procedure should also be considered in the different FDI designs.

2.3.5 UI distribution matrix estimation

An augmented state observer may be utilized to estimate the UI distribution matrix. Let E_u represent the UI distribution matrix and assume that $d_1 = E_u d$ is a slowly time-varying vector. The system model (2-33) can be formulated in augmented form as (Patton and Chen, 1993) and (Chen and Patton, 1999):

$$\begin{bmatrix} \dot{x} \\ \dot{d}_1 \end{bmatrix} = \begin{bmatrix} A & I \\ 0 & 0 \end{bmatrix} \begin{bmatrix} x \\ d_1 \end{bmatrix} + \begin{bmatrix} B \\ 0 \end{bmatrix} u$$

$$y = [C_a \quad 0] \begin{bmatrix} x \\ d_1 \end{bmatrix} \tag{2-54}$$

If the system inputs and outputs $\{u, y\}$ are available, an observer based on the model of (2-54) can be used to estimate d_1 directly. The distribution matrix E_u is calculated as the ratio of the elements of estimation of d_1 ($\hat{d}_1$). The necessary condition for observability is given in Theorem 2.4:

Theorem 2.4 The system (2-54) is observable if and only if the following conditions are satisfied (Chen and Patton, 1999):

(1) $rank(C) = n$

(2) $rank(C, A)$ is an observable pair

Remark 2.13: Theoretically, the condition (1) in Theorem 2.4 could limit the application of this estimation approach. For a practical application, the states are normally available from measurements, e.g. as for the model aircraft studied in Chapters 3 & 4, so that the above observability and rank conditions are not difficult to satisfy.

Remark 2.14: For the UIO design, the necessary rank condition $rank(E_u) \leq m$ has been given in Theorem 2.3. If this condition is not satisfied, a sub-optimal matrix E_u^* can be approximated as follows via an SVD expansion of E_u (Chen and Patton, 1999).

$$E_u = S\Sigma T^T \tag{2-55}$$

where,

$$\Sigma = \begin{bmatrix} diag\{\sigma_{1,\cdots,}\sigma_k\} & 0 \\ 0 & 0 \end{bmatrix} \tag{2-56}$$

S and T are orthogonal matrices, k is the rank, and $\sigma_{1,\cdots,}\sigma_k$ are the singular values of E_u, respectively. A low rank approximation for E_u by minimising $\|E_u - E_u^*\|_F^2$ is given by:

$$E_u^* = S\hat{\Sigma}T^T \tag{2-57}$$

where,

$$\hat{\Sigma} = \begin{bmatrix} diag\{0,\cdots,0,\sigma_{k-q,\cdots,}\sigma_k\} & 0 \\ 0 & 0 \end{bmatrix} \tag{2-58}$$

$q = rank(E_u^*) \leq m$ to satisfy Theorem 2.3 (for E_u^* instead of E_u).

Assume the $d_1(t)$ is estimated as $\hat{d}_1 = \{\hat{d}_1(1), \hat{d}_1(2), \cdots, \hat{d}_1(n)\}$. In some fairly simple systems, $\hat{d}_1, \hat{d}_2, \cdots, \hat{d}_n$ varies slightly, then the distribution matrix E_u can be considered as a constant vector and calculated approximately by using average algorithms, i.e.

$$E_u = \frac{1}{n}\sum_{k=1}^{n} \hat{d}_1(k) \tag{2-59}$$

This simple process for obtaining E_u is illustrated by a simple nonlinear tutorial example in Section 2.3.6.

2.3.6 Tutorial example

It is necessary to clarify how the UIO works to generate robust residuals with the capability of rejecting the UI influence. A simple nonlinear tutorial system example is used here to demonstrate the robust UIO design procedure as well as the computation of the UI distribution matrix. Although this example does not consider the fault isolation

issue, it strongly focuses on the robustness issue accompanying the FD in the presence of modelling uncertainty.

In this nonlinear tutorial example, a sensor fault is included to illustrate the following two main UIO design procedures.

(i) Estimate the optimum value of the 'distribution matrix/vector E_u' according to Section 2.3.5.

(ii) Construct the UIO structure depending on the E_u computed in (i). This step introduces the realisation of UIO-based residual generator. Accordingly, UI de-coupling principle is demonstrated clearly.

Consider a simple nonlinear system (Leigh, 1983) in terms of the state variables x_1, x_2 and outputs y_1, y_2, a single sensor fault f_s as follows:

$$\left.\begin{aligned} \dot{x}_1 &= -4x_1 + x_2 + 4x_1^2 \\ \dot{x}_2 &= x_1 - 4x_2 - x_1^2 \\ y_1 &= x_1 + f_s \\ y_2 &= x_2 \end{aligned}\right\} \tag{2-60}$$

The system is conditionally stable and requires no control input. A time-varying sensor fault f_s is considered as an abrupt fault corresponding to different severity levels (different magnitudes). A stable UIO is used to generate the robust residual that can be used to detect the presence of each fault in the residual signals. The UI in this example arises from the effect of the non-linearity via the linearisation process, namely, the difference between the time responses of the nonlinear and linearised systems.

This system has two equilbria (0, 0) and (1, 0) of which (0, 0) is the stable mode and (1, 0) is the unstable mode. It can be assumed for simplicity that the state motions are bounded close to the stable node solution, i.e. the system (2-60) is stable within a region of the stable node. Hence, the linearisation around the stable node equilibrium (0, 0) gives rise to the following state space model:

$$\begin{bmatrix} \dot{x}_1 \\ \dot{x}_2 \end{bmatrix} = \begin{bmatrix} -4 & 1 \\ 1 & -4 \end{bmatrix} \begin{bmatrix} x_1 \\ x_2 \end{bmatrix} \tag{2-61}$$

Let $A = \begin{bmatrix} -4 & 1 \\ 1 & -4 \end{bmatrix}$ which has eigenvalues $\lambda_1 = -5$ and $\lambda_1 = -3$.

Two steps of robust UIO designs are given as follows.

Step1: Estimate the distribution matrix E_u.

The stable linear model is used to construct the augmented state observer corresponding to the nonlinear model of (2-60) for the fault-free case, i.e. with $f_s = 0$. It is assumed that the system is driven by two Schroeder phase noise excitation signals $u = [u_1 \quad u_2]'$ in Figure 2-4 (Godfrey, 1993). The signal $d_1 = E_u d_u$ is determined via the augmented observer approach (described in Section 2.3.5) and the estimates of the elements of d_1 are generated from the additional states of the augmented system as:

$$\begin{bmatrix} \dot{x} \\ \dot{d}_1 \end{bmatrix} = \begin{bmatrix} A & I \\ 0 & 0 \end{bmatrix} \begin{bmatrix} x \\ d_1 \end{bmatrix} + \begin{bmatrix} B \\ 0 \end{bmatrix} u$$

$$y = [C \quad 0] \begin{bmatrix} x \\ d_1 \end{bmatrix} \tag{2-62}$$

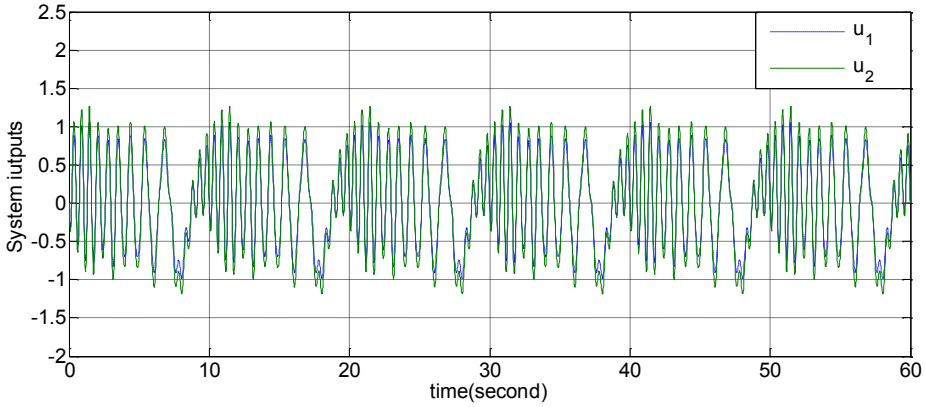

Figure 2-4 Generated Schroeder-phased signals

The observability conditions given in Theorem 2.4 are satisfied for this system and thus the elements of d_1 can be estimated progressively. Figure 2-5 illustrates the time behaviour of the elements of d_1 subject to the input stimuli. It can be seen that d_1 varies periodically in every 10s approximately. Therefore, 80 samples of d_1 in Table 2-1 which cover a 10s time interval are selected to represent the characteristic of d_1, i.e. are used to calculate the optimum $E_u{}^*$. The relative magnitudes of the two elements of this vector reveal an interesting phenomenon in the direction (distribution) of the term d_1. It can be observed that an approximately constant ratio of the components of d_1 is maintained and this is further illustrated by Table 2-1 which shows a sample of these values including the calculated ratios and the average values of the ratio. The response

shows a clear sign difference between d_1^* and d_2^*. It should be noted that that this system contains simple nonlinear functions of x_1 (but not of x_2), i.e. $g_1(x_1^2) = 4x_1^2$ and $g_2(x_1^2) = -x_1^2$.

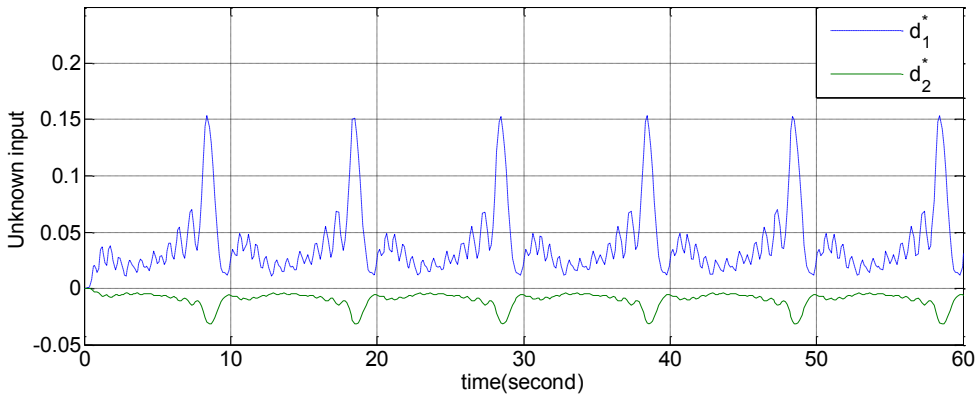

Figure 2-5 UI vector d_1 computed from augmented observer

Table 2-1 Sample values of d_1^* and d_2^*

Sample No.	d_1^*	d_2^*	d_1^*/d_2^*	Sample No.	d_1^*	d_2^*	d_1^*/d_2^*
1	0.00648	-0.0021	-3.084	41	0.00202	-0.00074	-2.7174
2	0.00615	-0.00201	-3.0649	42	0.00204	-0.0007	-2.9282
3	0.00577	-0.0019	-3.0299	43	0.00218	-0.00067	-3.2589
4	0.00572	-0.00183	-3.1317	44	0.0023	-0.00065	-3.5182
5	0.00536	-0.00171	-3.135	45	0.00336	-0.00074	-4.5452
6	0.0053	-0.00164	-3.2312	46	0.00678	-0.00109	-6.206
7	0.00493	-0.00155	-3.1766	47	0.0112	-0.00163	-6.8897
8	0.00476	-0.00148	-3.2274	48	0.0146	-0.00215	-6.7799
9	0.00362	-0.00129	-2.8028	49	0.01594	-0.00251	-6.3389
10	0.00295	-0.00113	-2.617	50	0.01547	-0.0027	-5.7245
11	0.00254	-0.00102	-2.4885	51	0.01359	-0.00272	-5.0011
12	0.00223	-0.00093	-2.4071	52	0.0117	-0.00263	-4.4471
13	0.00223	-0.00084	-2.658	53	0.00998	-0.00251	-3.9806
14	0.0023	-0.00077	-2.9758	54	0.00855	-0.00237	-3.6052
15	0.00223	-0.00072	-3.113	55	0.00761	-0.00225	-3.377
16	0.00228	-0.00069	-3.3139	56	0.00677	-0.00213	-3.1824
17	0.00268	-0.0007	-3.8375	57	0.00642	-0.00204	-3.1527
18	0.00664	-0.00109	-6.0828	58	0.00601	-0.00194	-3.1057
19	0.01118	-0.00163	-6.8447	59	0.00592	-0.00186	-3.1881
20	0.01464	-0.00217	-6.7504	60	0.0055	-0.00174	-3.1669
21	0.01594	-0.00253	-6.3092	61	0.0054	-0.00166	-3.2439
22	0.01538	-0.00271	-5.671	62	0.00494	-0.00156	-3.1598

23	0.01384	-0.00273	-5.0783	63	0.00479	-0.00149	-3.215
24	0.01194	-0.00265	-4.5094	64	0.00347	-0.00129	-2.6942
25	0.0102	-0.00253	-4.0337	65	0.00253	-0.00108	-2.3356
26	0.0087	-0.00239	-3.6405	66	0.00201	-0.00094	-2.1378
27	0.00771	-0.00227	-3.3985	67	0.00188	-0.00084	-2.254
28	0.00684	-0.00214	-3.1923	68	0.0019	-0.00076	-2.4823
29	0.00645	-0.00205	-3.1522	69	0.00205	-0.00072	-2.8435
30	0.00602	-0.00194	-3.0992	70	0.00205	-0.00067	-3.0536
31	0.00591	-0.00186	-3.1777	71	0.00237	-0.00067	-3.5407
32	0.00549	-0.00174	-3.1563	72	0.00278	-0.00069	-4.0357
33	0.00539	-0.00166	-3.2356	73	0.0061	-0.00102	-5.9836
34	0.00492	-0.00156	-3.1496	74	0.01069	-0.00156	-6.8614
35	0.00478	-0.00149	-3.2077	75	0.01481	-0.00218	-6.7821
36	0.00348	-0.00129	-2.6981	76	0.01611	-0.0026	-6.1867
37	0.00239	-0.00105	-2.2665	77	0.01535	-0.00274	-5.5996
38	0.0021	-0.00097	-2.1735	78	0.01367	-0.00274	-4.9868
39	0.00189	-0.00089	-2.1212	79	0.01178	-0.00265	-4.437
40	0.00196	-0.0008	-2.438	80	0.01012	-0.00254	-3.9897
				Average	0.006676	-0.00163	-4.08865

Assume now that the ratio is constant, it then follows that:

$$d_1 = E_u d_u \tag{2-63}$$

It is clear for this example that the "optimum" approximation $E_u{}^*$ to the matrix E_u that also satisfies the rank condition (for UI de-coupling) of Section 2.3.5 is simply given by the average values $\bar{d}_1^*$ and $\bar{d}_2^*$ of the elements of d_1^* and d_2^*, respectively, i.e. $E_u^* = \begin{bmatrix} 1 \\ \bar{d}_1^* / \bar{d}_2^* \end{bmatrix}$. For this example, $E_u^* = \begin{bmatrix} 4 \\ -1 \end{bmatrix}$. On inspection of (2-60), it is immediately obvious that E_u^* represents the ratio of the nonlinear terms $g_1(x_1^2)$ and $g_2(x_1^2)$. This example is a simple case for which it is clear that since the non-linearity only depends on x_1^2 the average values d_1^* and d_2^* can be used to get the accurate result. This simple structure (constant nonlinear coefficients) does not occur in more realistic examples (containing more complex nonlinear forms) and it is necessary to consider a more general procedure as in Section 2.3.5.

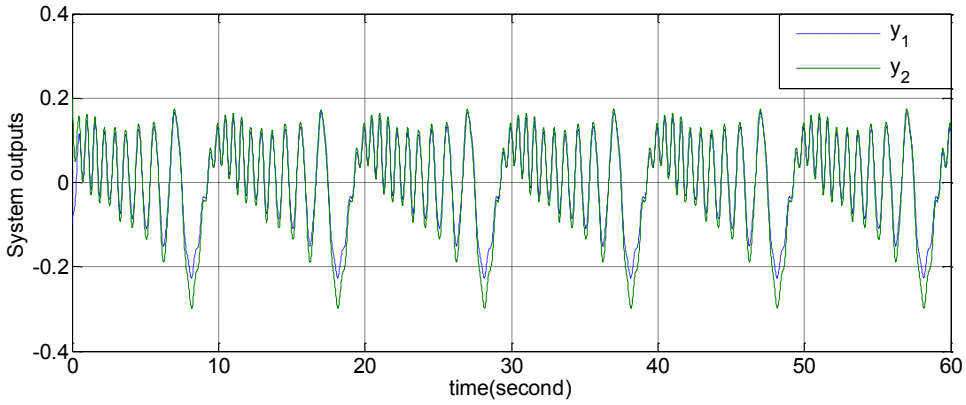

Figure 2-6 Nonlinear system outputs excited by Schroeder-phased signals

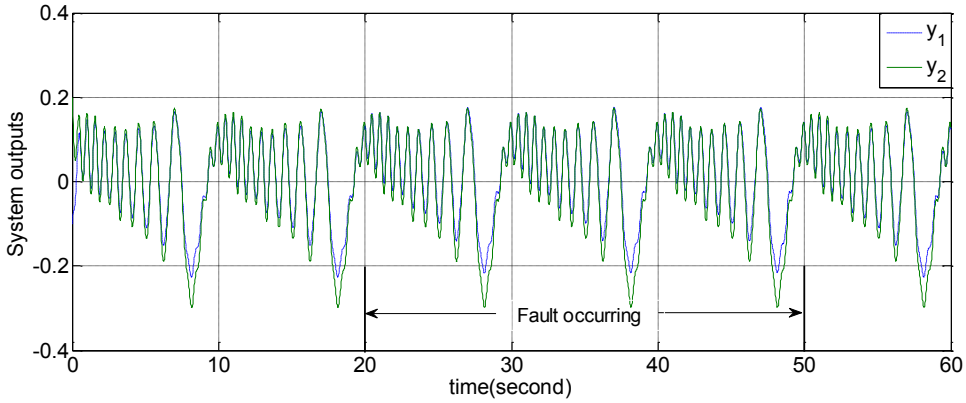

Figure 2-7 Nonlinear system outputs for step fault ($f_s = 0.01$)

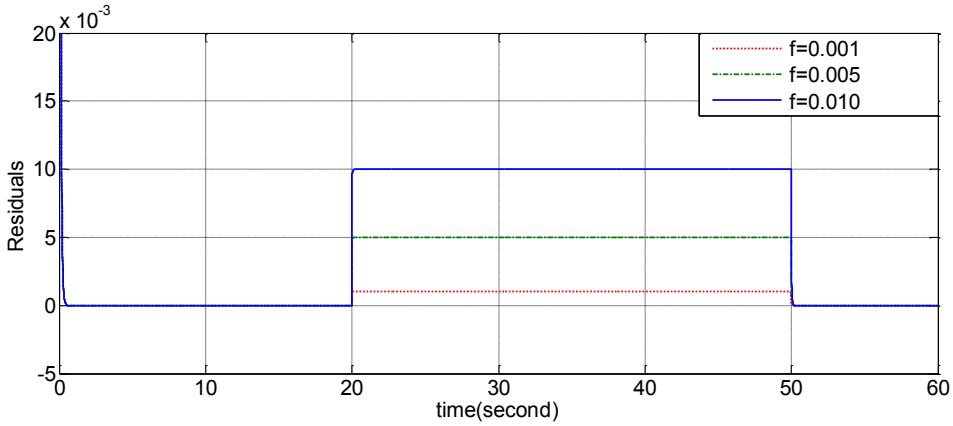

Figure 2-8 Residuals with different step fault magnitudes

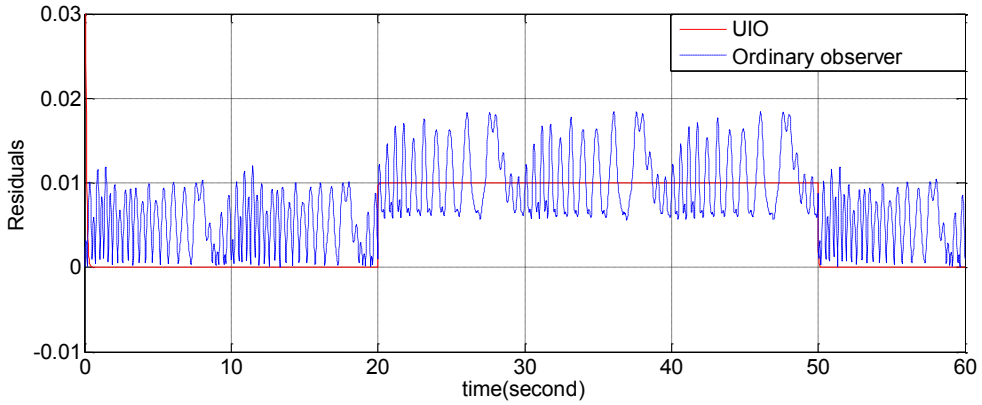

Figure 2-9 Residuals with optimal E_u (UIO) and $E_u = 0$ (Ordinary observer)

Figure 2-6 shows the system output excited by Schroeder-phased signals in fault-free case. It can be assumed that the UIO is driven by the modelling uncertainty represented by the UI and a sensor fault.

Figure 2-7 shows the nonlinear system outputs y with small fault ($f_s = 0.01$). It is difficult to see the effect of the fault on the outputs, i.e. the fault cannot easily be detected from the two output signals. The effects of the step fault are hidden in the larger output variations. Results illustrate clearly the effect of having different suitable "worst case" level of incipient (hard to detect) faults acting as well as low magnitude disturbances (in a sensor fault case). A robust residual will show a strong response to this fault. This is an important criterion when quantifying the robustness properties of an FDI scheme. This robustness is illustrated very clearly in the residual results shown in Figure 2-8. The faults can be detected even with very small value.

In Figure 2-9, the red line is the response of the residual norm corresponding to the use of the optimal E_u in the UIO design, for step faults: $f_s = 0.01$. The blue line corresponds to the residual norm derived once again using the UIO design procedure but with $E_u = 0$ (i.e. for no UI de-coupling). It can be see easily that the residual generated by UIO leads to good fault sensitivity with a low FA probability. However, for the case, it is hard to detect the fault by setting a fixed threshold. Lower fault detection robustness in the presence of the uncertainty has been demonstrated.

By using this simple tutorial nonlinear system example the robust fault detection approach of estimation of UI distribution matrix direction and UIO design has been

illustrated. The UIO approach to FDI/FDD shows good promise for further study in this thesis.

2.4 Conclusion

This Chapter provides a review of model-based strategies for FDI/FDD. The residual generation-based FDI and the FE-based FDD are outlined respectively. The most important features of FDI/FDD design strategies are introduced and the central issues of the model-based approach are discussed, focussing particularly on the robustness problem. After that, the observer-based FDI/FDD is described as one of the widely used model-based FDI/FDD strategies and providing a background for new developments later in the thesis. The basic concepts and fundamental representations of model-based FDI/FDD are defined using mathematical descriptions chosen to provide a framework for work described in later chapters of the thesis. The fault detectability and isolability of the monitored system are given as two important conditions in FDI/FDD design which guarantee that the fault is detectable and isolable. Finally, the fundamental theory of this thesis, the UIO' is introduced. The theoretical concepts behind the notion of UI de-coupling are described as a mechanism for tackling the robustness issue in FDI design along with methods of computing the UI distribution matrix. A simple nonlinear tutorial system example is used to demonstrate the UI estimation and de-coupling based on UIO FDI strategy.

In Chapter 3, an industrial application of a residual-based UIO design is implemented on a high fidelity commercial aircraft based on the *ADDSAFE* FP7 project. In this application study, A bank of unknown input observers (UIOs) is designed in a multiple observer scheme used to realise reliable isolation of the aircraft elevator runaway faults.

Chapter 3
UIO Theory and Application for FDI on a Commercial Aircraft

3.1 Introduction

The UIO is one of the well accepted approaches for robust residual generation-based FDI. When the structured UI (modelling uncertainties/exogenous disturbance) are concerned, to achieve robust FDI performance, the UIO can be used successfully to design the robust residual (residuals) that are de-coupled from the UI. In UIO design, the solution to the appropriate robustness problem (de-coupling the effects of the UI) strongly relies on an assumption that can be made about the UI distribution matrix, i.e. whether the columns are known or not or can be approximated. However, in certain real application cases, for example for the aircraft system described in this Chapter, the UI distribution is unknown due to the lack of knowledge of the nonlinear system dynamics. This results in a significant challenge to obtain the appropriate UI directions using mathematical tools. Hence, it is necessary to focus on methods for generating the structure of the UI in terms of identification and estimation of the UI directions. Once these distributions are estimated, the unexpected UI effects on the residuals can be de-coupled using the UIO description given in Section 2.3.

As introduced in Chapter 1, the main proposal of this thesis is to evolve the traditional UIO approach, focusing on residual generation-based FDI to some novel UIO FE-based FDD, as a consequence of modern demands for FDD/AFTC systems (see Section 1.2 for discussion). From this background this Chapter is mainly devoted to applying the conventional UIO design approach for the detection and isolation of sensor faults on a nonlinear commercial aircraft benchmark system simulation provided by the FP7 project 'Advanced Fault Diagnosis for Sustainable Flight Guidance and Control (ADDSAFE, 2009)'.

Section 3.2 reviews the literature on studies of UIO approaches to FDI for aircraft flight control problems.

3.2 Review of aircraft FDI application

Some published statistics show that between 1993 and 2007 about 16% of commercial aircraft accidents are caused by Loss of Control In-flight (LoC-I), involving technical malfunctions or unusual flight conditions due to external disturbances. LoC-I is regarded as the second largest accident category after Controlled Flight Into Terrain (CFIT) accounting for 23% of air accidents worldwide (Goupil, 2011). Loss-of-Control (LoC) is intrinsically related to the guidance and control (G&C) system of the aircraft, and includes sensors and actuators failures. Improvement using FDI on LoC aircraft failures will have a direct impact on reducing the number of aircraft accidents. Hence, the development of the application of model-based FDI methods for civil aircraft to increase aircraft safety and sustainability clearly plays an important role in aircraft research.

The traditional approach to detect and isolate faults in a flight control system makes use of hardware redundancy by a replication of hardware (sensors, actuators or even flight control computers). This replication increases the aircraft net weight leading to higher fuel demand and increased cost as well as causing more harmful noise and atmospheric pollution. Furthermore, hardware replication is problematic to apply in conjunction with many innovative solutions being developed by the aeronautical sector. The use of conventional hardware redundancy can even limit the aircraft sustainability. This technological barrier limits the full realisation of the next generation of aircraft by an inability to guarantee the current highest levels of required aircraft safety when implementing novel green and efficient technologies (Goupil, 2011).

As an alternative to hardware redundancy, the model-based approach has attracted significant attention. Although the fault information generated via the model-based approach to FDI for actuators (or sensors) generally increases the flight control system computational load, it can on the other hand increase the aircraft sustainability by improving fault diagnosis performance. Linked with this is a potential for optimising aircraft structural design with net weight saving. All of which can help to achieve the European Vision 2020 (ACARE, 2002) challenges related to the “safety” and “greening” of the aircraft. Model-based FDD has often been considered for fault detection, fault location and even diagnosis of fault severity in aircraft flight control systems (Varga, 2010; Chen and Patton, 2011).

Many approaches to robust model-based FDD have been proposed on aircraft fault diagnosis system in the past decades. The major challenge is that the fault information signal should be robust to the UI, which are assumed to be structured according to known (or estimated) UI directions linked to modelling uncertainty. To achieve the robust design, different methods have been studied, e.g. the use of optimisation methods (Varga, 2010), the UIO approach of (Wang and Lum, 2007), the sliding mode observer (Alwi and Edwards, 2011) and geometric design approaches (Vanek, Seiler, Bokor and Balas, 2011). Although the awareness of the potential and demand of advanced FDI/FDD approach is increasing, limited understanding of the theory involved by technician's means that it is impractical to carry out the performance assessment and design verifications within the aircraft industry. It is not realistic to expect aircraft flight control engineers and technicians to spend time in gaining familiarization with advanced model-based FDI/FDD methods. The practitioners prefer to use methods which use simple algorithms, clear design procedures with few tuning parameters, avoiding the use of complicated methods that appear to be beyond their limit of understanding. However, a huge gap exists between the in the academic research and industrial sectors. Within this scenario, a European FP7 project 'ADDSAFE' (ADDSAFE, 2009) was launched to seek to narrow the gap between the academia and the industry.

In this Chapter, a conventional UIO is applied to a nonlinear simulation of a generic aircraft model provided by ADDSAFE project as a benchmark study. As discussed above, in the light of the industrial demands, UIO is a good candidate to implement on the aircraft for FDI/FDD purpose, since it possesses simple algorithms and explicit procedures. The benchmark considered is highly representative of the flight physics and aircraft handling qualities. For realisation the purpose of elevator sensor fault isolation, particularly, UIOs (the generalised observer design scheme proposed in (Patton, Frank and Clark, 1989) are used. At the end of the design, in order to evaluate the FDI performance, the UIO is implemented using the FES environment (Fernández and Ramón, 2011) by considering the right elevator sensor runaway fault. The detected fault scenario and benchmark system description are addressed briefly within the context of the ADDAFE project.

3.3 Robust FDI scheme based on UIO for sensor faults

The preliminary UIO-based FD design scheme outlined in Section 2.3 in general does not enable fault isolation to be achieved since all the output estimates may react to any faults affecting the system. To provide robust FD as well as fault isolation, in this Section, an FDI scheme comprising a bank of UIOs is introduced based on the theory described in Section 2.3 to generate residuals that are sensitive to specific faults (or sets of faults). The ADDSAFE aircraft study as described in Section 3.4. Considering the elevator sensor fault leads to a requirement for the design of only two UIOs.

The system described by (3-1) is affected by UI signals and involves two sensor faults (all actuators are assumed to fault-free) as follows:

$$\left.\begin{aligned} \dot{x} &= Ax + Bu + E_u d_u \\ y_j &= c_j x \\ y^j &= C^j x + C^j f_s^j \end{aligned}\right\} \quad \text{for } j = 1, 2 \qquad (3\text{-}1)$$

where, $x \in \Re^n$ denotes the system state vector. $u \in \Re^r$ denotes the input and measurement vectors and $d_u \in \Re^p$ is a vector of UI. A, B, C are known system matrices with appropriate dimensions. The matrix $E_u \in \Re^{n \times p}$ represents the distribution matrix for the UI. $y_j \in \Re^1$ is the fault-free sensor output. $c_j \in \Re^{1 \times n}$ is one row of the matrix C corresponding to fault-free sensor y_j. $y^j \in \Re^{m-1}$ is obtained from the vector y by deleting y_j. $C^j \in \Re^{(m-1) \times n}$ is the matrix C created by deleting the row c_j. It can be seen that C^j contains the measurement that is corrupted by the sensor fault f_s^j.

Remark 3.1: Consider the aircraft application (elevator sensor fault) in the following Section 3.4, only two UIOs are designed, because the monitored aircraft system has only two elevators (the left and the right). Therefore, the system is structured as (3-1) and the UIOs design as well as the decision making logic is simpler compared with that in case of more than two sensor fault cases, i.e. ($j > 2$). If $j > 2$, the solution refers to the work in (Chen and Patton, 1999).

In terms of the above description, two UIO-based residual generators can be constructed as:

$$\left.\begin{aligned} \dot{z}^j &= N^j z^j + T^j B u + K^j y^j \\ r^j &= \left(I - C^j H^j\right) y^j + C^j z^j \end{aligned}\right\} \tag{3-2}$$

The corresponding UIO matrix parameters must satisfy the following in the light of the UIO-based FD design in Section 2.3.2:

$$\left.\begin{aligned} \left(H^j C^j - I\right) E_u &= 0 \\ T^j &= I - H^j C^j \\ N^j &= T^j A - K_1^j C^j = A_1^j - K_1^j C^j \\ K_2^j &= N^j H^j \\ K^j &= K_1^j + K_2^j \end{aligned}\right\} \quad \text{for } j = 1, 2 \tag{3-3}$$

According to (3-3), the particular solution of H^j is given as:

$$H^j = [(C^j E_u)^T (C^j E_u)]^{-1} (C^j E_u)^T = E_u (C^j E_u)^+ \tag{3-4}$$

Considering the fault isolation task, all the eigenvalues of N^j should be assigned to be stable with satisfaction of the relations in (3-3) so that the required FDI performance can be achieved. The necessary and sufficient conditions of the UIOs can be reformed as Theorem 3.1 in terms of Theorem 2.3.

Theorem 3.1. The necessary and sufficient conditions for the existence of UIOs (3-1) of system (3-2) are:

(1) $rank\left(C^j E_u\right) = rank(E_u)$

(2) $rank\left(C^j, A_1^j\right)$ is a detectable pair

In the case of system of (3-1) with sensor faults (all actuators are assumed to be fault-free) and UI, the generated residual signals r^j have been given in (3-2) in terms of UIOs. Obviously, the residual generators r^j are driven by all the control inputs and all the outputs except the fault-free sensor in each case, which means that the j_{th} residual only includes the j_{th} sensor information where the fault occurs. The UI signals are specified as corresponding only to modelling uncertainties, so that the generated residual r^j based on the UI de-coupling principle is insensitive to modelling uncertainty whilst sensitive to a dedicated fault signal, as long as the UI signal is de-coupled according to (3-3) & (3-4) and Theorem 3.1.

Finally, decision-making logic for detecting and isolating faults is set by the threshold logics in (3-5) for each of the two observers corresponding to each sensor fault:

$$\begin{cases} \|r^j\| > T_{SFI}^j \\ \|r^k\| \leq T_{SFI}^k \end{cases} \quad \text{for } j = 1,2; \quad k = 2,1 \tag{3-5}$$

It is defined that, if the residual values are less than the threshold value, a '0' signal is generated, or if the residual values are larger than the threshold value, a '1' signal is flagged in the UIO. Both '0' and '1' are used for to detect and isolate faults.

3.4 Robust UIO-based FDI approach on a commercial aircraft

In this Section, the two UIOs design outlined above are applied to a nonlinear simulation of a generic aircraft provided by ADDSAFE project for the benchmark study. The main work is to detect and isolate the elevator sensor runaway fault described in Section 3.4.1.

3.4.1 Elevator sensor runaway fault

Right elevator sensor runaway fault: This is a typical fault scenario dealing with actuator/sensor faults located in the servo-loop control of an elevator surface. The fault is considered to occur between the flight control computer (FCC) and an individual control surface. This runaway fault gives rise to an unwanted hardover deflection of one control surface if the runaway fault remains undetected. Runaway faults may occur in any flight condition corresponding to generally unknown dynamics. Under specific circumstances, depending on the control surface impacted, catastrophic consequences may result from an undetected runaway. This is why a runaway fault must be detected very quickly, in particular for structural load aspects. In this scenario, the root cause can be (ADDSAFE, 2009):

- A mechanical dysfunction: actuator servo-valve runaway, etc...
- A sensor malfunction: bias, etc…
- A FCC malfunction: servo-loop gain coding error, etc...

It is required to detect the elevator sensor runaway before the control surface exceeds a certain degree, whatever the runaway speed (from the slowest to the fastest), in order to reconfigure on a healthy adjacent actuator (system reconfiguration).

In Section 3.4.2, the LTI longitudinal aircraft model dynamics are derived as required by the UIO FDI method for detecting the elevator sensor runaway fault.

3.4.2 LTI longitudinal aircraft model dynamics

The proposed UIO is implemented on a longitudinal LTI model derived from the ADDSAFE benchmark model. Two parts constitute the LTI longitudinal aircraft model: one is the aircraft body axis LTI model. The other part comprises the locally linear aircraft actuator models representing the right and left elevators on the aircraft tail surface. The linearised system is obtained by choosing the trimming parameters given in Table 3-1.

Table 3-1 Trimming points for longitudinal aircraft LTI model

Trimming parameter	Value
MASS (Net mass in Kg)	200000
XG (Centre gravity of the aircraft)	0.30
ZP (Altitude in feet)	20000
VC (Calibrate aircraft speed in kts)	290

The LTI state space representation of the aircraft body axis dynamics can be expressed as:

$$\left.\begin{aligned}\dot{x}_b &= A_b x_b + B_b u_b \\ y_b &= C_b x_b + D_b u_b\end{aligned}\right\} \tag{3-6}$$

where, $x_b = [V_{tas},\ \alpha,\ q, \theta]'$ and $y_b = [V_{tas},\ \alpha,\ q, \theta]'$ are the aircraft body axis states and outputs, respectively. u_b is equal to y_{ac} in (3-7). V_{tas} is the true air speed in m s^{-1}, α is the angle of attack in deg, q is the pitch rate in deg s^{-1}, θ is pitch angle in deg. A_b, B_b, C_b, D_b are the corresponding system matrices.

The LTI elevator model is represented by a first order system dynamic. For the longitudinal motion, the left and right elevator dynamics combined together have the structure:

$$\left.\begin{aligned}\dot{x}_{ac} &= A_{ac} x_{ac} + B_{ac} u_c \\ y_{ac} &= C_{ac} x_{ac} + D_{ac} u_c\end{aligned}\right\} \tag{3-7}$$

where, $x_{ac} \in \Re^{2\times 1}$ is the augmented state vector for both the left and right elevators. $u_c \in \Re^{2\times 1}$ is the vector of elevator control inputs (the actuator input signals fed by the FCC), y_{ac} is the actuator output. A_{ac}, B_{ac}, C_{ac}, D_{ac} are corresponding system matrices with proper dimensions.

The complete LTI longitudinal motion model is formulated as:

$$\begin{bmatrix} \dot{x}_b \\ \dot{x}_{ac} \end{bmatrix} = \begin{bmatrix} A_b & B_b C_{ac} \\ 0 & A_{ac} \end{bmatrix} \begin{bmatrix} x_b \\ x_{ac} \end{bmatrix} + \begin{bmatrix} B_b D_{ac} \\ B_{ac} \end{bmatrix} u_c$$

$$\begin{bmatrix} y_b \\ y_{ac} \end{bmatrix} = \begin{bmatrix} C_b & D_b C_{ac} \\ 0 & C_{ac} \end{bmatrix} \begin{bmatrix} x_b \\ x_{ac} \end{bmatrix} + \begin{bmatrix} D_b D_{ac} \\ D_{ac} \end{bmatrix} u_c \tag{3-8}$$

(3-8) can be re-written as:

$$\left.\begin{aligned} \dot{x} &= Ax + Bu \\ y &= Cx + Du \end{aligned}\right\} \tag{3-9}$$

where, $x = \begin{bmatrix} x_b \\ x_{ac} \end{bmatrix}$, $y = \begin{bmatrix} y_b \\ y_{ac} \end{bmatrix}$, $A = \begin{bmatrix} A_b & B_b C_{ac} \\ 0 & A_{ac} \end{bmatrix}$, $B = \begin{bmatrix} B_b D_{ac} \\ B_{ac} \end{bmatrix}$, $C = \begin{bmatrix} C_b & D_b C_{ac} \\ 0 & C_{ac} \end{bmatrix}$, $D = \begin{bmatrix} D_b D_{ac} \\ D_{ac} \end{bmatrix}$. In ADDSAFE benchmark model, it is defined that $D = 0$.

The nonlinear aircraft model is not available for publication due to confidential issues. However, the results in this Chapter have been generated by applying the UIO FDI strategy to the fully nonlinear aircraft system dynamics via the ADDSAFE project. Following a procedure in Section 2.3.5, the discrepancies (modelling uncertainties) between the nonlinear and LTI aircraft model give rise to the UI signal should be de-coupled in the UIO designs to cover the robustness issue. Hence, the FDI consists of the following two steps:

In step (i) of the UIO design, the influences of the UI are estimated by estimating the "directions" (i.e. distributions) of these terms into the state space model as described in Section 2.3.5. The off-line design of the augmented observer scheme for estimating the UI distribution matrix E_u is carried by running the nonlinear aircraft ADDSAFE benchmark. The lower rank technique via SVD approach is applied to post-process the modelling uncertainty data, so that condition (1) of Theorem 2.3 is satisfied.

The second step is based on the philosophy of UI de-coupling design, namely to de-couple the UI following the E_u estimation of step 1. The robust UIO FDI schemes for sensor faults introduced in Section 3.3 are used to develop the sensor faults FDI scheme involving both fault detection and isolation. Each of the two observer residuals (in the observer bank) is made specifically sensitive to one fault, so that the faults can be isolated. According to the structure of the UIO, two constant observer gains should be designed for each of the sensor faults using standard procedures aimed at de-coupling the UI signals from each of the generated residuals.

A logical decision mechanism is developed to achieve this goal. The two dedicated UIO design steps for the ADDSAFE benchmark FDI problem are illustrated as Figure 3-1. The complete FDI strategy including UIO design and the tuning scheme are shown in Figure 3-2.

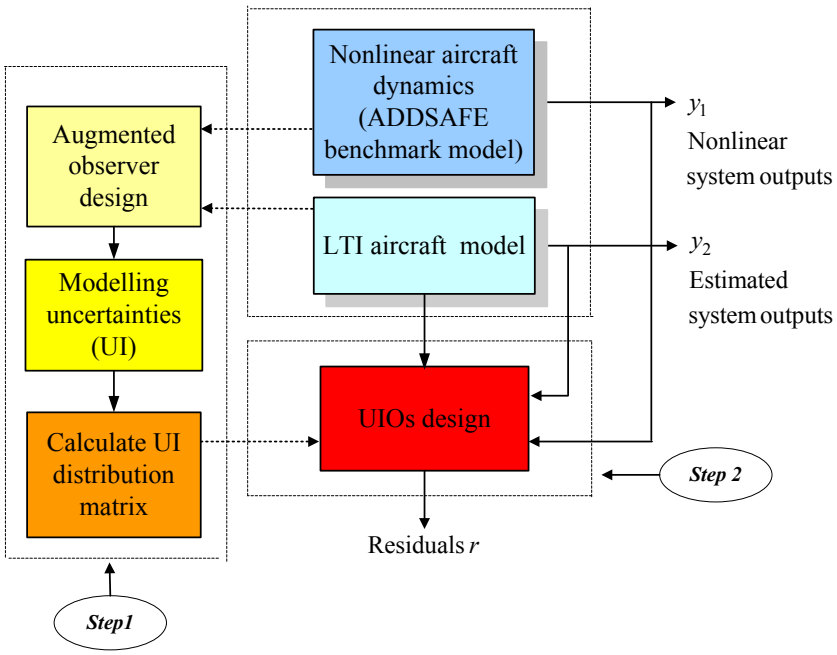

Figure 3-1 UIO application on ADDSAFE benchmark

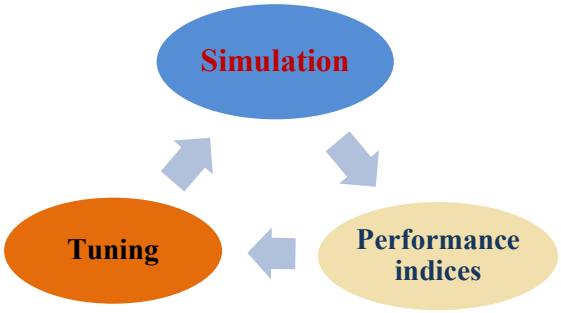

Figure 3-2 FDD complete design and final tuning scheme

(Patton, Uppal, Simani and Polle, 2010)

3.4.3 Simulation results

The nominal aircraft flight behaviour is defined under the trimming point defined in Table 3-1. Results corresponding to a right elevator sensor runaway fault occurring at 5s are shown below. The design meets the UIO FDI performance indices which along with the abbreviations used are defined in Section 1.5 (Maximum detection time, Minimum detection time, MDT, FDR, MAR, FAR). The performance evaluated in the ADDSAFE FES system environment within a predefined flight envelope (see below for full description of the FES environment). The parameters for defining the flight envelope are given in Table 3.2. In the following plots, the red line is referred to as the *nominal* flight condition which means the aircraft operates at the trimming point. The blue lines represent other evaluation results.

A brief description of the FES system environment is introduced here to provide a better understanding of the simulation results and to acknowledge the ownership. FES is a term used to describe a software simulator operating at the functional level of system components (including the operating environment) used to support the specification, design, verification and operations of space systems. The FES concept can be used across the spacecraft development life-cycle, including activities such as system design validation, software verification & validation, spacecraft unit and sub-system test activities (Fernández, De Zaiacomo and Mafficini, 2010). The FES developed by Deimos Space S.L.U. for the ADDSAFE project (Fernández and Ramón, 2011) is a non-real-time simulator based on Simulink, Matlab and XML that includes the Airbus

benchmark as well as the robustness and performances metrics for all the fault scenarios defined in the project (Goupil and Marcos, 2012)

Table 3-2 Parameter values chosen in flight envelope

Parameter notation	**Value**			
ZP (Altitude in feet)	8	18	28	38
MASS (Net mass in Kg)	120	180	233	
VC (Calibrate aircraft speed in kts)	160	220	300	
XG (Centre gravity of the aircraft)	0.17	0.3	0.41	

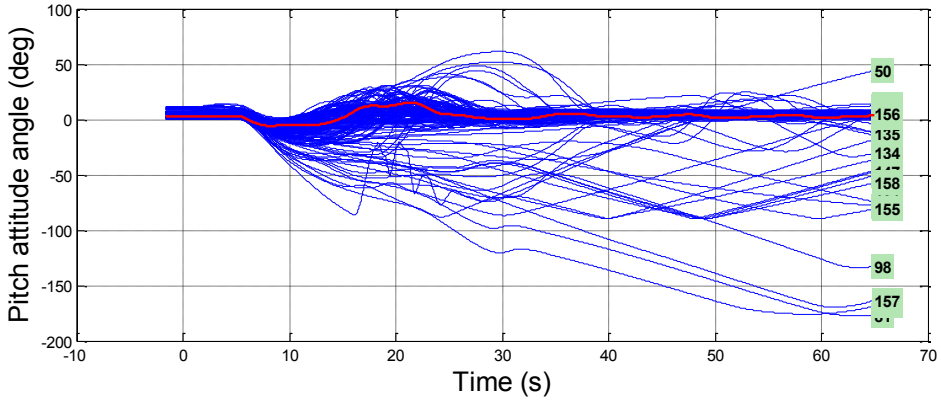

Figure 3-3 Pitch angle in runaway fault scenario

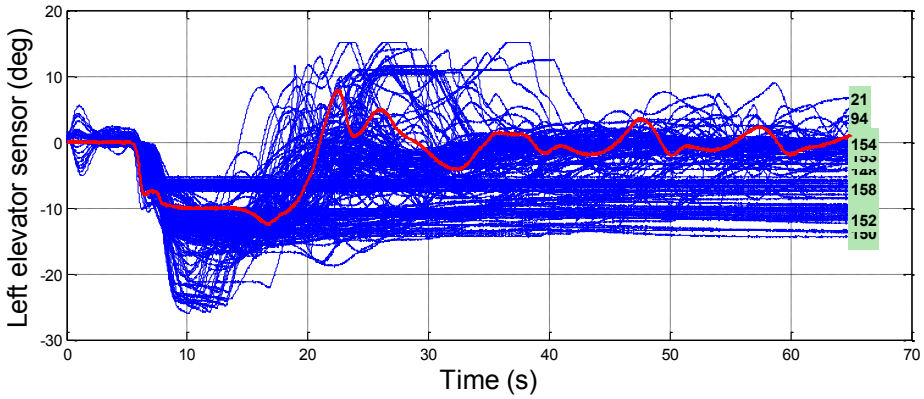

(a) Left elevator sensor value in runaway fault scenario

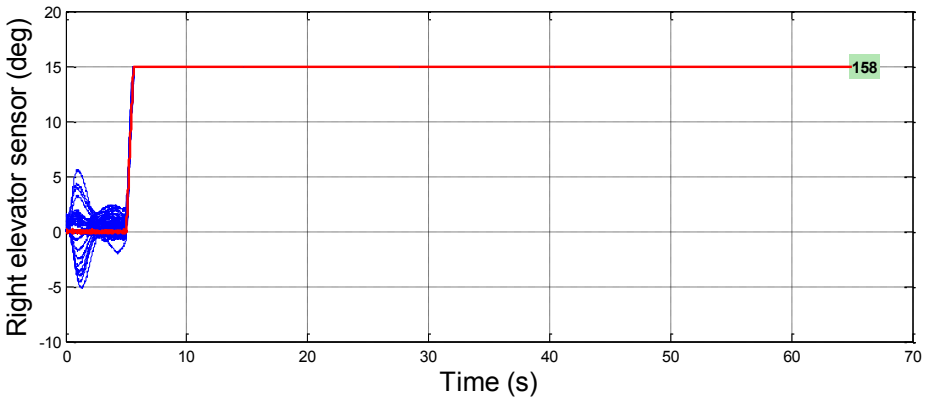

(b) Right elevator sensor value in runaway fault scenario

Figure 3-4 Left and Right elevator sensor value in runaway fault scenario

Since the runaway fault occurs during cruise flight but before a pitch-up manoeuver, it makes sense to compare the pitch angle in both the cruise flight and the runaway fault scenarios. From Figures 3-3 & 3-4, the large pitch angle change occurring at 5s can be clearly seen, reflecting the impact of the right elevator sensor runaway fault on the pitch angle.

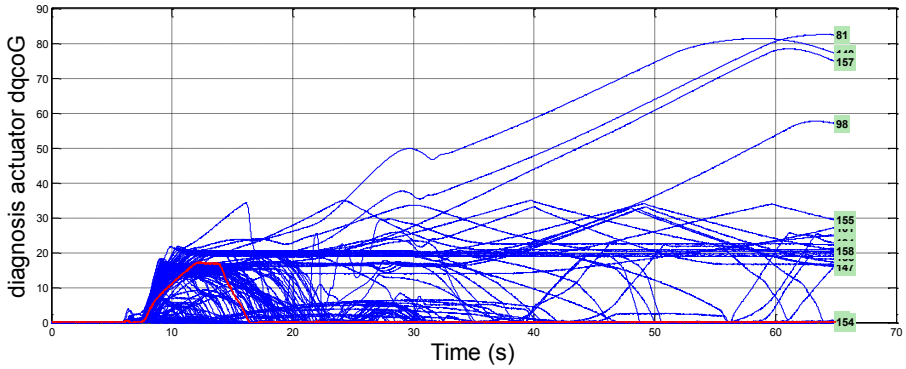

(a) Left elevator UIO residuals in runaway fault scenario

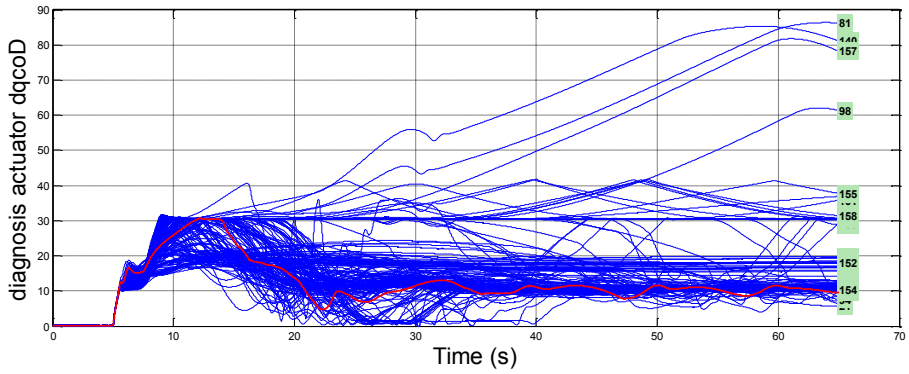

(b) Right elevator UIO residuals in runaway fault scenario

Figure 3-5 Left and Right elevator UIO residuals in runaway fault scenario

Figure 3-5 shows the left and right elevator UIO residuals. In terms of the UIO theory, the right elevator residual (r_D) is driven by two inputs (left and right elevator control command) and all the outputs except left elevator sensor measurement, which means that r_D includes the fault information. The left elevator residual (r_G) is driven by two inputs (left and right elevator control command) and all the outputs except right elevator sensor value) which means that (r_G) does not include the information of the fault onset until the control command change. No sudden deflection occurs in r_G at 5s as shown in Figure 3-5(a). Following the same theory, in Figure 3-5(b), it can be seen that a sudden deflection appears on the right elevator residual (r_D) at 5s. According to the threshold setting principle described in Section 2.3.4, thresholds for the left and right elevator residuals are $T_G = 0.9$ and $T_D = 1.2$, respectively. In terms of the (3-5), the decision-making logic is formed as Table 3-3 using both '0' and '1' to detect and isolate fault.

Table 3-3 Decision-making logic

Left elevator decision signal	**Right elevator decision signal**	**Fault occurring in left elevator**	**Fault occurring in right elevator**
0	1	0	1
1	0	1	0

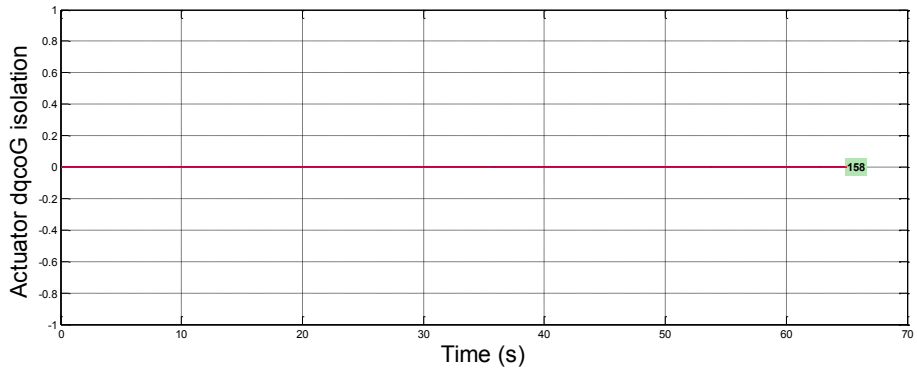

(a) Fault isolation signals of left elevator

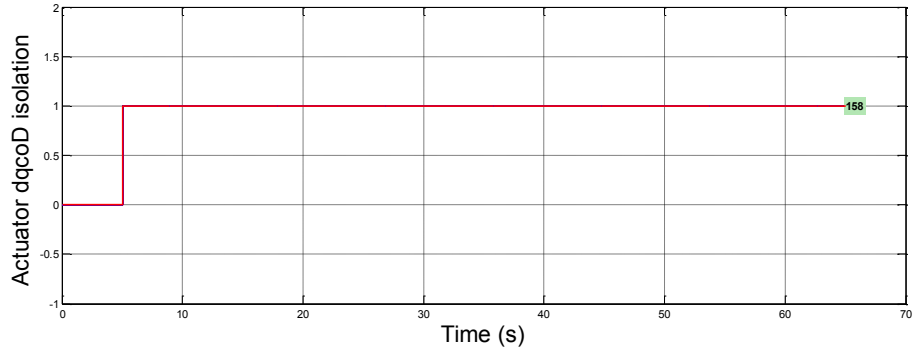

(b) Fault isolation signals of right elevator

Figure 3-6 Fault isolation signal of left and right elevators in runaway fault scenario

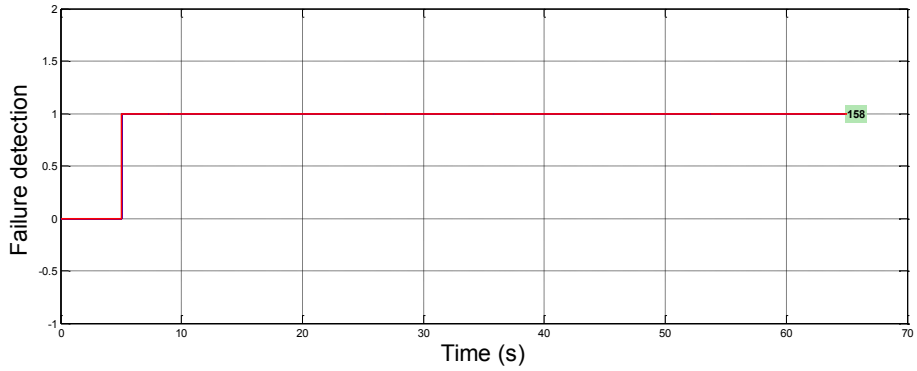

Figure 3-7 FDI signals of right elevator in runaway fault scenario

Figure 3-6 shows the isolation results for left and right elevator, respectively. Figure 3-7 illustrates right elevator isolation results using Figure 3-6 and decision-making logic in Table 3-3. The FDI performance by FES system environment test is given in Table 3-4.

Table 3-4 FES test results

Maximum detection time(s)	Minimum detection time(s)	MDT (s)	FDR%	MAR%	FAR%
0.09	0.08	0.0801	100	0	0

Remark 3.2: A logical decision mechanism should be designed for the two elevator UIO residuals in order to detect the fault occurrences in the individual elevators as well as to isolate the fault locations, i.e. to know which elevator is affected by the fault. By correctly isolating each actuator sensor, FA alarms can be avoided, i.e. if a fault occurs in the right elevator this will not influence the sensor fault residual of the left elevator, etc. This is very important for the FDI global design to identify the fault location. To achieve this purpose, appropriate residual thresholds should be set.

Remark 3.3: The threshold can be considered as a tuning parameter in the UIO FDI designs. In each of these UIO designs, static thresholds are set for each fault detection residual signal corresponding to each UIO. Meanwhile, a good FDI performance (Low MD and low FA and Fast FDT) can be achieved by tuning the appropriate thresholds.

The FES system evaluation of the UIO designs simulates the given flight envelope and the right elevator sensor runaway fault scenario. It requires that the appropriate threshold value should be larger than the maximum peak value for each of the left and right elevator separately in any of the fault-free time periods in order to avoid false alarms. Actually, this is not the only factor to define the threshold in each UIO. As described above, the FDI performance indices in Section 1.5 are used to evaluate the FDI design performance which do not only concern the 100% FDR, but also 0% MAR, 0% FAR and fast FDT. Hence, the philosophy of UIO parameter tuning is detailed as follows:

For isolation purposes, the residual for each elevator sensor fault is set individually by comparing the residuals in both the fault-free and fault scenario cases. The thresholds should be larger than each of the peak residual values for the corresponding fault-free cases. Meanwhile in theory a smaller threshold can guarantee a high FDR as well as lower FDT. However, the threshold values should be set no less than the peak values during the fault-free period to avoid FA. Therefore, in the UIO designs, the thresholds are tuned in both the right and left elevator residual generators by considering the FDI

performance indices and all the simulation results for both the fault-free and the right runaway scenario. Finally, the threshold values are set as 0.9 in the left elevator and 1.2 in the right elevator. Consequently, 100% FDR, 0% MAR and 0% FAR are obtained.

3.5 Conclusion

In this Chapter, the UIO approach introduced in Chapter 2 is applied to a benchmark simulation of a high fidelity commercial Airbus generic aircraft based on the *ADDSAFE* FP7 project concerning a real industry focussed application study of FDI in collaboration with the company Airbus. The right elevator sensor runaway fault scenario is detected and isolated using a bank of observers design principle. The preliminary design of the UIO method for FDI has been introduced and the philosophy of de-coupling the structured UI signals from the generated residuals, i.e. to tackle the FDI robustness issue associated with the UI matrix estimation problem. The integrated UIO design procedures together with the UI distribution matrix estimation are addressed explicitly in terms of typical flight control requirements arising from the aircraft. Finally, a performance evaluation procedure for the proposed FDI design is carried out by in FES system environment.

In Chapter 4, the interest turns to the use of FE-based FDD approaches based on the residual-based UIO introduced in Chapters 2 & 3. However, the UI de-coupling principle is kept to handle the robustness problem in all design approaches.

Chapter 4
RFAFE for a Commercial Aircraft Oscillatory Fault[1]

4.1 Introduction

Following the literature review on model-based FDI/FDD in Chapter 2 and the UIO developments described in Chapters 2 & 3, the focus of interest in this Chapter is on the use of FE-based FDD approaches rather than residual-based FDI.

It turns out that the residual approach to FDI has significant complexity whilst still not easily providing an ideal residual. The ideal residual is one which follows the fault signal in shape and time variation as precisely as possible. Hence, it can be argued that the residual approach can, in the most part, now be replaced by FE approach based on the availability of powerful FE methods. Furthermore, FDI residual signals are not so useful in FTC systems using reconfigurable control etc, so that even in FTC design attention is turning very rapidly to the use of FE.

Amongst the observer-based FDD methods, the adaptive observer is one of the acceptable methodologies and has been studied more during two decades. For the adaptive FE, two alternative strategies have been considered in the literature, for example, works in (Wang, Huang and Daley, 1997) and (Gao and Ho, 2004), respectively. (Wang, Huang and Daley, 1997) estimate the fault using input-output data. Following that, the system states are estimated by appropriate updating of fault information. (Gao and Ho, 2004) consider the fault signals as additional state variables of the system. A state observer is constructed to estimate the augmented states including the faults. (Zhang, 2005) give comparison amongst different adaptive observers in a unified approach.

Theoretically, the estimated fault signal should follow the real fault signal precisely, i.e. there should be no time delay compared with the real fault signal. From this point of view, the so-called fast adaptive fault estimation (FAFE) based on the aforementioned

[1] The work presented in this Chapter has been published in: Sun, X. Y., Patton, R. J. and Goupil, P. (2012). Robust adaptive fault estimation for a commercial aircraft oscillatory fault scenario. *Proc. of the 2012 UKACC International Conference on Control*, Cardiff, 595-600, 3-5 Sept.

adaptive observer structure in (Wang, Huang and Daley, 1997) is presented by (Zhang, Jiang and Cocquempot, 2008) to achieve the rapidity of FE. In the FAFE design, the adaptive estimated fault signals comprise proportional and integral terms to guarantee both dynamical and steady-state FE performance. There is also a robustness problem in FDD design which has not been taken into consideration by (Zhang, Jiang and Cocquempot, 2008). As discussed in Section 2.2.2, if an FE approach is to be used, the estimated fault signals must be accurate and robust to changes in system operation involving modelling uncertainty and disturbance. Hence, the robustness in FE is an important topic in this Chapter.

This provides the motivation for the development of a design approach for a robust fast adaptive fault estimator (RFAFE) that incorporates with a UI de-coupling function. As a background to this work (Wang and Lum, 2007) and (Zhao, Xie, Hong and Zhang, 2011) worked separately on UI de-coupling approaches to adaptive FE enhancing the robustness of the adaptive observer approaches outlined above. In (Wang and Lum, 2007), the full measurements are needed, and this is either considered as an ideal situation in practice or is not general enough for many problems. (Zhao, Xie, Hong and Zhang, 2011) attempt to resolve some of the limitations imposed by the requirement to have a full set of measurements. However, in their work it is assumed that the fault time derivative is zero, thus limiting the type of FE structure that can be used. Aside from using UIO approaches, these two papers share one feature in common, which is that the fault estimators are constructed with one integral term depending on system output error dynamics.

Hence, the work in this Chapter is inspired by the so-called FAFE approach of (Zhang, Jiang and Cocquempot, 2008). The proposed approach is termed a RFAFE, based on a combination of the UIO proposed in (Chen, Patton and Zhang, 1996) and the FAFE of (Zhang, Jiang and Cocquempot, 2008). It should be noted that (Zhang, Jiang and Cocquempot, 2008) do not consider the robustness of the FE to modelling uncertainty. So from the FDD robustness perspective, the contribution in the current work provides an extension to the (Zhang, Jiang and Cocquempot, 2008) study using a UIO to take into account the effects of the so-called UI signals.

In this RFAFE structure, the FE signal is a function of the combination of the proportional and integral action realised by a full order identity observer. When

compared with (Wang and Lum, 2007) and (Zhao, Xie, Hong and Zhang, 2011), FE signal not only involves integral action but also includes proportional action to enhance the FE speed. Furthermore, the proposed approach is not restricted to the use of a full set of measurements. Therefore, this robust adaptive fast FE method can enhance the robustness of the fault estimator to UI as well as the rapidity of the FE.

The RFAFE design problem is divided into two stages of (i) UI distribution matrix estimation followed by (ii) the actual FE, with inclusion of proportional (not only integral) action to enhance to FE speed. Finally, the RFAFE is applied to estimate the OFC acting on an elevator of the ADDSAFE benchmark system introduced in Chapter 3. The benefit of the proposed RFAFE is that the robustness of the FE is improved by making the output error of the observer insensitive to modelling uncertainty.

However, the results in this Chapter have been generated by applying the new RFAFE FE strategy to the fully nonlinear aircraft system dynamics via the ADDSAFE project. By using the same procedure as described in Chapter 3, modelling uncertainty between the nonlinear and LTI aircraft models is accounted for using UI terms that appear in the linear model state space format used for the development of the fault estimator. In stage (i) of the RFAFE design, the influences of the UI are estimated by estimating the "directions" (i.e. distributions) of these terms into the state space model as described in Chapter 3. In stage (ii) the fault estimator is then applied directly to estimate the OFC fault activity in one elevator actuator (referred to as the "left" actuator in the light of the requirement of the FP7 ADDSAFE project).

4.2 RFAFE theory description

4.2.1 FAFE with UI de-coupling

An LTI system considering actuator faults (all sensors are assumed to be fault-free) and with modelling uncertainty, represented by the UI term $E_u d_u$ is represented as:

$$\left.\begin{aligned} \dot{x} &= Ax + Bu + E_u d_u + F_a f_a \\ y &= Cx \end{aligned}\right\} \tag{4-1}$$

where, $x \in \Re^n$ denotes the system state vector, $u \in \Re^r$ and $y \in \Re^m$ denote the input and measurement vectors, respectively and $d_u \in \Re^p$ is a vector of UI. $f_a \in \Re^l$ represents a vector of time-varying actuator faults. A, B, C are known system matrices

with appropriate dimensions. The matrix $E_u \in \Re^{n\times p}$ represents the distribution matrix for the UI. The columns of the matrix $F_a \in \Re^{n\times l}$ denote the independent fault directions. It is thus considered that both E_u and F_a act as system inputs.

A functional observer in full order is constructed as:

$$\left.\begin{aligned} \dot{z} &= Nz + TBu + Ky + TF_a\hat{f}_a \\ \hat{x} &= z + Hy \end{aligned}\right\} \tag{4-2}$$

where, $\hat{x} \in \Re^n$ is the estimated state vector and $z \in \Re^n$ is the observer state vector, $\hat{f}_a \in \Re^l$ is the FE signal of f_a, and N, T, K and H are design matrices as described below.

Definition 4.1: The observer (4-2) is defined as a RFAFE for the system (4-1), if its state and FE errors $e_x = x - \hat{x}$ and $e_f = f_a - \hat{f}_a$ approach zero asymptotically, in the presence of the system UI and faults.

Assuming that E_u is known, the estimation error dynamics are governed by:

$$\begin{aligned} \dot{e}_x = {} & (A - HCA - K_1C)e_x \\ & + [N - (A - HCA - K_1C)]z \\ & + [K_2 - (A - HCA - K_1C)H]y \\ & + [T - (I - HC)]Bu \\ & + (HC - I)E_u d_u + TF_a e_f \end{aligned} \tag{4-3}$$

where,

$$K = K_1 + K_2 \tag{4-4}$$

If the following relations are satisfied:

$$(HC - I)E_u = 0 \tag{4-5}$$

$$T = I - HC \tag{4-6}$$

$$N = A - HCA - K_1C = A_1 - K_1C \tag{4-7}$$

$$K_2 = NH \tag{4-8}$$

The state estimation error is then refined as:

$$\dot{e}_x = Ne_x + TF_a e_f \tag{4-9}$$

$$e_y = Ce_x \tag{4-10}$$

$$r = y - C\hat{x} = Ce_x = e_y \tag{4-11}$$

Furthermore, if all the eigenvalues of N are stable, r will approach a small set of value asymptotically, i.e. $\hat{x} \to x$ and $\hat{f}_a \to f_a$. The observer (4-2) is an UI de-coupling *fast adaptive fault estimator* for the system (4-1) when conditions (4-5) – (4-8) are satisfied. Therefore, this RFAFE design involves the solution of (4) to (8) whilst placing all the eigenvalues of the system matrix N to be stable. Meanwhile, N, T, K and H in (4-2) are designed to achieve the required FE performance.

A particular solution to (4-5) can be calculated as follows:

$$H = E_u(CE_u)^+ \tag{4-12}$$

where, $(CE_u)^+ = [(CE_u)^T(CE_u)]^{-1}(CE_u)^T$ denotes the Moore-Penrose pseudo-inverse.

Theorem 4.1. The necessary and sufficient conditions for the existence of RFAFE of system (4-1) comply with Theorem 2.3 in (Chen and Patton, 1999):

(1) $rank(CE_u) = rank(E_u)$

(2) $rank(C, A_1)$ is a detectable pair

Lemma 4.1 is used to verify the RFAFE existence conditions:

Lemma 4.1 (Jiang, Wang and Soh, 2002): Given a scalar $\theta > 0$ and a symmetric positive definite (S.P.D) matrix P, the following inequality holds:

$$2x^T y \leq \frac{1}{\theta}(x^T P x) + \theta y^T P^{-1} y \quad x, y \in \Re^n \tag{4-13}$$

Assume that $\dot{f}_a \neq 0$, e.g. a sinusoidal perturbation (as required for the OFC fault case). The derivative of e_f is represented as:

$$\dot{e}_f = \dot{f}_a - \dot{\hat{f}}_a \tag{4-14}$$

The system error dynamics can be guaranteed by Theorem 4.2.

Theorem 4.2: With the assumption of Theorem 4.1, given the scalar parameters $\alpha, \theta > 0$, if there exist S.P.D matrices $P \in \Re^{n\times n}$, $Q \in \Re^{n\times n}$, $G \in \Re^{l\times l}$, and matrices $Y \in \Re^{n\times m}$, $N \in \Re^{n\times n}$ such that the following conditions hold.

$$\begin{bmatrix} PN + N^T P & -\frac{1}{\alpha} N^T P(TF_a) \\ * & -2\frac{1}{\alpha}(TF_a)^T P(TF_a) + \frac{1}{\alpha\theta} G \end{bmatrix} < 0 \tag{4-15}$$

$$(TF_a)^T P = MC \tag{4-16}$$

$*$ denotes the elements of a symmetric matrix. The UI de-coupling fast adaptive fault estimator can be defined as:

$$\dot{\hat{f}}_a = \Gamma M(\dot{r} + \alpha r) \tag{4-17}$$

(4-17) can be realised when r and e_f are uniformly bounded functions. $\Gamma \in \Re^{l\times l}$ is an S.P.D learning rate matrix.

Proof:

Consider the following Lyapunov function:

$$V = e_x^T P e_x + \frac{1}{\alpha} e_f^T \Gamma^{-1} e_f \tag{4-18}$$

Substituting (4-9) and (4-17) into (4-18), the derivative of V with respect to time is derived as:

$$\dot{V} = \dot{e}_x^T P e_x + e_x^T P \dot{e}_x^T + 2\frac{1}{\alpha} e_f^T \Gamma^{-1} \dot{e}_f$$

$$= e_x^T (PN + N^T P) e_x + 2 e_x^T P(TF_a) e_f$$

$$-2\frac{1}{\alpha}\, e_f^T M(\dot{r} + \sigma r) - 2\frac{1}{\alpha} e_f^T \Gamma^{-1} \dot{f}_a \tag{4-19}$$

Using (4-16), the term $-2\frac{1}{\alpha}\, e_f^T M(\dot{r} + \sigma r)$ on the left hand side of (4-19) can be re-written as:

$$-2\frac{1}{\alpha}\, e_f^T M(\dot{r} + \sigma r) = -2\frac{1}{\alpha} e_f^T (TF_a)^T P(\dot{e}_x + \sigma e_x) \tag{4-20}$$

Substituting (4-9) and (4-20) into (4-19), $\dot{V}$ can be formulated as:

$$\dot{V} = \dot{e}_x^T (PN + N^T P) e_x - 2\frac{1}{\alpha} e_f^T (TF_a)^T PN e_x$$

$$-2\frac{1}{\alpha} e_f^T (TF_a)^T P(TF_a) e_f - 2\frac{1}{\alpha} e_f^T \Gamma^{-1} \dot{f}_a \tag{4-21}$$

By using Lemma 4.1, the (4-22) is obtained as:

$$-2\frac{1}{\alpha}\, e_f^T \Gamma^{-1} \dot{f}_a \leq \frac{1}{\alpha\theta} e_f^T G e_f + \frac{\theta}{\alpha} f_a^2 \lambda_{max}(\Gamma^{-1} G^{-1} \Gamma^{-1}) \tag{4-22}$$

Substituting (4-22) into (4-21), $\dot{V}$ can be reformulated as:

$$\dot{V} = \varphi^T \, \Xi \, \varphi + \delta \tag{4-23}$$

where,

$$\varphi = \begin{bmatrix} e_x \\ e_f \end{bmatrix}, \qquad \delta = \frac{\theta}{\alpha} f_a^2 \lambda_{max}(\Gamma^{-1} G^{-1} \Gamma^{-1}),$$

$$\Xi = \begin{bmatrix} PN + N^T P & -\frac{1}{\alpha} N^T P(TF_a) \\ * & -2\frac{1}{\alpha}(TF_a)^T P(TF_a) + \frac{1}{\alpha\theta} G \end{bmatrix}$$

(TF_a) is full column rank, under the condition of $\Xi < 0$, and $\epsilon = \lambda_{min}(-\Xi)$, then:

$$\dot{V} < -\epsilon \|\varphi\|^2 + \delta \tag{4-24}$$

for

$$\delta < \epsilon \|\varphi\|^2 \tag{4-25}$$

Then, it follows that:

$$\dot{V} < 0 \tag{4-26}$$

In terms of (4-24) & (4-25), (4-26) indicates that e_x and e_f converge to a small set of δ.

This ends the proof.

If the fault signal is defined as:

$$f_a(t) = \begin{cases} 0 & t \in [0,\ t_f) \\ f_a(t) & t \in [t_f,\ \infty) \end{cases} \tag{4-27}$$

The FE signal $\hat{f}_a$ can be derived by (4-17) and given as:

$$\hat{f}_a = \Gamma M(r + \alpha \int_{tf}^{t} r\, d\tau) \tag{4-28}$$

From (4-28), it can be seen that the $\hat{f}_a$ includes both proportional and integral actions. The proportional part enhances the fault estimator dynamic performance giving improved FE speed as well as relaxing the constraint with zero value of first derivative of the estimated fault.

Remark 4.1: Although (4-15) can be solved easily via the Matlab LMI tool box, the simultaneous solution of (4-15) and (4-16) is difficult to achieve using functions in the LMI tool box. However, the problem can be solved by reformulating (4-16) into (4-29), as an inequality optimisation problem (Corless and Tu, 1998):

$$\begin{bmatrix} -\gamma I & (TF_a)^T P - MC \\ * & -\gamma I \end{bmatrix} < 0 \tag{4-29}$$

The RFAFE derivation is complete with proof of stability.

4.2.2 Regulation of $\mathcal{D}$-stable theory on RFAFE

Apart from guaranteeing the observer stability, the observer dynamic response plays an important role in obtaining a qualified observer performance achieved by forcing the poles to lie within suitable complex plane sub-regions comprising either vertical strips, discs, conic sectors etc. (or their combinations) using LMIs optimisation (Chilali and Gahinet, 1996). Here, the disc and ζ-stability regions are employed as a further refinement to improve the fault estimator dynamics with LMIs defined as:

Definition 4.2: N is defined as in (4-7). Let $\mathcal{D}$ be an LMI sub-region with characteristic function in the left hand side of the complex plane as a disc of radius r and centre $(-q, 0)$. Then there exist an S.P.D matrix P such that:

$$\begin{pmatrix} -rP & qP + N^T P \\ * & -rP \end{pmatrix} < 0 \qquad P > 0 \tag{4-30}$$

Then, N is called disc–stable.

Definition 4.3: N is defined as in (4-7). Let $\mathcal{D}$ be a subregion which presents a ζ-stability region in the left-half plane. $\mathcal{D}$ is an LMI region with characteristic function, so that there exists an S.P.D matrix P such that:

$$N^T P + PN + 2\zeta P < 0 \qquad P > 0 \tag{4-31}$$

Then, N is called ζ–stable. Figure 4-1 shows the RFAFE poles assignment within a sub-region $\mathcal{D}$ of an intersection between a specified disc and ζ-stability regions by solving (4-30) & (4-31).

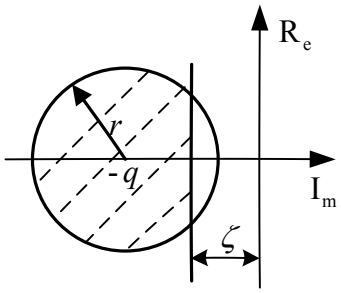

Figure 4-1 $\mathcal{D}$-subregion (hatched)

Consequently, a complete RFAFE with UI de-coupling can be designed by solving (4-15), (4-29), (4-30), (4-31) and conditions (4-4)–(4-8), together with Theorem 4.2.

4.3 RFAFE application on a commercial aircraft

In this Chapter, the RFAFE design is implemented on a generic AIRBUS aircraft model to estimate the left elevator OFC fault. This typical fault is an actuator fault modelled as a discrepancy between the computed control input signal and the delivered actuator input value.

4.3.1 OFC fault scenario

One of the often considered fault scenarios is the OFC {sometimes referred to as the "oscillatory failure case"} which can be caused, for example by electronic system component faults (Goupil, 2010). The moving flight surface of the aircraft can sometimes experience oscillation generated within the servo-loop control, i.e. between the FCC and the actual control surface itself. The spurious sinusoidal signals can propagate through the FCC and hence the control surface, as shown in Figure 4-2. As the

fault is a local phenomenon within a single actuator, it only has an impact on one control surface.

Two types of OFC are classified, the “liquid” and “solid” faults. The liquid fault is considered as an additive fault which adds to the control command inside the control loop. The solid fault is considered as a ‘disconnected’ fault which substitutes the control command completely inside the control loop. Both of these two OFC faults lead to the control surface performing with a spurious control command. In this project, the OFC faults are simulated as sinusoidal signals within a range of magnitudes and frequencies. The estimated OFC fault signals are normalized into the entire interval [0, 1] according to the elevator control surface deflection range of operation. In this Section, the OFC signals 0.016 and 0.33 (in normalized units) are estimated to (a) demonstrate the effect that the OFC has on the elevator operation and (b) the effectiveness of the RFAFE design.

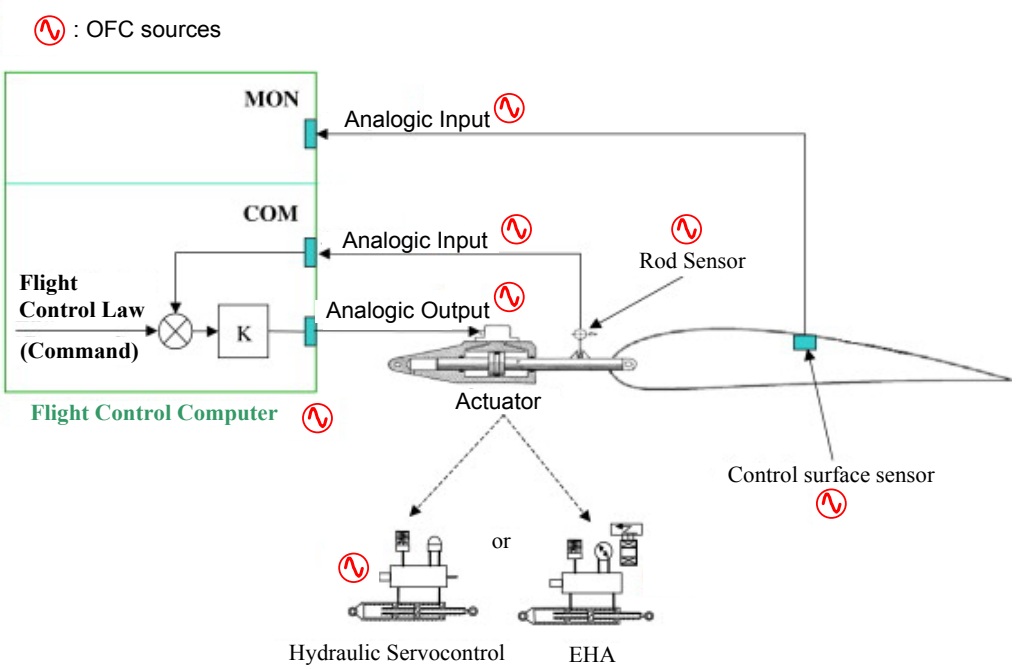

Figure 4-2 OFC source location in the control loop (Goupil, 2010)

Note: In Figure 4-2, a command channel (COM) and a monitoring channel (MON) are the two parts of flight-by-wire FCC.

4.3.2 Simulation results

The first step of the RFAFE design is to estimate the UI distribution matrix as an off-line analysis. The modelling uncertainties between the nominal nonlinear aircraft model and the LTI aircraft longitudinal model are considered as a UI. The off-line design for E_u estimation is made by running the ADDSAFE benchmark model as introduced in Section 3.4. The lower rank technique via the SVD approach is applied to post-process the modelling uncertainty data, so that condition (1) in Theorem 4.1 is satisfied. The design described in this Section uses the same aircraft longitudinal LTI model as that in Section 3.4. The corresponding operating point has been given in Table 3-1. The design approach described here uses the same notation for E_u as derived in Section 3.4.

The second step of the RFAFE design is to construct the UI de-coupling fast adaptive estimator in terms of the matrix E_u estimated in step 1. A set of conditions should be satisfied first and a group of LMIs should be solved, as discussed in Section 4.2. The left elevator fault direction F_a is the first column of $B = [B_G, B_D]$, i.e. $F_a = B_G$.

Figure 4-3 & 4-4 show the left elevator control surface position for two fault cases compared with the fault-free case, respectively. The control surface deflection is apparent, i.e. the OFC fault leads to unwanted control surface oscillation.

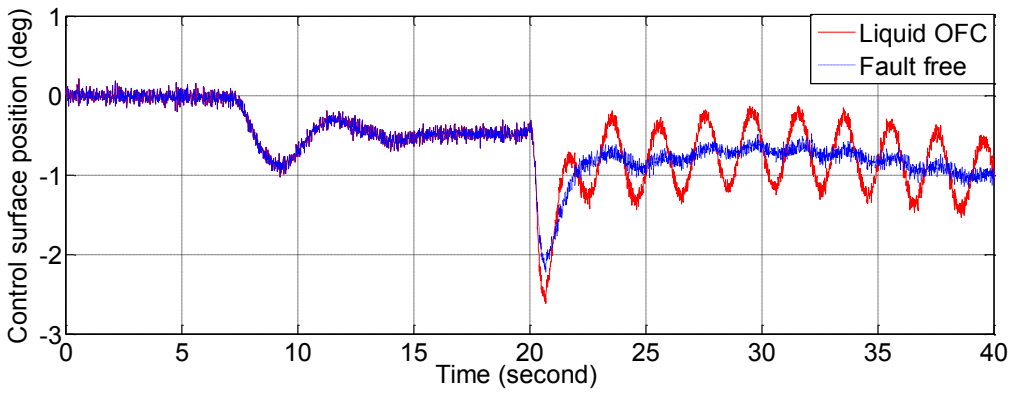

Figure 4-3 Left elevator control surface position (liquid OFC & fault-free cases)

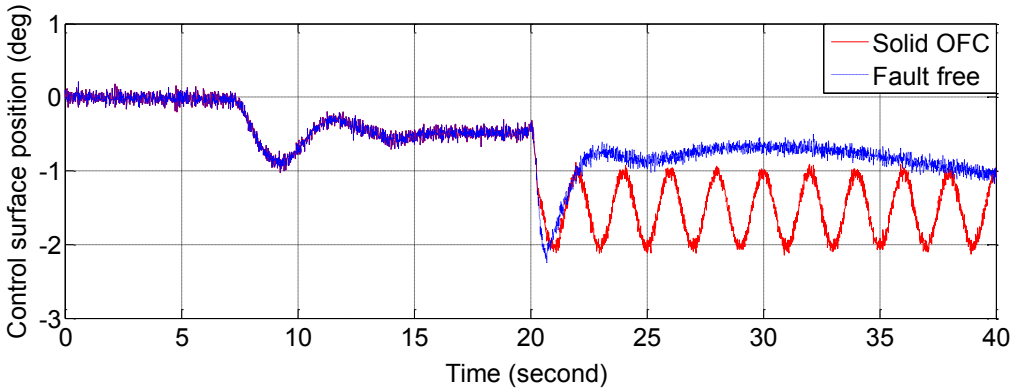

Figure 4-4 Left elevator control surface position (solid OFC and fault-free cases)

Figure 4-3 corresponds to the liquid OFC. A sinusoidal signal is added to the normal control surface position. Figure 4-4 shows the control surface movement trajectory is totally substituted by a sinusoidal signal for the solid OFC "disconnection" behaviour.

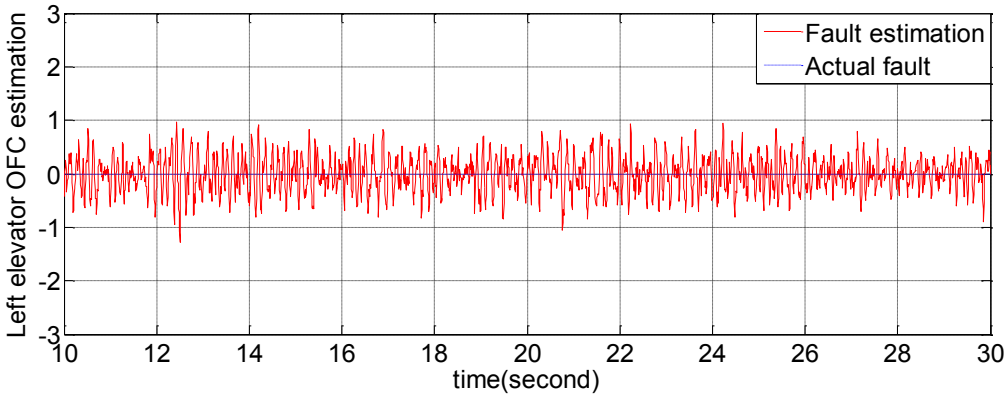

Figure 4-5 Left elevator FE signal for the fault-free case

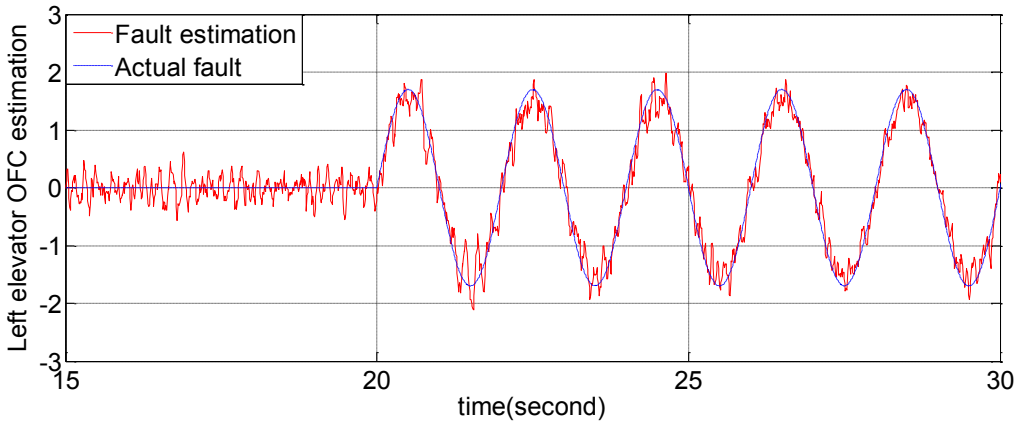

Figure 4-6 Left elevator FE signal for the liquid OFC fault

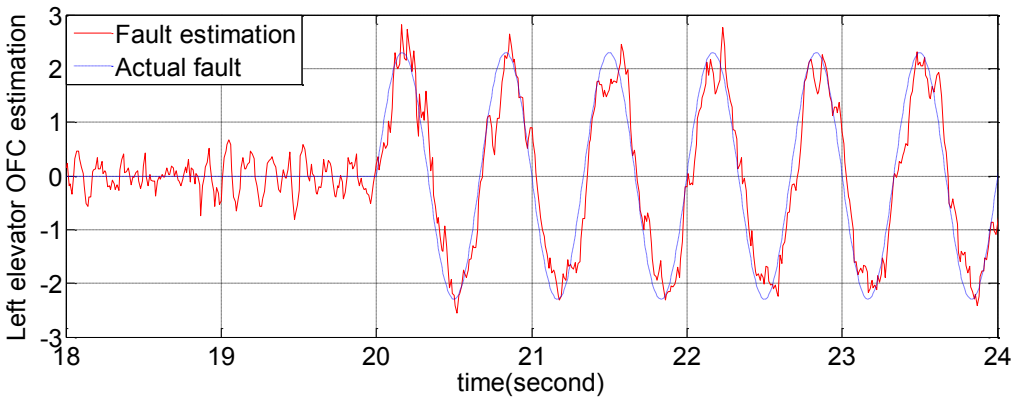

Figure 4-7 Left elevator FE signal for the Solid OFC fault

Figure 4-5 shows that in the fault-free case (left elevator) the estimates are comparable with the noise level. In Figures 4-6 & 4-7, the estimation of the so-called liquid OFC (0.016 OFC) and solid OFC (0.033 OFC) are shown, respectively. For each fault scenario, the faults occur at 20s and the FE signals track the actual fault signals in magnitude and frequency.

The RFAFE design learning rate is tuned to a suitable value to achieve accurate and fast FE. It can also be seen that the FE signal is not significantly affected by the modelling uncertainties, but is influenced by high frequency sensor noise. Hence, the FE signal obtained is considered robust to modelling uncertainties.

4.4 Conclusion

In this Section, the RFAFE approach to fast FE response has been applied to the problem of an aircraft actuator OFC, taking modelling uncertainties into account through UI estimation. The UI reflects the modelling mismatch between the linear and nonlinear aircraft systems and the UI estimation provides a structured approach to robust FE design. The UI estimation is completed off-line considering a range of flight conditions with the UI de-coupling utilized in the RFAFE design. The results show that the signals track the actual fault signals accurately under both liquid and solid OFC faults in different magnitudes and frequencies, demonstrating the effectiveness and efficiency of the RFAFE method.

As pointed out in Section 4.3.2, the measurement noise signals are not taken into account in this RFAFE design. Hence, in Chapter 5, the work is to develop a robust UI-PIO design which enables to de-coupling the UI from FE signals as well as to

minimise the effect of measurement noise on the FE signals using the H_∞ optimisation approach.

Chapter 5

Robust Actuator Multiplicative FE with UI De-coupling for a Wind Turbine System[2]

5.1 Introduction •

The residual generation-based FDI and FE-based FDD designs described in Chapters 3 & 4 are constructed using a proportional Luenberger UIO framework relying on current state estimation information. In these approaches, the steady state estimation error cannot be avoided due to an only proportional gain in observer design. In this Chapter, an integral gain will be inserted into the observer to achieve a better state estimation performance.

The earliest work on PIO was described by (Wojciechowski, 1978) for single input single output (SISO) LTI systems. Following this several studies proposed approaches focussed on multivariable systems (Kaczorek, 1979; Shafai and Carroll, 1985; Saif, 1993; Busawon and Kabore, 2000). (Shafai and Carroll, 1985) explored the properties of the PIO further with the purpose of improving the robustness against slow time-varying parameter variations and step disturbances. In (Söffker, Yu and Müller, 1995), the proposed PIO is capable of estimating the state of a system with arbitrary UI. Studies of the application of PIO to the FE problem have been described in (Shafai, Pi and Nork, 2002; Marx, Koenig and Georges, 2003; Xiong and Saif, 2003). In (Koenig and Mammar, 2002), PIO with UI de-coupling strategy was used to handle the robustness against the effect of UI acting on the system states. In (Marx, Koenig and Georges, 2003), H_∞ theory was adopted to attenuate the effect of the disturbance acting in the estimation error. Also, studies on PIO for descriptor system designs can be seen in (Marx, Koenig and Georges, 2003; Wu and Duan, 2006; Gao, Breikin and Wang, 2008; Hamdi, Mickael, Chokri, Theilliol and Naceur Benhadj, 2012).

It is noticed that among these studies, the sensor noise acting on the measurement is rarely taken into account in the PIO design. However, in some practical applications,

[2]The work proposed in this chapter has been published in: Sun, X., Patton, R. J., Robust actuator multiplicative fault estimation with unknown input decoupling for a wind turbine system. IEEE Conference on Control and Fault-Tolerant Systems SysTol'13, October 9-11, 2013, Nice, France (accepted)

sensor noise can be problematic for FDI/FDD design since the FE signal reconstruction requires the measurement information. For instance, the measurements of a wind turbine system can be severely influenced by sensor noise which can degrade the FDI/FDD as well as the state estimation performance. It is interesting that only a few studies on PIO designs involving sensor noise have been reported in the literature using designs that are strictly constrained by a number of idealised assumptions. Specifically, in (Saif, 1993), a PIO design for a monitored system with constant measurement disturbances was proposed. In (Busawon and Kabore, 2001), their PIO is only applied to minimise a certain bounded noise in a single output system. These papers indicated that further research in PIO design would be required that should be based on more practical considerations to take into account a variety of measurement noises for more general applications.

This Chapter develops a robust PIO design with the capability of attenuating the measurement noises and de-coupling the effects of the UI signals on the FE signals. Hence, a Unknown input-proportional integral observer (UI-PIO) system for fault and state estimation is proposed in which the faults are appended as additional states in an augmented system structure.

As an example, an LTI wind turbine model is chosen to build the proposed UI-PIO. The LTI wind turbine model is derived from a nonlinear wind turbine benchmark model described in (Odgaard, Stoustrup and Kinnaert, 2009). The nonlinear benchmark model (assumed to emulate the dynamic behaviours of a real wind turbine) operates in the high wind speed range and linearisation is made corresponding to a wind speed of 16m s^{-1} in its range. The linearised model is then used in the UI-PIO design. Modelling uncertainties relating to the wind force are derived via the linearisation, since the appropriate partial derivatives are available. As a consequence, both the linearisation error and exogenous disturbance (the wind force) are derived as UI signals. Therefore, the UI de-coupling principle is utilized to remove the UI effect from the FE signals corresponding to abnormal parameter changes in the wind turbine dynamics. The effects of output measurement noise signals acting on the rotor speed, generator speed and actuator pitch angle sensors are minimised in the FE signals by combined use of H_∞ optimisation to enhance the FE robustness.

In order to achieve a required FE performance, the observer poles are regulated using the $\mathcal{D}$ sub-region pole assignment. Parametric changes are multiplicative faults, which are estimated by this scheme. To facilitate the FE design by the proposed observer a modification is required to transform the multiplicative faults into additive fault format acting on the system states. An application example of a hydraulic leakage fault occurring on a three blade horizontal wind turbine pitch system is provided to demonstrate the efficiency of the proposed estimation methodology. The leakage affects the values of the pitch actuator damping and natural frequency parameters.

5.2 Review of wind turbine FDI/FDD application

It is noticeable that the focus on renewable energy sources has significantly increased due to the limitation of fossil-based fuels and environmental contamination of the usages of these fuels. Wind power is currently showing a lot of promise in certain regions of the world and there has been an explosion in the development of the appropriate wind turbine technologies for both off-shore and on-shore applications. In certain regions offshore wind power has become very important, e.g. in the North sea (Wikipedia, 2013) and Irish sea (Wikipedia, 2012). The various technologies for offshore wind power face significant challenges which have led to new research and development into attractive systems and structural design and manufacturing methods.

However, with the increasing demands from the wind turbine, new problems have to be overcome. For instance, some new technologies are not fully tested before going to application and the designed performance is sometimes hard to demonstrate. In this context, a survey given by (Ribrant and Bertling, 2007) discusses the issue of failures occurring on wind turbine systems in Sweden, Finland and Germany based on the maintenance records. (Hameed, Hong, Cho, Ahn and Song, 2009) and (Lu, Li, Wu and Yang, 2009) review the general fault scenarios as well as the state of art techniques for the monitoring system for faults on wind turbine system. There is no doubt that the performance and operational safety of wind turbine systems can be significantly degraded when faults occur, decreasing the efficiency and availability or sustainability of the wind power for transmission into the electrical grid system. Hence, the issues of improving the safety, reliability and sustainability of offshore wind turbine are considered necessary and valuable.

Motivated by all the aforementioned issues, real-time FDD or FDD related-AFTC schemes on wind turbine components have attracted much attention with the purpose of enhancing the reliability and reducing the operations and maintenance costs. This is especially true for offshore wind turbine installations due to challenging access restrictions.

(Pourmohammad and Fekih, 2011) provide a general review of the primarily concepts and issues corresponding to the development of FTC schemes for wind turbines including fault diagnosis. (Odgaard, Stoustrup and Kinnaert, 2009) describe a wind turbine benchmark model which is a useful tool for FDD/FTC analysis and design studies. Attractive competitions have been launched based on this benchmark model system for (a) FDD robustness in 2011, (b) FTC design in 2012, (c) FDD/FTC for wind farms (Kk-Electronic, 2013). An international workshop "Sustainable Control of Offshore Wind Turbines" was held at Hull University in September 2012 (Turbine-control-workshop, 2012). A significant number of useful papers on this subject have been presented and published. For example, (Sloth, Esbensen and Stoustrup, 2011) have described an interesting study of the use of LPV model-based FDD/FTC design and (Sami and Patton, 2012) describe an approach to FTC for a wind turbine systems using T-S fuzzy modelling (in control and FE).

Focusing on FDD (Odgaard and Stoustrup, 2010) use a conventional residual based-UIO to detect three different sensor faults (rotor, generator and the converter). (Wei and Liu, 2010) describe an H_∞ filter (in the finite frequency domain) design for sensor fault detection. (Zhang, Zhang, Zhao, Ferrari, Polycarpou and Parisini, 2011) described a unified adaptive method to detect sensor and actuator faults. In (Wei, Verhaegen and van Engelen, 2010), the blade root moment sensor faults are detected by using residual-based dual Kalman filters. (Chen, Ding, Sari, Naik, Khan and Yin, 2011) use the Kalman filter approaches to detect pitch actuator and sensor faults. (Esbensen and Sloth, 2009) explore the use of an extended Kalman filter to estimate the paramter faults of a three blade horizontal wind turbine pitch system. In this Chapter, the same paramter faults caused by hydraulic leakage are estimated by an observer-based FE approach, i.e. using a UI-PIO. It is shown that this leads to acceptable FE performance. Additionally, the design provides a way to estimate the parameter variations using

observer-based methods instead of stochastic estimator methods such as the extended Kalman filter.

5.2.1 Actuator additive FE with UI-PIO

Before introducing the proposed UI-PIO, an LTI system with additive actuator fault $F_a f_a$ (all sensors are assumed to be fault-free) and exogenous disturbance expressed by the UI term $E_u d_u$ is represented firstly as:

$$\left.\begin{aligned} \dot{x} &= Ax + Bu + E_u d_u + F_a f_a \\ y &= Cx \end{aligned}\right\} \tag{5-1}$$

where, $x \in \Re^n$ denotes the system state vector, $u \in \Re^r$ denotes the input vector, $y \in \Re^m$ is the measurement vector, $d_u \in \Re^p$ is UI vector, $f_a \in \Re^l$ is actuator fault. A, B, C are known system matrices with appropriate dimensions. $E_u \in \Re^{n \times p}$ denotes the UI distribution matrix, $F_a \in \Re^{n \times l}$ denotes the fault distribution matrix with full rank.

An augmented state observer is considered to estimate the actuator fault f_a. Assume that $\dot{f}_a = 0$, i.e. f_a is a slowly time-varying vector. Then the system model can be expressed in an augmented form as:

$$\left.\begin{aligned} \dot{x}_a &= A_a x_a + B_a u + E_a d_a \\ y &= C_a x_a \end{aligned}\right\} \tag{5-2}$$

where, $x_a = \begin{bmatrix} x \\ f_a \end{bmatrix}$, $A_a = \begin{bmatrix} A & F_a \\ 0 & 0 \end{bmatrix}$, $B_a = \begin{bmatrix} B \\ 0 \end{bmatrix}$, $E_a = \begin{bmatrix} E_u \\ 0 \end{bmatrix}$, $C_a = [C \quad 0]$.

If the system inputs and outputs $\{u, y\}$ are available, a functional observer (5-3) of the system (5-2) is constructed as (5-3) to estimate the f_a:

$$\left.\begin{aligned} \dot{z} &= Nz + TB_a u + Ky \\ \hat{x}_a &= z + Hy \end{aligned}\right\} \tag{5-3}$$

where, $\hat{x}_a \in \Re^{\bar{n}}$ is the estimated state vector and $z \in \Re^{\bar{n}}$ is the augmented observer state vector with $\bar{n} = n + l$. Note that , T, K and H are design matrices.

Definition 5.1: Observer (5-3) is defined as a robust UI-PIO for the system (5-2), if its state estimation error $e_x = x_a - \hat{x}_a$ converges to zero asymptotically, regardless of the presence of the UI and faults in the system.

Assuming that E_a is known, the estimation error dynamics are governed by the equation:

$$\begin{aligned}\dot{e}_x = {} & (A_a - HC_aA_a - K_1C_a)e_x \\ & +[N - (A_a - HC_aA_a - K_1C_a)]z \\ & +[K_2 - (A_a - HC_aA_a - K_1C_a)H]y \\ & +[T - (I - HC_a)]B_au \\ & +(HC_a - I)E_ad_u \end{aligned} \tag{5-4}$$

where,

$$K = K_1 + K_2 \tag{5-5}$$

If the following relations are satisfied:

$$(HC_a - I)E_a = 0 \tag{5-6}$$

$$T = HC_a - I \tag{5-7}$$

$$N = A_a - HC_aA_a - K_1C_a = A_1 - K_1C_a \tag{5-8}$$

$$K_2 = NH \tag{5-9}$$

Then the state estimation error is rearranged to be:

$$\dot{e}_x = Ne_x \tag{5-10}$$

$$e_y = C_ae_x \tag{5-11}$$

If all the eigenvalues of N are stable, $e_x(t)$ will approach zero asymptotically, i.e. $\hat{x}_a \rightarrow x_a$. The observer (5-3) is a UI-PIO for an additive actuator FE of the system (5-2) when conditions (5-5) to (5-9) are satisfied. Therefore, this observer design involves the solution of (5-5) to (5-9) whilst placing all the eigenvalues of the system matrix N on the left half of complex plane. Meanwhile, N, T, K and H in (5-3) are designed to achieve the required FE performance.

A particular solution to (5-6) can be sought as defined by (Chen and Patton, 1999):

$$H = E_a(C_aE_a)^+ \tag{5-12}$$

where, $(C_aE_a)^+ = [(C_aE_a)^T(C_aE_a)]^{-1}(C_aE_a)^T$ denotes the Moore-Penrose pseudo-inverse.

Theorem 5.1: (Chen and Patton, 1999). The necessary and sufficient conditions for the existence of UI-PIO for the system (5-2) based on functional observer (5-3) are:

(1) $rank(C_aE_a) = rank(E_a)$

(2) (C_a, A_1) is a detectable pair

5.2.2 Measurement noise attenuation by H_∞ theory

A UI-PIO for additive actuator FE has been introduced in Section 5.2.1 without consideration the of the output measurement sensor noise. In this sub-section, the sensor noise is taken into account and the H_∞ optimisation is applied to minimise the influence of the sensor noise on the FE signal based on the proposed observer in Section 5.2.1. Hence, a new robust UI-PIO is constructed. In order to enhance the observer dynamic performance, the $\mathcal{D}$ sub-region pole assignment method is explored to regulate the pole locations.

When the output measurement is corrupted by sensor noise, (5-1) is re-written as:

$$\left.\begin{aligned} \dot{x} &= Ax + Bu + E_u d_u + F_a f_a \\ y &= Cx + E_s d_s \end{aligned}\right\} \tag{5-13}$$

$d_s \in \Re^m$ represents the sensor noise. E_s is the distribution matrix of the sensor noise.

The augmented state observer (5-3) are reorganised as follows:

$$\left.\begin{aligned} \dot{x}_a &= A_a x_a + B_a u + E_a d_a \\ y &= C_a x_a + E_s d_s \end{aligned}\right\} \tag{5-14}$$

where, $x_a = \begin{bmatrix} x \\ f_a \end{bmatrix}$, $A_a = \begin{bmatrix} A & F_a \\ 0 & 0 \end{bmatrix}$, $B_a = \begin{bmatrix} B \\ 0 \end{bmatrix}$, $E_a = \begin{bmatrix} E_u \\ 0 \end{bmatrix}$, $C_a = [C \quad 0]$.

By using the same functional observer as (5-3), the state estimation error dynamics of (5-14) based on the theory in Section 5.2.1 are obtained as:

$$\dot{e}_x = Ne_x - K_1E_sd_s - HE_s\dot{d}_s \tag{5-15}$$

$$e_y = Ce_x + E_sd_s \tag{5-16}$$

The observer design considering both the influence of exogenous disturbance and sensor noise involves the solution of (5-5) to (5-9) with assignment of all the eigenvalues of the system matrix N to be stable. The design parameters are N, T, K and H in (5-3).

The sensor noise present in (5-15) & (5-16) affects the system estimation error which can degrade the FE performance. Here, H_∞ optimisation theory is used to minimise the sensor noise effect to improve the robustness of the proposed UI-PIO.

Theorem 5.2: For a given positive constant γ_0, if there exists an S.P.D matrix P and a matrix M, such that the LMI (5-17) holds, then a robust UI-PIO defined by (5-3) for (5-14) is solvable with the gain $K_1 = P^{-1}M$. The state estimation error dynamics (5-15) are robustly stable and the H_∞ norm of the output estimation error satisfies $\|e_y\|_2 < \gamma_0\|\omega_d\|_2$ for any nonzero $\omega_d \in l_2[0, \infty)$, where:

$$\begin{bmatrix} \Xi & -PK_1E_s + C_a^TE_s & -PHE_s \\ * & E_s^TE_s - \gamma_0 I & 0 \\ * & * & -\gamma_0 I \end{bmatrix} < 0 \tag{5-17}$$

with $\Xi = PA_1 + A_1^TP - MC_a - M^TC_a^T + C_a^TC_a$, $\omega_d = [d_s \quad \dot{d}_s]$, $*$ denotes a symmetric term.

***Proof*:** Consider the following Lyapunov function:

$$V = e_x^TPe_x \tag{5-18}$$

According with $\dot{e}_x$ derived in (5-15), the time derivative of the candidate Lyapunov function $\dot{V}(e_x)$ for the system (5-15) is derived as:

$$\begin{aligned} \dot{V} &= 2e_x^TP\dot{e}_x \\ &\leq e_x^T[P(A_1 - K_1C_a) + (A_1 - K_1C_a)^TP]e_x \\ &\quad -2e_x^TPK_1E_sd_s - 2e_x^TPHE_s\dot{d}_s \end{aligned}$$

$$= \begin{bmatrix} e_x \\ d_s \\ \dot{d}_s \end{bmatrix}^T \begin{bmatrix} \Theta & -PK_1E_s & -PHE_s \\ * & 0 & 0 \\ * & * & 0 \end{bmatrix} \begin{bmatrix} e_x \\ d_s \\ \dot{d}_s \end{bmatrix} \quad (5\text{-}19)$$

where, $\Theta = P(A_1 - K_1C_a) + (A_1 - K_1C_a)^T P$, $*$ denotes a mean symmetric term.

Define

$$J = \int_0^\infty e_y^T e_y - \gamma_0^2 \omega_d^T \omega_d] \, dt \quad (5\text{-}20)$$

$$J \leq \int_0^\infty [e_y^T e_y - \gamma_0^2 \omega_d^T \omega_d] + \dot{V} dt \quad (5\text{-}21)$$

$$J \leq \int_0^\infty \phi^T X \phi dt \quad (5\text{-}22)$$

where, $\phi = [e_x \quad d_s \quad \dot{d}_s]^T$

$$X = \begin{bmatrix} \Xi & -PK_1E_s + C_a^T E_s & -PHE_s \\ * & E_s^T E_s - \gamma_0 I & 0 \\ * & * & -\gamma_0 I \end{bmatrix} \quad (5\text{-}23)$$

with, $\Xi = P(A_1 - K_1C_a) + (A_1 - K_1C_a)^T P + C_a^T C_a$.

Let $K_1 = P^{-1}M$, then Ξ can be re-written as:

$\Xi = PA_1 + A_1^T P - MC_a - M^T C_a^T + C_a^T C_a$.

where, $*$ denotes a symmetric term. $X < 0$ is equal to $\|e_y\|_2 < \gamma_0 \|\omega_d\|_2$ for any nonzero $\omega_d \in l_2[0, \infty)$. Hence, for $P > 0$, the robust UI-PIO is quadratically stable with the dynamical output error satisfying $\|e_y\|_2 < \gamma_0 \| \omega_d\|_2$.

This completes the proof.

In the following, a disc LMI region (Chilali and Gahinet, 1996) is defined to regulate the robust augmented fault estimator poles.

Definition 5.2: Θ is defined as that in Theorem 5.2. Let $\mathcal{D}$ be a sub-region which represents a disc of radius r and centre $(-q, 0)$ in the left-half plane. $\mathcal{D}$ is an LMI region with characteristics of disc function. There exists an S.P.D matrix P such that

$$\begin{pmatrix} -rP & qP + \Theta^T \\ * & -rP \end{pmatrix} < 0 \qquad P > 0 \tag{5-24}$$

Then, Θ is referred to as disc–stable.

Based on the Definition 5.1, the poles of the proposed UI-PIO can be assigned in the disc LMI region by solving (5-24) to regulate the FE performance. Consequently, a robust UI-PIO with the effect of the sensor noise in the estimation error e_x can be designed by solving (5-17), (5-24) and conditions (5-5)–(5-9) subject to Theorem 5.1.

5.2.3 Transformation from multiplicative fault to additive fault

The component fault which is expressed as a multiplicative fault can be reformulated into an additive fault format. Then, the actuator component FE can be realised by using the additive FE theory introduced in Sections 5.2.1 & 5.2.2. In the following, a wind turbine state representation with a multiplicative fault in the pitch system actuator described by (5-25) is re-written by (5-26) in a form containing a pitch system actuator additive fault.

Consider a system with multiplicative fault in the system matrix A described as:

$$\left.\begin{aligned} \dot{x} &= (A + \Delta A_f)x + Bu + E_u d_u \\ y &= Cx + E_s d_s \end{aligned}\right\} \tag{5-25}$$

By rewriting (5-25) in an actuator additive fault format:

$$\left.\begin{aligned} \dot{x} &= Ax + Bu + E_u d_u + F_a f_a\,(x,t) \\ y &= Cx + E_s d_s \end{aligned}\right\} \tag{5-26}$$

where,

$$F_a f_a\,(x,t) = \Delta A_f x \tag{5-27}$$

In general formulation, F_a is a matrix whose columns represent the fixed fault directions. $f_a\,(x,t)$ is the re-constructed fault which has an affine dependence on the faulty parameters. The transformation will be used to estimate the wind turbine hydraulic leakage fault scenario described in Section 5.4.

5.3 Robust UI-PIO based FE on a wind turbine

In this Section，the faults occurring on the pitch system dynamics are detected and estimated by using the UI-PIO strategy proposed in Section 5.2. The design facilitates an extension of the observer-based FDD scheme not only to estimate additive faults but also to enable multiplicative faults to be estimated, for example in the parameter estimation problem of the wind turbine pitch actuator system. In this example, the UI de-coupling principle is used to de-couple the UI (in this case the so-called wind speed) signal from the FE signals.

A 4.8 MW Offshore wind turbine benchmark system developed by (Odgaard, Stoustrup and Kinnaert, 2009) operating in the high wind speed region is used for the proposed FE design. The corresponding wind turbine MATLAB/SIMULINK model with required parameters is available from (Odgaard, Stoustrup and Kinnaert, 2009; and Sloth, Esbensen and Stoustrup, 2011; Kk-Electronic, 2013). In this simulation model, the wind turbine actuator hydraulic leakage fault scenario is estimated by using the proposed robust augmented actuator additive fault estimator.

5.3.1 Wind turbine model description

The wind turbine benchmark system is represented by its nonlinear behaviour and a stochastic uncontrollable wind force as a driving signal. A three blade horizontal wind turbine model comprising the aerodynamic, drive train and power and pitch system models is described as follows (Odgaard, Stoustrup and Kinnaert, 2009).

The aerodynamic model

The aerodynamic torque T_a represents the source of the nonlinear nature of the wind turbine aerodynamics. T_a depends on the rotor speed ω_r, the blade pitch angle β and the effective wind speed v_r.

The power available from the wind passing through the entire rotor swept area can be expressed as:

$$P_w = \frac{1}{2}\rho A_R v_r^3 = \frac{1}{2}\rho\pi R^2 v_r^3 \tag{5-28}$$

$A_R = \pi R^2$ is the rotor swept area [m^2]

P_w is the power available from the wind [W]

v_r is the rotor effective wind speed [m s^{-1}]

ρ is the air density [kg m^{-3}]

R is the radius of the rotor [m]

C_p is the power coefficient which depends on the blade pitch angle β and the tip-speed-ratio λ.

The aerodynamic power captured by the rotor is given by:

$$P_{cap} = \frac{1}{2}\rho\pi R^2 C_p(\lambda,\beta)v_r^3 = P_w C_p(\lambda,\beta) \quad (5\text{-}29)$$

P_{cap} is the power captured by the rotor [W]

β is the pitch angle [°]

λ is the tip-speed-ratio.

The tip-speed-ratio (λ) is defined as the ratio between the tip speed of the blades and the rotor effective wind speed:

$$\lambda = \frac{\omega_r R}{v_r} \quad (5\text{-}30)$$

where, ω_r is the rotor speed [rad s^{-1}].

The aerodynamic torque T_a acting on the blades is:

$$T_a = \frac{P_{cap}}{\omega_r} \quad (5\text{-}31)$$

$$T_a = \frac{1}{2}\rho\pi R^3 C_q(\lambda,\beta){v_r}^2 \quad (5\text{-}32)$$

where, C_q is the torque coefficient given as:

$$C_q = \frac{C_p}{\lambda} \quad (5\text{-}33)$$

The aerodynamic torque of (5-32) can be linearised as follows in order to provide and estimate of the hydraulic leakage fault described in Section 5.4 based on the theory in Section 5.2.

$$T_a = T_{a0} + \bar{T}_a \tag{5-34}$$

$$\bar{T}_a = \left.\frac{\partial T_a}{\partial v_r}\right|_{v_r=\bar{v}} \bar{v} + \left.\frac{\partial T_a}{\partial \beta}\right|_{v_r=\bar{v}} \bar{\beta} + \left.\frac{\partial T_a}{\partial \omega_r}\right|_{v_r=\bar{v}} \bar{\omega}_r \tag{5-35}$$

where, $\bar{T}_a$ is the deviation of rotor torque and $\left.\frac{\partial T_a}{\partial v_r}\right|_{v_r=\bar{v}}$, $\left.\frac{\partial T_a}{\partial \beta}\right|_{v_r=\bar{v}}$ and $\left.\frac{\partial T_a}{\partial \omega_r}\right|_{v_r=\bar{v}}$ are instantaneous partial derivatives of the aerodynamic torque, $\bar{v}$ is the deviation of v_r from an appropriate operating point. Finally, the linearised $\bar{T}_a$ is obtained as (5-35).

The drive train model

The drive train is responsible for scaling up the rotor rotational speed to a higher generator rotational speed. The drive train model includes low and high speed shafts linked together by a gearbox modelled as a gear ratio. The dynamics of the low-speed shaft is:

$$J_r \dot{\omega}_r = T_a - T_{ls} - B_r \omega_r \tag{5-36}$$

where, J_r is the rotor inertia, T_{ls} is the low speed shaft torque, and B_r is the rotor external damping.

The dynamics of the high speed shaft is:

$$J_g \dot{\omega}_g = T_{hs} - T_g - B_g \omega_g \tag{5-37}$$

where, J_g is the generator inertia, T_{hs} is the high speed shaft torque, B_g is the generator external damping, and ω_g is the generator speed. If an ideal gearbox with a ratio n_g is assumed and n_g is defined as:

$$n_g = \frac{T_{ls}}{T_{hs}} = \frac{\omega_g}{\omega_{ls}} \tag{5-38}$$

The drive train twisting is modelled using a torsion spring and a friction coefficient model, described as shown in:

$$T_{ls} = K_{dt}(\theta_r - \theta_{ls}) - B_{dt}\left(\dot{\theta}_r - \dot{\theta}_{ls}\right) \tag{5-39}$$

$$\theta_\Delta = \theta_r - \theta_{ls} = \theta_r - \frac{\theta_g}{n_g} \tag{5-40}$$

where, θ_Δ is the torsion angle, θ_r θ_g and θ_{ls} are the rotor side, generator side and gearbox side angular deviation respectively. The entire state space drive train model is described as:

$$\begin{bmatrix} \dot{\omega}_r \\ \dot{\omega}_g \\ \dot{\theta}_\Delta \end{bmatrix} = \begin{bmatrix} -\frac{B_{dt}+B_r}{J_r} & \frac{B_{dt}}{N_g J_r} & \frac{-K_{dt}}{J_r} \\ \frac{B_{dt}}{N_g J_g} & \frac{-\frac{B_{dt}}{N_g^2}-B_g}{J_g} & \frac{K_{dt}}{N_g J_g} \\ 1 & -\frac{1}{N_g} & 0 \end{bmatrix} \begin{bmatrix} \omega_r \\ \omega_g \\ \theta_\Delta \end{bmatrix} + \begin{bmatrix} \frac{1}{J_r} & 0 \\ 0 & -\frac{1}{J_g} \\ 0 & 0 \end{bmatrix} \begin{bmatrix} T_a \\ T_g \end{bmatrix} \tag{5-41}$$

The power system

The electrical power system basically consists of a generator and a converter, allowing variable speed operation. Currents flow in the generator is controlled using power electronics. The power electronic converters connect the wind turbine generator output to the local wind farm power network.

The converter dynamics can be modelled by a first order transfer function.

$$\frac{T_g(s)}{T_{g,r}(s)} = \frac{1}{1+\tau_g s} \tag{5-42}$$

where, $T_{g,r}$ is the reference for the generator torque and τ_g is the time constant of the first order generator dynamics:.

$$\dot{T}_g = -\frac{1}{\tau_g} T_g + \frac{1}{\tau_g} T_{g,r} \tag{5-43}$$

The power is produced by the generator which depends on the rotational speed of the rotor and the applied load. Then, the following equation is obtained as:

$$P_g = \eta_g \omega_g T_g \tag{5-44}$$

where, P_g is the power produced by generator, and η_g is the efficiency of the generator.

Pitch system model

The hydraulic pitch actuator adjusts the pitch of a blade by rotating it. It is modelled as a second order closed-loop transfer function with natural frequency $\omega_{n,0}$ and damping ratio ς.

$$\frac{\beta(s)}{\beta_r(s)} = \frac{\omega_{n,0}^2}{s^2+2\varsigma\omega_{n,0}s+\omega_{n,0}^2} \tag{5-45}$$

Using the transformation $\dot{\beta}_0 = \frac{1}{\omega_n^2}\dot{\beta}$, a wind turbine model working in the high speed region (above rated speed) is described as in (5-46) by linearising T_a as shown in (5-35) at a certain effective wind speed $v_r = \bar{v}$:

$$\dot{x} = A_w x + B_w \begin{bmatrix} T_{g,r} \\ \beta_r \end{bmatrix} + E_w v_w \tag{5-46}$$

where, $x = \begin{bmatrix} \omega_r & \omega_g & \theta_\Delta & \beta & \dot{\beta}_0 & T_g \end{bmatrix}^T$

$$A_w = \begin{bmatrix} a_{11} & \frac{B_{dt}}{n_g J_r} & -\frac{K_{dt}}{J_r} & a_{14} & 0 & 0 \\ \frac{B_{dt}}{n_g J_g} & a_{22} & \frac{K_{dt}}{n_g J_g} & 0 & 0 & -\frac{1}{J_g} \\ 1 & -\frac{1}{n_g} & 0 & 0 & 0 & 0 \\ 0 & 0 & 0 & 0 & \omega_{n,0}^2 & 0 \\ 0 & 0 & 0 & -1 & -2\varsigma_0\omega_{n,0} & 0 \\ 0 & 0 & 0 & 0 & 0 & -\frac{1}{\tau_g} \end{bmatrix},$$

where, $a_{11} = -\frac{(B_{dt}+B_r)}{J_r} + \frac{1}{J_r}\frac{\partial T_a}{\partial \omega_r}\Big|_{v_r=\bar{v}}$, $a_{14} = \frac{3}{J_r}\frac{\partial T_a}{\partial \beta}\Big|_{v_r=\bar{v}}$, $a_{22} = -\frac{(B_{dt}+n_g^2 B_g)}{n_g^2 J_g}$,

$$B_w = \begin{bmatrix} 0 & 0 & 0 & 0 & 0 & \frac{1}{\tau_g} \\ 0 & 0 & 0 & 0 & 1 & 0 \end{bmatrix}^T, E_w = \begin{bmatrix} \frac{3}{J_r}\frac{\partial T_a}{\partial v_r}\Big|_{v_r=\bar{v}} & 0 & 0 & 0 & 0 & 0 \end{bmatrix}^T, v_w = v_r - \bar{v}.$$

v_w is the wind speed error [m s^{-1}]. The corresponding values of the model parameters for system (5-46) are listed in Table 5-1.

Table 5-1 Model parameters for system (5-46)

$A_R = 10387$ m^2	$\rho = 1.225$ kg m^{-3}
$C_p(\lambda, \beta)$ is a coefficient which is not expressed as a mathematical function, but has to be looked up in a	$B_r = 27.8$ kNm (rad s^{-1})$^{-1}$

table given in (Sloth, Esbensen and Stoustrup, 2011)	
$B_{dt} = 945$ kNm $(\text{rad s}^{-1})^{-1}$	$B_g = 3.034$ Nm $(\text{rad s}^{-1})^{-1}$
$J_g = 390 \text{ kg m}^2$	$J_r = 55 \cdot 10^6 \text{ kg m}^2$
$N_g = 95$	$K_{dt} = 2.7$ GNm rad^{-1}
$T_g \in [0 \text{ Nm}, \ 35.3\text{kNm}]$	$\tau_g = 10$ ms
$\dot{T}_g \in [-50 \text{ MNm s}^{-1}, 50 \text{ MNm s}^{-1}]$	$\varsigma \quad = 0.6$
$\omega_{n,0} = 11.11$ rad s^{-1}	

Via linearising of T_a as shown in (5-35) at a certain effective wind speed $v_r = \bar{v}$, it can be seen that the linearisation error and exogenous disturbance (wind) are constructed in the structure of the unknown signals 'wind speed error v_w' and its distribution matrix E_w. Therefore, the $E_w v_w$ in (5-46) can be considered as UI signals and de-coupled via the UI de-coupling principle.

5.3.2 Wind turbine hydraulic leakage fault scenario

In the wind turbine system, variation in the hydraulic pressure affects the dynamics of the pitch system represented by changing the damping ratio and the natural frequency from their nominal values ς and $\omega_{n,0}$ to their values corresponding to the changed hydraulic pressure, i.e. ς_{lp} and $\omega_{n,lp}$. The hydraulic pressure change affects the control action of the wind turbine (Sloth, Esbensen and Stoustrup, 2011). The changes in parameters ς and $\omega_{n,0}$ are considered as component faults. According to Section 5.2.3 a component fault can always be expressed as a multiplicative fault and reconstructed into a state representation having an equivalent additive fault. Then, the actuator component FE can be realised by using the additive FE design approach introduced in Sections 5.2.1 & 5.2.2. The parameters ς and $\omega_{n,0}$ vary within the intervals $\varsigma_f \in [0.6, \ 0.9]$ and $\omega_{n,f} \in [11.11, 3.42]$ rad s^{-1} respectively.

In the following, a wind turbine state representation with pitch system actuator multiplicative fault in (5-47) is transformed into a state representation with the pitch system actuator additive fault structure as (5-48).

First, consider a system with multiplicative faults $\Delta A_f x$ in the system matrix A described as:

$$\left.\begin{aligned}\dot{x} &= (A+\Delta A_f)x + Bu + E_u d_u \\ y &= Cx + E_s d_s\end{aligned}\right\} \tag{5-47}$$

(5-47) is now re-written in the actuator additive fault format:

$$\left.\begin{aligned}\dot{x} &= Ax + Bu + E_u d_u + F_a f_a\,(x,t) \\ y &= Cx + E_s d_s\end{aligned}\right\} \tag{5-48}$$

where,

$$F_a f_a\,(x,t) = \Delta A_f x \tag{5-49}$$

F_a is the fault distribution direction, $f_a\,(x,t)$ is the constructed fault which is a time-varying signal related to the system states.

In the wind turbine benchmark supplied by Kk-Electronic, a hydraulic leakage is considered as one kind of pitch system actuator fault which affects the hydraulic pressure. The pitch actuator fault is derived as follows in multiplicative fault format.

In the fault-free case, $\Delta A_f = 0$

$$A_w = A \tag{5-50}$$

where, A_w is defined in (5-46).

In the fault case $\Delta A_f \neq 0$

$$A_w = A + \Delta A_f = \begin{bmatrix} a_{11} & \frac{B_{dt}}{n_g J_r} & -\frac{K_{dt}}{J_r} & a_{14} & 0 & 0 \\ \frac{B_{dt}}{n_g J_g} & a_{22} & \frac{K_{dt}}{n_g J_g} & 0 & 0 & -\frac{1}{J_g} \\ 1 & -\frac{1}{n_g} & 0 & 0 & 0 & 0 \\ 0 & 0 & 0 & 0 & \omega_n^2(\theta_f) & 0 \\ 0 & 0 & 0 & -1 & -2\varsigma(\theta_f)\omega_{n,0}(\theta_f) & 0 \\ 0 & 0 & 0 & 0 & 0 & -\frac{1}{\tau_g} \end{bmatrix} \tag{5-51}$$

where, $a_{11} = -\frac{(B_{dt}+B_r)}{J_r} + \frac{1}{J_r}\frac{\partial T_a}{\partial \omega_r}\Big|_{v_r\,(t)=\bar{v}}$, $a_{14} = \frac{3}{J_r}\frac{\partial T_a}{\partial \beta}\Big|_{v_r\,(t)=\bar{v}}$, $a_{22} = -\frac{(B_{dt}+n_g^2 B_g)}{n_g^2 J_g}$,

$$\omega_n^2(\theta_f) = (1-\theta_f)\omega_{n,0}^2 + \theta_f \omega_{n,hl}^2$$

$$= \omega_{n,0}^2 + \theta_f\left(\omega_{n,hl}^2 - \omega_{n,0}^2\right) \tag{5-52}$$

$$-2\varsigma(\theta_f)\omega_{n,0}(\theta_f) = -2(1-\theta_f)\varsigma\omega_{n,0} - 2\theta_f\varsigma_f\omega_{n,hl}$$

$$= -2\varsigma\omega_{n,0} + \theta_f(2\varsigma\omega_{n,0} - 2\varsigma_{hl}\omega_{n,hl}) \quad (5\text{-}53)$$

where, $\theta_f \in [0,1]$ is an indicator function for the fault with $\theta_f = 0$ corresponding to normal pressure i.e. for the fault-free case and $\theta_f = 1$ corresponding to the low pressure fault case. Therefore, the pitch system actuator component faults can be identified by estimating the variation in the parameter θ_f (Sloth, Esbensen and Stoustrup, 2011).

From (5-51) - (5-53), ΔA_f is given as:

$$\Delta A_f = \begin{bmatrix} 0 & 0 & 0 & 0 & 0 & 0 \\ 0 & 0 & 0 & 0 & 0 & 0 \\ 0 & 0 & 0 & 0 & 0 & 0 \\ 0 & 0 & 0 & 0 & \theta_f(\omega_{n,hl}^2 - \omega_{n,0}^2) & 0 \\ 0 & 0 & 0 & 0 & \theta_f(2\varsigma\omega_{n,0} - 2\varsigma_{hl}\omega_{n,hl}) & 0 \\ 0 & 0 & 0 & 0 & 0 & 0 \end{bmatrix} \quad (5\text{-}54)$$

In terms of (5-46), (5-49) can be expressed as:

$$F_a f_a(x,t) = \Delta A_f x$$

$$= \begin{bmatrix} 0 & 0 & 0 & \theta_f f_{41} & \theta_f f_{51} & 0 \end{bmatrix}^T \dot{\beta}_0$$

$$= [0 \quad 0 \quad 0 \quad f_{41} \quad f_{51} \quad 0]^T \theta_f \dot{\beta}_0 \quad (5\text{-}55)$$

where, $f_{41} = (\omega_{n,hl}^2 - \omega_{n,0}^2)$, $f_{51} = (2\varsigma\omega_{n,0} - 2\varsigma_{hl}\omega_{n,hl})$.

Then, the additive fault format is structured as in (5-51) and (5-54) by decomposing (5-55) as follows:

$$F_a = [0 \quad 0 \quad 0 \quad f_{41} \quad f_{51} \quad 0]^T \quad (5\text{-}56)$$

$$f_a(x,t) = \theta_f \dot{\beta}_0 \quad (5\text{-}57)$$

where, the fault distribution matrix F_a is in this case a constant vector. f_a is a time-varying fault coupled with the system states.

So far, the hydraulic leakage fault (multiplicative fault) of the pitch system is reorganized as an additive fault. Also, f_a and $\dot{\beta}_0$ can be estimated by using the UI-PIO

proposed in Section 5.2. Let $\hat{f}_a(x,t)$ and $\hat{\dot{\beta}}_0$ represent the estimation signals of $f_a(x,t)$ and $\dot{\beta}_0$, respectively. Then, the fault indicator signal θ_f can be estimated as follows:

$$\hat{f}_a(x,t) = \hat{\theta}_f \hat{\dot{\beta}}_0 \tag{5-58}$$

$$\hat{\theta}_f = \frac{\hat{f}_a(x,t)}{\hat{\dot{\beta}}_0} = \frac{\hat{\theta}_f \hat{\dot{\beta}}_0}{\hat{\dot{\beta}}_0} \qquad if\ \hat{\dot{\beta}}_0 \neq 0 \tag{5-59}$$

However, the particular case $\hat{\dot{\beta}}_0 = 0$ is hardly avoided since $\hat{\dot{\beta}}_0$ represents the estimation of $\dot{\beta}_0$. Therefore, the following modification to (5-59) is used to handle this problem as:

$$\hat{\theta}_f = sgn(\hat{\dot{\beta}}_0) \frac{\hat{\theta}_f \hat{\dot{\beta}}_0}{\left|\hat{\dot{\beta}}_0\right| + \sigma} \tag{5-60}$$

where, $\left|\hat{\dot{\beta}}_0\right| \gg \sigma$. A suitable σ should be chosen to guarantee a sufficiently close approximation to $\hat{\theta}_f$ (Tan and Edwards, 2004).

5.4 Simulation results

A 4.8 MW offshore wind turbine model operating in the high wind speed region is used for testing the proposed FE design. The corresponding wind turbine MATLAB/SIMULINK model with required parameters is available in (Kk-Electronic, 2013). In this simulation, the hydraulic leakage fault in the wind turbine pitch system is estimated by using the robust UI-PIO, described in Section 5.2.

The wind turbine model has been given in Section 5.3. The operating point in (5-35) is defined as the effective wind speed at 16m s^{-1}. The system measurable outputs are: rotor speed ω_r, and generator speed ω_g, pitch angle β, with the measurement noise modelled as a zero-mean white Gaussian noise (the standard deviation of $\delta_r = 0.025$ rad s^{-1}, $\delta_\beta = 0.2°$, $\delta_g = 0.0158$ rad s^{-1}). Two different levels of hydraulic leakage faults are estimated in the simulation. The corresponding parameter variation values in different fault levels as well as the fault-free case can be found in a look up table as given in Table 5-2.

Table 5-2 Parameter variations in hydraulic leakage fault scenario

Fault scenario	**Parameters**	$\boldsymbol{\theta_f}$
Fault-free case	$\varsigma = 0.6$ $\omega_{n,0} = 11.11$ rad s^{-1}	0
Moderate fault case	$\varsigma_{n,f} = 0.65$ $\omega_{n,f} = 5.84$ rad s^{-1}	0.8
Extreme fault case	$\varsigma_{n,hl} = 0.9$ $\omega_{n,hl} = 3.42$ rad s^{-1}	1

In the wind turbine model, the wind speed is regarded as the UI with distribution vector $E_u = [0.004\ 0\ 0\ 0\ 0\ 0]^T$, F_a is given according to (5-56) and Table 5-1. The simulation results are demonstrated as follows.

The proposed observer gain is calculated by using the Matlab LMI Toolbox as:

$$K = \begin{bmatrix} 0 & 4.1939 & -0.0023 \\ 0.2030 & 886.7084 & 2.1731 \\ 1.0000 & 2.1811 & -0.0030 \\ 0 & 0.1100 & 71.6988 \\ 0 & -0.0071 & -3.8730 \\ 0 & -0.0010 & 0.0250 \\ 0 & -0.0034 & -2.6584 \end{bmatrix}$$

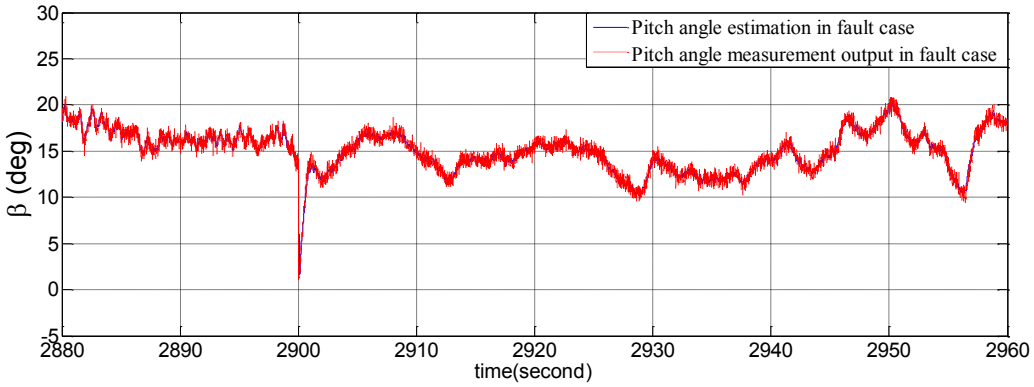

Figure 5-1 Extreme fault case

Figure 5-1 illustrates the pitch angle β estimation where the extreme fault ($\theta_f = 1$) occurs at 2900 s. A peak are shown in the pitch angle at 2900s caused by the two pitch dynamic parameters (ς and $\omega_{n,0}$) sudden variations as. It can also be seen that, by comparing the estimated signal $\hat{\beta}$ with the actual measured β is highly influenced by the sensor noise. This makes a strong case for dealing with the noise effect.

Figures 5-2 & 5-3 show the FE signals $\hat{f}_a$, state estimation signal $\hat{\dot{\beta}}_0$ as well as fault indicator parameter $\hat{\theta}_f$.

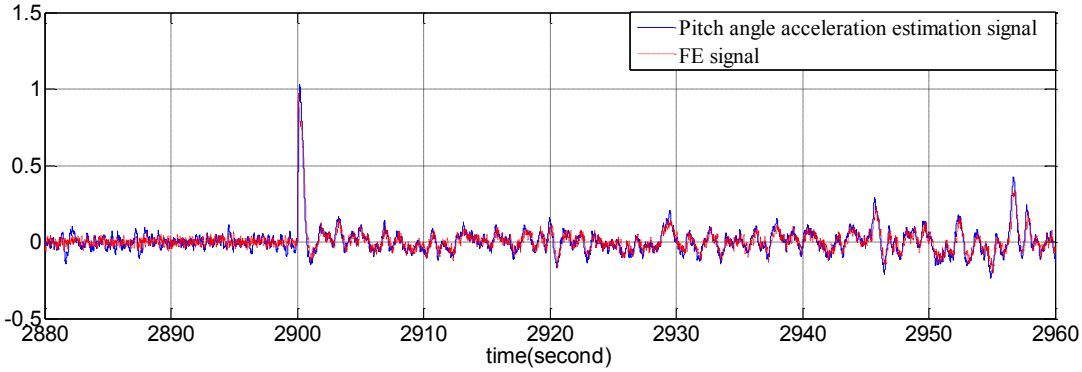

(a) FE signal $\hat{f}_a$ and state estimation signal $\hat{\dot{\beta}}_0$ (rad s^{-1})

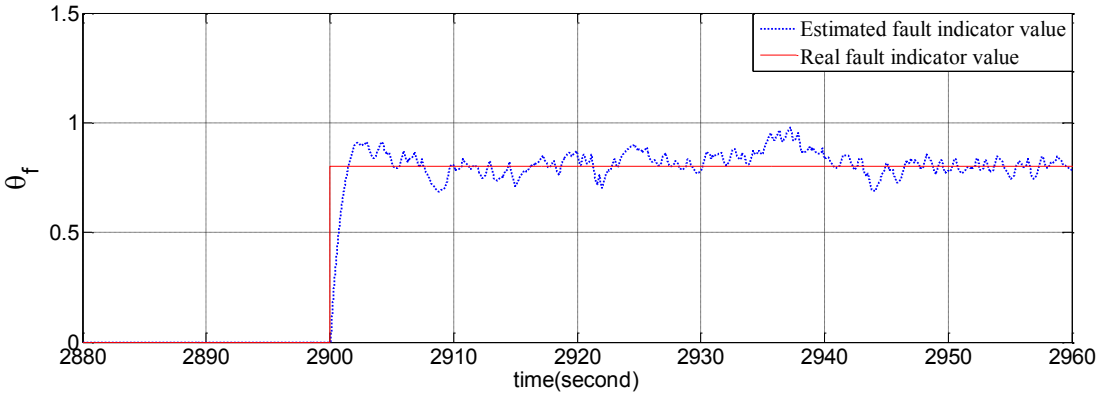

(b) Fault indicator θ_f and corresponding estimation $\hat{\theta}_f$

Figure 5-2 FE signal of hydraulic leakage fault in the moderate fault case

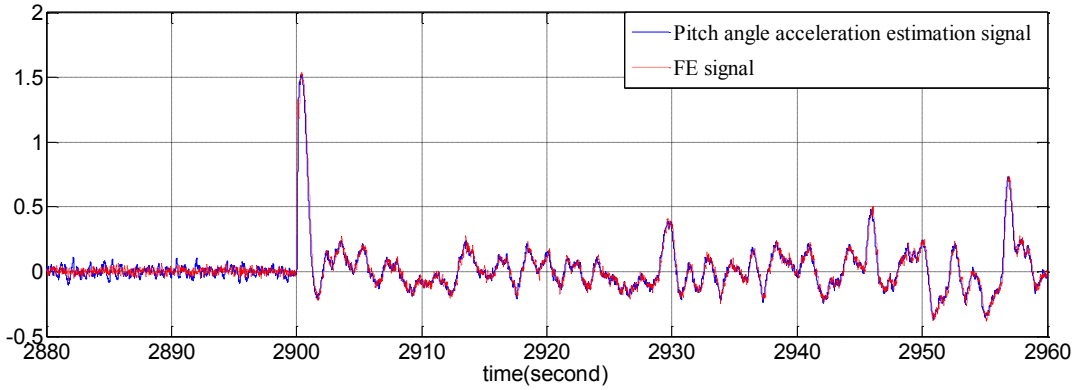

(a) FE signal $\hat{f}_a$ and state estimation signal $\hat{\dot{\beta}}_0$ (rad s^{-1})

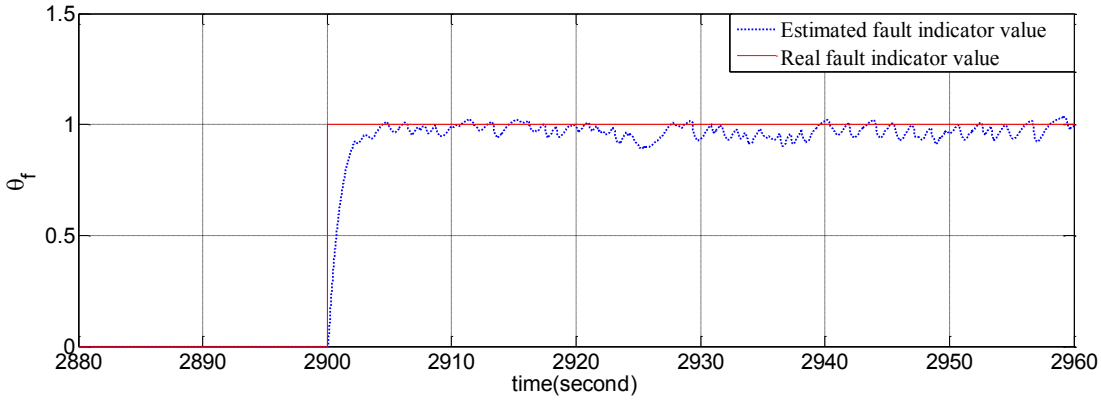

(b) Fault indicator θ_f and corresponding estimation $\hat{\theta}_f$

Figure 5-3 FE of hydraulic leakage fault in the extreme fault case

The wind turbine system is simulated with two different fault severities (moderate and extreme). Figures 5-2(a) and 5-3(a) show the fault estimate $\hat{f}_a$ and the wind turbine system state estimate $\hat{\hat{\beta}}_0$. Figures 5-2(b) & 5-3(b) display the real values of the fault indicator parameter θ_f and its estimation $\hat{\theta}_f$.

To make a comparison with the results of Figure 5-1, the faults for both scenarios are simulated to occur at 2900s. The transient after 2900s simulates the impacts on both the estimated fault and the system states due to the hydraulic leakage fault. This faulty behaviour is immediately sensed by the fault indicator. In Figure 5-2(a) & 5-3(a), the FE signal $\hat{f}_a$ is much smaller in magnitude than the estimation signal $\hat{\hat{\beta}}_0$ in the fault-free case (before $t \leq$ 2900s). Figures 5-2(b) & 5-3(b) show that the value of the fault indicator $\hat{\theta}_f$ varies around zero in the fault-free case. The variations of the FE signal $\hat{f}_a$ follow the shape of the signal $\hat{\hat{\beta}}_0$ when the fault occurs ($t \geq$ 2900s). The fault indicators of $\hat{\theta}_f \approx 0.8$ and $\hat{\theta}_f \approx 1$, in Figures 5-2(b) & 5-3(b), respectively, correspond to the cases of moderate and extreme faults. The simulated estimates of $\hat{\theta}_f$ vary between 0 and 1 which comply with the theoretical range of $\theta_f \in [0, 1]$ proposed in Table 5-1.

5.5 Conclusion

In this Chapter, a multiplicative FE approach is designed by combining a UI de-coupling observer with H_∞ optimisation theory. The proposed observer can

de-couple the effect of the UI (wind force) and minimise the effect of the output measurement sensor noise on the FE signal simultaneously to obtain an accurate FE signal. In order to estimate the multiplicative fault, a fault model modification is adopted to reformulate the system description with the multiplicative fault into an additive fault format which facilitates the fault estimator design. Consequently, the hydraulic leakage fault occurring on the wind turbine pitch system is used to test the FE design. The simulation results show that the UI-PIO is capable of estimating the hydraulic leakage fault precisely and robustly in the extreme and moderate fault cases.

Starting with Chapter 6, the studies in this thesis consider much wider time derivative characteristics of various faults using multiple integral actions for FE design.

Chapter 6
Proportional Multiple Integral Observer-based FE with UI De-coupling Approach

6.1 Introduction

Chapter 5 has discussed that in the PIO FDD structure, the fault is augmented as an additive state vector assumed to be a constant or slowly time-varying signal, i.e. the first time derivative of the fault is considered to be zero or approximately zero. With this assumption, the PIO with a single integral action can provide sufficiently good FE FDD performance.

An extension to the PIO has been made by (Jiang, Wang and Song, 2000) who designed a proportional multiple integral observer (PMIO) to account for the purpose of estimating fault signals with the characteristic of zero values for the finite time derivatives. In (Gao and Ho, 2004) and (Koenig, 2005), the PMIO research was extended to not only estimate if the signal whose finite time derivatives is zero, but also to explore if the finite time derivatives is bounded. The PMIO structure includes multiple integrators to augment the observer structure with each additional states corresponding to the individual integrators, hence providing a more powerful way to estimate more complex fault signals, i.e. with complex time-variations. For example, one kind of oscillatory fault is a sinusoidal signal which has a bounded finite time derivatives.

(Gao and Ho, 2006) apply the PMIO design in (Gao and Ho, 2004) to estimate sensor faults. (Gao and Ho, 2006) also show that the state estimation error convergence condition is guaranteed by solving an appropriate Lyapunov equation with a tuning parameter to attenuate the effects of the UI signals, i.e., as a method of improving the PMIO robustness to modelling uncertainty and exogenous disturbance. In this design, the selection of the tuning parameter is adjusted experimentally via simulation.

The PMIO principle has been used by several other researchers. More recently, an actuator fault estimation using PMIO can be seen in (Gao and Ding, 2007). About the

same time two investigators (Koenig, 2005) and (Ichalal, Marx, Ragot and Maquin, 2009) addressed another robustness approach to the PMIO design problem based on the UIO structure, focussing on the problem of de-coupling the effects that the UI have on the state estimates and FE signals, with observer stability using the Hurwitz theorem.

Interesting developments were described by (Ichalal, Marx, Ragot and Maquin, 2009;Hamdi, Mechmeche, Rodrigues and BenHadjBraiek, 2011) by extending the LTI PMIO design approaches to take into account the properties of multiple-model system structures. In their approaches these authors design the PMIO state estimation error global convergence condition using an LMI formulation. This approach has suitably wide application to the general problem of UI estimation including the faults needed to be estimated.

Hence, from this background the goal of this Chapter is to investigate a method of PMIO based on UIO structure which can be applicable to the robust FE problem. With some motivation from the work of (Koenig, 2005) and (Hamdi, Mechmeche, Rodrigues and BenHadjBraiek, 2011) summarised above, this is referred to here as the UI-PMIO. In this approach it is anticipated to estimate the system states and faults simultaneously regardless of the existence of any UI that may act on the system dynamics.

When suitably developed this approach could lead to a wider class of estimation problems as a consequence of the possibility of numerically solving the finite time fault derivatives subject to suitable bounds. The work described here thus provides an enhancement to the UI-PIO observer described in Chapter 5 considering the time derivative characteristics of various faults.

In this UI-PMIO structure, the UI associated with the system states are de-coupled using the UIO design approach of (Chen, Patton and Zhang, 1996; Chen and Patton, 1999). As an additional feature, the H_∞ optimisation theory within an LMI formulation is used to minimising the effect of the non-zero finite time fault derivative on FE as well as guaranteeing the asymptotic stability. This approach is considered here to be more systematic than other methods in the literature, e.g. by (Koenig, 2005) who did not provide a specific stability optimisation strategy. In Section 6.3 a numerical example with an actuator fault is given to demonstrate the effectiveness of the proposed

UI-PMIO approach and the results of this study are carefully analysed. Before describing this example Section 6.2 describes the UI-PMIO design strategy.

6.2 UI-PMIO based FE

In this Section, the proposed UI-PMIO method is described in detail. First, the existence conditions are given according to the requirements for UI de-coupling in the FDD design problem requiring robust FE (in the presence of UI signals). It is shown that the detailed convergence conditions of the augmented state estimation error are guaranteed using LMIs derived in conjunction with H_∞ optimisation theory.

6.2.1 UI-PMIO structure

Consider a linear system described by (6-1) with actuator faults (all sensors are assumed to be fault-free) and with UI, represented as:

$$\left.\begin{aligned} \dot{x} &= Ax + Bu + E_u d_u + F_a f_a \\ y &= Cx \end{aligned}\right\} \tag{6-1}$$

where, $x \in \Re^n$ denotes the system state vector, $u \in \Re^r$ and $y \in \Re^m$ denote the input and measured system vectors, respectively and $d_u \in \Re^p$ is a vector of UI. $f_a \in \Re^l$ is a vector of time-varying actuator faults. A, B, C are known system matrices with appropriate dimensions. The matrix $E_u \in \Re^{n\times p}$ represents the distribution matrix for the UI. The columns of the matrix $F_a \in \Re^{n\times l}$ denote the independent fault directions. Both E_u and F_a are regarded as system input matrices.

Assume that the k_{th} derivative of the fault signal f, i.e. $f^{(k)}$, is bounded. Then let

$$\varepsilon_i = f^{(k-i)} \qquad (i = 1,2,\cdots,k) \tag{6-2}$$

One thus has that:

$$\begin{aligned} \dot{\varepsilon}_1 &= f^{(k)} \\ \dot{\varepsilon}_2 &= \varepsilon_1 \\ &\vdots \\ \dot{\varepsilon}_k &= \varepsilon_{k-1} \end{aligned} \tag{6-3}$$

Let

$$\bar{x} = [x^T \quad \varepsilon_1^T \quad \varepsilon_2^T \quad \cdots \quad \varepsilon_k^T]^T \in \Re^{\bar{n}} \tag{6-4}$$

By using (6-3) to (6-4), an augmented state-space representation with the structure of (6-5) and (6-6) is to be constructed.

$$\left.\begin{aligned} \dot{\bar{x}} &= \bar{A}\bar{x} + \bar{B}u + \bar{E}d + \bar{G}f^{(k)} \\ y &= \bar{C}\bar{x} \end{aligned}\right\} \tag{6-5}$$

where,

$$\bar{A} = \begin{pmatrix} A & 0 & \cdots & 0 & F_a \\ 0 & 0 & \cdots & 0 & 0 \\ 0 & I & \cdots & 0 & 0 \\ \vdots & \vdots & \ddots & \vdots & \vdots \\ 0 & 0 & \cdots & I & 0 \end{pmatrix} \in \Re^{\bar{n}\times\bar{n}}$$

$$\bar{B} = [B^T \quad 0 \quad 0 \quad \cdots \quad 0]^T \in \Re^{\bar{n}\times r}$$

$$\bar{E} = [E_u^T \quad 0 \quad 0 \quad \cdots \quad 0]^T \in \Re^{\bar{n}\times p}$$

$$\bar{G} = [0 \quad I_l \quad 0 \quad \cdots \quad 0]^T \in \Re^{\bar{n}\times l}$$

$$\bar{C} = [C \quad 0 \quad 0 \quad \cdots \quad 0] \in \Re^{m\times\bar{n}}$$

$$\bar{n} = n + lk \tag{6-6}$$

A functional observer is formed as:

$$\left.\begin{aligned} \dot{z} &= Nz + T\bar{B}u + Ky \\ \hat{\bar{x}} &= z + Hy \end{aligned}\right\} \tag{6-7}$$

where， $\hat{\bar{x}} \in \Re^{\bar{n}}$ is the estimated augmented state vector, $z \in \Re^{\bar{n}}$ is the functional observer state vector, and N, T, K and H are design matrices.

Noticeably, an augmented state vector $\bar{x}$ is formulated from the original state vector x, the fault vector f, and the i_{th} derivative $\{1,2,\cdots,l-1\}$ of the fault vector $f^{(i)}$, as (6-5). Hence, by using the functional observer (6-7), the original system state vector x, the fault vector f and its derivatives $\varepsilon_i = f^{(k-i)}$ $(i = 1,2,\cdots,k)$ can be deduced at the same time. This UI-PMIO is constructed according to the UIO theory in Section 2.3.3.

Definition 6.1: Observer (6-7) is defined as a UI-PMIO for the system (6-5), if its augmented state estimation errors $\bar{e} = \bar{x} - \hat{\bar{x}}$ approaches zero asymptotically, in the presence of the system UI and faults.

Assuming that $\bar{E}$ is known, the estimation error dynamics are governed by:

$$\begin{aligned}\dot{e} = {} & (\bar{A} - H\bar{C}\bar{A} - K_1\bar{C})\bar{e} \\ & + [N - (\bar{A} - H\bar{C}\bar{A} - K_1\bar{C})]z \\ & + [K_2 - (\bar{A} - H\bar{C}\bar{A} - K_1\bar{C})H]y \\ & + [T - (I - H\bar{C})]\bar{B}u \\ & + (H\bar{C} - I)\bar{E}d_u + \bar{G}f^{(k)}\end{aligned} \tag{6-8}$$

where,

$$K = K_1 + K_2 \tag{6-9}$$

The state estimation error dynamics are rearranged into the form of (6-14), if the following relations (6-10) to (6-13) are satisfied (Chen and Patton, 1999):

$$(H\bar{C} - I)\bar{E} = 0 \tag{6-10}$$

$$T = I - H\bar{C} \tag{6-11}$$

$$N = (\bar{A} - H\bar{C}\bar{A} - K_1\bar{C}) = \bar{A}_1 - K_1\bar{C} \tag{6-12}$$

$$K_2 = NH \tag{6-13}$$

The state estimation error dynamics are defined as:

$$\dot{\bar{e}} = N\bar{e} + \bar{G}f^{(k)} \tag{6-14}$$

Furthermore, if all the eigenvalues of N are stable, $\bar{e}$ will approach zero asymptotically, which means that $\hat{\bar{x}} \to \bar{x}$. The observer (6-7) is thus a UI-PMIO for the system (6-5) when conditions (6-9) – (6-13) are satisfied.

Hence, this UI-PMIO design involves the solution of (6-9) – (6-13) whilst placing all the eigenvalues of the system matrix N to be stable. Meanwhile, N, T, K and H in (6-7) are designed to achieve the required FE performance.

Theorem 6.1 The necessary and sufficient conditions for the existence of UI-PMIO of system (6-5) are (Chen and Patton, 1999):

(1) $rank(\bar{C}\bar{E}) = rank(\bar{E})$

(2) $(\bar{C}, \bar{A}_1)$ is a detectable pair

A particular solution to (6-10) can be calculated as follows:

$$H = \bar{E}(\bar{C}\bar{E})^{+} \tag{6-15}$$

where, $(\bar{C}\bar{E})^{+} = [(\bar{C}\bar{E})^{T}(\bar{C}\bar{E})]^{-1}(\bar{C}\bar{E})^{T}$ denotes the Moore-Penrose pseudo-inverse.

6.2.2 UI-PMIO design in H_∞ optimisation frame work

Theorem 6.2 with the Definition 6.1 and the assumption of Theorem 6.1, for $t > 0$ the system (6-7) is asymptotically stable. Furthermore, the H_∞ optimisation theory is used to guarantee that $f^{(k)}$ is minimised with a minimum level γ_m, if there exists an S.P.D matrix $\bar{P} > 0$ and matrices $\bar{A}_1$, K_1 such that the following conditions hold:

$$\begin{bmatrix} \bar{P}\bar{A}_1 + \bar{A}_1^T\bar{P} - \bar{Y}_m\bar{C} - \bar{C}^T\bar{Y}_m^T & \bar{P}\bar{G} & \bar{C}^T \\ * & -\gamma_m I & 0 \\ * & * & -\gamma_m I \end{bmatrix} < 0 \quad \bar{P} > 0 \tag{6-16}$$

***Proof*:**

Using the state estimation error $\bar{e}$ defined in Definition 6.1, a suitable candidate Lyapunov function $V(\bar{e})$ for the augmented system (6-14) is given as:,

$$V(\bar{e}) = \bar{e}^T\bar{P}\bar{e} \tag{6-17}$$

Then, in terms of $\dot{\bar{e}}$ defined in (6-14), the time derivative of the candidate Lyapunov function $\dot{V}(\bar{e})$ is derived as:

$$\dot{V}(\bar{e}) = \bar{e}^T[\bar{P}(\bar{A}_1 - K_1\bar{C}) + (\bar{A}_1 - K_1\bar{C})^T\bar{P}]\bar{e} + 2\bar{e}^T\bar{P}\bar{G}f^{(k)} \tag{6-18}$$

with $N = \bar{A}_1 - K_1\bar{C}$,

$$\dot{V}(\bar{e}) = \bar{e}^T[\bar{P}N + N^T\bar{P}]\bar{e} + 2\bar{e}^T\bar{P}\bar{G}f^{(k)} \tag{6-19}$$

Then the H_∞ optimisation theory is used to attenuate the effect of $f^{(k)}$ on the state estimation error $\bar{e}$. Hence, the stability of the system (6-17) is ensured simultaneously in terms of minimum level γ_m, if the following inequality holds:

$$\dot{V}(\bar{e}) + \frac{1}{\gamma_m}\bar{C}^T\bar{e}^T\bar{e}\bar{C} - \gamma_m {f^{(k)}}^T f^{(k)} < 0 \tag{6-20}$$

It follows that to the minimum value of γ_m must be found so that:

$$\begin{bmatrix} \bar{e} \\ f^{(k)} \end{bmatrix}^{\mathrm{T}} \begin{bmatrix} \bar{P}N + N^T\bar{P} + \frac{1}{\gamma_m}\bar{C}^T\bar{C} & \bar{P}\bar{G} \\ * & -\gamma_m \end{bmatrix} \begin{bmatrix} \bar{e} \\ f^{(k)} \end{bmatrix} < 0 \tag{6-21}$$

Then, by using the Schur Complement Lemma, the following LMI can be stated:

$$\begin{bmatrix} \bar{P}N + N^T\bar{P} & \bar{P}\bar{G} & \bar{C}^T \\ * & -\gamma_m I & 0 \\ * & 0 & -\gamma_m I \end{bmatrix} < 0 \qquad \bar{P} > 0 \tag{6-22}$$

Let

$$\bar{Y}_m = \bar{P}K_1 \tag{6-23}$$

Then, (6-22) can be replaced by:

$$\begin{bmatrix} \bar{P}\bar{A}_1 + \bar{A}_1^T\bar{P} - \bar{Y}_m\bar{C} - \bar{C}^T\bar{Y}_m^T & \bar{P}\bar{G} & \bar{C}^T \\ * & -\gamma_m I & 0 \\ * & 0 & -\gamma_m I \end{bmatrix} < 0 \qquad \bar{P} > 0 \tag{6-24}$$

This completes the proof.

Remark 6.1: The proposed UI-PMIO has the ability to de-couple the UI completely instead of minimising or attenuating the UI e.g. by using H_∞ or H_2 optimisation if the UI distribution matrix satisfies the condition (1) in Theorem 6.1. Hence, it is considered as a straightforward approach to remove the effect of the UI since the de-coupling procedure does not require the use of signal attenuation.

Remark 6.2: In fact, $\bar{G}f^{(k)}$ can also be considered to have the same effect as the UI. However it does not satisfy the UIO design rank condition specified in Theorem 6.1 Hence, in the UI-PMIO design, the H_∞ optimisation theory is applied to minimise the

effect of the $\bar{G}f^{(k)}$ signal on the augmented state estimation error by optimisation of γ_m. In the above description the optimisation parameter γ_m only relates to the minimisation of $\bar{G}f^{(k)}$ and does not apply to the joint minimisation of both the UI and the $\bar{G}f^{(k)}$ as discussed in (Gao and Ho, 2004).

Remark 6.3: In this Section, the robustness problem involving measurement sensor noise is not taken into account. However, two candidate methods are recommended for this study. One is to use H_∞ optimisation theory to minimise the measurement noise effect on the estimated fault signal as described in Chapter 5. An alternative way to take the additive sensor noise into account is to construct a new augmented state system in the PMIO design that takes the sensor noise into account as an additional state (Koenig, 2005). In this approach, the sensor noise is considered as a UI with bounded finite time derivatives and reconstructed using a multiple-integral observer.

Remark 6.4: To help to develop a better understanding of the purpose and structure of the UI-PMIO an alternative description can be given using a new state partitioning with a clear distinction between the proportional and integral action roles as follows:

Let

$$\hat{\bar{x}} = [\hat{x}^T \quad \hat{\varepsilon}_1^T \quad \hat{\varepsilon}_2^T \quad \cdots \quad \hat{\varepsilon}_k^T]^T \tag{6-25}$$

$$\bar{L} = [L_P^T \quad L_{I1}^T \quad L_{I2}^T \quad \cdots \quad L_{Ik}^T]^T \tag{6-26}$$

The observer (6-7) can be re-written as

$$\left.\begin{aligned} \dot{\hat{x}} &= A\hat{x} + Bu + L_P(y - C\hat{x}) + B_f\hat{\varepsilon}_k \\ \dot{\hat{\varepsilon}}_1 &= L_{I1}^T(y - C\hat{x}) \\ \dot{\hat{\varepsilon}}_2 &= L_{I2}^T(\,(y - C\hat{x}) + \hat{\varepsilon}_1) \\ &\vdots \\ \dot{\hat{\varepsilon}}_k &= L_{Ik}^T(\,(y - C\hat{x}) + \hat{\varepsilon}_{k-1}) \end{aligned}\right\} \tag{6-27}$$

$$\left.\begin{aligned} \hat{\varepsilon}_1 &= L_{I1}^T \textstyle\int_t^\infty Ce \\ \hat{\varepsilon}_2 &= L_{I2}^T \textstyle\int_t^\infty (Ce + \hat{\varepsilon}_1\,) \\ &\vdots \\ \hat{\varepsilon}_k &= L_{Ik}^T \textstyle\int_t^\infty (Ce + \hat{\varepsilon}_{k-1}\,) \end{aligned}\right\} \tag{6-28}$$

Clearly, $\dot{\hat{x}} = A\hat{x} + Bu + L_P(y - C\hat{x}) + B_f\hat{\varepsilon}_k$ in (6-27) represents the proportional (or P) part of this new state space PMIO. The Multiple Integral (or MI part) is represented by the integral calculations in (6-28).

Remark 6.5: In some previous studies, the fault signal is often assumed to be bounded. However, practical systems may encounter a complete actuator break-down and the outputs of actuators and/or sensors are likely to become irregular and unbounded. In the proposed UI-PMIO structure, it is important to consider a set of unbounded faults as one possible fault scenario. It actually makes sense to consider carefully what the true value of using the estimator integral action is. In the UI-PMIO design, the integer k can be determined as the order of the highest non-zero fault time derivative from which if know *a priori* can be useful information for FE in a practical setting. In theoretical terms a large number k can be used to guarantee that the fault k_{th} derivative is zero value or bounded. It would be interesting to attempt to estimate a suitable value of k as a precursor to design for a real application study. The k can be chosen in terms of the knowledge of the estimated fault or adjusted compromisingly according to the observer design complexity and performance.

6.3 Example study

A numerical example system, described in (Gao, Ding and Ma, 2007), chosen to test the FE performance using the UI-PMIO strategy. It is assumed that the only faults present are the actuator faults f_a, although the effect of a disturbance d_u is also considered. The state space system description of this example is given as:

$$\left.\begin{aligned} \dot{x} &= Ax + Bu + E_u d_u + F_a f_a \\ y &= Cx \end{aligned}\right\} \tag{6-29}$$

where, $A = \begin{bmatrix} 0 & 1 \\ -2 & -2 \end{bmatrix}$, $B = \begin{bmatrix} 1 \\ 1.5 \end{bmatrix}$, $F_a = \begin{bmatrix} 1 \\ 1.5 \end{bmatrix}$, $E_u = \begin{bmatrix} 0.5 \\ -1 \end{bmatrix}$, $C = \begin{bmatrix} 1 & 0 \\ 2 & 1 \end{bmatrix}$,

d_u is represented by a band-limited white noise signal (covariance = 0.001). An oscillatory fault $f_a(t)$ expressed by a sinusoidal signal is used to represent the actuator fault which is considered as the k_{th} derivative is bounded.

$$f_a(t) = \begin{cases} 4.6 + 0.3\sin(t) & t \geq 3 \\ 0 & t < 3 \end{cases}$$

Substituting A, B, F_a, E_u, C defined above into (6-6), an augmented observer system is described for which $k = 2$ and where:

$$\bar{A} = \begin{bmatrix} 0 & 1 & 0 & 1 \\ -2 & -2 & 0 & 1.5 \\ 0 & 0 & 0 & 0 \\ 0 & 0 & 1 & 0 \end{bmatrix}, \bar{B} = \begin{bmatrix} 1 \\ 1.5 \\ 0 \\ 0 \end{bmatrix}, \bar{F}_a = \begin{bmatrix} 1 \\ 1.5 \\ 0 \\ 0 \end{bmatrix}, \bar{E}_u = \begin{bmatrix} 0.5 \\ -1 \\ 0 \\ 0 \end{bmatrix},$$

$$\bar{C} = \begin{bmatrix} 1 & 0 & 0 & 0 \\ 2 & 1 & 0 & 0 \end{bmatrix}, G = \begin{bmatrix} 0 \\ 0 \\ 1 \\ 0 \end{bmatrix}.$$

By setting $u = 0$, the simulation results for states and faults are shown in the following.

Based on the theory in Section 6.2, the designed observer gain matrix K is:

$$K = \begin{bmatrix} 0 & -16.5642 \\ -2 & 39.4260 \\ 0 & 217.8799 \\ 0 & 50.3576 \end{bmatrix}.$$

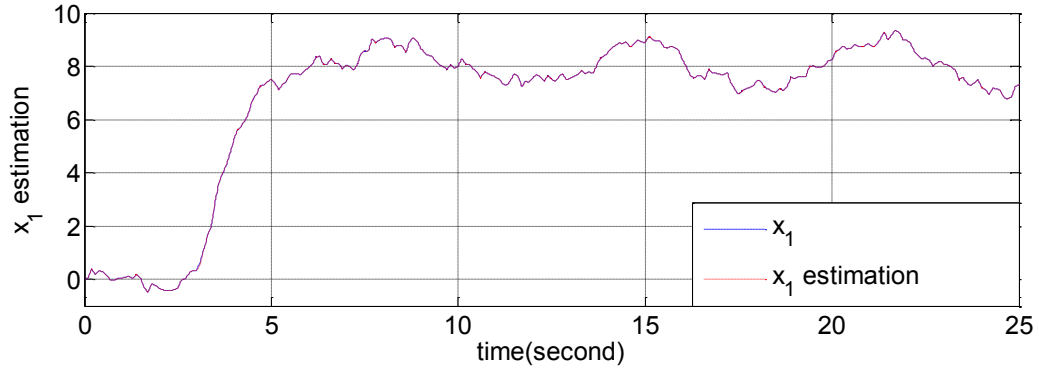

Figure 6-1 State x_1 and its estimated value $\hat{x}_1$

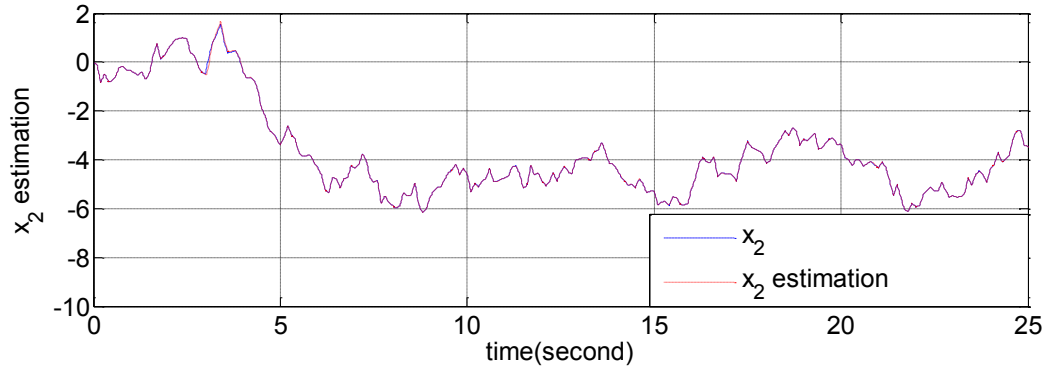

Figure 6-2 State x_2 and its estimated value $\hat{x}_2$

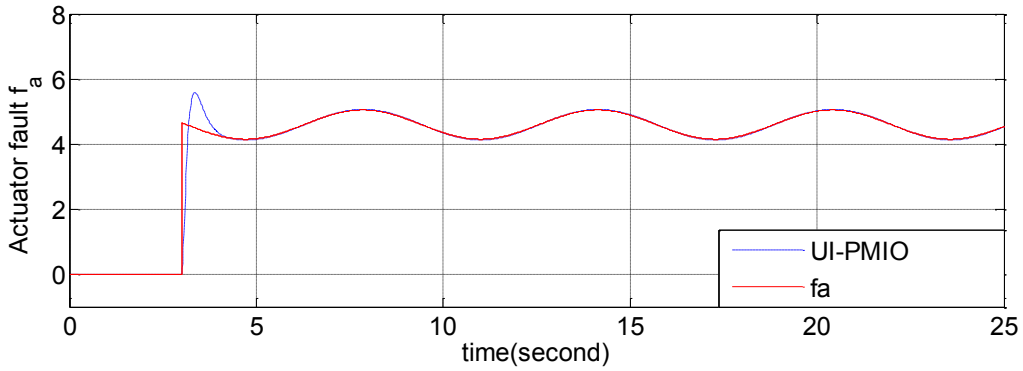

Figure 6-3 Actuator fault f_a and its estimate $\hat{f}_a$ (a)

Figures 6-1 to 6-3 show the states and FE signals, respectively. From Figures 6-1 & 6-2 it can be seen that the estimated signals $\hat{x}_1$ and $\hat{x}_2$ can almost follow the system states x_1 and x_2 regardless of the exogenous disturbance. Figure 6.3 shows that after a short transient, the FE signal can almost track the actual fault with good accuracy.

Now consider a $\times 3$ increase in the frequency of the fault as:

$$f_a = \begin{cases} 4.6 + 0.3\sin(3t) & t \geq 3 \\ 0 & t < 3 \end{cases}$$

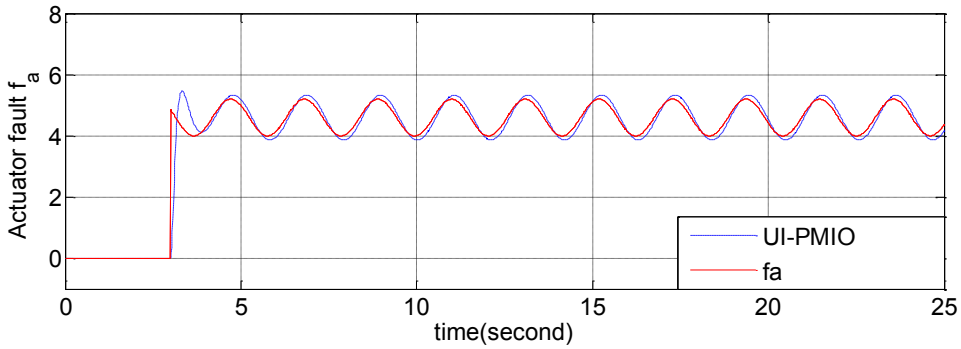

Figure 6-4 Actuator fault f_a and its estimate $\hat{f}_a$ (b)

Figure 6-4 shows that after the short transient, the FE signal trajectory has a small delay and there is also a small magnitude error compared with the actual fault signal. However, it can still track the actual fault with relatively good accuracy.

6.4 Conclusion

In this Chapter, the mathematical properties of the UI-PMIO comprising state and FE are developed and tested through a numerical simulation comprising a single actuator fault.

A particular feature of the UI-PMIO is the ability to de-couple the effect of the UI on system state as well as the FE signals so that system state and FE can be estimated simultaneously regardless of the existence of UI. Compared with the UI-PIO approach the UI-PMIO has a more extensive range of FE properties making use of the concept of the finite time fault derivatives. In the UI-PIO the first time derivative of the fault is assumed to be zero-valued and this is unrealistic for many real application problems. In contrast in the UI-PMIO the finite time fault derivatives is zero-valued or bounded. Hence, this framework for observer design has a wider application area than the UI-PIO, making use of the bounded nature of a finite time fault derivative signal.

It is shown how H_∞ optimisation theory can be used to minimise the state estimation error caused by a small but bounded k_{th} fault derivative. Finally, a numerical example with an actuator fault is used to demonstrate the effectiveness of the proposed UI-PMIO approach.

Whilst the UI-PMIO concentrates on providing good fault estimates in the presence of bounded fault derivatives. Chapter 7 shows that including a derivative action in the UI-PMIO, a UI-PMIDO approach to joint state and FE can provide more design freedom to achieve improved FE performance.

Chapter 7
Proportional Multiple Integral Derivative Observer-based FE with UI De-coupling Approach

7.1 Introduction

Chapter 6 has proposed UI-PMIO FE strategy that has the ability to estimate the system state and the finite time derivatives of fault as well as the fault signal simultaneously. It is clear that multiple integral functions are applied in an observer design to guarantee good estimates of the k_{th} derivatives bounded faults. The robustness issue is handled by using the UI de-coupling principle.

As an extension to the work of Chapter 6, it is also interesting to include derivative action in the FE observer design. The derivative action can be used to provide additional degrees of design freedom, which can be used, for example, to handle the robustness problem and provide robust estimation performance.

The role of the derivative action in the observer design in general, the so-called PDO problem (D' presents the 'derivative' action), has been the subject of several studies during the last decade principally applied using a descriptor system (Gao, 2005; Gao and Wang, 2006; Gao, Ding and Ma, 2007; Gao and Ding, 2007; Wu and Duan, 2007; Ren and Zhang, 2010; Ting, Chang and Chen, 2011; Gu, Ming and Dan, 2012; Hamdi, Rodrigues, Mechmeche and BenHadjBraiek, 2012).

In the above observer designs, the PMIDO is presented to involve both multiple integral and derivative actions. These studies focus on descriptor systems and use derivative action to provide more design freedom for improving observer performance and robustness. Also, it is promising to see that the developed PMIDO approach to FE as contributions (Gao, Ding and Ma, 2007; Gao and Ding, 2007; Gu, Ming and Dan, 2012; Hamdi, Rodrigues, Mechmeche and BenHadjBraiek, 2012).

In this Chapter, a novel UI-PMIDO design is inspired by the properties of the RFAFE for normal FE in LTI systems outlined in Chapter 4 and the UI-PMIO including multiple integral actions in Chapter 6 It is interesting to see that the derivative action in

UI-PMIDO design provides extra freedom to achieve an improved FE speed (albeit without the use of the descriptor system structure). A detailed derivation as to how the UI-PMIDO is structured from RFAFE theory is given in Section 7.2.1. The UI-PMIDO is developed from the UI-PMIO methodology of Chapter 6, based on the UI de-coupling strategy for rejecting the effect of UI (as an approach to handling the robust issue).

Consequently, the UI-PMIDO structure for FE involves multiple integral action as well as derivative action. This Chapter shows how this facilitates the derivation of fault with finite time derivatives and also give rise to faster estimation performance. This Chapter can therefore be considered as an extension to the work of Chapters 4 & 6. The stability analysis and estimator gains are derived using an appropriate set of LMIs via the Matlab LMI Toolbox. A numerical example is adopted to demonstrate the effectiveness of the novel UI-PMIDO FE methodology. This Chapter also provides a comparison of the UI-PMIDO with the UI-PMIO approach described in Chapter 6 based on simulation results.

7.2 UI-PMIDO-based FE

7.2.1 Derivation of UI-PMIDO structure

For clarity (7-1) is a re-statement of the system defined in (6-1) as an LTI system encompassing actuator faults $F_a f$ (all sensors are assumed fault-free), including a UI term $E_u d_u$.

$$\left.\begin{aligned} \dot{x} &= Ax + Bu + E_u d_u + F_a f \\ y &= Cx \end{aligned}\right\} \tag{7-1}$$

where, $x \in \Re^n$ denotes the state vector, $u \in \Re^r$ and $y \in \Re^m$ denote the input and measurement vectors, respectively and $d_u \in \Re^p$ is a vector of UI. $f \in \Re^l$ represents a vector of time-varying actuator faults. A, B, C are known system matrices with appropriate dimensions. The matrix $E_u \in \Re^{n\times p}$ represents the UI distribution matrix. The columns of $F_a \in \Re^{n\times l}$ denote the independent fault directions. It is thus considered that both $E_u d_u$ and $F_a f$ act as system inputs.

The actuator FE is derived by (4-17) in Section 4.2.1 as:

$$\dot{\hat{f}} = \Gamma M(\dot{r} + \alpha r) \tag{7-2}$$

and

$$\hat{f} = \Gamma M(r + \alpha \int_{tf}^{t} r \, d\tau) \tag{7-3}$$

where, $r = Ce$. It can be seen that $\dot{\hat{f}}$ has a term which is a function of the derivative of r. It then follows that the fault estimate $\hat{f}$ contains both integral and proportional actions on r (and hence e) with the proportional action providing freedom for designing the speed of the FE response. The advantage of this FE observer design has been detailed in Chapter 4, this is the so-called RFAFE.

Recall that in Chapter 6, a UI-PMIO is designed as proposed in (6-27) from which the FE signal (6-28) is derived and re-stated in (7-4):

$$\left.\begin{aligned} \dot{\hat{x}} &= A\hat{x} + Bu + L_P(Cx - C\hat{x}) + B_f\hat{\varepsilon}_k \\ \dot{\hat{\varepsilon}}_1 &= L_{I1}^T(y - C\hat{x}) \\ \dot{\hat{\varepsilon}}_2 &= L_{I2}^T(y - C\hat{x}) + \hat{\varepsilon}_1 \\ &\vdots \\ \dot{\hat{\varepsilon}}_k &= L_{Ik}^T(y - C\hat{x}) + \hat{\varepsilon}_{k-1} \end{aligned}\right\} \tag{7-4}$$

where, $\hat{x}$ is the state estimation of system (7-1) and $\hat{\varepsilon}_i = \hat{f}^{(k-i)}$ $(i = 1,2,\cdots,k)$ are the finite time derivatives of the FE signals. $\hat{\varepsilon}_i$ are estimated as:

$$\left.\begin{aligned} \hat{\varepsilon}_1 &= L_{I1}^T \int_t^\infty Ce \\ \hat{\varepsilon}_2 &= L_{I2}^T \int_t^\infty (Ce + \hat{\varepsilon}_1) \\ &\vdots \\ \hat{\varepsilon}_k &= L_{Ik}^T \int_t^\infty (Ce + \hat{\varepsilon}_{k-1}) \end{aligned}\right\} \tag{7-5}$$

It is interesting here to reformulate the FE problem by combining (7-2) and (7-4) with the fault structure of (7-3) as follows:

$$\left.\begin{aligned} \dot{\hat{\varepsilon}}_1 &= L_{I1}^T(\left(y - C\hat{x}\right) + L_{d1}^T(\dot{y} - C\dot{\hat{x}}) \\ \dot{\hat{\varepsilon}}_2 &= L_2^T(\left(y - C\hat{x}\right) + L_{d1}^T(\dot{y} - C\dot{\hat{x}}) \\ &\vdots \\ \dot{\hat{\varepsilon}}_k &= L_{Ik}^T(\left(y - C\hat{x}\right) + L_{dk}^T(\dot{y} - C\dot{\hat{x}}) + \hat{\varepsilon}_{k-1} \end{aligned}\right\} \tag{7-6}$$

Hence, the $\hat{\varepsilon}_i = \hat{f}^{(k-i)}$ $(i = 1,2,\cdots,k)$ are represented as follows:

$$\left.\begin{aligned}\hat{\varepsilon}_1 &= L_{d1}^T Ce + L_{I1}^T \int_t^\infty Ce \\ \hat{\varepsilon}_2 &= L_{d2}^T Ce + L_{I2}^T (\int_t^\infty Ce) + \hat{\varepsilon}_1 \\ &\vdots \\ \hat{\varepsilon}_k &= L_{dk}^T Ce + L_{Ik}^T (\int_t^\infty Ce) + \hat{\varepsilon}_{k-1}\end{aligned}\right\} \tag{7-7}$$

where,

$$\hat{f} = \hat{\varepsilon}_k \tag{7-8}$$

Derivative actions appear in the estimated fault dynamics described in (7-7). A further derivation from (7-4) to (7-7) shows that proportional terms are involved in FE signals due to the derivative action. Compared with UI-PMIO, the derivative action means that that the new FE signals in (7-7) & (7-8) provide extra freedom to take into account the FE speed as discussed in RFAFE in Chapter 4. This new observer is referred to here as a UI-PMIDO.

7.2.2 UI-PMIDO design

Following the derivation of the UI-PMIDO in Section 7.2.1, the bounded k_{th} derivative of the fault *f*, i.e. $f^{(k)}$, is defined as:

$$\varepsilon_i = f^{(k-i)} \qquad (i = 1,2,\cdots,k) \tag{7-9}$$

Then, it is reorganized as:

$$\begin{aligned}\dot{\varepsilon}_1 &= f^{(k)} \\ \dot{\varepsilon}_2 &= \varepsilon_1 \\ &\vdots \\ \dot{\varepsilon}_k &= \varepsilon_{k-1}\end{aligned} \tag{7-10}$$

In order to construct the UI-PMIDO for FE, (7-4) can be reformulated by taking into account (7-6), yielding the augmented system format:

$$\left.\begin{aligned}\dot{\bar{x}} &= \bar{A}\bar{x} + \bar{B}u + \bar{E}d + \bar{G}f^{(k)} \\ y &= \bar{C}\bar{x}\end{aligned}\right\} \tag{7-11}$$

where, $\bar{x} = [x^T \quad \varepsilon_1^T \quad \varepsilon_2^T \quad \cdots \quad \varepsilon_k^T]^T \in \Re^{\bar{n}}$,

$$\bar{A} = \begin{pmatrix} A & 0 & \cdots & 0 & F_a \\ 0 & 0 & \cdots & 0 & 0 \\ 0 & I & \cdots & 0 & 0 \\ \vdots & \vdots & \ddots & \vdots & \vdots \\ 0 & 0 & \cdots & I & 0 \end{pmatrix} \in \Re^{\bar{n}\times\bar{n}}$$

$$\bar{B} = [B^T \quad 0 \quad 0 \quad \cdots \quad 0]^T \in \Re^{\bar{n}\times r}$$

$$\bar{E} = [E^T \quad 0 \quad 0 \quad \cdots \quad 0]^T \in \Re^{\bar{n}\times p}$$

$$\bar{G} = [0 \quad I_l \quad 0 \quad \cdots \quad 0]^T \in \Re^{\bar{n}\times l}$$

$$\bar{C} = [C \quad 0 \quad 0 \quad \cdots \quad 0] \in \Re^{m\times\bar{n}}$$

$$\bar{n} = n + lk \tag{7-12}$$

Then, a functional observer is constructed as for the augmented system (7-11) as follows:

$$\left.\begin{aligned} \dot{\bar{z}} &= N\bar{z} + T\bar{B}u + \bar{K}y + L_d(y - \hat{y}) \\ \hat{\bar{x}} &= \bar{z} + Hy \end{aligned}\right\} \tag{7-13}$$

The state estimation error dynamics of the augmented system (7-11) are thus formulated according to the functional observer of (7-13) as:

$$\begin{aligned} \dot{\bar{e}} = {} & (\bar{A} - H\bar{C}\bar{A} - \bar{K}_1\bar{C})\bar{e} \\ & + [N - (\bar{A} - H\bar{C}\bar{A} - \bar{K}_1\bar{C})]z \\ & + [\bar{K}_2 - (\bar{A} - H\bar{C}\bar{A} - \bar{K}_1\bar{C})H]y \\ & + [T - (I_{\bar{n}} - H\bar{C})]\bar{B}u \\ & + (H\bar{C} - I_{\bar{n}})\bar{E}d + \bar{G}f^{(k)} - L_d(\dot{y} - \dot{\hat{y}}) \end{aligned} \tag{7-14}$$

where,

$$\bar{K} = \bar{K}_1 + \bar{K}_2 \tag{7-15}$$

If the following relations of are satisfied (Chen and Patton, 1999):

$$(H\bar{C} - I_{\bar{n}})\bar{E} = 0 \tag{7-16}$$

$$T = I_{\bar{n}} - H\bar{C} \tag{7-17}$$

$$N = (\bar{A} - H\bar{C}\bar{A} - \bar{K}_1\bar{C}) = \bar{A}_1 - \bar{K}_1\bar{C} \tag{7-18}$$

$$\bar{K}_2 = NH \tag{7-19}$$

The augmented state estimation error dynamics are organised as:

$$\dot{\bar{e}} = N\bar{e} - L_d(\dot{\bar{y}} - \dot{\hat{\bar{y}}}) + \bar{G}f^{(k)} \tag{7-20}$$

(7-20) can be re-written as:

$$\dot{\bar{e}} = N\bar{e}(t) - L_d\bar{C}\left(\dot{\bar{x}} - \dot{\hat{\bar{x}}}\right) + \bar{G}f^{(k)}$$

$$= N\bar{e}(t) - L_d\bar{C}\dot{\bar{e}} + \bar{G}f^{(k)} \tag{7-21}$$

where, $\bar{G}f^{(k)}$ can be zero or a bounded small value.

$$(I_{\bar{n}} + L_d\bar{C})\dot{\bar{e}} = N\bar{e} + \bar{G}f^{(k)} \tag{7-22}$$

Let

$$R_d = I_{\bar{n}} + L_d\bar{C} \tag{7-23}$$

Then, (7-22) is reorganised as:

$$R_d\dot{\bar{e}} = N\bar{e} + \bar{G}f^{(k)} \tag{7-24}$$

(7-24) can be further transformed into:

$$\dot{\bar{e}} = R_d^{-1}N\bar{e} + R_d^{-1}\bar{G}f^{(k)} = N_R\bar{e} + R_d^{-1}\bar{G}f^{(k)} \tag{7-25}$$

where, $N_R = R_d^{-1}N$.

Definition 7.1 The observer (7-13) is defined as a UI-PMIDO for the system (7-11), if all the eigenvalues of $R_d^{-1}N$ are stable, so that $\bar{e} = \bar{x} - \hat{\bar{x}}$ will approach zero asymptotically even in the presence of UI and faults, i.e. $\hat{\bar{x}} \to \bar{x}$.

Remark 7.1: Based on Definition 7.1, the UI-PMIDO design objective is to solve the (7-15) to (7-19) whilst placing all the eigenvalues of the system matrix N_R to be stable.

Meanwhile, N_R, T, K and H in (7-13) are designed to achieve the required state estimation and FE performance.

In the light of this proposed UI-PMIDO structure and the augmented error dynamics, the following theorems can be stated.

Theorem 7.1 (Chen and Patton, 1999) The necessary and sufficient conditions for the existence of UI-PMIDO of system (7.1) are:

(1) $rank(\bar{C}\bar{E}) = rank(\bar{E})$

(2) $(\bar{C}, \bar{A}_1)$ is a detectable pair

A particular solution to (7-16) can be calculated as follows:

$$H = \bar{E}(\bar{C}\bar{E})^{+} \tag{7-26}$$

where: $(\bar{C}\bar{E})^{+} = [(\bar{C}\bar{E})^{T}(\bar{C}\bar{E})]^{-1}(\bar{C}\bar{E})^{T}$ denotes the Moore-Penrose pseudo-inverse.

Remark 7.2: In terms of (7-25), the robustness issue in the UI-PMIDO design involves both the UI and $\bar{G}f^{(k)}$ terms. From (7-15) to (7-19)，the UI are de-coupled from the augmented state estimation error by using the UI de-coupling structure, with only the term in $\bar{G}f^{(k)}$ remaining. $\bar{G}f^{(k)}$ cannot be de-coupled as it does not satisfy Condition (1) of Theorem 7.1.

Remark 7.3: Clearly, the existence of $\bar{G}f^{(k)}$ can reduce the observer estimation performance, i.e. degrade the FE accuracy. The impact of this can be interpreted as a robustness problem. Referring to the UI-PMIO theory in Chapter 6, the value of $f^{(k)}$ in (6-5) can be zero or a small bounded constant. In this case, H_∞ optimisation theory is applied to attenuate the effect of $\bar{G}f^{(k)}$ on the FE signal when $\bar{G}f^{(k)} \neq 0$ to solve the robustness issue rising from $\bar{G}f^{(k)}$. Finally, the observer stability problem can be viewed as an LMI design problem.

For the sake of simplicity, the proposed, UI-PMIDO design is now introduced step by step in terms of different values of $\bar{G}f^{(k)}$. Section 7.2.3 below only considers the case when the k_{th} fault derivative is zero ($\bar{G}f^{(k)} = 0$). A more complicated case dealing with the robustness issue related to the k_{th} derivative of the bounded fault ($\bar{G}f^{(k)} \neq 0$) is given in Section 7.2.4,.

7.2.3 UI-PMIDO design in the case of zero value of k_{th} fault derivatives

In this Section, a UI-PMIDO design is developed by assuming that $f^{(k)} = 0$. The augmented system estimation error dynamics (7-25) can then be re-written as:

$$\dot{\bar{e}} = R_d^{-1} N \bar{e} = N_R \bar{e} \tag{7-27}$$

where, $R_d = I_{\bar{n}} + L_d \bar{C}$ defined in (7-23).

The main purpose of the UI-PMIDO design is to develop an asymptotic observer which has the property that the estimation error has asymptotic stability. Hence, the UI-PMIDO design problem is to find an L_d and stabilize the augmented system estimation error dynamics in (7-27), i.e. place all the eigenvalues of N_R in the open left hand of the complex plane.

The stabilization procedure of the UI-PMIDO is established using an approach described by (Ren and Zhang, 2010) for the PD estimator problem which is modified here by considering multiple integral actions. As a result, the LMI formulation is constructed and solved conveniently via the Matlab LMI Toolbox. The formal derivation of the design procedure is developed via Theorem 7.2, Theorem 7.3 and Theorem 7.4 stated as follows.

Lemma 7.1 (Horn and Johnson, 1990) Define the matrices $\bar{\Phi} \in \Re^{\bar{n}\times\bar{n}}$, $\bar{\Psi} \in \Re^{\bar{n}\times\bar{n}}$, then (7-28) holds:

$$det(sI - \bar{\Phi}\bar{\Psi}) = det(sI - \bar{\Psi}\bar{\Phi}) \tag{7-28}$$

Theorem 7.2. With Definition 7.1, based on Lyapunov stability theory, the UI-PMIDO is stable and the augmented system state estimation error dynamics are asymptotically stable, if there exists an S.P.D matrix $\bar{P}_1$, such that (7-29) holds.

$$R_d^T \bar{P}_1 N + N^T \bar{P}_1 R_d < 0 \tag{7-29}$$

***Proof*:**

The eigenvalues of $R_d^{-1}N$ and NR_d^{-1} are identical in terms of Lemma 7.1. Hence, the stability of the UI-PMIDO error dynamics are guaranteed by placing all the eigenvalues

of NR_d^{-1} on the left hand of the complex plane. Based on Lyapunov theory, the UI-PMIDO error dynamics presented in (7-27) are stable only if there is an S.P.D matrix $\bar{P}_1$ such that the following LMI holds.

$$\bar{P}_1 N R_d^{-1} + R_d^{-1} N \bar{P}_1 < 0 \tag{7-30}$$

Pre and post multiply (7-30) by R_d^T and R_d respectively, and then (7-29) holds.

Remark 7.4: The observer design in Theorem 7.2 is difficult to solve because (7-30) involves the product of $\bar{P}_1$, R_d and N. Hence, Theorem 7.3 is proposed to tackle this problem, i.e. to separate the matrices $\bar{P}_1$ from the product of R_d and N in (7-30).

Theorem 7.3 With Definition 7.1 and Theorem 7.2, based on Lyapunov stability theory, the UI-PMIDO is stable and the augmented system state estimation error dynamics are asymptotically stable, if there exist an S.P.D matrix $\bar{P}_1$, and the matrices $\bar{P}_2$, $\bar{P}_3$ such that the following LMI is satisfied.

$$\begin{bmatrix} \bar{P}_2 + \bar{P}_2^T & \bar{P}_1 N - \bar{P}_2^T R_d + \bar{P}_3 \\ * & -\bar{P}_3^T R_d - R_d^T \bar{P}_3 \end{bmatrix} < 0 \tag{7-31}$$

where, N and R_d are defined as in (7-18) and (7-23), respectively.

Proof:

Necessity: If there exists a matrix $\bar{P}_1 > 0$ such that (7-29) holds, then (7-31) also holds since a matrix $\bar{P}_2$ can always be chosen.

$$\begin{bmatrix} \bar{P}_2 + \bar{P}_2^T & 0 \\ 0 & R_d^T \bar{P}_1 N + N^T \bar{P}_1 R_d \end{bmatrix} < 0 \tag{7-32}$$

Let

$$\bar{P}_3 = -\bar{P}_1 N - \bar{P}_2 R_d \tag{7-33}$$

Substituting (7-33) into (7-32), then (7-32) is re-formulated as:

$$\begin{bmatrix} \bar{P}_2 + \bar{P}_2^T & \bar{P}_1 N + \bar{P}_2 R_d + \bar{P}_3 \\ R_d^T \bar{P}_1 + R_d^T \bar{P}_2 + \bar{P}_3 & R_d^T \bar{P}_1 N + N^T \bar{P}_1 R_d \end{bmatrix} < 0 \tag{7-34}$$

By pre- and post-multiplying (7-34) by:

$$\begin{bmatrix} I & 0 \\ -R_d^T & I \end{bmatrix} \tag{7-35}$$

and its transpose respectively, it can then easily be shown that (7-31) holds.

Sufficiency: By (7-31) and the necessity proof above, (7-34) is obtained which indicates that (7-31) holds.

This completes the proof.

Theorem 7.4 If Theorem 7.3, based on Lyapunov stability theory, holds then the UI-PMIDO is stable and the augmented system state estimation error dynamics are asymptotically stable, if there exist an S.P.D. matrices $\bar{P}_1$, and matrices $\bar{P}_2$, $\bar{P}_3$, Y_1 Y_2, such that the following LMI is satisfied.

$$\begin{bmatrix} \bar{P}_2 + \bar{P}_2^T & \Pi_{12} \\ * & \Pi_{22} \end{bmatrix} < 0 \tag{7-36}$$

where, N and R_d are defined as (7-18) and (7-23) respectively, and $\Pi_{12} = \bar{P}_1\bar{A}_1 - \bar{P}_2^T + \bar{P}_3 + Y_1^T\bar{C}$ and $\Pi_{22} = -\bar{P}_3^T - \bar{P}_3 - \bar{C}^T Y_2 + Y_2^T\bar{C}$. The UI-PMIDO gains are thus generated by:

$$K_1^T = -[Y_1 \quad Y_2]\begin{bmatrix} \bar{P}_1^{-1} \\ -\bar{P}_3^{-1}\bar{P}_2\bar{P}_1^{-1} \end{bmatrix} \tag{7-37}$$

$$L_d^T = -[Y_1 \quad Y_2]\begin{bmatrix} 0 \\ -\bar{P}_3^{-1} \end{bmatrix} \tag{7-38}$$

where, if $\bar{P}_3$ is singular, a suitable ε_0 should be chosen so that $\bar{P}_3 + \varepsilon_0 \neq 0$ holds.

***Proof*:**

Sufficiency: Let

$$\varphi_1 = \begin{bmatrix} \bar{P}_2 + \bar{P}_2^T & \bar{P}_1 N - \bar{P}_2^T R_d + \bar{P}_3 \\ * & -\bar{P}_3^T R_d - R_d^T \bar{P}_3 \end{bmatrix} \tag{7-39}$$

$$\varphi_2 = \begin{bmatrix} 0 \\ \bar{C}^T \end{bmatrix}[Y_1 \quad Y_2] + [Y_1 \quad Y_2]^T \begin{bmatrix} 0 \\ \bar{C}^T \end{bmatrix}^T \tag{7-40}$$

Hence, (7-36) can be expressed as:

$$\varphi_1 + \varphi_2 < 0 \tag{7-41}$$

By re-formulating (7-37) & (7-38) as:

$$[-K_1^T \quad -L_d^T] = [Y_1 \quad Y_2]\begin{bmatrix}\bar{P}_1 & 0\\ \bar{P}_2 & \bar{P}_3\end{bmatrix}^{-1} \tag{7-42}$$

Which can be re-written as:

$$[Y_1 \quad Y_2] = [-K_1^T \quad -L_d^T]\begin{bmatrix}\bar{P}_1 & 0\\ \bar{P}_2 & \bar{P}_3\end{bmatrix} \tag{7-43}$$

Substituting (7-43) into (7-40) and by means of (7-41), leads to (7-36).

Necessity: By Theorem 7.2, if (7-13) is an UI-PMIDO, there exist an S.P.D. matrix $\bar{P}_1$, and matrices $\bar{P}_2$, $\bar{P}_3$, K_1, L_d, such that the following (7-44) holds. Then re-write (7-36) as:

$$\varphi_1 + \begin{bmatrix}0\\ \bar{C}^T\end{bmatrix}[-K_1^T \quad -L_d^T]\begin{bmatrix}\bar{P}_1 & 0\\ \bar{P}_2 & \bar{P}_3\end{bmatrix} + \begin{bmatrix}\bar{P}_1 & 0\\ \bar{P}_2 & \bar{P}_3\end{bmatrix}^T [-K_1^T \quad -L_d^T]^T \begin{bmatrix}0\\ \bar{C}^T\end{bmatrix}^T < 0 \tag{7-44}$$

with φ_1 is defined as (7-36).

Define a new matrix $[Y_1 \quad Y_2]$ in terms of (7-44) as:

$$[Y_1 \quad Y_2] = [-K_1^T \quad -L_d^T]\begin{bmatrix}\bar{P}_1 & 0\\ \bar{P}_2 & \bar{P}_3\end{bmatrix} \tag{7-45}$$

Then substituting (7-45) into (7-44) gives (7-36).

This completes the proof.

7.2.4 UI-PMIDO design in the case of bounded k_{th} fault derivatives

In this Section, a more general UI-PMIDO design is developed by extending the FE signal to a small bounded and non-zero k_{th} fault derivative, i.e. $\bar{G}f^{(k)} \neq 0$.

If $\bar{G}f^{(k)} \neq 0$, the augmented system error dynamics are given as (7-25), i.e.,

$$\dot{\bar{e}} = N_R\bar{e} + R_d^{-1}\bar{G}f^{(k)} \tag{7-46}$$

Let $\bar{G}_R = R_d^{-1}\bar{G}$ (7-46) can be further transformed to:

$$\dot{\bar{e}} = N_R \bar{e} + R_d^{-1} \bar{G} f^{(k)} = N_R \bar{e} + \bar{G}_R f^{(k)} \tag{7-47}$$

where, $N_R = R_d^{-1} N$.

Thus the UI-PMIDO design involves finding a suitable N_R to stabilize the augmented system estimation error depicted in (7-47), i.e. place all the eigenvalues of N_R into the left hand of the complex plane.

It should be noted that the robustness problem involves the influence of $\bar{G}_R f^{(k)}$ on $\dot{\bar{e}}$ in (7-47). This requirement has already been discussed in *Remark 6.2*, although for this case the $\bar{G}_R f^{(k)}$ action is now included. The rank condition (1) in Theorem 7.3 is not satisfied and hence an H_∞ optimisation design procedure is used to attenuate the effect of the term $\bar{G}_R f^{(k)}$, leading to a robust UI-PMIDO. Theorem 7.5 & Theorem 7.6 describe the construction of the corresponding optimisation design in an LMI framework which can be solved via the Matlab LMI Toolbox.

Theorem 7.5 For $t > 0$ the system (7-47) is asymptotically stable and the H_∞ performance is guaranteed with an attenuation level γ_a required to degrade the effect of $f^{(k)}$ in the estimation error if there exist an S.P.D. matrix $\bar{P}_1$ and matrices $\bar{P}_2$, $\bar{P}_3$, such that the following LMI is satisfied:

$$\begin{bmatrix} \bar{P}_2 + \bar{P}_2^T & \bar{P}_1 N - \bar{P}_2^T R_d + \bar{P}_3 & \bar{P}_1 \bar{G} & 0 \\ * & -\bar{P}_3^T R_d - R_d^T \bar{P}_3 & 0 & \bar{C}^T \\ * & * & -\gamma_a & 0 \\ * & * & * & -\gamma_a \end{bmatrix} < 0 \tag{7-48}$$

where, N and R_d are defined as in (7-18) and (7-23), respectively.

Proof:

In the light of the state estimation error $\bar{e} = \bar{x} - \hat{\bar{x}}$ defined in Definition 7.1, the candidate Lyapunov function $V(\bar{e})$ for the augmented system (7-1) is given as:

$$V(\bar{e}) = \bar{e}^T \bar{P} \bar{e} \tag{7-49}$$

$\dot{V}(\bar{e})$ is the time derivative of the candidate Lyapunov function for the augmented system (7-47) expressed as (7-50) using $\dot{\bar{e}}$ defined in (7-47):

$$\dot{V}(\bar{e}) = \bar{e}^T (\bar{P}_1 N_R + N_R^T \bar{P}_1) \bar{e} + 2 \bar{e}^T \bar{P}_1 \bar{G}_R f^{(k)} \tag{7-50}$$

To achieve the desired performance and required closed-loop stability of (7-47) and reduce the effect of $\bar{G}_R f^{(k)}$ on the augmented system estimation error dynamics, the following inequality must hold:

$$\dot{V}(\bar{e}) + \frac{1}{\gamma_a}\,\bar{C}^T \bar{e}^T \bar{e} \bar{C} - \gamma_a {f^{(k)}}^T f^{(k)} < 0 \tag{7-51}$$

To achieve the minimum value γ_a the following LMI must be satisfied:

$$\begin{bmatrix} \bar{e} \\ f^{(k)} \end{bmatrix}^T \begin{bmatrix} \bar{P}_1 N_R + N_R^T \bar{P}_1 + \frac{1}{\gamma_a} \bar{C}^T \bar{C} & \bar{P}_1 \bar{G}_R \\ * & -\gamma_a \end{bmatrix} \begin{bmatrix} \bar{e} \\ f^{(k)} \end{bmatrix} < 0 \tag{7-52}$$

Using the Schur Complement Lemma, (7-53) is obtained as:

$$\begin{bmatrix} \bar{P}_1 N_R + N_R^T \bar{P}_1 & \bar{P}_1 \bar{G}_R & \bar{C}^T \\ * & -\gamma_a & 0 \\ * & * & -\gamma_a \end{bmatrix} < 0 \qquad \bar{P}_1 > 0 \tag{7-53}$$

Substituting $N_R = R_d^{-1} N$ and $\bar{G}_R = R_d^{-1} \bar{G}$ into (7-53), then:

$$\begin{bmatrix} \bar{P}_1 R_d^{-1} N + (R_d^{-1} N)^T \bar{P}_1 & \bar{P} R_d^{-1} \bar{G} & \bar{C}^T \\ * & -\gamma_a & 0 \\ * & * & -\gamma_a \end{bmatrix} < 0 \qquad \bar{P}_1 > 0 \tag{7-54}$$

It can be seen that the (7-54) involves the inverse R_d^{-1} and thus (7-54) is difficult to solve. Hence, the following reformulation should be used with (7-54) re-written as:

$$\begin{bmatrix} \bar{P}_1 & 0 & 0 \\ 0 & I & 0 \\ 0 & 0 & I \end{bmatrix} \left(\begin{bmatrix} R_d^{-1} & 0 & 0 \\ 0 & I & 0 \\ 0 & 0 & I \end{bmatrix} \begin{bmatrix} N & \bar{G} & 0 \\ 0 & -\frac{\gamma_a}{2} & 0 \\ \bar{C} & 0 & -\frac{\gamma_a}{2} \end{bmatrix} \right)$$

$$+ \left(\begin{bmatrix} R_d^{-1} & 0 & 0 \\ 0 & I & 0 \\ 0 & 0 & I \end{bmatrix} \begin{bmatrix} N & \bar{G} & 0 \\ 0 & -\frac{\gamma_a}{2} & 0 \\ \bar{C} & 0 & -\frac{\gamma_a}{2} \end{bmatrix} \right)^T \begin{bmatrix} \bar{P}_1 & 0 & 0 \\ 0 & I & 0 \\ 0 & 0 & I \end{bmatrix}^T < 0 \tag{7-55}$$

In terms of the Lemma 7.1, i.e. $det(sI - \bar{\Phi}\bar{\Psi}) = det(sI - \bar{\Psi}\bar{\Phi})$, then (7-55) is identical to:

$$\begin{bmatrix} \bar{P}_1 & 0 & 0 \\ 0 & I & 0 \\ 0 & 0 & I \end{bmatrix} \left(\begin{bmatrix} N & \bar{G} & 0 \\ 0 & -\frac{\gamma_a}{2} & 0 \\ \bar{C} & 0 & -\frac{\gamma_a}{2} \end{bmatrix} \begin{bmatrix} R_d^{-1} & 0 & 0 \\ 0 & I & 0 \\ 0 & 0 & I \end{bmatrix} \right)$$

$$+ \left(\begin{bmatrix} N & \bar{G} & 0 \\ 0 & -\frac{\gamma_a}{2} & 0 \\ \bar{C} & 0 & -\frac{\gamma_a}{2} \end{bmatrix} \begin{bmatrix} R_d^{-1} & 0 & 0 \\ 0 & I & 0 \\ 0 & 0 & I \end{bmatrix} \right)^T \begin{bmatrix} \bar{P}_1 & 0 & 0 \\ 0 & I & 0 \\ 0 & 0 & I \end{bmatrix}^T < 0 \quad (7\text{-}56)$$

After some manipulation the LMI (7-56) becomes:

$$\begin{bmatrix} R_d^T \bar{P}_1 N + N^T \bar{P}_1 R_d & R_d^T \bar{P}_1 \bar{G} & \bar{C}^T \\ * & -\gamma_a & 0 \\ * & * & -\gamma_a \end{bmatrix} < 0 \quad (7\text{-}57)$$

There always exists a $\bar{P}_2$ which satisfies:

$$\bar{P}_2 + \bar{P}_2^T < 0 \quad (7\text{-}58)$$

Hence, combining (7-57) and (7-58) leads to:

$$\begin{bmatrix} R_d^T \bar{P}_1 N + N^T \bar{P}_1 R_d & R_d^T \bar{P}_1 \bar{G} & \bar{C}^T \\ * & -\gamma_a - \bar{C}^T \bar{P}_1 (\bar{P}_2 + \bar{P}_2^T)^{-1} \bar{P}_1 \bar{G} & 0 \\ * & * & -\gamma_a \end{bmatrix} < 0 \quad (7\text{-}59)$$

Using the Schur Complement Lemma, it follows that:

$$\begin{bmatrix} \bar{P}_2 + \bar{P}_2^T & 0 & \bar{P}_1 \bar{G} & 0 \\ 0 & R_d^T \bar{P}_1 N + N^T \bar{P}_1 R_d & R_d^T \bar{P}_1 \bar{G} & \bar{C}^T \\ * & * & -\gamma_a & 0 \\ * & * & * & -\gamma_a \end{bmatrix} < 0 \quad (7\text{-}60)$$

Let

$$\bar{P}_3 = -\bar{P}_1 N - \bar{P}_2 \quad (7\text{-}61)$$

To separate the products N^T, $\bar{P}_1$ and R_d, pre and post multiplying (7-60) by $\begin{bmatrix} I & 0 & 0 & 0 \\ -R_d^T & I & 0 & 0 \\ 0 & 0 & I & 0 \\ 0 & 0 & 0 & I \end{bmatrix}$ and $\begin{bmatrix} I & 0 & 0 & 0 \\ -R_d^T & I & 0 & 0 \\ 0 & 0 & I & 0 \\ 0 & 0 & 0 & I \end{bmatrix}^T$ respectively, leading to (7-62):

$$\begin{bmatrix} \bar{P}_2 + \bar{P}_2^T & \bar{P}_1 N - \bar{P}_2^T R_d + \bar{P}_3 & \bar{P}_1 \bar{G} & 0 \\ * & -\bar{P}_3^T R_d - R_d^T \bar{P}_3 & 0 & \bar{C}^T \\ * & * & -\gamma_a & 0 \\ * & * & * & -\gamma_a \end{bmatrix} < 0 \tag{7-62}$$

It can be seen that (7-62) is identical to (7-48).

This completes the proof.

Theorem 7.6 From Theorem 7.5, the UI-PMIDO is stable and the augmented system state estimation error dynamics are asymptotically stable, if there exist an S.P.D matrix $\bar{P}_1$, and matrices $\bar{P}_2$, $\bar{P}_3$, Y_1, Y_2, such that the following LMI holds.

$$\begin{bmatrix} \bar{P}_2 + \bar{P}_2^T & \Omega_{12} & \bar{P}_1 \bar{G} & 0 \\ * & \Omega_{22} & 0 & \bar{C}^T \\ * & * & -\gamma_a & 0 \\ * & * & * & -\gamma_a \end{bmatrix} < 0 \tag{7-63}$$

where, $\Omega_{12} = \bar{P}_1 \bar{A}_1 - \bar{P}_2^T + \bar{P}_3 + Y_1^T \bar{C}$ and $\Omega_{22} = -\bar{P}_3^T - \bar{P}_3 - \bar{C}^T Y_2 + Y_2^T \bar{C}$. The UI-PMIDO gains are determined by:

$$K_1^T = -[Y_1 \quad Y_2] \begin{bmatrix} \bar{P}_1^{-1} \\ -\bar{P}_3^{-1} \bar{P}_2 \bar{P}_1^{-1} \end{bmatrix} \tag{7-64}$$

$$L_d^T = -[Y_1 \quad Y_2] \begin{bmatrix} 0 \\ -\bar{P}_3^{-1} \end{bmatrix} \tag{7-65}$$

where, if $\bar{P}_3$ is singular, a suitable $\bar{\varepsilon}_0$ should be chosen so that $\bar{P}_3 + \bar{\varepsilon}_0 \neq 0$ holds.

***Proof*:**

Sufficiency: Let

$$\psi_1 = \begin{bmatrix} \bar{P}_2 + \bar{P}_2^T & \bar{P}_1 N - \bar{P}_2^T R_d + \bar{P}_3 & \bar{P}_1 \bar{G} & 0 \\ * & -\bar{P}_3^T R_d - R_d^T \bar{P}_3 & 0 & \bar{C}^T \\ * & * & -\gamma_a & 0 \\ * & * & * & -\gamma_a \end{bmatrix} \tag{7-66}$$

$$\psi_2 = \begin{bmatrix} 0 \\ \bar{C}^T \\ 0 \\ 0 \end{bmatrix} [Y_1 \quad Y_2 \quad 0 \quad 0] + [Y_1 \quad Y_2 \quad 0 \quad 0]^T \begin{bmatrix} 0 \\ \bar{C}^T \\ 0 \\ 0 \end{bmatrix}^T \tag{7-67}$$

Hence, (7-68) is given as:

$$\psi_1 + \psi_2 < 0 \tag{7-68}$$

Now, (7-64) & (7-65) can be re-formulated as:

$$[-K_1^T \quad -L_d^T] = [Y_1 \quad Y_2]\begin{bmatrix}\bar{P}_1 & 0\\ \bar{P}_2 & \bar{P}_3\end{bmatrix}^{-1} \tag{7-69}$$

Then substituting (7-69) into (7-68) gives (7-63), which can be re-written as:

$$[Y_1 \quad Y_2] = [-K_1^T \quad -L_d^T]\begin{bmatrix}\bar{P}_1 & 0\\ \bar{P}_2 & \bar{P}_3\end{bmatrix} \tag{7-70}$$

Substituting (7-70) into (7-67) and by means of (7-68), (7-63) is obtained.

Necessity: By Theorem 7.5, if (7-13) is an UI-PMIDO, there exist an S.P.D matrix $\bar{P}_1$, and matrices $\bar{P}_2$, $\bar{P}_3, K_1$, L_d such that (7-63) is satisfied. Then by rewriting (7-63) as:

$$\psi_1 + \begin{bmatrix}0\\ \bar{C}^T\\ 0\\ 0\end{bmatrix}[-K_1^T \quad -L_d^T]\begin{bmatrix}\bar{P}_1 & 0\\ \bar{P}_2 & \bar{P}_3\end{bmatrix}\begin{bmatrix}1 & 0 & 0 & 0\\ 0 & 1 & 0 & 0\end{bmatrix}$$

$$+ \begin{bmatrix}1 & 0 & 0 & 0\\ 0 & 1 & 0 & 0\end{bmatrix}^T\begin{bmatrix}\bar{P}_1 & 0\\ \bar{P}_2 & \bar{P}_3\end{bmatrix}^T[-K_1^T \quad -L_d^T]^T\begin{bmatrix}0\\ \bar{C}^T\end{bmatrix}^T < 0 \tag{7-71}$$

ψ_1 is defined as (7-66).

Now define a new matrix $[Y_1 \quad Y_2]$ according to (7-71) as:

$$[Y_1 \quad Y_2] = [-K_1^T \quad -L_d^T]\begin{bmatrix}\bar{P}_1 & 0\\ \bar{P}_2 & \bar{P}_3\end{bmatrix} \tag{7-72}$$

Substituting (7-72) into (7-71) gives (7-63).

This completes the proof.

Remark 7.5: The new structure of the UI-PMIDO observer is inspired by the work of the RFAFE estimator given in Chapter 4 and the UI-PMIO of Chapter 6 by synthesizing the feature of fast FE with the combined use of multiple integrators. Although the observer structure in (Gao and Ding, 2005) is also a PMIDO FDD design for facilitating the descriptor system by involving the derivative action, the motivations to explore the derivative action in the observer designs are different. However, the fundamental

principle is the same in both cases of increasing the design freedom to achieve a better FE performance.

Remark 7.6: The robustness against the measurement sensor noise is not taken into account. Again the typical literature for solving this robustness issue is referred to as *Remark 6.3* in Section 6.2.2.

7.3 Example study

A numerical example in (Gao, Ding and Ma, 2007) which is the same as in Chapter 6 is used to illustrate the proposed UI-PMIDO for the FE strategy. Here, only the additive actuator fault is taken into account. The example also provides a comparison of the UI-PMIDO with the UI-PMIO approach described in Chapter 6 to demonstrate the effectiveness of the developed UI-PMIDO.

Consider a state space system as follows:

$$\left.\begin{aligned} \dot{x} &= A\,x + Bu + E_u d_u + F_a f_a \\ y &= Cx \end{aligned}\right\} \tag{7-73}$$

where, $A = \begin{bmatrix} 0 & 1 \\ -2 & -2 \end{bmatrix}$, $B = \begin{bmatrix} 1 \\ 1.5 \end{bmatrix}$, $F_a = \begin{bmatrix} 1 \\ 1.5 \end{bmatrix}$, $E_u = \begin{bmatrix} 0.5 \\ -1 \end{bmatrix}$, $C = \begin{bmatrix} 1 & 0 \\ 2 & 1 \end{bmatrix}$,

d_u is represented by the output of a filter used to provide a band-limited signal from a zero-mean white noise signal (covariance = 0.001). A sinusoidal signal is used to denote the additive actuator fault for which the k_{th} derivative of the fault signal is bounded.

$$f_a = \begin{cases} 4.6 + 0.3\sin(t) & t \geq 3 \\ 0 & t < 3 \end{cases}$$

Then, an augmented system is constructed according to the (7-12) with $k = 2$, where,

$$\bar{A} = \begin{bmatrix} 0 & 1 & 0 & 1 \\ -2 & -2 & 0 & 1.5 \\ 0 & 0 & 0 & 0 \\ 0 & 0 & 1 & 0 \end{bmatrix},\ \bar{B} = \begin{bmatrix} 1 \\ 1.5 \\ 0 \\ 0 \end{bmatrix},\ \bar{F}_a = \begin{bmatrix} 1 \\ 1.5 \\ 0 \\ 0 \end{bmatrix},\ \bar{E}_u = \begin{bmatrix} 0.5 \\ -1 \\ 0 \\ 0 \end{bmatrix},$$

$$\bar{C} = \begin{bmatrix} 1 & 0 & 0 & 0 \\ 2 & 1 & 0 & 0 \end{bmatrix},\ G = \begin{bmatrix} 0 \\ 0 \\ 1 \\ 0 \end{bmatrix}.$$

The UI-PMIDO gains are calculated in terms of the Theorem 7.6 as:

$$K = \begin{bmatrix} 0 & 9.8077 \\ -2.0000 & 42.5537 \\ 0 & 615.8717 \\ 0 & 223.1617 \end{bmatrix}, \quad L_d = \begin{bmatrix} 5.9544 & 1.7821 \\ -4.7634 & 2.0801 \\ 24.3120 & -10.3095 \\ -3.5635 & 10.7187 \end{bmatrix}.$$

To evaluate the system capability of estimating both fault and system states, the system input, u, is set to $u = 0$. The simulation results for the state and fault estimates are shown in the following Figures 7-1to 7-4.

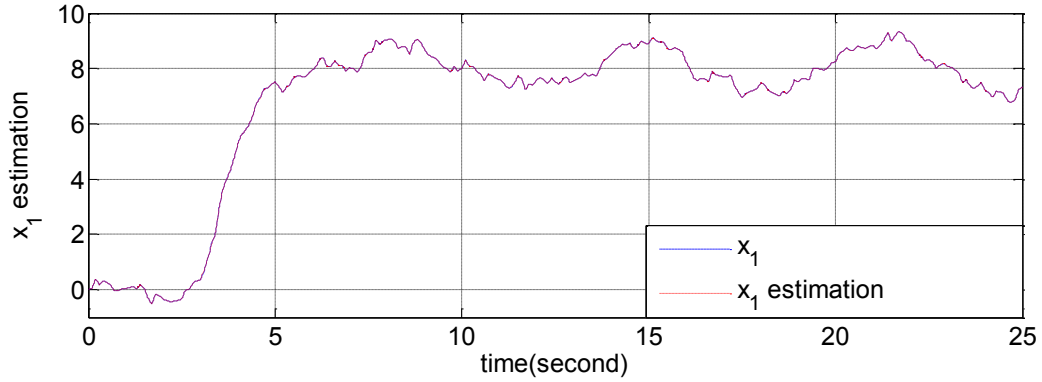

Figure 7-1 State x_1 and its estimation $\hat{x}_1$

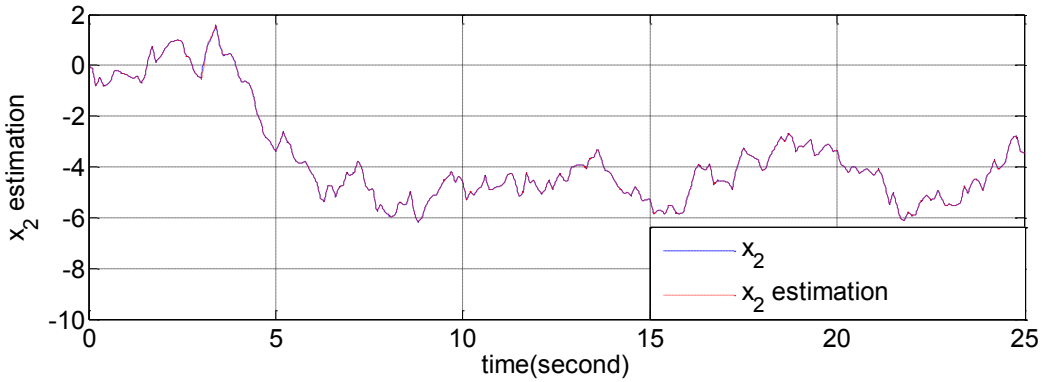

Figure 7-2 State x_2 and its estimation $\hat{x}_2$

Figures 7-1 & 7-2 exhibit the simulated system states (x_1, x_2) and their respective state estimates ($\hat{x}_1, \hat{x}_2$) provided by the UI-PMIDO. It can be seen that the reconstruction of the system states through the UI-PMIDO are adequately close to the original system state variables, which suggests that the observer system dynamics are removed from the injected UI, d_u due to the UI de-coupling effect.

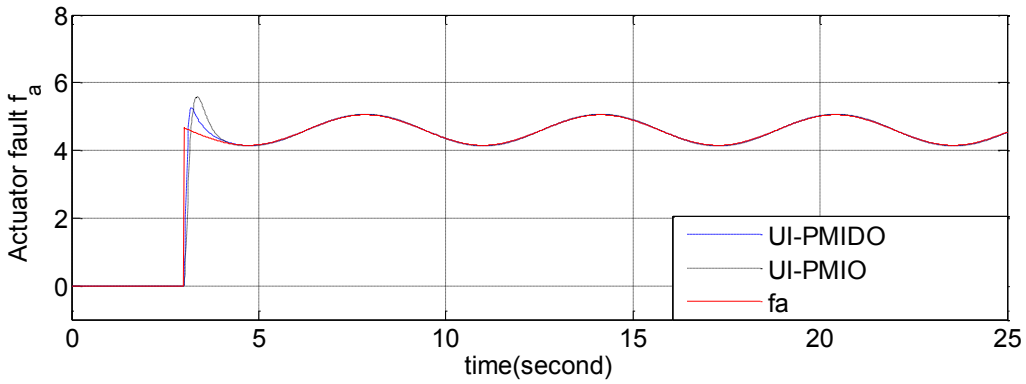

Figure 7-3 UI-PMIO & UI-PMIDO FE comparison (a)

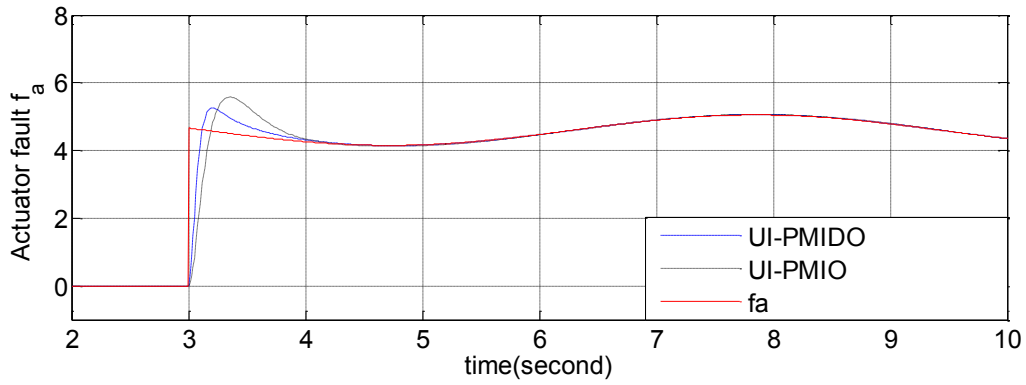

Figure 7-4 UI-PMIO & UI-PMIDO FE comparison (a) (zoom in)

Figure 7-3 shows the FE signals generated via the UI-PMIO and UI-PMIDO, respectively. Figure 7-4 shows a zoomed-in plot of Figure 7-3. The observer FE capability for each of the UI-PMIO and UI-PMIDO are illustrated and compared via Figures 7-3 & 7-4. Although the fault estimates from both the UI-PMIO and UI-PMIDO present accurate fault tracking during the steady-state period, the UI-PMIDO has better transient performance with a faster settling time and a lower overshoot than the transient response of the UI-PMIO. Meanwhile, the impact on FE signals using both observers caused by UI, d_u, is rarely noticeable, which proves that the UI is de-coupled completely from each of the observer FE subsystems.

In the second experiment, consider a $\times 7$ increase in the fault frequency as follows:

$$f_a = \begin{cases} 4.6 + 0.3\sin(7t) & t \geq 3 \\ 0 & t < 3 \end{cases}$$

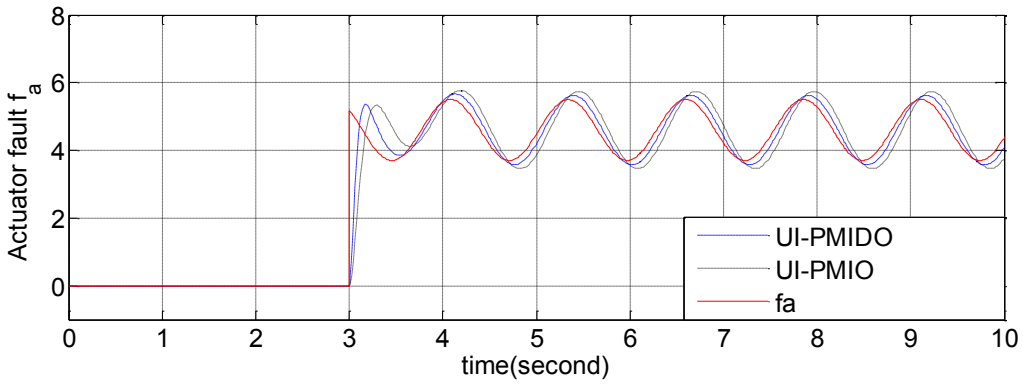

Figure 7-5 UI-PMIO & UI-PMIDO FE comparison (b)

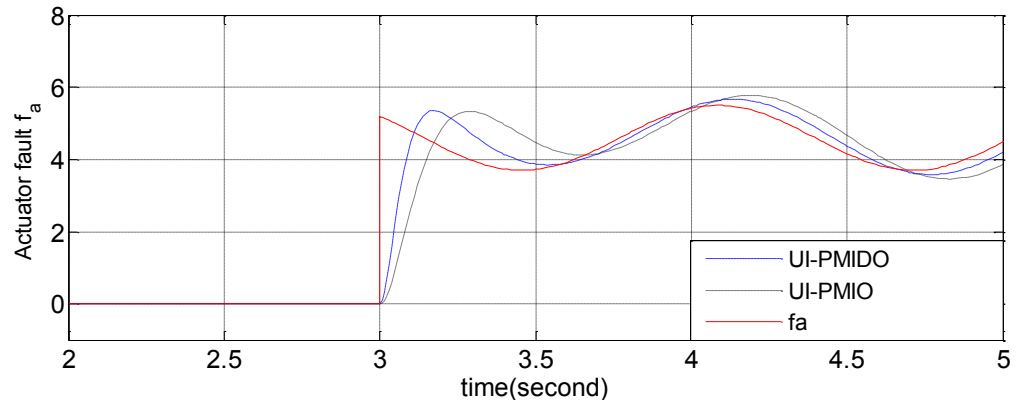

Figure 7-6 UI-PMIO & UI-PMIDO FE comparison (b) (zoom in)

The second simulation experiment is used to examine the responses of both the UI-PMIO and UI-PMIDO subjected to the higher frequency fault signal representing a more severe fault scenario. Figures 7-5 & 7-6 (showing an amplified region around the transient response) show a clear error of steady state after a short transient period. Compared with the results in Figure 7-3, the fault estimator demonstrates a reduced tracking accuracy which can be seen from both the UI-PMIDO and UI-PMIO when the higher frequency fault signal is considered. This phenomenon implies that the FE performance can be reduced when the fault characteristics change. However, the transient response of the UI-PMIDO estimation to the fault signal is still faster than the UI-PMIO's though an increase in the overshoot magnitude of the UI-PMIDO estimate can be seen. Hence, the above simulation results indicate that the UI-PMIO when structured to include a derivative term, is capable of adjusting the FE speed and reducing the settling time.

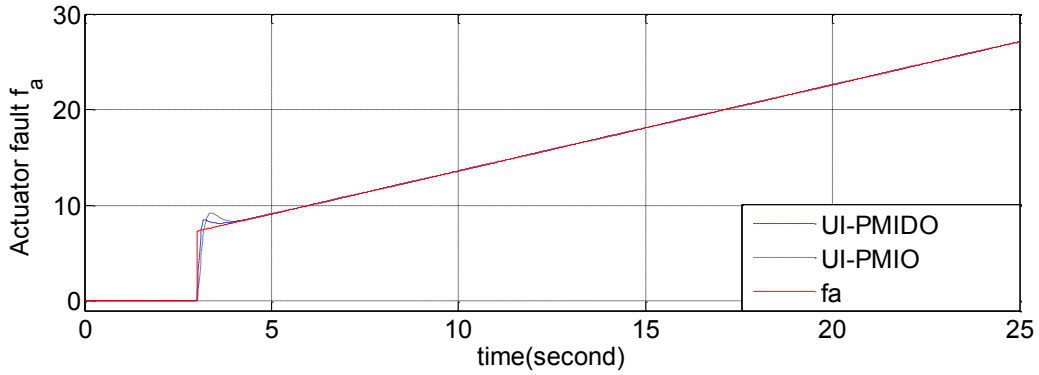

Figure 7-7 UI-PMIO & UI-PMIDO FE comparison in ramp fault case
(initial = 0, slope = 3, offset = 8)

The third simulation experiment tests the FE performance of the two kinds of observers when a different shape of the fault signal is chosen. In this case, a ramp fault with initial position = 0, slope = 3 and offset = 8 is applied to replace the sinusoidal fault.

Figure 7-7 contains the fault estimates following the ramp fault using each of the UI-PMIDO and UI-PMIO estimators. The simulation results demonstrate a similar and acceptable tracking performance in both cases for the ramp fault with a marked improvement in the transient speed when using the UI-PMIDO compared with the transient response of the UI-PMIO. The estimated fault signals can track the actual fault closely.

7.4 Conclusion

This Chapter presents an extension to the RFAFE estimator described in Chapter 4 and the UI-PMIO (Chapter 6). The UI-PMIDO inherits features of fast FE speed by including derivative action and the ability to estimate bounded finite time fault derivatives due to the multiple integral actions. The adopted UI de-coupling strategy successfully de-couples the exogenous disturbance, resulting in an unaffected fault estimate. The tutorial example is used to demonstrate the effectiveness of the novel UI-PMIDO FE methodology. The improved fault tracking performance of UI-PMIDO is given by a comparison with the simulation results resulting from the use of the UI-PMIO method proposed in Chapter 6.

In Chapter 8, a nonlinear FE design approach referred to as a polytopic UI-PMIDO is proposed based on LPV modelling. Compared with the LTI model-based FDI/FDD

design, it is promising to see that the polytopic UI-PMIDO design covers more modelling uncertainties. The practicality of this new approach is demonstrated using a nonlinear two-link manipulator system.

Chapter 8
Polytopic Proportional Multiple Integral and Derivative Observer-based FE with UI De-coupling

8.1 Introduction

Chapter 7 considers the observer design of the UI-PMIDO for LTI systems. However, the LTI approach to linear approximation of real systems is not always valid, because the un-modelled system dynamics can lead to stability issues and performance reduction not only for control system designs but also for observer designs.

Furthermore, the LTI system structure has the inability to take larger and more rapid smooth parameter variations into account. This is not only important for control but also for fault diagnosis using a mathematical model of the system being monitored.

Moreover, the dynamic behaviour of most practical systems is characterised by more than one operating point, so that linear model-based controller/observer designs are difficult to apply directly to nonlinear systems for lacking information of modelling uncertainties. From the standpoint of robust FDD for LTI system, it is ideally expected that the modelling uncertainties rising from operating point changes can be entirely represented by the UI distribution matrix, facilitating UI de-coupling or at least attenuation.

In (Chen and Patton, 1999), an industrial application on a gas turbine is given as an example to show how the UI distribution is derived and covers different operating points. Theoretically, the dimension and rank (number of independent columns) of the UI distribution depends on the nonlinear system complexity, i.e. in terms of the number of significant independent columns (i.e. rank) of the distribution matrix that are generated by the UI estimation. However, in reality, the UI distribution matrix is limited by the FDD design method, for example the UIO design requires that the maximum number of independent UI cannot be larger than the maximum number of independent measurements.

Even though the so-called low rank approximation (see Section 2.3.5) can be applied to approximate the UI matrix by one of a lower rank (to satisfy the dimension for satisfying the de-coupling condition), the loss of information through this approximation is itself a form of uncertainty that will compromise the performance of the FDD design. Furthermore, when more modelling uncertainties are taken into account, less freedom is left for handling the exogenous UI. In summary, the robustness that can be gained from using the UI de-coupling principle may be quite restrictive.

Above all, it is hoped to find a modelling approach that may be used to represent a wide class of smooth nonlinear systems efficiently so that modelling uncertainties can be taken into account in a non-conservative manner compared with the case that is apparent when LTI modelling is used. Following on from this discussion a potentially suitable approach to modelling some nonlinear or time-varying systems is to use an LPV model representation.

In recent years, an interesting 'LPV modelling approach' has been proposed in the context of gain-scheduling design (Becker, Packard, Philbrick and Balas, 1993; Apkarian and Adams, 1998). The gain-scheduling approaches are linked by overcoming the challenges imposed by attempting to deal with the overall system dynamics. This can be achieved by decomposing the smooth nonlinear system into a number of linear controller/observer design problems. Continuity is maintained with well-established linear methods and is generally lost when using gain-scheduling due to switching action between controller/observer sets. On the other hand LPV modelling is distinct from the conventional gain-scheduling approach due to the use of direct synthesis of a controller/observer rather than its construction from a family of local linear controllers designed by LTI methods. Especially, the induced L_2 norm is broadly used as a performance measure which means that the continuity can be maintained with well-known linear H_∞ theory.

Extensive research illustrates the high applicability of the LPV modelling approach in the domain of robust designs for control and estimation. Interesting application studies include vehicular systems, aerospace and aircraft as reported by (Wu, 2001; Bhattacharya, Balas, Kaya and Packard, 2002; Ganguli, Marcos and Balas, 2002; Henry and Zolghadri, 2004; Zolghadri, Castang and Henry, 2006).

The purpose of this Chapter is to extend the UI-PMIDO design methods studied in Chapter 7 by incorporating the UI-PMIDO within an LPV modelling framework to achieve robust FE design. The practicality of this FE strategy is considered based on a study involving a nonlinear two-link manipulator system example, in which the modelling uncertainties are not taken into account in the UI de-coupling design. Instead, they are handled by the LPV modelling structure that takes into account the errors arising from local approximation to the non-linearities. This provides freedom to handle the exogenous disturbance through the UI de-coupling principle. It is argued here that this approach to the use of UI-PMIDO has wide application for real engineering systems with smooth nonlinear structure.

The LPV system concept was first addressed by (Shamma and Athans, 1990) by defining as a set of state space linear system, where the time dependence in the state-space data enters through a known dependence on a vector-valued parameter signal (Shamma and Athans, 1992). The ideas about using LPV representations were motivated by the well-known use of gain scheduling control designs used for example in flight control (Shamma and Athans, 1990) and (Rugh, 1991). There was a need to develop a more systematic framework for accounting accurately for time-varying system behaviour using scheduling parameters. In the LPV approach the time dependence uses an on-line measurable vector-valued parameter signal, the so-called scheduling vector of parameters that relate to the state space description (not the exogenous independent variables) of the original nonlinear system.

Key studies on LPV can be found in (Rugh, 1991; Shamma and Athans, 1992; Becker, Packard, Philbrick and Balas, 1993; Becker, 1995; Apkarian and Adams, 1998; Leith and Leithead, 2000; Rugh and Shamma, 2000). In particular, (Shamma and Athans, 1992) discuss the issues of ‘stability and performance’ of LPV control theory design exploiting the concept of a parameter-dependent Lyapunov function. This is also discussed in the context of robustness analysis and synthesis in (Apkarian, Gahinet and Becker, 1995; Becker, 1995; Wu, Yang, Packard and Becker, 1995; Gahinet, Apkarian and Chilali, 1996). A well cited survey paper on gain-scheduling methods by (Leith and Leithead, 2000), refers to the LPV problem as a related issue.

Although the LPV modelling approach has been popularised in robust controller design it has also attracted significant attention from the FDI/FDD community in recent years.

There has been a substantial amount of work on the application of LPV methods for the design of observer/estimators for the fault monitoring role based on FDI/FDD. (Bokor, Szabo and Stikkel, 2002) introduced the LPV modelling approach for FDI/FDD design. Following that, many other researches on FDI/FDD schemes based on the LPV modelling approach have been developed (Bokor and Balas, 2004; Henry and Zolghadri, 2004; Rodrigues, Theilliol and Sauter, 2005c; Rodrigues, Theilliol and Sauter, 2005b; Zolghadri, Castang and Henry, 2006; Casavola, Famularo, Franze and Sorbara, 2007; Grenaille, Henry and Zolghadri, 2008; Bokor and Szabó, 2009; Hamdi, Rodrigues, Mechmeche, Theilliol and BenHadjBraiek, 2009; Zhang, Jiang and Chen, 2009; Patton and Klinkhieo, 2010; Chen and Patton, 2011; Patton, Chen and Klinkhieo, 2012; Rosa and Silvestre, 2012; Alwi, Edwards and Marcos, 2012).

The LPV modelling-based FDI/FDD design also faces the central 'robust issues' as introduced in Chapter 2. Therefore, the key problem is how to generate residuals or FE signals that are sensitive to faults but insensitive to the UI. Some efforts on norm-based work to minimise the UI effects on system states and fault indicator/estimator have been presented in (Henry and Zolghadri, 2004; Grenaille, Henry and Zolghadri, 2008; Patton and Klinkhieo, 2010; Chen, Patton and Goupil, 2012). However, few studies extend the UIO design problem to an LPV model framework for FDI/FDD (Rodrigues, Theilliol and Sauter, 2005a; Hamdi, Rodrigues, Mechmeche, Theilliol and BenHadjBraiek, 2009; Hamdi, Rodrigues, Mechmeche and BenHadjBraiek, 2012). Of particular interest is the work of (Rodrigues, Theilliol and Sauter, 2005a) which focuses on a residual generation-based FDI. The FE design can be found in (Hamdi, Mickael, Chokri, Theilliol and Naceur Benhadj, 2012).

This Chapter is motivated by an interest in developing an LPV model-based approach to polytopic UI-PMIDO design for actuator fault and state estimation. The main contribution of this work is to re-cast the UI-PMIDO LTI theory of Chapter 7 into an LPV framework for FE design. After first describing the mathematical background, the stability conditions that must be satisfied for the LPV form of the UI-PMIDO are investigated using an LMI formulation.

One of the objectives of this study is to examine if the proposed polytopic UI-PMIDO is a good candidate for estimating the faults and states of the nonlinear system being monitored.

The structure of the remainder of this Chapter is as follows: Section 8.2 describes the background of the LPV modelling representation based on polytopic-formalism, interpreted as a description of the system as a convex combination of subsystems defined by the vertices of a convex polytope. These sub-models are combined by a convex weighting function to construct the global model.

Section 8.3 describes the design of a polytopic UI-PMIDO for the purpose of estimating the bounded finite time derivatives of actuator faults and system states for a nonlinear system with non-unique equilibria. The system description allows for the presence of both UI (as exogenous disturbances) as well as faults. Note that to estimate the states and faults, all matrices of the LPV systems are considered with time-varying parameters and the proposed polytopic UI-PMIDO theory applies to a LPV polytopic-formalism with assumption that the state space description has an affine parameter dependence.

Finally, Section 8.4 provides an illustrative example, i.e. a nonlinear two-link manipulator is used to illustrate the effectiveness of the proposed LPV approach.

8.2 LPV modelling Preliminaries

Section 8.1 introduces the main concepts of LPV modelling. The design task is to establish the LPV modelling scheduled by the appropriate online measurable time-varying vector-valued parameters depending on the state space system (Rugh, 1991; Shamma and Athans, 1992; Leith and Leithead, 2000; Rugh and Shamma, 2000). The LPV model realisation obtains smooth semi-linear models that are smoothly dependent on an online measurable time-varying vector of scheduling parameters. The idea is that from a practical standpoint the nonlinear system can be mimicked in the LPV mathematical representation by using the linearisation along trajectories of the parameters. For example for an aircraft problem the scheduling parameters are typically mass, altitude and centre of gravity (Shamma and Athans, 1992; Chen, Patton and Goupil, 2012). Whereas for the two-link manipulator problem the main scheduling variables are the joint angles denoted by a vector.

The LPV mathematical description in continuous state space form is given in (8-1) with the parameter-dependent matrix quadruple $\left[A_p(\theta), B_p(\theta), C_p(\theta), D_p(\theta)\right]$:

$$\left.\begin{aligned} \dot{x}_p &= A_p(\theta)x_p + B_p(\theta)u \\ y_p &= C_p(\theta)x_p + D_p(\theta)u \end{aligned}\right\} \tag{8-1}$$

where, $A_p(\theta) \in \Re^{n\times n}$, $B_p(\theta) \in \Re^{n\times m}$, $C_p(\theta) \in \Re^{p\times n}$ and $D_p(\theta) \in \Re^{p\times n}$ are continuous functions of the measured scheduling parameter vector θ. In this Chapter, it is consider the case that $C_p(\theta)$ is constant, i.e. can be represented as C_p. Also, the input signal has no effect direct on the output channel which means the input to output distribution matrix is $D_p(\theta) = 0$.

In the light of the work in (Apkarian, Gahinet and Becker, 1995), two assumptions are given for the faulty LPV system (8-1) as follows:

Assumptions 8.1

(1) The parameter dependence is affine, that is, the state space matrices $A_p(\theta)$ and $B_p(\theta)$ depend affinely on time-varying vector θ.

(2) Time-varying vector θ varies in a convex polytope Θ of vertices $\{\theta_1, \theta_2, \cdots \theta_j \ (j = 2^s)\}$, i.e.

$$\theta \in \Theta := \{\theta_1, \theta_2, \cdots \theta_j\} = \left\{\sum_{i=1}^{j} \alpha_i\theta_i : \alpha_i \geq 0, \sum_{i=1}^{j} \alpha_i = 1\right\} \tag{8-2}$$

With the Assumptions 8.1(1) & (2), the state space matrices in (8-1) range in a polytope of matrices which are the image of the polytopic vertices $\{\theta_1, \theta_2, \cdots \theta_j \ (j = 2^s)\}$. s is the number of elements in vector . This is expressed as:

$$\begin{bmatrix} A_p(\theta) & B_p(\theta) \\ C_p & 0 \end{bmatrix} \in C_O \left\{ \begin{bmatrix} A_p(\theta_i) & B_p(\theta) \\ C_p & 0 \end{bmatrix} \right\}_{i=1,\cdots,j} \tag{8-3}$$

If θ is a given parameter vector then an LPV system can be reduced to a linear time varying (LTV) system with a constant trajectory. Furthermore, if θ is a constant parameter, i.e. the parameter trajectory is constant, an LPV system can be reduced to an LTI system.

The LPV system with actuator faults and UI is described as:

$$\left.\begin{aligned} \dot{x}_p &= A_p(\theta)x_p + B_p(\theta)u + E_p(\theta)d + F_{ap}(\theta)f_a \\ y_p &= C_p x_p(t) \end{aligned}\right\} \tag{8-4}$$

where, $x_p \in \Re^n$, $u \in \Re^r$, $y_p \in \Re^m$, and $d \in \Re^q$, are the system states, control inputs, outputs, disturbance and actuator faults $f_a \in \Re^l$, respectively. $\theta \in \Re^s$ is a time-varying vector. $A_p(\theta)$, $B_p(\theta)$, C_p are state space matrices with appropriate dimensions, $E_p(\theta)$ is the disturbance distribution matrix, $F_{ap}(\theta)$ is the fault distributed matrix.

With the Assumptions 8.1 (1) & (2), the state space matrices in (8-4) are spanned by a polytope of matrices which are the image of the polytopic vertices $\{\theta_1, \theta_2, \cdots \theta_j \ (j = 2^s)\}$. The representation is expressed as:

$$\begin{bmatrix} A_p(\theta) & B_p(\theta) & E_p(\theta) & F_{ap}(\theta) \\ C_p & 0 & 0 & 0 \end{bmatrix} \in C_O \left\{ \begin{bmatrix} A_p(\theta) & B_p(\theta) & E_p(\theta) & F_{ap}(\theta) \\ C_p & 0 & 0 & 0 \end{bmatrix} \right\}_{i=1,\cdots,j} \tag{8-5}$$

8.3 Polytopic PMIDO design

In the light of (7-9) & (7-10) in Chapter 7, the bounded k_{th} derivative of the fault f, i.e. $f^{(k)}$, is defined as:

$$\varepsilon_i = f^{(k-i)} \qquad (i = 1,2,\cdots,k) \tag{8-6}$$

$$\begin{aligned} \dot{\varepsilon}_1 &= f^{(k)} \\ \dot{\varepsilon}_2 &= \varepsilon_1 \\ &\vdots \\ \dot{\varepsilon}_k &= \varepsilon_{k-1} \end{aligned} \tag{8-7}$$

Then, (8-4) is formulated into an augmented state representation as:

$$\left.\begin{aligned} \dot{\bar{x}}_p &= \bar{A}_p(\theta)\bar{x}_p + \bar{B}_p(\theta)u + \bar{E}_p(\theta)d \\ y_p &= \bar{C}_p\bar{x}_p \end{aligned}\right\} \tag{8-8}$$

where, $\bar{x}_p = \begin{bmatrix} x_p^T & \bar{\varepsilon}_1^T & \bar{\varepsilon}_2^T & \cdots & \bar{\varepsilon}_k^T \end{bmatrix}^T \in \Re^{\bar{n}}$. $\bar{A}_p(\theta)$, $\bar{B}_p(\theta)$, $\bar{C}_p$, $\bar{E}_p(\theta)$, $\bar{F}_{ap}(\theta)$ are state space matrices with appropriate dimensions.

$$\bar{A}_p(\theta) = \begin{pmatrix} A_p(\theta) & 0 & \cdots & 0 & F_{ap}(\theta) \\ 0 & 0 & \cdots & 0 & 0 \\ 0 & I & \cdots & 0 & 0 \\ \vdots & \vdots & \ddots & \vdots & \vdots \\ 0 & 0 & \cdots & I & 0 \end{pmatrix} \in \Re^{\bar{n}\times\bar{n}}$$

$$\bar{B}_p(\theta) = \begin{bmatrix} B_p(\theta)^T & 0 & 0 & \cdots & 0 \end{bmatrix}^T \in \Re^{\bar{n}\times r}$$

$$\bar{E}_p(\theta) = \begin{bmatrix} E_p(\theta)^T & 0 & 0 & \cdots & 0 \end{bmatrix}^T \in \Re^{\bar{n}\times q}$$

$$\bar{G}_p = [0 \quad I_l \quad 0 \quad \cdots \quad 0]^T \in \Re^{\bar{n}\times l}$$

$$\bar{C}_p = [C_p \quad 0 \quad 0 \quad \cdots \quad 0] \in \Re^{m\times\bar{n}}$$

$$\bar{n} = n + lk \tag{8-9}$$

For the polytope design a polytopic UI-PMIDO is constructed as a polytopic extension of the functional observer given by (8-10) (with affine dependence on the parameter θ for the augmented system of (8-8):

$$\left.\begin{aligned} \dot{\bar{z}}_p &= \bar{N}_p(\theta)\,\bar{z}_p + \bar{T}_p(\theta)\,\bar{B}_p(\theta)u + \bar{K}_p(\theta)y + \bar{L}_{dp}(\theta)(y-\hat{y}) \\ \hat{\bar{x}}_p &= \bar{z}_p + \bar{H}_p(\theta)\,y \end{aligned}\right\} \tag{8-10}$$

The state estimation error dynamics (8-11) of the augmented system (8-8) are then formulated as a polytopic extension of the functional observer described in (Chen and Patton, 1999):

$$\begin{aligned} \dot{\bar{e}}_p = &\left[\left(\bar{A}_p(\theta) - \bar{H}_p(\theta)\bar{C}_p\bar{A}_p(\theta) - \bar{K}_{1p}(\theta)\bar{C}_p\right)\bar{e}_p\right. \\ &+\left[\bar{N}_p(\theta) - \left(\bar{A}_p(\theta) - \bar{H}_p(\theta)\bar{C}_p\bar{A}_p(\theta) - \bar{K}_{1p}(\theta)\bar{C}_p\right)\right]\bar{z}_p \\ &+\left[\bar{K}_{2p}(\theta) - \left(\bar{A}_p(\theta) - \bar{H}_p(\theta)\bar{C}_p\bar{A}_p(\theta) - \bar{K}_{1p}(\theta)\bar{C}_p\right)\bar{H}_p(\theta)\right]y \\ &+\left[\bar{T}_p(\theta) - \left(I_{\bar{n}} - \bar{H}_p(\theta)\bar{C}_p\right)\right]\bar{B}_p(\theta)u \\ &+\left(\bar{H}_p(\theta)\bar{C}_p - I_{\bar{n}}\right)\bar{E}_p(\theta)d + \bar{G}_p f^{(k)} - \bar{L}_{dp}(\theta)\left(\dot{y} - \dot{\hat{y}}\right) \end{aligned} \tag{8-11}$$

where,

$$\bar{K}_p(\theta) = \bar{K}_{1p}(\theta) + \bar{K}_{2p}(\theta) \tag{8-12}$$

If the following relations are satisfied:

$$\left(\bar{H}_p(\theta)\bar{C}_p - I_{\bar{n}}\right)\bar{E}_p(\theta) = 0 \tag{8-13}$$

$$\bar{T}_p(\theta) = I_{\bar{n}} - \bar{H}_p(\theta)\bar{C}_p \tag{8-14}$$

$$\begin{aligned}\bar{N}_p(\theta) &= \left(\bar{A}_p(\theta) - \bar{H}_p(\theta)\bar{C}_p\bar{A}_p(\theta) - \bar{K}_{1p}(\theta)\bar{C}_p\right) \\ &= (\bar{A}_{1p}(\theta) - \bar{K}_{1p}(\theta)\bar{C}_p\end{aligned} \tag{8-15}$$

$$\bar{K}_{2p}(\theta) = \bar{N}_p(\theta)\bar{H}_p(\theta) \tag{8-16}$$

Then,

$$\dot{\bar{e}}_p = \bar{N}_p(\theta)\bar{e}_p - \bar{L}_{dp}(\theta)(\dot{\bar{y}} - \dot{\hat{\bar{y}}}) + \bar{G}_p f^{(k)} \tag{8-17}$$

(8-17) can be re-written as:

$$\begin{aligned}\dot{\bar{e}}_p &= \bar{N}_p(\theta)\bar{e}_p - \bar{L}_{dp}(\theta)\bar{C}_p\left(\dot{\bar{x}}_p - \dot{\hat{\bar{x}}}_p\right) + \bar{G}_p f^{(k)} \\ &= \bar{N}_p(\theta)\bar{e}_p - \bar{L}_{dp}(\theta)\bar{C}_p\dot{\bar{e}}_p + \bar{G}_p f^{(k)}\end{aligned} \tag{8-18}$$

i.e.

$$\left(I_{\bar{n}} + \bar{L}_{dp}(\theta)\bar{C}_p\right)\dot{\bar{e}}_p = \bar{N}_p(\theta)\bar{e}_p + \bar{G}_p f^{(k)} \tag{8-19}$$

Then let

$$\bar{R}_{dp}(\theta) = I_{\bar{n}} + \bar{L}_{dp}(\theta)\bar{C}_p \tag{8-20}$$

Then, (8-15) is re-written as:

$$\bar{R}_{dp}(\theta)\dot{\bar{e}}_p = \bar{N}_p(\theta)\bar{e}_p + \bar{G}_p f^{(k)} \tag{8-21}$$

Hence, (8-18) can be reorganized to:

$$\begin{aligned}\dot{\bar{e}}_p &= \bar{R}_{dp}^{-1}(\theta)\bar{N}_p(\theta)\bar{e}_p + \bar{R}_{dp}^{-1}(\theta)\bar{G}_p f^{(k)} \\ &= \bar{N}_{Rp}(\theta)\bar{e}_p + \bar{G}_{Rp}(\theta)f^{(k)}\end{aligned} \tag{8-22}$$

where, $\bar{N}_{Rp}(\theta) = \bar{R}_{dp}^{-1}(\theta)\bar{N}_p(\theta)$ and $\bar{G}_{Rp}(\theta) = \bar{R}_{dp}^{-1}(\theta)\bar{G}_p$

Definition 8.1 Observer (8-10) is defined as a polytopic UI-PMIDO for (8-8), if all the eigenvalues of $\bar{N}_{Rp}(\theta)$ are stable, $\bar{e}_p = \dot{\bar{x}}_p - \dot{\hat{\bar{x}}}_p$ will approach zero asymptotically with the presence of both UI and faults, i.e. $\hat{\bar{x}}_p \to \bar{x}_p$. The observer (8-10) is a polytopic UI-PMIDO.

Remark 8.1: Based on Definition 8.1, the polytopic UI-PMIDO design objective for the LPV model is to solve the (8-12) to (8-16) whilst assigning the eigenvalues of the system matrix $\bar{N}_{Rp}(\theta)$ to the left hand of the complex plane uniformly. Meanwhile, $\bar{N}_{Rp}(\theta)$, $\bar{T}_p(\theta)$, $\bar{K}_p(\theta)$ and $\bar{H}_p(\theta)$ in (8-10) are designed to achieve the required state and FE performance.

Following the polytopic UI-PMIDO structure proposed above, the augmented error dynamics of (8-22) are derived in Theorem 8.1, Theorem 8.2 and Theorem 8.3.

Theorem 8.1: The necessary and sufficient conditions for the existence of a polytopic UI-PMIDO of system (8-5) are:

(1) $rank(\bar{C}_p\bar{E}_p(\theta)) = rank(\bar{E}_p(\theta))$

(2) $(\bar{C}_p,\ \bar{A}_{1p}(\theta))$ is a detectable pair

A particular solution to (8-13) can be determined as follows:

$$\bar{H}_p(\theta) = \bar{E}_p(\theta)(\bar{C}_p\bar{E}_p(\theta))^+ \tag{8-23}$$

where, $(\bar{C}_p\bar{E}_p(\theta))^+ = [(\bar{C}_p\bar{E}_p(\theta))^T(\bar{C}_p\bar{E}_p(\theta))]^{-1}(\bar{C}_p\bar{E}_p(\theta))^T$ denotes the Moore-Penrose pseudo-inverse.

Remark 8.2: The proof of Theorem 8.1 can be found by following the principle of LTI-based UIO design in (Chen and Patton, 1999).

Remark 8.3: Item $\bar{G}_{Rp}f^{(k)}$ in (8-22) cannot be de-coupled as the signal $\bar{G}_{Rp}f^{(k)}$ does not satisfy Condition (1) in Theorem 8.1. It is therefore appropriate to apply the H_∞ optimisation theory outlined in Theorem 8.2 to attenuate the effect of the signal $\bar{G}_{Rp}f^{(k)}$ on the augmented state estimation error dynamics $\dot{\bar{e}}_p$ of the functional observer (8-10).

Theorem 8.2 For $t > 0$ the system polytopic UI-PMIDO is asymptotically stable and the H_∞ performance is guaranteed with optimisation level γ_{ap} to attenuate the effect

of $f^{(k)}$, if there exist an S.P.D matrix $\bar{P}_{1p}$, and matrices $\bar{P}_{2p}$, $\bar{P}_{3p}$, such that the following LMI holds:

$$\begin{bmatrix} \bar{P}_{2p}+\bar{P}_{2p}^T & \bar{P}_{1p}\bar{N}_p(\theta)-\bar{P}_{2p}^T\bar{R}_{dp}(\theta)+\bar{P}_{3p} & \bar{P}_{1p}\bar{G} & 0 \\ * & -\bar{P}_{3p}^T\bar{R}_{dp}(\theta)-\bar{R}_{dp}^{-1}(\theta)\bar{P}_{3p} & 0 & \bar{C}_p^T \\ * & * & -\gamma_{ap} & 0 \\ * & * & * & -\gamma_{ap} \end{bmatrix} < 0 \qquad (8\text{-}24)$$

where, $\bar{N}_p(\theta)$ and $\bar{R}_{dp}(\theta)$ are defined in (8-15) and (8-20), respectively.

Proof:

Using the state estimation error $\bar{e}_p$ defined in Definition 8.1, the candidate Lyapunov function $V(\bar{e}_p)$ is given by:

$$V(\bar{e}_p) = \bar{e}_p^T\bar{P}_{1p}\bar{e}_p \qquad (8\text{-}25)$$

In terms of $\dot{\bar{e}}_p$ defined in (8-22), the time derivative of the candidate Lyapunov function $\dot{V}(\bar{e}_p)$ can be derived as (8-26) for the augmented system (8-22) as:

$$\dot{V}(\bar{e}_p) = \bar{e}_p^T\left[\bar{P}_{1p}\left(\bar{A}_{1p}(\theta)-\bar{K}_{1p}(\theta)\bar{C}_p\right)+\left(\bar{A}_{1p}(\theta)-\bar{K}_{1p}(\theta)\bar{C}_p\right)^T\bar{P}_{1p}\right]\bar{e}_p$$
$$+2\bar{e}_p^T\bar{P}_{1p}\bar{G}_{Rp}f^{(k)} \qquad (8\text{-}26)$$

with $\bar{N}_p(\theta) = \bar{A}_{1p}(\theta)-\bar{K}_{1p}(\theta)\bar{C}_p$.

$$\dot{V}(\bar{e}_p) = \bar{e}_p^T\left[\bar{P}_{1p}\bar{N}_{Rp}(\theta)+\bar{N}_{Rp}^T(\theta)\bar{P}_{1p}\right]\bar{e}_p + 2\bar{e}_p^T\bar{P}_{1p}\bar{G}f^{(k)} \qquad (8\text{-}27)$$

The H_∞ optimisation theory is used to attenuate the effect of $f^{(k)}$ on the state estimation error $\bar{e}_p$ to ensure that the system (8-22) is stabilized simultaneously by determining the minimum value of γ_{ap}.

$$\dot{V}(\bar{e}_p)+\frac{1}{\gamma_{ap}}\bar{C}_p^T\bar{e}_p^T\bar{e}_p\bar{C}_p-\gamma_{ap}{f^{(k)}}^T f^{(k)} < 0 \qquad (8\text{-}28)$$

(8-28) is identical to (8-29).

$$\begin{bmatrix}\bar{e}\\ f^{(k)}\end{bmatrix}^T\begin{bmatrix}\bar{P}_{1p}\bar{N}_{Rp}(\theta)+\bar{N}_{Rp}^T(\theta)\bar{P}_{1p}+\frac{1}{\gamma_a}\bar{C}_p^T\bar{C}_p & \bar{P}_{1p}\bar{G}_R\\ * & -\gamma_{ap}\end{bmatrix}\begin{bmatrix}\bar{e}\\ f^{(k)}\end{bmatrix} < 0 \qquad (8\text{-}29)$$

Using the Schur Complement Lemma, it can be shown that (8-30) holds.

$$\begin{bmatrix} \bar{P}_{1p}\bar{N}_{Rp}(\theta) + \bar{N}_{Rp}^{T}(\theta)\bar{P}_{1p} & \bar{P}_1\bar{G}_R & \bar{C}_p^T \\ * & -\gamma_{ap} & 0 \\ * & * & -\gamma_{ap} \end{bmatrix} \quad \bar{P}_1 > 0 \qquad (8\text{-}30)$$

Substituting $\bar{N}_{Rp}(\theta) = \bar{R}_{dp}^{-1}(\theta)\bar{N}_p(\theta)$ and $\bar{G}_{Rp} = \bar{R}_{dp}^{-1}(\theta)\bar{G}_p$ into (8-30), then,

$$\begin{bmatrix} \bar{P}_{1p}\bar{R}_{dp}^{-1}(\theta)\bar{N}_p(\theta) + \left(\bar{R}_{dp}^{-1}(\theta)\bar{N}_p(\theta)\right)^T\bar{P}_{1p} & \bar{P}_{1p}\bar{R}_{dp}^{-1}(\theta)\bar{G}_p & \bar{C}_p^T \\ * & -\gamma_{ap} & 0 \\ * & * & -\gamma_{ap} \end{bmatrix} < 0$$

$$\bar{P}_{1p} > 0 \qquad (8\text{-}31)$$

It can be seen that (8-31) involves $\bar{R}_{dp}^{-1}(\theta)$ presenting a challenge to determining the solution of (8-31). To simplify the approach to this solution the following reformulations are taken with (8-31) re-written as:

$$\begin{bmatrix} \bar{P}_{1p} & 0 & 0 \\ 0 & I & 0 \\ 0 & 0 & I \end{bmatrix}\left(\begin{bmatrix} \bar{R}_{dp}^{-1}(\theta) & 0 & 0 \\ 0 & I & 0 \\ 0 & 0 & I \end{bmatrix}\begin{bmatrix} \bar{N}_p(\theta) & \bar{G}_p & 0 \\ 0 & -\frac{\gamma_{ap}}{2} & 0 \\ \bar{C} & 0 & -\frac{\gamma_{ap}}{2} \end{bmatrix}\right)$$

$$+\left(\begin{bmatrix} \bar{R}_{dp}^{-1}(\theta) & 0 & 0 \\ 0 & I & 0 \\ 0 & 0 & I \end{bmatrix}\begin{bmatrix} \bar{N}_p(\theta) & \bar{G}_p & 0 \\ 0 & -\frac{\gamma_{ap}}{2} & 0 \\ \bar{C}_p & 0 & -\frac{\gamma_{ap}}{2} \end{bmatrix}\right)^T\begin{bmatrix} \bar{P}_{1p} & 0 & 0 \\ 0 & I & 0 \\ 0 & 0 & I \end{bmatrix}^T < 0 \qquad (8\text{-}32)$$

Following the concept of Lemma 7.1 ($det(sI - \bar{\Phi}\bar{\Psi}) = det(sI - \bar{\Psi}\bar{\Phi})$), as an extension to the polytopic case, (8-32) is identical to:

$$\begin{bmatrix} \bar{P}_{1p} & 0 & 0 \\ 0 & I & 0 \\ 0 & 0 & I \end{bmatrix}\left(\begin{bmatrix} \bar{N}_p(\theta) & \bar{G}_p & 0 \\ 0 & -\frac{\gamma_{ap}}{2} & 0 \\ \bar{C}_p & 0 & -\frac{\gamma_{ap}}{2} \end{bmatrix}\begin{bmatrix} \bar{R}_{dp}^{-1}(\theta) & 0 & 0 \\ 0 & I & 0 \\ 0 & 0 & I \end{bmatrix}\right)$$

$$+\left(\begin{bmatrix} \bar{N}_p(\theta) & \bar{G}_p & 0 \\ 0 & -\frac{\gamma_{ap}}{2} & 0 \\ \bar{C}_p & 0 & -\frac{\gamma_{ap}}{2} \end{bmatrix}\begin{bmatrix} \bar{R}_{dp}^{-1}(\theta) & 0 & 0 \\ 0 & I & 0 \\ 0 & 0 & I \end{bmatrix}\right)^T\begin{bmatrix} \bar{P}_{1p} & 0 & 0 \\ 0 & I & 0 \\ 0 & 0 & I \end{bmatrix}^T < 0 \qquad (8\text{-}33)$$

then, (8-33) is re-organised as:

$$\begin{bmatrix} \bar{R}_{dp}^T(\theta)\bar{P}_{1p}\bar{N}_p(\theta) + \bar{N}_p^T(\theta)\bar{P}_{1p}\bar{R}_{dp}(\theta) & \bar{R}_{dp}^T(\theta)\bar{P}_{1p}\bar{G}_p & \bar{C}_p^T \\ * & -\gamma_{ap} & 0 \\ * & * & -\gamma_{ap} \end{bmatrix} < 0 \quad \bar{P}_{1p} > 0 \tag{8-34}$$

There always exists $\bar{P}_{2p}$which satisfies:

$$\bar{P}_{2p} + \bar{P}_{2p}^T < 0 \tag{8-35}$$

Substituting (8-35) into (8-34):

$$\begin{bmatrix} \bar{\Omega}_p & \bar{R}_{dp}^T(\theta)\bar{P}_{1p}\bar{G}_p & \bar{C}_p{}^T \\ * & -\gamma_{ap} - \bar{C}_p^T\bar{P}_{1p}(\bar{P}_{2p} + \bar{P}_{2p}^T)^{-1}\bar{P}_{1p}\bar{G}_p & 0 \\ * & * & -\gamma_{ap} \end{bmatrix} < 0 \tag{8-36}$$

where, $\bar{\Omega}_p(\theta) = \bar{R}_{dp}^T(\theta)\bar{P}_{1p}\bar{N}_p(\theta) + N_p^T(\theta)\bar{P}_{1p}\bar{R}_{dp}(\theta)$.

In terms of the Schur Complement Lemma, it follows that:

$$\begin{bmatrix} \bar{P}_{2p} + \bar{P}_{2p}^T & 0 & \bar{P}_{1p}\bar{G}_p & 0 \\ 0 & \bar{\Omega}_p(\theta) & \bar{R}_{dp}^T(\theta)\bar{P}_{1p}\bar{G}_p & \bar{C}_p^T \\ * & * & -\gamma_{ap} & 0 \\ * & * & * & -\gamma_{ap} \end{bmatrix} < 0 \tag{8-37}$$

Let

$$\bar{P}_{3p} = -\bar{P}_{1p}\bar{N}_p(\theta) - \bar{P}_{2p} \tag{8-38}$$

To separate the product $\bar{N}_p^T(\theta)$, $\bar{P}_1$, and $\bar{R}_{dp}(\theta)$, pre- and post- multiplying (8-37) by $\begin{bmatrix} I & 0 & 0 & 0 \\ -R_{dp}^T(\theta) & I & 0 & 0 \\ 0 & 0 & I & 0 \\ 0 & 0 & 0 & I \end{bmatrix}$ and $\begin{bmatrix} I & 0 & 0 & 0 \\ -R_{dp}^T(\theta) & I & 0 & 0 \\ 0 & 0 & I & 0 \\ 0 & 0 & 0 & I \end{bmatrix}^T$ respectively. Then, (8-39) is obtained.

$$\begin{bmatrix} \bar{P}_{2p} + \bar{P}_{2p}^T & \bar{P}_{1p}\bar{N}_p(\theta) - \bar{P}_{2p}^T\bar{R}_{dp}(\theta) + \bar{P}_{3p} & \bar{P}_{1p}\bar{G}_p & 0 \\ * & -\bar{P}_{3p}^T\bar{R}_{dp}(\theta) - R_{dp}^T(\theta)\bar{P}_{3p} & 0 & \bar{C}_p^T \\ * & * & -\gamma_{ap} & 0 \\ * & * & * & -\gamma_{ap} \end{bmatrix} < 0 \tag{8-39}$$

It is easy to see that (8-39) is identical to (8-24).

This completes the proof.

Theorem 8.3 If Theorem 8.2 holds, then the polytopic UI-PMIDO is stable and the augmented system state estimation error dynamics are asymptotically stable, if there exist an S.P.D matrix $\bar{P}_{1p}$, and matrices $\bar{P}_{2p}$, $\bar{P}_{3p}, \bar{Y}_{1p}$, $\bar{Y}_{2p}$, such that the following LMI is satisfied.

$$\begin{bmatrix} \bar{P}_{2p}+\bar{P}_{2p}^T & \bar{\Omega}_{12}(\theta) & \bar{P}_{1p}\bar{G}_p & 0 \\ * & \bar{\Omega}_{22}(\theta) & 0 & \bar{C}_p^T \\ * & * & -\gamma_{ap} & 0 \\ * & * & * & -\gamma_{ap} \end{bmatrix} < 0 \tag{8-40}$$

where, $\bar{N}_p(\theta)$ and $\bar{R}_{dp}(\theta)$ are defined as in (8-15) and (8-20) respectively, and $\bar{\Omega}_{12}(\theta) = \bar{P}_{1p}\bar{A}_{1p}(\theta) - \bar{P}_{2p}^T + \bar{P}_{3p} + \bar{Y}_{1p}^T\bar{C}_p$ and $\bar{\Omega}_{22}(\theta) = -\bar{P}_{3p}^T - \bar{P}_{3p} - \bar{C}_p^T\bar{Y}_{2p} + \bar{Y}_{2p}^T\bar{C}_p$. Following this the polytopic UI-PMIDO gains are calculated as:

$$\bar{K}_{1p}^T(\theta) = -\begin{bmatrix}\bar{Y}_{1p} & \bar{Y}_{2p}\end{bmatrix}\begin{bmatrix}\bar{P}_{1p}^{-1} \\ -\bar{P}_{3p}^{-1}\bar{P}_{2p}\bar{P}_{1p}^{-1}\end{bmatrix} \tag{8-41}$$

$$\bar{L}_{dp}^T(\theta) = -\begin{bmatrix}\bar{Y}_{1p} & \bar{Y}_{2p}\end{bmatrix}\begin{bmatrix}0 \\ -\bar{P}_{3p}^{-1}\end{bmatrix} \tag{8-42}$$

where, if $\bar{P}_3$ is singular, a proper ϵ_0 should be chosen so that $\bar{P}_3 + \epsilon_0 \neq 0$ holds.

Proof:

Sufficiency: Let

$$\bar{\psi}_{1p}(\theta) = \begin{bmatrix} \bar{P}_{2p}+\bar{P}_{2p}^T & \bar{P}_{1p}\bar{N}_p(\theta) - \bar{P}_{2p}^T\bar{R}_{dp}(\theta) + \bar{P}_{3p} & \bar{P}_{1p}\bar{G}_p & 0 \\ * & -\bar{P}_{3p}^T\bar{R}_{dp}(\theta) - R_{dp}^T(\theta)\bar{P}_{3p} & 0 & \bar{C}_p^T \\ * & * & -\gamma_{ap} & 0 \\ * & * & * & -\gamma_{ap} \end{bmatrix} \tag{8-43}$$

$$\bar{\psi}_{2p}(\theta) = \begin{bmatrix}0 \\ \bar{C}_p^T \\ 0 \\ 0\end{bmatrix}\begin{bmatrix}\bar{Y}_{1p} & \bar{Y}_{2p} & 0 & 0\end{bmatrix} + \begin{bmatrix}\bar{Y}_{1p} & \bar{Y}_{2p} & 0 & 0\end{bmatrix}^T\begin{bmatrix}0 \\ \bar{C}_p^T \\ 0 \\ 0\end{bmatrix}^T \tag{8-44}$$

Hence, (8-45) is derived as:

$$\bar{\psi}_{1p} + \bar{\psi}_{2p} < 0 \tag{8-45}$$

Formulate the LMIs (8-41) & (8-42) as:

$$\begin{bmatrix} -\bar{K}_{1p}^{T}(\theta) & -\bar{L}_{dp}^{T}(\theta) \end{bmatrix} = \begin{bmatrix} \bar{Y}_{1p} & \bar{Y}_{2p} \end{bmatrix} \begin{bmatrix} \bar{P}_{1p} & 0 \\ \bar{P}_{2p} & \bar{P}_{3p} \end{bmatrix}^{-1} \tag{8-46}$$

Since the inverse in (8-46) exists it follows that:

$$\begin{bmatrix} \bar{Y}_{1p} & \bar{Y}_{2p} \end{bmatrix} = \begin{bmatrix} -\bar{K}_{1p}^{T}(\theta) & -\bar{L}_{dp}^{T}(\theta) \end{bmatrix} \begin{bmatrix} \bar{P}_{1p} & 0 \\ \bar{P}_{2p} & \bar{P}_{3p} \end{bmatrix} \tag{8-47}$$

Substituting (8-46) into (8-45), then (8-40) is obtained.

Necessity: If Theorem 8.2 holds, (8-10) is a polytopic UI-PMIDO, and there exist an S.P.D matrix $\bar{P}_{1p}$, and matrices $\bar{P}_{2p}$, $\bar{P}_{3p}$, $\bar{K}_{1p}(\theta)$, $\bar{L}_{dp}(\theta)$, such that (8-40) holds. Then rewriting (8-40) as:

$$\bar{\psi}_{1p}(\theta) + \begin{bmatrix} 0 \\ \bar{C}_p^T \\ 0 \\ 0 \end{bmatrix} \begin{bmatrix} -\bar{K}_{1p}^{T}(\theta) & -\bar{L}_{dp}^{T}(\theta) \end{bmatrix} \begin{bmatrix} \bar{P}_{1p} & 0 \\ \bar{P}_{2p} & \bar{P}_{3p} \end{bmatrix} \begin{bmatrix} 1 & 0 & 0 & 0 \\ 0 & 1 & 0 & 0 \end{bmatrix}$$

$$+ \begin{bmatrix} 1 & 0 & 0 & 0 \\ 0 & 1 & 0 & 0 \end{bmatrix}^T \begin{bmatrix} \bar{P}_{1p} & 0 \\ \bar{P}_{2p} & \bar{P}_{3p} \end{bmatrix}^T \begin{bmatrix} -\bar{K}_{1p}^{T}(\theta) & -\bar{L}_{dp}^{T}(\theta) \end{bmatrix}^T \begin{bmatrix} 0 \\ \bar{C}_p^T \end{bmatrix}^T < 0 \tag{8-48}$$

$\bar{\psi}_{1p}(\theta)$ is defined in (8-43).

Define a new matrix $\begin{bmatrix} \bar{Y}_{1p} & \bar{Y}_{2p} \end{bmatrix}$ in terms of (8-48) as:

$$\begin{bmatrix} \bar{Y}_{1p} & \bar{Y}_{2p} \end{bmatrix} = \begin{bmatrix} -\bar{K}_{1p}^{T}(\theta) & -\bar{L}_{dp}^{T}(\theta) \end{bmatrix} \begin{bmatrix} \bar{P}_{1p} & 0 \\ \bar{P}_{2p} & \bar{P}_{3p} \end{bmatrix} \tag{8-49}$$

Substituting (8-49) into (8-48) gives (8-40).

This completes the proof.

Remark 8.4: The observer gains of $\bar{K}_p(\theta)$ and $\bar{L}_{dp}(\theta)$ derived through Theorem 8.1, 8.2 and 8.3 depend on the parameter vector θ in polytopic form.

Remark 8.5: In this Chapter, the measurement noise is not included and hence the robustness to the measurement noise is not considered. However, an approach to this robustness problem could be developed with reference to *Remark 6.3*.

8.4 Polytopic UI-PMIDO FE design on a two-link manipulator

8.4.1 Introduction of two-link manipulator model

To illustrate the UI-PMIDO theory based on LPV model discussed in Section 8.3, an example of an actuator FE strategy is implemented via a nonlinear simulation of a two-link manipulator/robot demonstrator system which is very familiar to the control system community. The purpose of this Section is to describe a polytopic LPV modelling strategy applicable to the nonlinear two-link manipulator system.

The nonlinear dynamics of robot manipulator systems have been used in many research fields, e.g. in physics, mechanical design, motion analysis and planning, actuator drivers, control design, sensor systems, computer algorithms as well as in relation to the behaviour of machines, animals, and even human beings (Mckerrow, 1991 and Slotine and Li, 1991).

The motion of the manipulator comprises three dynamic torques: inertial, centripetal and Coriolis. The inertial torques are considered to be proportional to the acceleration of each joint in accordance with Newton's second law. Centripetal torques arise from the centripetal forces which constrain a body to rotate about a point. They are directed towards the centre of the uniform circular motion, and are proportional to the square of the velocity. Coriolis torques result from vertical forces derived from the interaction of two rotating links and are proportional to the product of the joint velocities of those links. Figure 8-1 describes the structure of a nonlinear two-link manipulator.

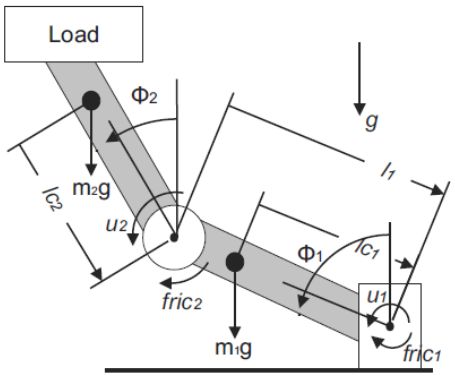

Figure 8-1 Two-link manipulator structure

For simplicity, the two-link manipulator is considered to rotate in the vertical plane whose position (joint angles) are constructed by a vector $\phi = [\phi_1, \phi_2]^T$, and whose actuator inputs (torques acted on the manipulator joints) are described by $u = [u_1, u_2]^T$. $\dot{\phi}$ and $\ddot{\phi}$ are used to are used to express the joint velocities and accelerations, respectively. A more general description of the two-link manipulator dynamics is given in (Mckerrow, 1991; Slotine and Li, 1991; (Kajiwara, Apkarian and Gahinet, 1999; Nie and Patton, 2011; Patton, Chen and Klinkhieo, 2012) and is shown as follows:

$$\Xi[\phi]\ddot{\phi} + O[\phi, \dot{\phi}]\dot{\phi} + G[\phi] = u \tag{8-50}$$

where, $\Xi[\phi] \in \Re^{2\times 2}$ is the manipulator inertia tensor matrix, $O[\phi, \dot{\phi}]\dot{\phi} \in \Re^2$ is the vector function with the centripetal and Coriolis torques; $G[\phi] \in \Re^2$ is the gravitational torque.

The physical parameters of the system are defined as:

I_1: Inertia of arm-1

I_2: Inertia of arm-2 and load

l_1: Distance between joint-1 and joint-2

l_{c1}: Distance of joint-1 from centre of mass arm-1

l_{c2}: Distance of joint-2 from centre of mass arm-2

m_1: Mass of arm-1

m_2: Mass of arm-2 and load

Table 8-1 Parameter values for the Two-link manipulator system

Parameters	I_1	I_2	l_1	l_{c1}	l_{c2}	m_1	m_2	g
Values	0.833	0.417	1.0	0.5	0.5	10.0	5.0	9.80
Units	Kg m^2	Kg m^2	m	m	m	Kg	Kg	m s^{-2}

The state space equations of motion are expressed as:

$$[m_1 lc_1^2 + m_2 lc_1^2 + I_1]\ddot{\phi}_1 + [m_2 l_1 l\, c_2 \cos(\phi_1 - \phi_2)]\ddot{\phi}_2 + [m_2 l_1 l\, c_2 \sin(\phi_1 - \phi_2)]\dot{\phi}_2^2$$

$$-[m_1 l c_1 + m_2 l_1] g \sin(\phi_1) = u_1 \tag{8-51}$$

$$[m_2 l_1 l\, c_2 \cos(\phi_1 - \phi_2)]\ddot{\phi}_1 + [m_2 l c_2^2 + I_2]\ddot{\phi}_2 - [m_2 l_1 l\, c_2 \sin(\phi_1 - \phi_2)]\dot{\phi}_1^2$$

$$-m_2 g\, c_2 \sin(\phi_2) = u_2 \tag{8-52}$$

(8-51) & (8-52) can be re-written into a single matrix equation as:

$$M(\phi)\ddot{\phi} + C\left(\phi, \dot{\phi}\right) + \tilde{g}(\phi) = u \tag{8-53}$$

where, the following parameters relate to (8-51) and (8-52):

$M(\phi)\ddot{\phi}$: Contains generalized mass terms;

$C\left(\phi, \dot{\phi}\right)$: Contains all the quadratic terms;

$\tilde{g}(\phi)$: Generalized force terms,

For the system of (8-53), a widely accepted approach is to take out the quadratic terms $C\left(\phi, \dot{\phi}\right)$ in the robust control design since they are unbounded. Hence, rewriting (8-53) as :

$$M(\phi)\ddot{\phi} + \tilde{g}(\phi) = u \tag{8-54}$$

where,

$$M(\phi) = \begin{bmatrix} m_1 l_{c1}^2 + m_2 l_{c1}^2 + I_1 & m_2 l_1 l_{c2} \cos(\phi_1 - \phi_2) \\ m_2 l_1 l_{c2} \cos(\phi_1 - \phi_2) & m_2 l_{c2}^2 + I_2 \end{bmatrix} \tag{8-55}$$

$$\tilde{g}(\phi) = \begin{bmatrix} -[m_1 l_{c1} + m_2 l_1] g \sin(\phi_1) \\ -m_2 g\, l_{c2} \sin(\phi_2) \end{bmatrix} \tag{8-56}$$

In the vector ϕ, both the angles ϕ_1 and ϕ_2 are in the ranges of $[-\pi, \pi]$. Then, (8-57) is given as:

$$\varphi(\phi) = \cos(\phi_1 - \phi_2) \in [-1 \quad 1] \tag{8-57}$$

It is clear that the nonlinear term in $M(\phi)$ is bounded and expressed in polytopic form as:

$$M(\phi) \in \mathrm{C_O}\{M_1 \quad M_2\} \tag{8-58}$$

where,

$$M_1(\phi) = \begin{bmatrix} m_1 l_{c1}^2 + m_2 l_{c1}^2 + I_1 & m_2 l_1 l_{c2} \\ m_2 l_1 l_{c2} & m_2 l_{c2}^2 + I_2 \end{bmatrix} \tag{8-59}$$

$$M_2(\phi) = \begin{bmatrix} m_1 l_{c1}^2 + m_2 l_{c1}^2 + I_1 & -m_2 l_1 l_{c2} \\ -m_2 l_1 l_{c2} & m_2 l_{c2}^2 + I_2 \end{bmatrix} \tag{8-60}$$

In order to form the state space representation, the two functions $\varphi_1(\phi_1) \in \Re^2$, $\varphi_2(\phi_2) \in \Re^2$ are defined as follows:

$$\sin(\phi_1) = \left(\frac{\sin(\phi_1)}{\phi_1}\right)\phi_1 = \varphi_1(\phi_1)\phi_1 \tag{8-61}$$

$$\sin(\phi_2) = \left(\frac{\sin(\phi_2)}{\phi_2}\right)\phi_2 = \varphi_2(\phi_2)\phi_2 \tag{8-62}$$

where, $\varphi_1(\phi_1)$, $\varphi_2(\phi_2)$ are bounded and $-0.2 \le \varphi_1(\phi_1) \le 1$, $-0.2 \le \varphi_2(\phi_2) \le 1$.

Re-arrange $\tilde{g}(\phi)$ into $G^g(\phi)\phi$ and based on the functions $\varphi_1(\phi_1)$, $\varphi_2(\phi_2)$. $G^g(\phi)$ these are constructed into a polytope representation as follows:

$$G^g(\phi) \in \mathrm{C_O}\{G_1^g, G_2^g, G_3^g, G_4^g\} \tag{8-63}$$

where,

$$G_1^g = \begin{bmatrix} 0.2(m_1 l_{c1} + m_2 l_1)g & 0 \\ 0 & 0.2 m_2 l_{c2} g \end{bmatrix}$$

$$G_2^g = \begin{bmatrix} -(m_1 l_{c1} + m_2 l_1)g & 0 \\ 0 & 0.2 m_2 l_{c2} g \end{bmatrix}$$

$$G_3^g = \begin{bmatrix} 0.2(m_1 l_{c1} + m_2 l_1)g & 0 \\ 0 & m_2 l_{c2} g \end{bmatrix}$$

$$G_4^g = \begin{bmatrix} -(m_1 l_{c1} + m_2 l_1)g & 0 \\ 0 & -m_2 l_{c2} g \end{bmatrix}$$

Let the state vector x to be defined as:

$$x = [\phi_1 \quad \phi_2 \quad \dot{\phi}_1 \quad \dot{\phi}_2]^T \tag{8-64}$$

and

$$W_b = \begin{bmatrix} 0 & 0 & 0 & 1 \\ 0 & 0 & 1 & 0 \end{bmatrix}^T \tag{8-65}$$

Then, the two-link manipulator nonlinear dynamics are described by the following descriptor system:

$$\begin{bmatrix} I & 0 \\ 0 & M(\phi) \end{bmatrix} \dot{x} = \begin{bmatrix} 0 & I \\ -G^g(\phi) & 0 \end{bmatrix} x + W_b u \tag{8-66}$$

Let Γ be a non-singular matrix defined as:

$$\Gamma = \begin{bmatrix} I & 0 \\ 0 & M(\phi) \end{bmatrix} \tag{8-67}$$

Then the state space representation for the system can be expressed as:

$$\dot{x} = A(\phi)x + B(\phi)u \tag{8-68}$$

where,

$$A(\phi) = \Gamma^{-1} \begin{bmatrix} 0 & I \\ -G^g(\phi) & 0 \end{bmatrix} \tag{8-69}$$

$$B(\phi) = \Gamma^{-1} W_b \tag{8-70}$$

Noticeably, Γ is a non-singular block diagonal matrix, since in the manipulator system, as shown in (8-67), the eigenvalues of Γ fully depend on the lower right-hand block $M(\phi)$. The determinant of the matrix $M(\phi)$ in (8-59) & (8-60) is a fixed value related to the mechanical parameters, for instance, the link length and link mass.

Consider an additive actuator fault occurring on the first torque in the nominal time-varying manipulator system. Then the faulty manipulator system description can be expressed as (8-4).

Hence, according to the description above, a polytopic LPV model of the two-link manipulator is constructed as an 8-vertex linear system with the combinations of A_i and B_i. In this structure, $B(\phi)$ changes sign due to changes in the diagonal elements of $M(\phi)$. The eight-vertex models are listed as follows:

Vertex system 1:

$$A_{p1} = \begin{bmatrix} 0 & 0 & 1 & 0 \\ 0 & 0 & 0 & 1 \\ 19.5947 & -8.0159 & 0 & 0 \\ -29.386 & 26.7184 & 0 & 0 \end{bmatrix}, \; B_1 = \begin{bmatrix} 0 & 0 \\ 0 & 0 \\ 0.2182 & -0.3272 \\ -0.3727 & 1.0905 \end{bmatrix}$$

Vertex system 2:

$$A_{p2} = \begin{bmatrix} 0 & 0 & 1 & 0 \\ 0 & 0 & 0 & 1 \\ 19.5947 & 1.6031 & 0 & 0 \\ -29.386 & -5.3436 & 0 & 0 \end{bmatrix}, \; B_1 = \begin{bmatrix} 0 & 0 \\ 0 & 0 \\ 0.2182 & -0.3272 \\ -0.3727 & 1.0905 \end{bmatrix}$$

Vertex system 3:

$$A_{p3} = \begin{bmatrix} 0 & 0 & 1 & 0 \\ 0 & 0 & 0 & 1 \\ -3.9189 & -8.0159 & 0 & 0 \\ 5.8772 & 26.7184 & 0 & 0 \end{bmatrix}, B_1 = \begin{bmatrix} 0 & 0 \\ 0 & 0 \\ 0.2182 & -0.3272 \\ -0.3727 & 1.0905 \end{bmatrix}$$

Vertex system 4:

$$A_{p4} = \begin{bmatrix} 0 & 0 & 1 & 0 \\ 0 & 0 & 0 & 1 \\ -3.9189 & 1.6031 & 0 & 0 \\ 5.8772 & -5.3436 & 0 & 0 \end{bmatrix}, B_1 = \begin{bmatrix} 0 & 0 \\ 0 & 0 \\ 0.2182 & -0.3272 \\ -0.3727 & 1.0905 \end{bmatrix}$$

Vertex system 5:

$$A_{p5} = \begin{bmatrix} 0 & 0 & 1 & 0 \\ 0 & 0 & 0 & 1 \\ 19.5947 & 8.0159 & 0 & 0 \\ 29.386 & 26.7184 & 0 & 0 \end{bmatrix}, \; B_2 = \begin{bmatrix} 0 & 0 \\ 0 & 0 \\ 0.2182 & 0.3272 \\ 0.3727 & 1.0905 \end{bmatrix}$$

Vertex system 6:

$$A_{p6} = \begin{bmatrix} 0 & 0 & 1 & 0 \\ 0 & 0 & 0 & 1 \\ 19.5947 & -1.6031 & 0 & 0 \\ 29.386 & -5.3436 & 0 & 0 \end{bmatrix}, \; B_2 = \begin{bmatrix} 0 & 0 \\ 0 & 0 \\ 0.2182 & 0.3272 \\ 0.3727 & 1.0905 \end{bmatrix}$$

Vertex system 7:

$$A_{p7} = \begin{bmatrix} 0 & 0 & 1 & 0 \\ 0 & 0 & 0 & 1 \\ -3.9189 & 8.0159 & 0 & 0 \\ -5.8772 & 26.7184 & 0 & 0 \end{bmatrix}, B_2 = \begin{bmatrix} 0 & 0 \\ 0 & 0 \\ 0.2182 & 0.3272 \\ 0.3727 & 1.0905 \end{bmatrix}$$

Vertex system 8:

$$A_{p8} = \begin{bmatrix} 0 & 0 & 1 & 0 \\ 0 & 0 & 0 & 1 \\ -3.9189 & -1.6031 & 0 & 0 \\ -5.8772 & -5.3436 & 0 & 0 \end{bmatrix}, \quad B_2 = \begin{bmatrix} 0 & 0 \\ 0 & 0 \\ 0.2182 & 0.3272 \\ 0.3727 & 1.0905 \end{bmatrix}$$

The common output matrix is $C = \begin{bmatrix} 1 & 0 & 0 & 0 \\ 0 & 1 & 0 & 0 \\ 0 & 0 & 1 & 0 \end{bmatrix}$.

It should pointed out that the matrix B_i changes sign according to the sign variations of the diagonal elements in matrix $M(\phi)$.

The additive fault distribution matrix is a time-varying matrix, which is the first column of the actuator distribution matrix F_a. In the polytopic UI-PMIDO design, it is represented as either the first column of B_1 or B_2 corresponding to the system state matrix A, i.e. $F_a = \begin{bmatrix} 0 \\ 0 \\ 0.2182 \\ -0.3727 \end{bmatrix}$ or $F_a = \begin{bmatrix} 0 \\ 0 \\ 0.2182 \\ 0.3727 \end{bmatrix}$.

8.4.2 Simulation results

Consider the nonlinear two manipulator system subject to the exogenous disturbance (UI) represented as the output of a band-limited filter with zero-mean white noise input of covariance =0.001. The model includes the exogenous disturbance distribution matrix $E = \begin{bmatrix} 1 \\ 1 \\ 0 \\ 0 \end{bmatrix}$.

In this example, two kinds of actuator fault scenarios OFC fault and runaway fault acting on the system states are applied respectively. As introduced in Chapter 4, OFC faults can be expressed as a sinusoid signal which is a bounded k_{th} order derivative signal. The runaway fault scenario describes that the actuator suffers from a runaway fault, in this case, simulated using a ramp signal of which the k_{th} order derivative is zero value.

Following the UI-PMIDO design approach in Chapter 8, the observer gains in this design are determined using MATLAB LMI Toolbox and given as follows:

$$\overline{K}_{p1} = 10^3 * \begin{bmatrix} 0.0470 & -0.0470 & 0.2117 \\ -0.0851 & 0.0851 & -0.0426 \\ -0.0150 & 0.0024 & 0.8471 \\ -0.7958 & 0.7932 & -1.0416 \\ -14.1750 & 14.1750 & 94.8620 \\ -2.4608 & 2.4608 & 35.1920 \end{bmatrix},$$

$$\overline{K}_{p2} = 10^3 * \begin{bmatrix} 0.0439 & -0.0439 & 0.2097 \\ -0.0847 & 0.0847 & -0.0386 \\ -0.0070 & 0.0141 & 0.8420 \\ -0.7875 & 0.7528 & -1.0008 \\ -15.5020 & 15.5020 & 94.4630 \\ -2.9126 & 2.9126 & 34.9830 \end{bmatrix},$$

$$\overline{K}_{p3} = 10^3 * \begin{bmatrix} 0.0493 & -0.0493 & 0.2030 \\ -0.0858 & 0.0858 & -0.0372 \\ -0.0045 & 0.0073 & 0.8314 \\ -0.7850 & 0.8167 & -0.9737 \\ -15.5568 & 15.5568 & 94.3380 \\ -2.7744 & 2.7744 & 34.8070 \end{bmatrix},$$

$$\overline{K}_{p4} = 10^3 * \begin{bmatrix} 0.0505 & -0.0505 & 0.2012 \\ -0.0891 & 0.0891 & -0.0338 \\ -0.0023 & 0.0005 & 0.8263 \\ -0.8156 & 0.8161 & -0.9452 \\ -16.0900 & 16.0900 & 93.9430 \\ -2.8483 & 2.8483 & 34.5830 \end{bmatrix}$$

$$\overline{K}_{p5} = 10^3 * \begin{bmatrix} 0.0659 & -0.0659 & 0.2036 \\ -0.0895 & 0.0895 & -0.0354 \\ 0.1129 & -0.0853 & 0.8170 \\ -0.8564 & 0.9125 & -0.9617 \\ -1.2253 & 1.2253 & 91.2760 \\ 2.0615 & -2.0615 & 33.8300 \end{bmatrix},$$

$$\overline{K}_{p6} = 10^3 * \begin{bmatrix} 0.0635 & -0.0635 & 0.2042 \\ -0.0869 & 0.0869 & -0.0376 \\ 0.1027 & -0.0847 & 0.8173 \\ -0.8316 & 0.8856 & -0.9776 \\ -2.0733 & 2.0733 & 91.1580 \\ 1.7019 & -1.7019 & 33.8290 \end{bmatrix},$$

$$\overline{K}_{p7} = 10^3 * \begin{bmatrix} 0.0071 & -0.0071 & 0.0196 \\ -0.0097 & 0.0097 & -0.0314 \\ 0.0129 & -0.1250 & 0.8055 \\ -0.9893 & 1.0102 & -0.9112 \\ 2.1619 & -2.1619 & 91.0750 \\ 3.4864 & -3.4864 & 33.5820 \end{bmatrix},$$

$$\overline{K}_{p8} = 10^3 * \begin{bmatrix} 0.0073 & -0.0073 & 0.0197 \\ -0.0093 & 0.0093 & -0.0335 \\ 0.0117 & -0.1234 & 0.8060 \\ -0.9530 & 0.9418 & -9.0974 \\ 1.1393 & -1.1393 & 91.0740 \\ 3.1176 & -3.1176 & 33.5870 \end{bmatrix},$$

$$\bar{L}_{dp1} = \begin{bmatrix} 0.4611 & 0.1144 & 0.2320 \\ 0.1172 & 0.6766 & -0.0667 \\ 0.2229 & -0.0690 & 0.8101 \\ -0.1373 & 0.0870 & 0.0440 \\ 0.0028 & -0.0006 & -0.0015 \\ -0.0291 & 0.0035 & 0.0153 \end{bmatrix}, \bar{L}_{dp2} = \begin{bmatrix} 0.4630 & 0.0998 & 0.2313 \\ 0.0876 & 0.7600 & 0.0020 \\ 0.2178 & 0.0022 & 0.8143 \\ -0.1366 & 0.0672 & 0.0437 \\ 0.0028 & -2.8522 & -0.0015 \\ -0.0290 & 0.0011 & 0.0150 \end{bmatrix},$$

$$\bar{L}_{dp3} = \begin{bmatrix} 0.7618 & 0.1075 & 0.0828 \\ 0.1269 & 0.6766 & -0.0649 \\ 0.0932 & -0.0591 & 0.8001 \\ -0.1348 & 0.0875 & 0.0523 \\ 0.0020 & -0.0006 & -0.0017 \\ -0.0270 & 0.0035 & 0.0168 \end{bmatrix}, \bar{L}_{dp4} = \begin{bmatrix} 0.7575 & 0.0042 & 0.0831 \\ 0.0050 & 0.7553 & -0.0035 \\ 0.0901 & -0.0078 & 0.8026 \\ -0.1344 & -0.0727 & 0.0520 \\ 0.0019 & -0.0001 & -0.0017 \\ -0.0264 & 0.0021 & 0.0165 \end{bmatrix},$$

$$\bar{L}_{dp5} = \begin{bmatrix} 0.5244 & -0.0063 & 0.2089 \\ -0.0198 & 0.6777 & 0.0367 \\ 0.1998 & 0.0274 & 0.8130 \\ -0.0969 & 0.0981 & 0.0442 \\ 0.0023 & -0.0002 & -0.0015 \\ -0.0247 & -0.0076 & 0.0138 \end{bmatrix}, \bar{L}_{dp6} = \begin{bmatrix} 0.5260 & 0.0037 & 0.2044 \\ -0.0074 & 0.7467 & -0.0080 \\ 0.1974 & -0.0200 & 0.8138 \\ -0.0975 & 0.0719 & 0.0447 \\ 0.0023 & -0.0002 & -0.0015 \\ -0.0247 & -0.0064 & 0.0139 \end{bmatrix},$$

$$\bar{L}_{dp7} = \begin{bmatrix} 0.7344 & -0.0009 & 0.0876 \\ -0.0009 & 0.6796 & 0.0235 \\ 0.0905 & 0.0211 & 0.8026 \\ -0.1416 & 0.0973 & 0.0523 \\ 0.0020 & -0.0002 & -0.0017 \\ -0.0205 & -0.0076 & 0.0152 \end{bmatrix}, \bar{L}_{dp8} = \begin{bmatrix} 0.7381 & 0.0425 & 0.0847 \\ 0.0463 & 0.7505 & -0.0183 \\ 0.0897 & -0.0187 & 0.8029 \\ -0.1419 & 0.0695 & 0.0525 \\ 0.0020 & -0.0002 & -0.0017 \\ -0.0206 & -0.0068 & 0.0152 \end{bmatrix}.$$

- ***Simulation Results for the System with OFC Fault***

The first fault scenario is an OFC fault acting on the first torque occurring at 10s. Different fault severities are tested by varying amplitudes and frequencies of the fault signal. The state estimation of angles 1 & 2 are illustrated in Figures 8-2 & 8-3. Figures 8-4 to 8-7 show the results of the simulated FE signals under various magnitude and frequency test conditions. It should be pointed that, in the following, the signals x_1e, x_2e and f_e represent the corresponding estimations of x_1, x_2, and f_a, respectively.

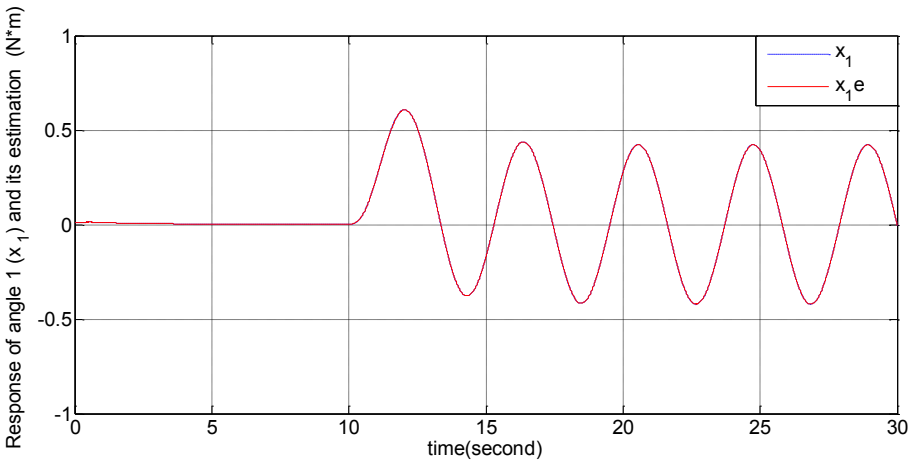

Figure 8-2 Response of angle 1 (x_1) and its estimation (x_1e) in OFC fault (Amplitude = 20 Nm; Frequency = 1.5 rad s^{-1})

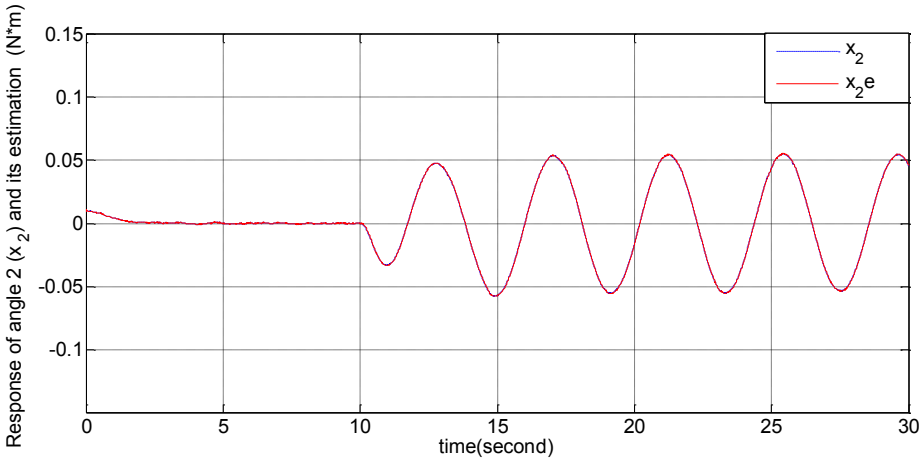

Figure 8-3 Response of angle 2 (x_2) and its estimation (x_2e) in OFC fault (Amplitude = 20 Nm; Frequency = 1.5 rad s^{-1})

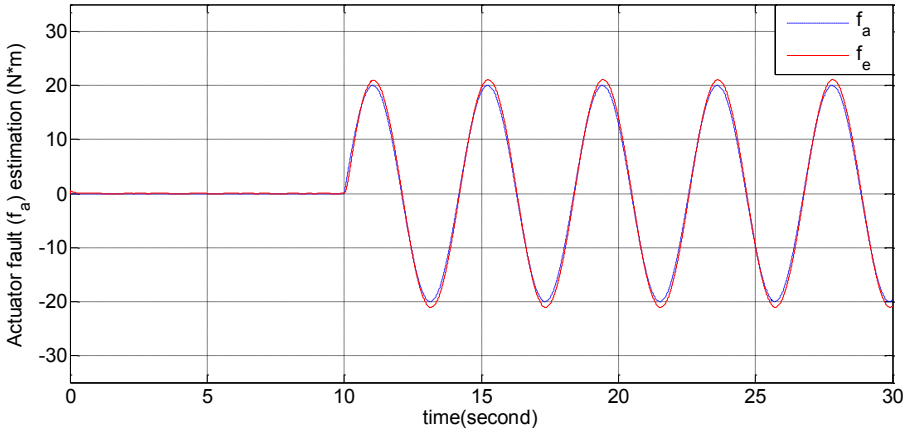

Figure 8-4 OFC fault f_a and FE signal f_e with fault occurring at 10s on actuator 1 (Amplitude = 20 Nm; Frequency = 1.5 rad s^{-1})

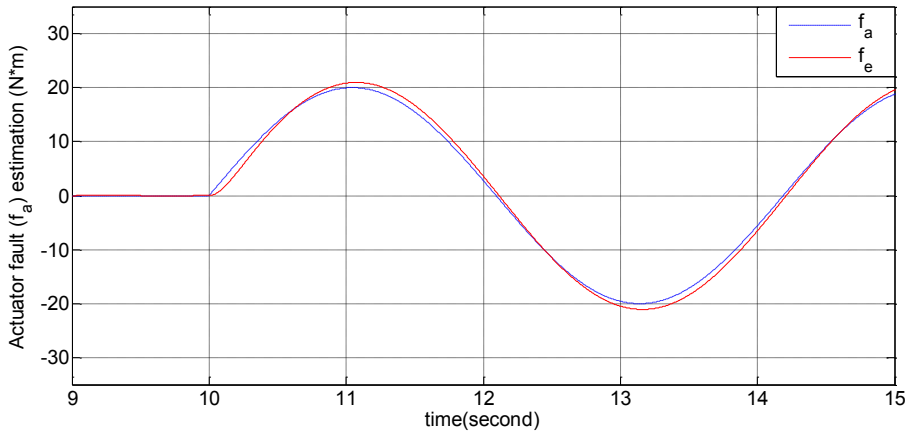

Figure 8-5 OFC fault f_a and FE signal f_e with fault occurring at 10s on actuator 1 (Amplitude = 20 Nm; Frequency = 1.5 rad s^{-1}) (zoom in)

Figures 8-2 & 8-3 are grouped to show the angle estimate and Figure 8-4 shows the OFC fault estimate for the two-link manipulator in the presence of the exogenous disturbance, both using the polytopic UI-PMIDO. The transient dynamic of the FE in Figure 8-4 is amplified in Figure 8-5. It can be observed that the state estimates shown in Figures 8-2 & 8-3 converge to the system states with a very short transient time, providing good estimates of the angle states 1 & 2.

Figure 8-4 shows that the observer generates a good estimate of the simulated fault that is fairly close in magnitude and frequency. However, it can be seen that the fault estimate lags behind the actual fault by a very small phase angle, with a small constant steady state error. This error is a likely consequence due to the minimisation procedure of $f^{(k)}$ which is not equivalent perfect UI de-coupling. Also, the impact of the UI (exogenous disturbance) on both the state estimates and the fault has been significantly attenuated by the UI de-coupling principle, which illustrates the effectiveness of UI de-coupling strategy.

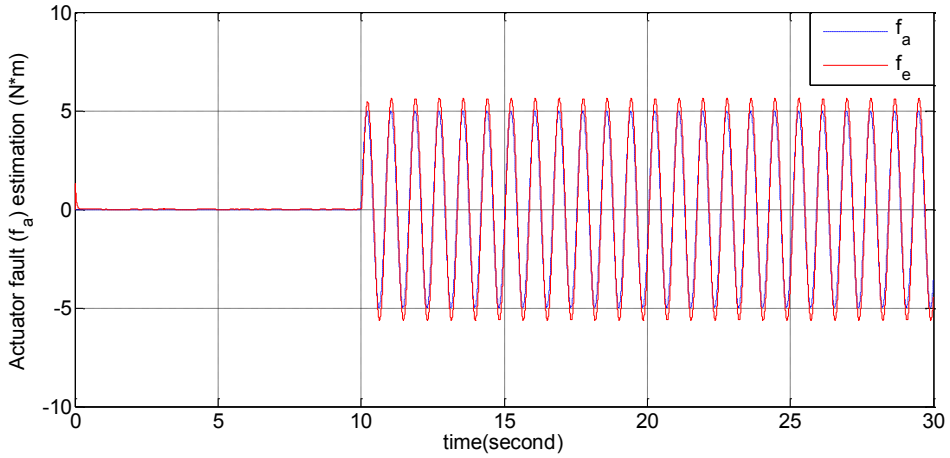

Figure 8-6 OFC fault f_a and FE signal f_e with fault occurring at 10s on actuator 1 (Amplitude = 5 Nm; Frequency = 7.5 rad s^{-1})

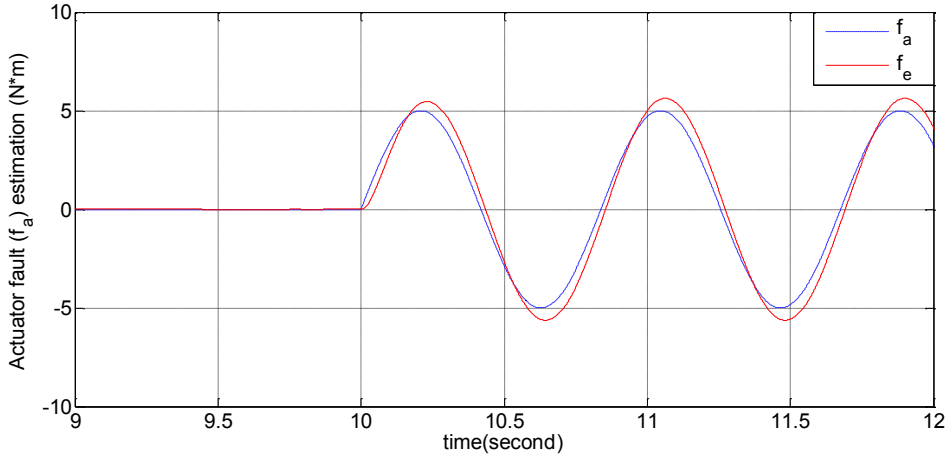

Figure 8-7 OFC fault f_a and FE signal f_e with fault occurring at 10s on actuator 1 (Amplitude = 5 Nm; Frequency = 7.5 rad s^{-1}) (zoomed in)

Figures 8-6 & 8-7 are the FE results stimulated by the OFC fault with different fault severities, where the amplitudes and frequencies are increased from 5 Nm to 20 Nm and 1.5 rad·s^{-1} to 7.5 rad·s^{-1}, respectively. Cases of either excessively high fault amplitude or fault frequency are considered to test to the FE performance. Fault signals with high amplitude and low frequency do not present a significant challenge for FE. However, the fault signal with low amplitude and higher frequency is too gentle and too fast to be followed. The simulation results show that the tracking error during steady-state can almost track the fault signal. Also, a very small phase angle lags behind the actual fault in the FE signal can be seen to be a bit larger than the fault with Frequency =1.5. The

implication is that the parametric changes in the fault signal attribute to a likely decrease in FE performance, compared with the results given in Figures 8-4 & 8-5.

- ***Simulation Results for the System with Runaway Fault***

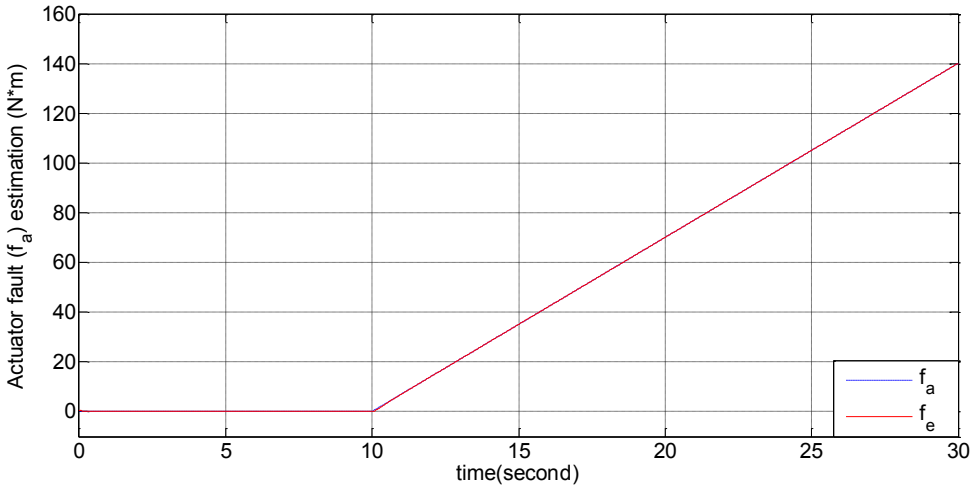

Figure 8-8 Ramp fault f_a and FE signal f_e with fault occurring at 10s on actuator 1 (slope=7, initial value =0)

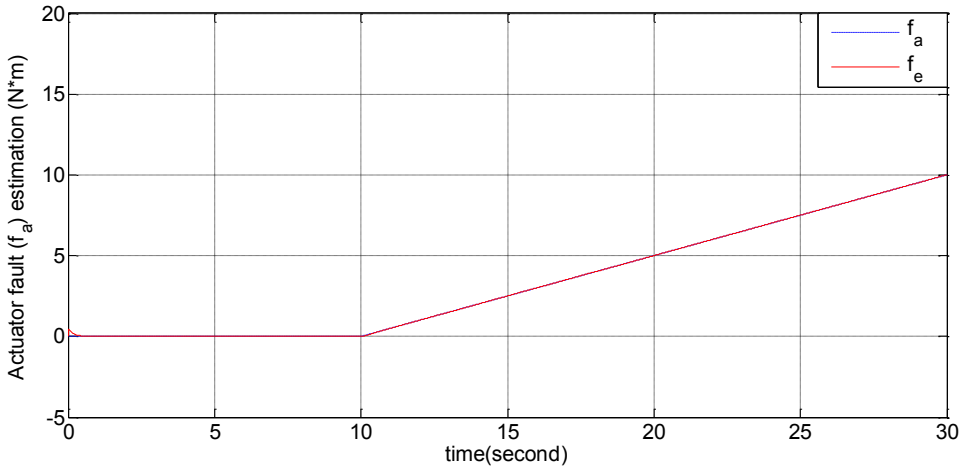

Figure 8-9 Ramp fault f_a and FE signal f_e with fault occurring at 10s on actuator 1 (slope=0.5, initial value=0)

The responses shown in Figures 8-8 & 8-9 correspond to ramp signal faults shown with their FE signals. The fault type is altered from a sinusoid to ramp signal which impacts on the actuator 1 at 10s. Two different ramp fault situations (fast and slow drift) are mimicked by changing the ramp slope to different levels (slope=7 and slope=0.5). Both estimates in Figures 8-8 & 8-9 reproduce the ramp fault with different slopes. The FE

responses show a very small steady-state estimation error. It is clear that satisfactory FE performances are achieved in both cases.

8.5 Conclusion

In this Chapter, the novel UI-PMIDO approach to FE in nonlinear systems is developed based on LPV modelling. Compared with LTI system, the several advantages of LPV modelling have been shown via the investigation. Firstly, the LPV approach can overcome the instability issues and performance reduction arising from the un-modelled when using on LTI systems. Also, compared with the use of the LTI modelling, the LPV modelling also has good capability of taking into account larger and more rapid parameter variations that may arise from the true nonlinear system. Finally, the LPV approach is considered to cover a wider class of modelling uncertainties and this facilitates an approach to less conservative robustness with improved controller and observer performances.

Bearing these advantages in mind, a new polytopic LPV UI-PMIDO is designed to provide robust FE in FDD considering systems taking modelling uncertainties into account as a development of the work proposed in Chapter 7. The proposed observer, using LPV modelling, is less affected by the nonlinear characteristics of the monitored system. Whilst it leaves the freedom for observer design to take into account the exogenous UI that act on the system and affect the FE performance. The UI-PMIDO design has demonstrated feasible simultaneous state and fault signal estimation for nonlinear systems in which the k_{th} derivative of the fault is bounded. The UI-PMIDO stability conditions are formulated using a computationally efficient LMI formulation that is suitable for implementation via the Matlab LMI Toolbox. A numerical example of a nonlinear two-link manipulator system with both OFC and ramp actuator fault scenarios is used to illustrate the power of this FE approach.

Chapter 9
Conclusion and Future Work

9.1 Conclusion and summary

It is argued that FE signals provide a powerful substitute for the more classical use of residual signals in terms of the fault information gained and this promotes the popularity of FE-based FDD. Given this, the goal of the thesis is to develop novel model-based FE methods as an alternative to use of the classical residual generation-oriented UIO approaches, considering the time derivative characteristics of various fault signals. The focus of the study is on the development of robust FE methods. As a consequence, the FE signals have accurate tracking performance, i.e. with small steady state estimation error as well as good estimation time response.

The literature in this subject shows that the biggest challenge of model-based methods for FDI/FDD is the influence of uncertainty (combining effects of modelling uncertainty and exogenous disturbances) on the monitored system. Hence, this thesis concentrates on using the UI de-coupling principle underlying the UIO FDI design for dealing with the robustness problem. In UIO design, uncertainty described by UI signals is designed to be de-coupled from fault indicators (residuals/FE signals), i.e. the residuals/FE signals are robust to the UI influence.

In this context, the thesis starts with reviewing the literature and basic principles of FDI/FDD and the model-based FDI/FDD in Chapters 1 & 2, respectively. Particularly, Section 2.3 introduces the foundation of the thesis 'residual-based UIO design' associating with a tutorial example that aims to illustrate the effectiveness of the UI de-coupling principle for handing the robustness problem. Chapter 3 focuses entirely on an industry application study arising from an FP7 project ADDSAFE involving testing of FDI designs on an Airbus generic nonlinear aircraft system using a FES system environment developed by Deimos Space in Madrid and with performance evaluation performed at Airbus in Toulouse.

Following Chapter 3 the main emphasis and contribution of the remainder of the thesis is on the development of FE strategies to obtain robust FE signals based on residual-based UIO.

In Chapter 4, the FE signals generated by the developed RFAFE are functions of the system output estimation error that is de-coupled from the UI. Furthermore, the FE signals include not only the conventional integral action but also a proportional action to improve the FE fault tracking performance. An LMI procedure, based on Lyapunov stability is used to guarantee stability of the RFAFE. An application example of an OFC fault acting on an elevator actuator in a generic model of an Airbus nonlinear aircraft (the same as in Chapter 3) is used to illustrate the method.

Chapter 5 considers the development of a new scheme the UI-PIO FE which uses the PIO structure in which the faults are considered as augmented state variables in the augmented observer. Besides considering the UI de-coupling function, H_∞ optimisation is to incorporate within an UIO structure to attenuate the effects of exogenous disturbance (sensor noise here) on the FE signals to avoid the noise-corrupted FE signals. As a result, a performance-improved FE is obtained. Additionally, a procedure for re-formulating the multiplicative faults in an additive fault representation is used to estimate the hydraulic leakage fault (multiplicative fault) scenario occurring on a wind turbine pitch system. The effectiveness and efficiency are demonstrated through the simulation results.

Chapters 4 & 5 provide further review of this subject concentrating on methods of taking account of fault derivative information. Following on from this the *robust adaptive* approach RFAFE design approach proposed in Chapter 4 removes the common assumption that the first fault derivative is not limited to be zero-valued, whereas in contrast the *proportional integral observer* UI-PIO discussed in Chapter 5 assumes that the first time fault derivative is zero. From the standpoint of fault derivative information this is more restrictive than RFAFE.

These restrictions limit the availability of the estimated faults and consequently narrow the potential applications that these FE approaches can be applied to. Hence, the approaches proposed in Chapters 6, 7 & 8 consider much wider time derivative characteristics of various faults by considering multiple integral actions as well as

derivative action. Hence, Chapter 6 proposes a *proportional multiple integral* UI-PMIO approach, whereas Chapter 7 introduces a *proportional multiple integral plus derivative* UI-PMIDO approach. It is known from the literature that with multiple integral actions (PMIO), the faults can be estimated in the case that the finite time fault derivatives have zero value or are bounded. The UI-PMIO contribution takes this up further by combining the original PMIO within the UIO structure with UI de-coupling. The methods proposed in Chapters 6 & 7 relax the restrictions that apply in Chapters 4 & 5. The UI-PMIO gives good potential for applying the FE approach to real applications by dealing with more types of faults through the use of the multiple integral actions.

Chapter 6 develops the so-called UI-PMIO with the capability of estimating the system states and fault simultaneously, based on the UI de-coupling structure. As it is, the UI de-coupling is responsible for dealing with UI acting on the system states to cover the robustness issue. Additionally, the H_∞ estimation theory is explored to stabilize the designed observer and minimising the bounded finite time fault derivative errors. At the end of Chapter 6, a numerical example with an actuator fault is used to test the effectiveness of the proposed UI-PMIO approach.

An interesting derivation is described in Chapter 7 inspired by the RFAFE and UI-PMIO FE methods of Chapters 4 & 6, respectively. A novel UI-PMIDO design is described which includes derivative action as well as the multiple-integral action. This is the UI-PMIDO derived by combining the 'derivative' action obtained from a modified RFAFE design with the UI-PMIO design proposed in Chapter 6. As a consequence, the UI-PMIDO structure that involves the multiple integral actions as well as the derivative action enables the resulting UI-PMIDO FE scheme to provide faster response to a fault, with bounded finite time derivatives. A numerical example is used to demonstrate the effectiveness of this new FE methodology. The advantage of UI-PMIDO is given by comparison with the simulation results using UI-PMIO method proposed in Chapter 6.

Finally, as an extension to the work described in Chapter 7, Chapter 8 extends the earlier ideas further by developing a linear time-varying approach to FE design based on using time-varying affine dependence on a scheduling parameter vector. The so-called polytopic LPV modelling and design framework is used to develop the new "polytopic UI-PMIDO" for system state estimation and FE design. Compared with the LTI system approaches, the advantages of LPV modelling can be seen as: a) A powerful approach

to deal with performance and stability for systems with global time-varying behaviour; b) A good strategy for taking into account rapid (but smooth) parameter changes as an extension to any LTI system approach; c) More modelling uncertainties may be taken into account than when using LTI systems, and this can facilitate a direct approach to gaining a better desired performance for FE. Advantage c) means that the use of LPV modelling has an impact on relaxing the degrees of design freedom in LTI UI de-coupling design.

It is therefore proposed that the polytopic LPV approach to UI-PMIDO can enhance the value of model-based FE applied to many real systems. Systems that have smooth nonlinearity can be considered suitable candidates since the linear time-varying characteristics can be easily defined. As introduced in Chapter 7, this UI-PMIDO possesses the ability to estimate the bounded k_{th} derivative actuator fault robustly by de-coupling the UI influence (exogenous disturbance) from the FE signals. A nonlinear two-link manipulator example is explored to demonstrate the effectiveness of this new approach in which the manipulator joint angles are considered as the scheduling parameters.

9.2 Future work

Although in this thesis new FE-oriented UIO schemes have been developed to satisfy the state-of-the-art fault diagnosis system and AFTC design, there is still considerable scope for further of development of this work and some suggestions of developments are as follows:

- The UIO-based FE design methods in this thesis are developed considering one of the two fundamental UIO conditions: that the maximum number of independent UI cannot be larger than the maximum number of independent measurements, as outlined in Section 2.3.3. There is no doubt that this condition severely limits the application of the UIO-based approach. Therefore, it could be valuable to investigate new approaches to, at least in part, remove this condition to ease the constraints and make UIO-based FDI/FDD design more applicable.
- Besides the residual-generation FDI applications, all the proposed FE methods in this thesis are based on the assumption that the faults acting on the system are additive. A multiplicative fault scenario is considered in which the multiplicative

actuator fault parameters are transformed into equivalent additive actuator faults. However, whilst this can be achieved for some component fault problems this approach is not generally applicable to all component fault cases. Future work could focus on more general approaches for dealing with component faults, retaining good robustness and fault isolation properties.

- Dealing with the general context of additive actuator faults, further work could focus well on approaches to provide simultaneous FE for combined actuator and sensor faults.
- Finally, it would be of value to explore the applicability of the UI de-coupling FE methods developed in this thesis to AFTC schemes. The robust FE methods have greater potential value in AFTC schemes compared with the use of robust residual approaches.

References

ACARE. (2002). http://www.acare4europe.org/ [Accessed 22/05/2013].

ADDSAFE. (2009). http://addsafe.deimos-space.com/ [Accessed 10/05/2013].

Alwi, H. and Edwards, C. (2010). Fault tolerant control using sliding modes with on-line control allocation, *in* C. Edwards, T. Lombaerts and H. Smaili (eds), *Fault Tolerant Flight Control*, Springer: 247-272.

Alwi, H. and Edwards, C. (2011). Oscillatory failure case detection for aircraft using an adaptive sliding mode differentiator scheme. *Proc. of the 2011 American Control Conference*, San Francisco, 1384-1389, 29, June-01, July.

Alwi, H., Edwards, C. and Marcos, A. (2012). Fault reconstruction using a LPV sliding mode observer for a class of LPV systems. *J. of the Franklin Institute*, 349(2): 510-530.

Alwi, H., Edwards, C. and Tan, C. P. (2009). Sliding mode estimation schemes for incipient sensor faults. *Automatica*, 45(7): 1679-1685.

Apkarian, P. and Adams, R. J. (1998). Advanced gain-scheduling techniques for uncertain systems. *IEEE Trans. on Control Systems Technology*, 6(1): 21-32.

Apkarian, P., Gahinet, P. and Becker, G. (1995). Self-scheduled *H*_ control of linear parameter-varying systems: a design example. *Automatica*, 31(9): 1251-1261.

Baca, A. (1993). Examples of Monte Carlo methods in reliability estimation based on reduction of prior information. *IEEE Trans. on Reliability*, 42(4): 645–649.

Bara, G. I., Daafouz, J., Kratz, F. d. r. and Ragot, J. (2001). Parameter-dependent state observer design for affine LPV systems. *Int. J. Contr*, 74(16): 1601-1611.

Bartys, M., Patton, R. J., Syfert, M., De las Heras, S. and Quevedo, J. (2006). Introduction to the DAMADICS actuator FDI benchmark study [Invited special issue paper] *Control Engineering Practice*, 14 (6): 577-596.

Becker, G. (1995). Parameter-dependent control of an under-actuated mechanical system. *Proc. of the 34th IEEE Conference on Decision and Control CDC'95*, New Orleans, 543-548, 13-15 Dec.

Becker, G., Packard, A., Philbrick, D. and Balas, G. (1993). Control of parametrically-dependent linear systems: a single quadratic Lyapunov approach. *Proc. of the 1993 American Control Conference*, San Francisco, 2795-2799, 2-4 June.

Bhattacharya, R., Balas, G. J., Kaya, M. A. and Packard, A. (2002). Nonlinear receding horizon control of an F-16 aircraft. *Journal of Guidance, Control, and Dynamics*, 25(5): 924-931.

Blanke, M., Kinnaert, M., Lunze, J. and Staroswiecki, M. (2003). *Diagnosis and fault-tolerant control*. Berlin, Germany, Springer Verlag.

Blanke, M., Kinnaert, M., Lunze, J. and Staroswiecki, M. (2006). Diagnosis and Fault-Tolerant Control, *in* M. Blanke, M. Kinnaert, J. Lunze and M. Staroswiecki (eds), *Diagnosis and Fault-Tolerant Control*, Berlin, Germany, Springer: 1-32.

Blanke, M., Staroswiecki, M. and Wu, N. E. (2001). Concepts and methods in fault-tolerant control. *Proc. of the 2001 American Control Conference*, Arlington, VA, 2606-2620, 25-27 June.

Bokor, J. and Balas, G. (2004). Detection filter design for LPV systems-a geometric approach. *Automatica*, 40(3): 511-518.

Bokor, J. and Szabó, Z. (2009). Fault detection and isolation in nonlinear systems. *Annual Reviews in Control*, 33(2): 113-123.

Bokor, J., Szabo, Z. and Stikkel, G. (2002). Failure detection for quasi LPV systems. *Proc. of the 41st IEEE Conference on Decision and Control CDC'02*, Las Vegas, Nevada, USA, 3318-3323, 10-13 Dec.

Busawon, K. and Kabore, P. (2000). On the design of integral and proportional integral observers. *Proc. of the 2000 American Control Conference*, Chicago,Illinois, 3725-3729, 28-30 Jun.

Busawon, K. K. and Kabore, P. (2001). Disturbance attenuation using proportional integral observers. *Int. J. Control*, 74(6): 618-627.

Casavola, A., Famularo, D., Franze, G. and Sorbara, M. (2007). A fault-detection, filter-design method for linear parameter-varying systems. *Proc. of the Institution of Mechanical Engineers, Part I: Journal of Systems and Control Engineering*, 221(6): 865-874.

Chadli, M. and Karimi, H. (2012). Robust Observer Design for Unknown Inputs Takagi-Sugeno Models. *IEEE Trans. on Fuzzy Systems*, 21(1): 158-164.

Chen, J. and Patton, R. J. (1999). *Robust model-based fault diagnosis for dynamic systems*. Kluwer Academic Publishers.

Chen, J., Patton, R. J. and Zhang, H. Y. (1995). Design of robust structured and directional residuals for fault isolation via unknown input observers. *Proc. of the European Control Conference*, Rome, 348-353, 5-8 Sept.

Chen, J., Patton, R. J. and Zhang, H. Y. (1996). Design of unknown input observers and robust fault detection filters. *Int. J. Contr.*, 63(1): 85-105.

Chen, L. and Patton, R. J. (2011). Polytope LPV Fault Estimation for Non-Linear Flight Control. *Proc. of the 18th IFAC World Congress*, Milano, Italy, 6680-6685, 28 Aug-02 Sept.

Chen, L., Patton, R. J. and Goupil, P. (2012). Robust Fault Estimation and Performance Evaluation Based Upon the ADDSAFE Benchmark Model. *Proc. of the 8th IFAC Symposium on SAFEPROCESS'12*, Mexico City, 1364-1369, 29-31 Aug.

Chen, L., Patton, R. J. and Klinkhieo, S. (2010). An LPV Pole-placement approach to friction compensation as an FTC problem. *Int. J. of Applied Mathematics and Computer Science*: 149-160.

Chen, W., Ding, S. X., Sari, A., Naik, A., Khan, A. and Yin, S. (2011). Observer-based FDI Schemes for Wind Turbine Benchmark. *Proc. of the 18th IFAC World Congress*, Milan, 7073-7078, 28 Aug-2 Sept.

Chen, W. and Saif, M. (2010). Fuzzy nonlinear unknown input observer design with fault diagnosis applications. *J. of Vibration and Control*, 16(3): 377-401.

Chen, W. T. and Saif, M. (2006a). Fault detection and isolation based on novel unknown input observer design. *Proc. of the 2006 American Control Conference*, Minneapolis, Minnesota, 5129-5134, 14-16, June.

Chen, W. T. and Saif, M. (2006b). Unknown input observer design for a class of nonlinear systems: an LMI approach. *Proc. of the 2006 American Control Conference*, Minneapolis, Minnesota, 834-838, 14-16 June.

Chilali, M. and Gahinet, P. (1996). H-infinity design with pole placement constraints: An LMI approach. *IEEE Trans. On Automatic Control*, 41(3): 358-367.

Clark, R. N., Fosth, D. C. and Walton, V. M. (1975). Detecting instrument malfunctions in control systems. *IEEE Trans. on Aerospace and Electronic Systems*, AES-11(4): 465-473.

Corless, M. and Tu, J. (1998). State and input estimation for a class of uncertain systems. *Automatica*, 34(6): 757-764.

Darouach, M., Zasadzinski, M. and Xu, S. J. (1994). Full-order observers for linear systems with unknown inputs. *IEEE Trans. on Automatic Control*, 39(3): 606-609.

Ding, S. (2008). *Model-based fault diagnosis techniques: design schemes, algorithms, and tools*. Berlin, Germany, Springer Verlag.

Ding, S., Jeinsch, T., Frank, P. M. and Ding, E. (2000). A unified approach to the optimization of fault detection systems. *Int. J. of Adapt. Control and Signal Processing*, 14(7): 725-745.

Ding, S. X., Zhang, P., Jeinsch, T., Ding, E., Engel, P. and Gui, W. (2011). A survey of the application of basic data-driven and model-based methods in process monitoring and fault diagnosis. *Proc. of the 18th IFAC World Congress*, Milan, 28 Aug-02 Sept.

Duan, G. and Patton, R. J. (2001). Robust fault detection using Luenberger-type unknown input observers-a parametric approach. *Int. J. of Systems Science*, 32(4): 533-540.

Edwards, C. (2004). A comparison of sliding mode and unknown input observers for fault reconstruction. *Proc. of the 43rd IEEE Conference on Decision and Control CDC'04*, Atlantis, 5279-5284, 14-17 Dec.

Edwards, C., Lombaerts, T. and Smaili, H. (2010). *Fault Tolerant Flight Control: A Benchmark Challenge*. Springer Verlag.

Esbensen, T. and Sloth, C. (2009). Fault Diagnosis and Fault-Tolerant Control of Wind Turbines. in Faculty of Engineering, Science and Medicine Department of Electronic Systems Section for Automation and Control. Fredrik Bajers, Denmark, Aalborg Univeristy. Master.

Falcoz, A., Henry, D. and Zolghadri, A. (2010). Robust fault diagnosis for atmospheric reentry vehicles: a case study. *IEEE Trans. on Systems, Man and Cybernetics, Part A: Systems and Humans*, 40(5): 886-899.

Fernández, V., De Zaiacomo, G. and Mafficini, A., Peñín, L. F (2010). he IXV GNC Functional Engineering Simulator. 11th ESA-ESTEC International Workshop on Simulation & EGSE facilities for Space Programmes.

Fernández, V. and Ramón, J. M. (2011). FES software users manual, ADDSAFE Technical Note D1.2.1, DEIMOS in ADDSAFE 2009.

Frank, P. M. (1987). Fault diagnosis in dynamic systems via state estimation-a survey, *in* S. Tzafestas, M. Singh and G. Schmidt (eds), *System fault diagnostics, reliability and related knowledge-based approaches*, Dordrecht, D.Reidel Press: 35-98.

Frank, P. M., Ding, S. X. and Köppen-Seliger, B. (2000). Current developments in the theory of FDI. *Proc. of the 5th IFAC Symposium on SAFEPROCESS'00*, Budapest, 16-27, 14-16 June.

Gahinet, P., Apkarian, P. and Chilali, M. (1996). Affine parameter-dependent Lyapunov functions and real parametric uncertainty. *IEEE Trans. on Automatic Control*, 41(3): 436-442.

Ganguli, S., Marcos, A. and Balas, G. (2002). Reconfigurable LPV control design for Boeing 747-100/200 longitudinal axis. *Proc. of the 2002 American Control Conference*, Anchorage, AK 3612-3617, 8-10 May.

Gao, Z. W. (2005). PD observer parametrization design for descriptor systems. *J. of the Franklin Institute*, 342(5): 551-564.

Gao, Z. W., Breikin, T. and Wang, H. (2008). Discrete-time proportional and integral observer and observer-based controller for systems with both unknown input and output disturbances. *Optimal Control Applications and Methods*, 29(3): 171-189.

Gao, Z. W. and Ding, S. X. (2005). PMID observer design for unknown input generalized dynamical systems. *Proc. of the 16th IFAC World Congress*, Prague, 01-03 Sept.

Gao, Z. W. and Ding, S. X. (2007). Actuator fault robust estimation and fault-tolerant control for a class of nonlinear descriptor systems. *Automatica*, 43(5): 912-920.

Gao, Z. W., Ding, S. X. and Ma, Y. (2007). Robust fault estimation approach and its application in vehicle lateral dynamic systems. *Optimal Control Applications and Methods*, 28(3): 143-156.

Gao, Z. W. and Ho, D. W. (2006). State/noise estimator for descriptor systems with application to sensor fault diagnosis. *IEEE Trans. on Signal Processing*, 54(4): 1316-1326.

Gao, Z. W. and Ho, D. W. C. (2004). Proportional multiple-integral observer design for descriptor systems with measurement output disturbances. *IEE Proc.-Control Theory Appl.*, 151(3): 279-288.

Gao, Z. W. and Wang, H. (2006). Descriptor observer approaches for multivariable systems with measurement noises and application in fault detection and diagnosis. *Systems & Control Letters*, 55(4): 304-313.

GARTEUR (2004). http://www.faulttolerantcontrol.nl/ [Accessed 01/06/2013].

Gertler, J. (1991). Analytical redundancy methods in fault detection and isolation. *Proc. of IFAC/IAMCS Symposium on SAFEPROCESS'91*, Baden-Baden, 9-21.

Gertler, J. (1998). *Fault detection and diagnosis in engineering systems*. New York, Marcel Dekker.

Godfrey, K. E. (1993). *Perturbation signals for system identification*. Prentice Hall New Jersey.

Golub, G. H. and Van Loan, C. F. (1996). *Matrix computations*. Baltimore, The Johns Hopkins University Press.

Goupil, P. (2010). Oscillatory failure case detection in the A380 electrical flight control system by analytical redundancy. *Control Engineering Practice*, 18(9): 1110-1119.

Goupil, P. (2011). AIRBUS state of the art and practices on FDI and FTC in flight control system. *Control Engineering Practice*, 19(6): 524-539.

Goupil, P. and Marcos, A. (2012). Industrial benchmarking and evaluation of ADDSAFE FDD designs. *Proc. of the 8th IFAC Symposium on SAFEPROCESS'12*, Mexico City, 29-31 Aug.

Grenaille, S., Henry, D. and Zolghadri, A. (2008). A method for designing fault diagnosis filters for LPV polytopic systems. *J. of Control Science and Engineering*, 2008: 1-11.

Gu, Y., Ming, H. F. and Dan, Y. (2012). Fault reconstruction for linear descriptor systems using PD observer in finite frequency domain. *Proc. of the 24 th IEEE Chinese Conference on Decision and Control*, Taiyuan, China, 2281-2286, 23-25 May.

Guan, Y. and Saif, M. (1991). A novel approach to the design of unknown input observers. *IEEE Trans. on Automatic Control*, 36(5): 632-635.

Hamdi, H., Mechmeche, C., Rodrigues, M. and BenHadjBraiek, N. (2011). State and unknown inputs estimations for multi-model descriptor systems. *Proc. of the 8th International Multi-Conference on Systems, Signals and Devices*, Sousse, Tunisia, 22-25 Mar.

Hamdi, H., Mickael, R., Chokri, M., Theilliol, D. and Naceur Benhadj, B. (2012). Fault detection and isolation in linear parameter varying descriptor systems via

proportional integral observer. *Int. J. of Adapt. Control and Signal Processing*, 26(3): 224-240.

Hamdi, H., Rodrigues, M., Mechmeche, C. and BenHadjBraiek, N. (2012). Robust fault detection and estimation for descriptor systems based on multi-models concept. *Int. J. of Control, Automation, and Systems*, 10(6): 1260-1266.

Hamdi, H., Rodrigues, M., Mechmeche, C., Theilliol, D. and BenHadjBraiek, N. (2009). State estimation for polytopic LPV descriptor systems: application to fault diagnosis. *Proc. of the 7th IFAC Symposium on SAFEPROCESS'09*, Barcelona, 30 June-03 July.

Hameed, Z., Hong, Y., Cho, Y., Ahn, S. and Song, C. (2009). Condition monitoring and fault detection of wind turbines and related algorithms: A review. *Renewable and Sustainable Energy Reviews*, 13(1): 1-39.

Henry, D. and Zolghadri, A. (2004). Robust fault diagnosis in uncertain linear parameter-varying systems. *Proc. of the IEEE International Conference on Systems, Man and Cybernetics*, The Hague, Netherlands, 5165-5170, 10-13 Oct.

Henry, D. and Zolghadri, A. (2005). Design and analysis of robust residual generators for systems under feedback control. *Automatica*, 41(2): 251-264.

Hokayem, P. and Abdallah, C. T. (2003). Quasi-Monte Carlo methods in robust control design. *Proc. of the Joint 44th IEEE CDC'03, and ECC'03*, Hawaii, 2435-2440, 9-12 Dec.

Horn, R. A. and Johnson, C. R. (1990). *Matrix analysis*. Cambridge University Press.

Hou, M. and Müller, P. C. (1992). Design of observers for linear systems with unknown inputs. *IEEE Trans. on Automatic Control* 37(6): 871-875.

Hou, M. and Patton, R., J (1996). An LMI approach to $H\_/H_\infty$ fault detection observers. *Proc. Int. Conf. Control'96*, Exter, 305-310.

Hwang, I., Kim, S., Kim, Y. and Seah, C. E. (2010). A survey of fault detection, isolation, and reconfiguration methods. *IEEE Trans. on Control Systems Technology*, 18(3): 636-653.

Ichalal, D., Marx, B., Ragot, J. and Maquin, D. (2009). Simultaneous state and unknown inputs estimation with PI and PMI observers for Takagi Sugeno model with unmeasurable premise variables. *Proc. of the 17th IEEE Mediterranean Conference on Control and Automation*, Thessaloniki, 353-358, 24-26 June.

Isermann, R. (1993). Fault diagnosis of machines via parameter estimation and knowledge processing-tutorial paper. *Automatica*, 29(4): 815-835.

Isermann, R. (2005). Model-based fault-detection and diagnosis-status and applications. *Annual Reviews in Control*, 29(1): 71-85.

Isermann, R. (2006). *Fault-diagnosis systems: an introduction from fault detection to fault tolerance*. Berlin, Germany, Springer.

Isermann, R. (2011). *Fault-Diagnosis Applications: Model-Based Condition Monitoring: Actuators, drives, machinery, plants, sensors, and fault-tolerant systems*. Berlin, Springerverlag.

Isermann, R. and Ballé, P. (1997). Trends in the application of model-based fault detection and diagnosis of technical processes. *Control Engineering Practice*, 5(5): 709-719.

Jiang, B., Wang, J. L. and Soh, Y. C. (2002). An adaptive technique for robust diagnosis of faults with independent effects on system outputs. *Int. J. of Control*, 75(11): 792-802.

Jiang, G. P., Wang, S. P. and Song, W. Z. (2000). Design of observer with integrators for linear systems with unknown input disturbances. *Electronics Letters*, 36(13): 1168-1169.

Kaczorek, T. (1979). Proportional-integral observers for linear multivariable time-varying systems. *Regelungstechnik*, 27(6): 359-362.

Kajiwara, H., Apkarian, P. and Gahinet, P. (1999). LPV techniques for control of an inverted pendulum. *IEEE Control Systems Magazine*, 19(1): 44-54.

Kk-Electronic. (2013). http://www.kk-electronic.com/wind-turbine-control/competition-on-fault-detection.aspx [Accessed 22/05/2013].

Koenig, D. (2005). Unknown input proportional multiple-integral observer design for linear descriptor systems: application to state and fault estimation. *IEEE Trans. on Automatic Control*, 50(2): 212-217.

Koenig, D. and Mammar, S. (2001). Design of a class of reduced order unknown inputs nonlinear observer for fault diagnosis. *Proc. of the 2001 American Control Conference*, Arlington, 2143-2147, 25-27 June.

Koenig, D. and Mammar, S. (2002). Design of proportional-integral observer for unknown input descriptor systems. *IEEE Trans. on Automatic Control*, 47(12): 2057-2062.

Kudva, P., Viswanadham, N. and Ramakrishna, A. (1980). Observers for linear systems with unknown inputs. *IEEE Trans. On Automatic Control*, AC-25(2): 113-115.

Leigh, R., J (1983). *Essentials of nonlinear control theory*. London, Peter Peregrinus.

Leith, D. and Leithead, W. (2000). Survey of gain-scheduling analysis and design. *Int. J. of Control*, 73(11): 1001-1025.

Lieber, D., Nemirovskii, A. and Rubinstein, R. Y. (1999). A fast Monte Carlo method for evaluating reliability indexes. *IEEE Trans. on Reliability*, 48(3): 256-261.

Lu, B., Li, Y., Wu, X. and Yang, Z. (2009). A review of recent advances in wind turbine condition monitoring and fault diagnosis. *Proc. of the IEEE Power Electronics and Machines in Wind Applications*, Lincoln, Nebraska, 24-26 June.

Luenberger, D. (1966). Observers for multivariable systems. *IEEE Trans. on Automatic Control*, 11(2): 190-197.

Ma, J. and Jiang, J. (2011). Applications of fault detection and diagnosis methods in nuclear power plants: A review. *Progress in nuclear energy*, 53(3): 255-266.

Maciejowski, J. M. and Jones, C. N. (2003). MPC fault-tolerant flight control case study: Flight 1862. *Proc. of the 5th IFAC Symposium on SAFEPROCESS'03*, Washington, D.C., USA, 121-126, 9-11 June.

Mangoubi, R. S. (1998). *Robust estimation and failure detection: A concise treatment*. New York, Springer-Verlag.

Marx, B., Koenig, D. and Georges, D. (2003). Robust fault diagnosis for linear descriptor systems using proportional integral observers. *Proc. of the 42nd IEEE Conference on Decision and Control CDC'03*, Hawaii, 457-462, 9-12 Dec.

Marx, B., Koenig, D. and Ragot, J. (2007). Design of observers for Takagi-Sugeno descriptor systems with unknown inputs and application to fault diagnosis. *Control Theory & Applications, IET*, 1(5): 1487-1495.

Marzat, J., Piet-Lahanier, H., Damongeot, F. and Walter, E. (2012). Model-based fault diagnosis for aerospace systems: a survey. *Proc. of the Institution of Mechanical Engineers, Part G: Journal of Aerospace Engineering*, 226(10): 1329-1360.

Mckerrow, P. (1991). *Introduction to robotics*. Addison-Wesley Longman.

Nie, C. and Patton, R. J. (2011). Fault Estimation and MRC-Based Active FTC. *Proc. of the 18th IFAC World Congress*, Milan, 14808-14813, 28 Aug-02 Sept.

Odgaard, P. F. and Stoustrup, J. (2010). Unknown input observer based detection of sensor faults in a wind turbine. *Proc. of the IEEE International Conference on Control Applications CCA'10*, Yokohama, 310-315, 8-10 Sept.

Odgaard, P. F., Stoustrup, J. and Kinnaert, M. (2009). Fault tolerant control of wind turbines a benchmark model. *Proc. of the 7th IFAC Symposium on SAFEPROCESS'09*, Barcelona, 155-160, 30 June-03 July.

Orjuela, R., Marx, B., Ragot, J. and Maquin, D. (2009). On the simultaneous state and unknown input estimation of complex systems via a multiple model strategy. *Control Theory & Applications, IET*, 3(7): 877-890.

Pasand, M. S. and Taghirad, H. (2010). Descriptor approach to unknown input PI observer design: Application to fault detection. *Proc. of the 2010 International Conference on Control Automation and Systems ICCAS'10*, Gyeonggi-do, Korea, 600-604, 27-30 Otc.

Patton, R. J. (1997a). Fault-tolerant control systems: The 1997 situation. *Proc. of the 3rd IFAC Symposium on SAFEPROCESS'97*, Hull, 1033-1054.

Patton, R. J. (1997b). Robustness in model-based fault diagnosis: The 1995 situation. *Annual Reviews in Control*, 2(1): 103-123.

Patton, R. J. and Chen, J. (1991). A re-examination of the relationship between parity space and observer-basedapproaches in fault diagnosis. *European J. of Diagnosis and Safety in Automation*, 1(2): 183-200.

Patton, R. J. and Chen, J. (1993). Optimal unknown input distribution matrix selection in robust fault diagnosis. *Automatica*, 29(4): 837-841.

Patton, R. J., Chen, L. and Klinkhieo, S. (2012). An LPV pole-placement approach to friction compensation as an FTC problem. *Int. J. of Applied Mathematics and Computer Science*, 22(1): 149-160.

Patton, R. J., Frank, P. M. and Clark, R. N., Eds. (1989). *Fault diagnosis in dynamic systems: theory and application*. Control Engineering Series. New York, Prentice-Hall.

Patton, R. J., Frank, P. M. and Clark, R. N. (2000). *Issues of fault diagnosis for dynamic systems*. Springer Verlag.

Patton, R. J. and Klinkhieo, S. (2010). LPV fault estimation and FTC of a two-link manipulator. *Proc. of the 2010 American Control Conference*, Baltimore, 4647-4652, 30 June-02 July.

Patton, R. J., Uppal, F. J., Simani, S. and Polle, B. (2010). Robust FDI applied to thruster faults of a satellite system. *Control Engineering Practice*, 18(9): 1093-1109.

Pourmohammad, S. and Fekih, A. (2011). Fault-Tolerant Control of Wind Turbine Systems-A Review. *Proc. of the 2011. IEEE Green Technologies Conference (IEEE-Green)*, Louisiana, 14-15 April.

Rajamani, R. and Ganguli, A. (2004). Sensor fault diagnostics for a class of non-linear systems using linear matrix inequalities. *Int. J. of Control*, 77(10): 920-930.

Ren, J. and Zhang, Q. (2010). PD observer design for descriptor systems: an LMI approach. *Int. J. of Control, Automation and Systems*, 8(4): 735-740.

Ribrant, J. and Bertling, L. (2007). Survey of failures in wind power systems with focus on Swedish wind power plants during 1997-2005. *IEEE Trans. Energy Conversion*, EC22(1): 167-173.

Rodrigues, M., Theilliol, D. and Sauter, D. (2005a). Design of a robust polytopic unknown input observer for FDI: Application for systems described by a multi-model representation. *Proc. of the Joint 44th IEEE CDC'05, and ECC'05*, Plaza de Espaňa Seville, 6268-6273, 12-15 Dec.

Rodrigues, M., Theilliol, D. and Sauter, D. (2005b). Design of an active fault tolerant control and polytopic unknown input observer for systems described by a multi-model representation. *Proc. of the Joint 44th IEEE CDC'05, and ECC'05*, Plaza de Espaňa Seville, 3815-3820, 12-15 Dec.

Rodrigues, M., Theilliol, D. and Sauter, D. (2005c). Fault tolerant control design of nonlinear systems using LMI gain synthesis. *Proc. of the 16th IFAC World Congress*, Prague, 01-03 Sept.

Rogovin, M. (1979). Three Mile Island: A report to the Commissioners and to the public, Nuclear Regulatory Commission, Washington, DC (USA).

Rosa, P. and Silvestre, C. (2012). Fault detection and isolation of LPV systems using set-valued observers: An application to a fixed-wing aircraft. *Control Engineering Practice*,(21): 242-252.

Rugh, W. J. (1991). Analytical framework for gain scheduling. *IEEE Control Systems Magazine*, 11(1): 79-84.

Rugh, W. J. and Shamma, J. S. (2000). Research on gain scheduling. *Automatica*, 36(10): 1401-1425.

Saif, M. (1993). Reduced order proportional integral observer with application. *AIAA J. of Guidance, Control, and Dynamics*, 16(5): 985-988.

Saif, M. and Guan, Y. (1993). A new approach to robust fault detection and identification. *IEEE Trans. on Aerospace and Electronic Systems*, 29(3): 685-695.

Sami, M. and Patton, R. J. (2012). An FTC Approach to Wind Turbine Power Maximisation Via TS Fuzzy Modelling and Control. Fault Detection, Supervision and Safety of Technical Processes, 349-354.

Shafai, B. and Carroll, R. L. (1985). Design of proportional-integral observer for linear time-varying multivariable systems. *Proc. of the 24th IEEE Conference on Decision and Control CDC'85*, Ft. Lauderdale, 597-599, 11-13 Dec.

Shafai, B., Pi, C. and Nork, S. (2002). Simultaneous disturbance attenuation and fault detection using proportional integral observers. *Proc. of the 2002 American Control Conference*, Anchorage, AK 1647-1649, 8-10 May.

Shamma, J. S. and Athans, M. (1990). Analysis of gain scheduled control for nonlinear plants. *IEEE Trans. on Automatic Control*, 35(8): 898-907.

Shamma, J. S. and Athans, M. (1992). Gain scheduling: Potential hazards and possible remedies. *IEEE Control Systems Magazine*, 12(3): 101-107.

Simani, S., Fantuzzi, C. and Patton, R. J. (2003). *Model-based fault diagnosis in dynamic systems using identification techniques*. Berlin, Germany, Springer.

Sloth, C., Esbensen, T. and Stoustrup, J. (2011). Robust and fault-tolerant linear parameter-varying control of wind turbines. *Mechatronics*, 21(4): 645-659.

Slotine, J.-J. E. and Li, W. (1991). *Applied nonlinear control*. Prentice-Hall Englewood Cliffs, NJ.

Smaili, H. M., Breeman, J., Lombaerts, T. J. J. and Stroosma, O. (2008). A simulation benchmark for aircraft survivability assessment. 26th International Congress of The Aeronautical Sciences, Anchorage, 14-19 Sept.

Smaili, M. H. and Mulder, J. A. (2000). Flight data reconstruction and simulation of the 1992 Amsterdam Bijlmermeer airplane accident. *Proc. of AIAA Modelling and Simulation Technologies Conference*, Colorado, 14-17 Aug.

Söffker, D., Yu, T. J. and Müller, P. C. (1995). State estimation of dynamical systems with nonlinearities by using proportional-integral observer. *Int. J. of Systems Science*, 26(9): 1571-1582.

Sreedhar, R., Fernandez, B. and Masada, G. (1993). Robust fault detection in nonlinear systems using sliding mode observers. *Proc. of the 2nd IEEE International Conference on Control Applications CCA'13*, Vancouver, B.C., 715-721, 13-16 Sept.

Stoustrup, J. and Niemann, H. (2002). Fault estimation - a standard problem approach. *Int. J. of Robust and Nonlinear Control*, 12(8): 649-673.

Tan, C. P. and Edwards, C. (2002). Sliding mode observers for detection and reconstruction of sensor faults. *Automatica*, 38(10): 1815-1821.

Tan, C. P. and Edwards, C. (2004). Multiplicative fault reconstruction using sliding mode observers. *Proc. of the 5th Asian Control Conference, ASCC'04*, Melbourne, 957-962, 20-23 July.

Theilliol, D., Noura, H. and Ponsart, J. C. (2002). Fault diagnosis and accommodation of a three-tank system based on analytical redundancy. *ISA Transactions*, 41(3): 365-382.

Ting, H. C., Chang, J. L. and Chen, Y. P. (2011). Proportional-derivative unknown input observer design using descriptor system approach for non-minimum phase systems. *Int. J. of Control, Automation and Systems*, 9(5): 850-856.

Turbine-control-workshop. (2012). http://www2.hull.ac.uk/newsandevents-1/newsarchive/2012newsarchive/august/turbinecontrolworkshop.aspx [Accessed 01/06/2013].

Vanek, B., Seiler, P., Bokor, J. and Balas, G. J. (2011). Robust Model Matching for Geometric Fault Detection Filters: A Commercial Aircraft Example. 18th IFAC World Congress, Milano, Italy, 7256-7261, 28 Aug.-2ep.

Varga, A. (2010). Integrated algorithm for solving H_2-optimal fault detection and isolation problems. *Proc. of the 1st Conference on Control and Fault-Tolerant Systems SysTol'10*, Nice, 353-358, 6-8 Oct.

Venkatasubramanian, V., Rengaswamy, R., Yin, K. and Kavuri, S. (2003). A review of process fault detection and diagnosis: Part I: Quantitative model-based methods. *Computers & Chemical Engineering*, 27(3): 293-311.

Wang, D. and Lum, K. Y. (2007). Adaptive unknown input observer approach for aircraft actuator fault detection and isolation. *Int. J. of Adapt. Control and Signal Processing*, 21(1): 31-48.

Wang, H. and Daley, S. (1996). Actuator fault diagnosis: an adaptive observer-based technique. *IEEE Trans. on Automatic Control*, 41(7): 1073-1078.

Wang, H., Huang, Z. J. and Daley, S. (1997). On the use of adaptive updating rules for actuator and sensor fault diagnosis. *Automatica*, 33(2): 217-225.

Wei, X. and Liu, L. (2010). Fault detection of large scale wind turbine systems. *Proc. of the 5th International Conference on Computer Science and Education ICCSE'10*, Hefei, China, 1299-1304, 24-27 Aug.

Wei, X., Verhaegen, M. and van Engelen, T. (2010). Sensor fault detection and isolation for wind turbines based on subspace identification and Kalman filter techniques. *Int. J. of Adapt. Control and Signal Processing*, 24(8): 687-707.

Wikipedia. (1992). http://en.wikipedia.org/wiki/El_Al_Flight_1862 [Accessed 01/06/2013].

Wikipedia. (2011). http://en.wikipedia.org/wiki/Wenzhou_train_collision [Accessed 01/06/2013].

Wikipedia. (2012). http://en.wikipedia.org/wiki/List_of_offshore_wind_farms_in_the_Irish_Sea [Accessed 01/06/2013].

Wikipedia. (2013). http://en.wikipedia.org/wiki/List_of_offshore_wind_farms_in_the_North_Sea [Accessed 01/06/2013].

Wojciechowski, B. (1978). Analysis and synthesis of proportional-integral observers for single-input-single-output time-invariant continuous systems. Ph.D. thesis. Poland, University of Gliwice.

Wu, A. and Duan, G. (2007). Design of PD observers in descriptor linear systems. *Int. J. of Adapt. Control, Automation and Systems*, 5(1): 93-98.

Wu, A. G. and Duan, G. R. (2006). Design of PI observers for continuous-time descriptor linear systems. *IEEE Trans. on Systems, Man, and Cybernetics, Part B: Cybernetics*, 36(6): 1423-1431.

Wu, F. (2001). A generalized LPV system analysis and control synthesis framework. *Int. J. of Control*, 74(7): 745-759.

Wu, F., Yang, X. H., Packard, A. and Becker, G. (1995). Induced L2-norm control for LPV system with bounded parameter variation rates. *Proc. of the 1995 American Control Conference*, Seatle, Washington, 2379-2383, 21-23 June.

Xian, J. Q., Chun, Z. Y., Yu, G. and Na, W. L. (2011). Robust nonlinear unknown input observer-based fault diagnosis for satellite attitude control system. *Proc. of 2nd International Conference on Intelligent Control and Information Processing ICICIP'11*, Harbin, China, 345-350, 25-28 July.

Xiong, Y. and Saif, M. (1998). A novel design for robust fault diagnostic observer. *Proc. of the 37th IEEE Conference on Decision and Control CDC'98*, Tampa, Florida, 592-597, 14-17 Dec.

Xiong, Y. and Saif, M. (2003). Unknown disturbance inputs estimation based on a state functional observer design. *Automatica*, 39(8): 1389-1398.

Yacine, Z., Ichalal, D., Oufroukh, N. A., Mammar, S. and Djennoune, S. (2012). Unknown input observer for vehicle lateral dynamics based on a Takagi-Sugeno model with unmeasurable premise variables. *Proc. of the 51th IEEE Conference on Decision and Control CDC'12*, Hawaii, 6211-6216, 10-13 Dec.

Yang, F. Y. and Wilde, R. W. (1988). Observers for linear systems with unknown inputs. *IEEE Trans. on Automatic Control* 33(7): 677-681.

Yang, H. and Saif, M. (1995). Fault detection in a class of nonlinear systems via adaptive sliding observer. *Proc. of the IEEE International Conference on Systems, Man and Cybernetics: Intelligent Systems for the 21st Century*, Piscataway, 2199-2204, 22-25 Oct.

Zhang, K., Jiang, B. and Chen, W. (2009). An improved adaptive fault estimation design for polytopic LPV systems with application to helicopter models. *Proc. of the 7th Asian Control Conference, ASCC'09*, Hong Kong, 1108-1113, 27-29 Aug.

Zhang, K., Jiang, B. and Cocquempot, V. (2008). Adaptive observer-based fast fault estimation. *Int. J. of Adapt. Control, Automation and Systems*, 6(3): 320-326.

Zhang, K., Jiang, B. and Shi, P. (2009). Fast fault estimation and accommodation for dynamical systems. *Control Theory & Applications, IET*, 3(2): 189-199.

Zhang, Q. (2005). Revisiting different adaptive observers through a unified formulation. *Proc.of the Joint 44th IEEE CDC'05, and ECC'05*, Seville, 3067-3072, 12-15 Dec.

Zhang, X. D., Zhang, Q., Zhao, S. L., Ferrari, R., Polycarpou, M. M. and Parisini, T. (2011). Fault detection and isolation of the wind turbine benchmark: An estimation-based approach. *Proc. of the 18th IFAC World Congress*, Milan, 8295-8300, 28 Aug-02 Sept.

Zhang, Y. and Jiang, J. (2008). Bibliographical review on reconfigurable fault-tolerant control systems. *Annual Reviews in Control*, 32(2): 229-252.

Zhao, Z., Xie, W. F., Hong, H. and Zhang, Y. (2011). A disturbance decoupled adaptive observer and its application to faulty parameters estimation of a hydraulically driven elevator. *Int. J. of Adapt. Control and Signal Processing*, 25(6): 519-534.

Zhu, F. and Cen, F. (2010). Full-order observer-based actuator fault detection and reduced-order observer-based fault reconstruction for a class of uncertain nonlinear systems. *J. of Process Control*, 20(10): 1141-1149.

Zolghadri, A., Castang, F. and Henry, D. (2006). Design of robust fault detection filters for multivariable feedback systems. *Int. J. of Modelling and Simulation*, 26(1): 17-26.